



Durham E-Theses

S-nitrosothiols: novel decomposition pathways including reactions with sulfur and nitrogen nucleophiles

Munro, Andrew P.

How to cite:

Munro, Andrew P. (1999) *S-nitrosothiols: novel decomposition pathways including reactions with sulfur and nitrogen nucleophiles*, Durham theses, Durham University. Available at Durham E-Theses Online:
<http://etheses.dur.ac.uk/4605/>

Use policy

The full-text may be used and/or reproduced, and given to third parties in any format or medium, without prior permission or charge, for personal research or study, educational, or not-for-profit purposes provided that:

- a full bibliographic reference is made to the original source
- a [link](#) is made to the metadata record in Durham E-Theses
- the full-text is not changed in any way

The full-text must not be sold in any format or medium without the formal permission of the copyright holders.

Please consult the [full Durham E-Theses policy](#) for further details.

Academic Support Office, Durham University, University Office, Old Elvet, Durham DH1 3HP
e-mail: e-theses.admin@dur.ac.uk Tel: +44 0191 334 6107
<http://etheses.dur.ac.uk>

**S-NITROSTHIOLS : NOVEL DECOMPOSITION PATHWAYS
INCLUDING REACTIONS WITH SULFUR AND
NITROGEN NUCLEOPHILES**

by

Andrew P. Munro, B.Sc. (Hons.)

(Graduate Society)

The copyright of this thesis rests
with the author. No quotation
from it should be published
without the written consent of the
author and information derived
from it should be acknowledged.

A thesis submitted for the degree of Doctor of Philosophy in the
Department of Chemistry, University of Durham

September 1999



27 JAN 2000

**S-NITROSO THIOLS : NOVEL DECOMPOSITION PATHWAYS
INCLUDING REACTIONS WITH SULFUR AND
NITROGEN NUCLEOPHILES**

by Andrew P. Munro

A thesis submitted for the degree of Doctor of Philosophy in the Department of Chemistry, University of Durham, September 1999.

ABSTRACT

Spectrophotometric (including stopped-flow) techniques were used to examine the kinetics of NO-group transfer reactions (transnitrosation) between S-nitrosothiols (RSNO) and a wide range of sulfur/nitrogen nucleophiles in aqueous solution. A metal-ion chelator was added in all experiments to prevent RSNO decay and NO liberation catalysed by copper ions. In most cases reaction was envisaged as rate-determining attack of the nucleophile at the nitrogen atom of the -SNO moiety, and hence S-nitrosothiols essentially acted as electrophilic nitrosating agents.

Sulfite, thiosulfate, thiourea, thiocyanate and thiomethoxide, were sufficiently nucleophilic to induce nitrosothiol decomposition at physiological pH. Reaction with sulfide (pH > 7.4) afforded the orange-yellow anion, $^-\text{SSNO}$, and embodies a potential quantitative test for RSNOs. S-Nitrosopenicillamine was reactive enough to allow a thorough investigation into its reaction at basic pH with primary, secondary (creating carcinogenic N-nitrosamines), and tertiary amines, as well as ambident (e.g. thiomorpholine) and alpha nucleophiles (e.g. azide ion). Parallels could be made with analogous studies using other nitroso compounds such as MNTS.

The generality of the reaction of a S-nitrosothiol with a large excess of the corresponding or a different thiol was also assessed. Ammonia and not nitric oxide was confirmed as the primary nitrogenous product of this highly complicated process.

Mechanistic details of the copper(I) catalysed decomposition of some novel S-nitroso derivatives (e.g. a synthesised S-nitroso-1-thiosugar) are reported. The two-stage degradation pathway involved an initial Cu^+ promoted component that halted at incomplete conversion, and was accompanied by a large thermal reaction. An explanation of this unique pattern has been offered in terms of the generation of a disulfide- Cu^{2+} complex, in which copper is/is not accessible to reduction.

ACKNOWLEDGEMENTS

I am indebted to my supervisor, Professor D. Lyn H. Williams for his guidance and friendship throughout the course of my studies. The regular discussions about the turbulent state of Welsh sport will be greatly missed. Many thanks go to the exceptional computer magician (and story teller), Mr. Colin 'Ceeg' Greenhalgh, and I appreciate the time and effort spent by Dr. Andy Dicks in proof reading this thesis.

It is impossible to name everyone who has made my time in Durham so memorable, but a few people deserve a particular mention. Firstly, I wish to express my gratitude to my lab colleagues and friends; Ian, Gibbo, Coupie, Lynsey, Kathryn, Tony, Darren, Seve, Dave Moss, Parkin, Geordie Dave, Jeanette, Anna and E. I must also thank the Jas Pal lads, Bedders, Pricey, Alex, Phil, Fraggie, and Stella, for making the social life as entertaining as the work life. Coffee breaks will never be the same without the 'girls', Hazel and Jean.

Additional recognition goes to my grandparents, Chris, the Neath boys, Brian and Marian, and I am extremely grateful to my parents for their unremitting moral and financial support. Finally, but most importantly, I would like to say a special thank you to Madeleine for her patience, humour, and care, over the past few months.

Acknowledgement is made to the EPSRC for funding this research.

DECLARATION

The material in this thesis is the result of research carried out in the Department of Chemistry, University of Durham, between October 1996 and September 1999. It has not been submitted for any other degree and is the authors own work, except where acknowledged by reference.

STATEMENT OF COPYRIGHT

The copyright of this thesis lies with the author. No quotation from it should be published without his prior written consent and information derived from it should be acknowledged.

To my parents

CONTENTS

Chapter 1 : Introduction	1
1.1 Nitric Oxide	2
1.1.1 Introduction	2
1.1.2 Physical Properties	3
1.1.3 The Early Reputation of NO	3
1.1.4 The Physiological Functions of Nitric Oxide	5
1.1.4.1 Vasodilation	5
1.1.4.2 Biosynthesis of NO	7
1.1.4.3 Macrophage Cytotoxicity	8
1.1.4.4 Neurotransmission	9
1.1.4.5 Platelet Aggregation	9
1.1.5 Nitric Oxide Donor Compounds	10
1.1.5.1 Nitrovasodilators	10
1.1.5.2 Organic Nitrates and Nitrites	10
1.1.5.3 Metal Nitrosyls	12
1.1.5.4 S-Nitrosothiols	13
1.1.5.5 Furoxans	13
1.1.5.6 C-Nitroso Compounds	14
1.1.5.7 Sydnones	14
1.1.5.8 Oxatriazole-5-imine Derivatives	15
1.1.5.9 NONOates	15
1.1.5.10 N-Hydroxyguanidine Compounds	16
1.1.5.11 N-Nitropyrazoles	16
1.2 S-Nitrosothiols	17
1.2.1 Introduction	17
1.2.2 Physical Properties	17
1.2.3 History of S-Nitrosothiols	18
1.2.4 S-Nitrosothiol Formation	23
1.2.4.1 S-Nitrosation and Nitrosating Agents	23
1.2.4.2 Kinetics of S-Nitrosation	28

1.3	Reactions of S-Nitrosothiols	30
1.3.1	Introduction	30
1.3.2	Thermal/Photochemical Decomposition	30
1.3.3	Metal Ion Induced Decay	31
1.3.3.1	Copper Ion Catalysed Decomposition	31
1.3.3.2	Decomposition Induced by Mercury and Silver Salts	35
1.3.3.3	Iron Ion Catalysed Decomposition	36
1.3.3.4	Decomposition Induced by Other Metal Ions	37
1.3.4	Acid Catalysed Hydrolysis	38
1.3.5	S-Nitrosothiols as a Source of NO ⁺	39
1.3.5.1	Reactions with Nucleophiles	39
1.3.5.2	Reactions with Thiols (Transnitrosation)	39
1.3.5.3	Reactions with Amines	42
1.3.5.4	Reactions with Ascorbate (Vitamin C)	44
1.3.5.5	Reactions with Iodide/Iodine	45
1.3.5.6	Reactions with Hydrogen Peroxide	45
1.3.5.7	Reactions with Diethyl Dithiocarbamate	46
1.3.5.8	Reactions with Phenolic Nucleophiles	47
1.3.6	Decomposition Induced by Other Species	48
1.3.6.1	Reactions with Inorganic Complexes	48
1.3.6.2	Reactions with Seleno Compounds and Glucose Peroxidase	49
1.3.6.3	Reactions with Superoxide	50
1.3.6.4	Enzymatic and Cell-Mediated Reactions	51
1.3.7	Analytical Reactions	51
	References	52
	Chapter 2 : The Reaction of S-Nitrosothiols with Thiols at High Thiol Concentration	59
2.1	Introduction	60

2.2	Thiol Induced S-Nitrosothiol Decomposition	61
2.2.1	Kinetic Studies	61
2.2.2	Reactions of S-Nitrosothiols with the Parent Thiol	63
2.2.3	Reactions of S-Nitrosothiols with Thiols other than the Parent Thiol	69
2.2.4	Reactions of S-Nitrosothiols with Mixed Thiols	71
2.3	Determination of Reactive Species	73
2.4	Product Analysis	77
2.4.1	Detection of Ammonia	77
2.4.2	Detection of Nitrite	78
2.4.3	Detection of Nitrous Oxide	79
2.4.4	Detection of Disulfide	79
2.4.5	Composition of Reaction Products	80
2.5	Anaerobic Reaction	82
2.6	Proposed Decay Mechanism	84
2.7	Conclusion	86

References	87
------------	----

Chapter 3 : Reactivity of Nitrogen Nucleophiles Towards S-Nitrosopenicillamine 89

3.1	Introduction	90
3.2	Reactions of Secondary Amines	92
3.2.1	Effect of Amine Concentration on S-Nitrosopenicillamine Decomposition	92
3.2.2	Active Form of the Amine	96
3.2.3	Second Order Rate Constants	100
3.2.4	Reactivity	103
3.2.5	Reaction under Anaerobic Conditions	104
3.2.6	Identification of Decomposition Products	105
3.2.6.1	Nitrogen-Derived Species	105
3.2.6.2	Sulfur-Derived Species	107

3.2.7	Activation Parameters of Reaction	109
3.2.8	Deduced Reaction Mechanism	113
3.2.9	Alkaline Hydrolysis	114
3.3	Reactions of Primary Amines	121
3.3.1	Interactions at Low Amine Concentration	121
3.3.1.1	Effect of pH and Amine Basicity upon Reactivity	121
3.3.1.2	End Products	125
3.3.1.3	Proposed Mechanism of Deamination	126
3.3.2	Interactions at High Amine Concentration	127
3.3.2.1	Kinetic Characteristics	127
3.3.2.2	Nitrosothiol-Amine Complex Formation	129
3.4	Reactions of Tertiary Amines	133
3.5	Reactions of Other Nitrogen Nucleophiles	135
3.6	Reactions of Ambident Nucleophiles	139
3.7	Correlation and Discussion of Kinetic Results	143
3.8	Conclusion	147

References	148
------------	-----

Chapter 4 : Reactivity of Sulfur Nucleophiles 151

Towards S-Nitrosothiols

4.1	Introduction	152
4.2	Reactions of S-Nitrosothiols with Sulfites	153
4.2.1	Kinetic Analysis and Procedure	153
4.2.2	pH Dependence	158
4.2.3	Structure/Reactivity Investigation	161
4.2.4	Reaction using Different Forms of Sulfitite	167
4.2.5	Denitrosation Products	168
4.2.6	Reaction over a Temperature Range	169
4.2.7	Mechanistic Interpretations	171
4.3	Reactions of S-Nitrosothiols with Thiourea, Thiocyanate, Thiosulfate, and Thiomethoxide	173

4.4	Reactions of S-Nitrosothiols with Sulfides	177
4.4.1	Denitrosation of S-Nitrosoglutathione	177
4.4.2	Denitrosation of Other S-Nitrosothiols	179
4.4.3	Denitrosation of O- and N-Nitroso Compounds	181
4.4.4	Nitrosated Product	183
4.4.5	Promotion of Reaction by Added Disulfide	183
4.4.6	Mechanism of Anion Formation	186
4.5	Conclusion	187

References	188
------------	-----

Chapter 5 : Synthesis and Kinetics of Decomposition of Some New S-Nitrosothiols 190

5.1	Introduction	191
5.2	Synthetic Approaches and Biological Activity	191
5.2.1	2-Acetamido-2-deoxy-S-nitroso-1-thio- β -D-glucopyranose 3,4,6-triacetate (GPSNO)	191
5.2.2	S-Nitroso-1-thio- β -D-glucose (SNTG)	192
5.2.3	S-Nitroso-N-carbamyl-D,L-penicillamine (SNCP)	193
5.2.4	S-Nitroso-1-thioglycerol (TGSNO)	193
5.3	S-Nitrosothiol Decomposition	194
5.3.1	Spectral Characteristics	194
5.3.1.1	Effect of Varying Added Cu^{2+}	194
5.3.1.2	Addition of Metal Ion Chelating Agents	197
5.3.1.3	Addition of Ascorbate	199
5.3.1.4	Formation of a Copper(II)-Disulfide Complex	201
5.3.2	Nitrogenous Product Detection	202
5.3.3	Mechanism of S-Nitrosothiol Decay	204
5.4	Conclusion	206

References	207
------------	-----

Chapter 6 :	Experimental Details	208
6.1	Experimental Techniques	209
6.1.1	UV-Visible Spectrophotometry	209
6.1.2	Stopped-Flow Spectrophotometry	211
6.1.3	NMR Spectroscopy	212
6.1.4	IR Spectroscopy	212
6.1.5	Elemental Analysis	212
6.1.6	Melting Points	213
6.1.7	pH Measurements	213
6.1.8	Nitric Oxide Specific Electrode	213
6.2	Experimental Methods	214
6.2.1	Product Detection	214
6.2.1.1	Ammonia Analysis	214
6.2.1.2	Nitrite Analysis	215
6.2.1.3	Thiol Analysis	215
6.2.2	Enzymatic Deaeration of Solutions	215
6.3	Experimental Materials	215
6.3.1	Reagents	215
6.3.2	Synthesis of Stable S-Nitrosothiols	216
6.3.2.1	Symbols and Abbreviations	216
6.3.2.2	Preparation of 2-Acetamido-2-deoxy-S-nitroso- 1-thio- β -D-glucopyranose 3,4,6-triacetate (GPSNO)	216
6.3.2.3	Preparation of S-Nitroso-N-carbamyl- D,L-penicillamine (SNCP)	217
	APPENDIX	218

Chapter 1

Introduction

Chapter 1 : Introduction

1.1 Nitric Oxide

1.1.1 Introduction

Nitric Oxide..... “a startlingly simple molecule unites neuroscience, physiology, and immunology, and revises scientists’ understanding of how cells communicate and defend themselves.”¹ (*Science 1992*)

Only in the latter part of this century has nitric oxide (NO) emerged as a fundamental component in science’s interpretation of how many biochemical and physiological systems function.

Since the initial discovery of NO by Priestley in 1772², the important role of nitric oxide in nature and the human body has been largely disguised by the detrimental environmental effects and potential toxicity linked to the molecule. Photochemical smog, acid rain and the depletion of the ozone layer, are some of the highly publicised concerns attributable to NO pollutants.

Nevertheless the early use of nitric oxide products in explosives and agricultural fertilisers has evolved into a vast area of research during recent years, specifically highlighting the involvement of this species in many essential physiological pathways. Conclusive evidence now illustrates that biological processes including immune defences, platelet anti-aggregation, smooth muscle relaxation, and neurotransmission, are all governed by NO in some manner. Understandably this influence has elevated the chemical profile of NO. At present over one thousand literature articles are published annually on NO related topics, and the molecule has even made an appearance in high street magazines such as *Cosmopolitan*.

The 1998 Nobel Prize for medicine was awarded to three American scientists, namely Furchgott, Ignarro, and Murad, in recognition of their pioneering work on the role of nitric oxide within the human body’s cardiovascular system. Additionally the mode of action of the drug of the moment, *Viagra*, is based upon the NO pathway.

This compound has been globally marketed and administered as a temporary remedy for penile dysfunction³.

1.1.2 Physical Properties

At room temperature nitric oxide is a stable colourless gas, with a melting point of -163.6°C and a boiling point of -151.8°C . NO contains one unpaired electron in its $2p-\pi^*$ orbital⁴, and is therefore an example of a neutral paramagnetic molecule. The solubility in water is comparable to that of oxygen and carbon dioxide (i.e. $1.8 \times 10^{-3} \text{ mol dm}^{-3}$ at 1 atm and 25°C).

The free radical nature of NO has created confusion in determining its structure. Factors such as a reluctance to dimerise in solution have been attributed to delocalisation of the lone electron. Using valence bond theory the canonical forms in figure 1.1 have been proposed. The oxidation state of nitrogen is +2, the bond order ~ 2.5 , and N-O bond length $\sim 1.15\text{\AA}$.

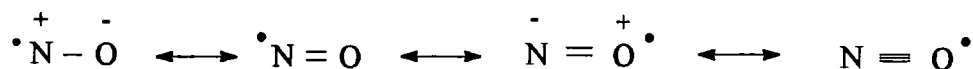
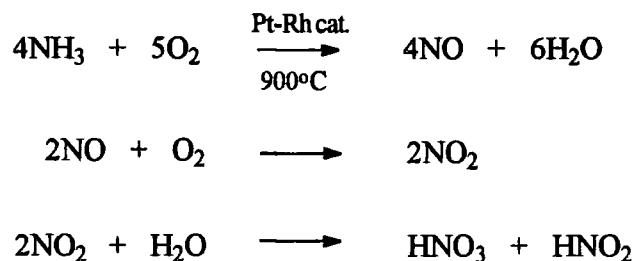


Figure 1.1

1.1.3 The Early Reputation of NO

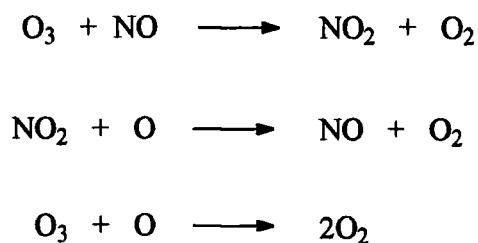
In the past NO has been labelled a 'villain' of the chemical world.

Many industrial procedures involve the generation of NO as a by-product. An example is the Ostwald Process. This is utilised in the commercial manufacture of nitric acid⁵ and involves catalytic oxidation of ammonia to yield NO (scheme 1.1).



Scheme 1.1

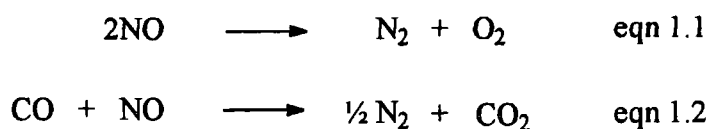
The unhindered release of NO into the upper reaches of the atmosphere can assist in the conversion of ozone into molecular oxygen (scheme 1.2). This erodes the earth's protective layer that filters out damaging radiation from the sun.



Scheme 1.2

A more immediate problem is present at ground level within the troposphere. Prolonged exposure to a dense photochemical smog composed of stagnant clouds of NO₂ (derived from NO) mixed with other chemical impurities, can destroy wildlife and seriously impair human health. Los Angeles, Mexico City and Tokyo are major cities known to suffer from such chronic atmospheric effects.

Catalytic converters have been designed with the intention of reducing the output of noxious exhaust emissions into the surrounding environment. Consequently, common pollutants such as NO_x (x = 1 or 2) gases and hydrocarbons are broken down into substances such as nitrogen and carbon dioxide (equations 1.1 and 1.2)⁶.

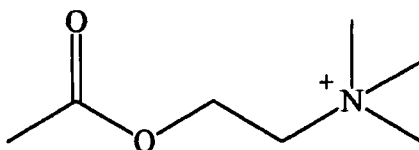


1.1.4 The Physiological Functions of Nitric Oxide

Contrary to early opinion, nitric oxide is today renowned as somewhat of a 'hero' of both the chemical and physiological worlds.

1.1.4.1 Vasodilation

A discovery by Furchgott and Zawadzki⁷ in 1980 has proved vital in shaping the present day understanding of the physiological mechanism involved in vasodilation. They noted that the aortic relaxation invoked by endogenous vasodilators such as acetylcholine (1.1), was somehow related to the endothelial cells lining the walls of an artery.



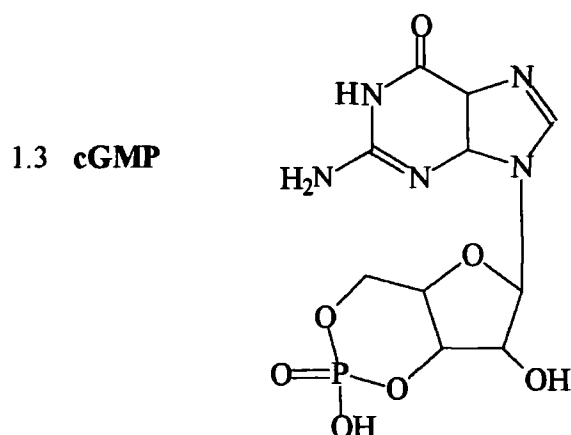
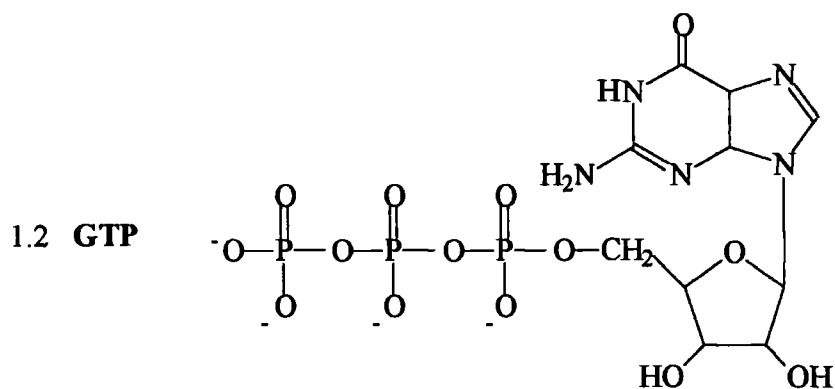
1.1

The conclusion reached was that acetylcholine did not act directly upon the vascular smooth muscle, moreover it interacted with receptors in the endothelium. This produced a new messenger molecule with a lifetime of only seconds, which has been assigned the label "endothelium-derived relaxing factor" (EDRF). The EDRF diffuses into underlying muscle and stimulates the soluble enzyme guanylate cyclase (GC), which catalyses the transformation of guanosine triphosphate (GTP, 1.2) into cyclic guanosine monophosphate (cGMP, 1.3). cGMP then initiates a series of protein phosphorylations linked to smooth muscle relaxation⁸.

One paramount question still remained however - what was the chemical identity of the mysterious EDRF ?

In 1986 Furchgott⁹ first speculated that the EDRF may be related to the diatomic gas, NO. Subsequent independent observations by Ignarro *et al*¹⁰ and Palmer *et al*¹¹ did indeed allow the EDRF to be conclusively assigned as NO. Both groups

highlighted the close relationship of the two species in biological tests, e.g. comparable half-lives. Furthermore, superoxide dismutase (SOD) (an enzyme that removes superoxide ions, so inhibiting reaction with NO) enhanced the vasodilatory effect of the EDRF. Haemoglobin (which reacts readily with NO) retarded its activity.

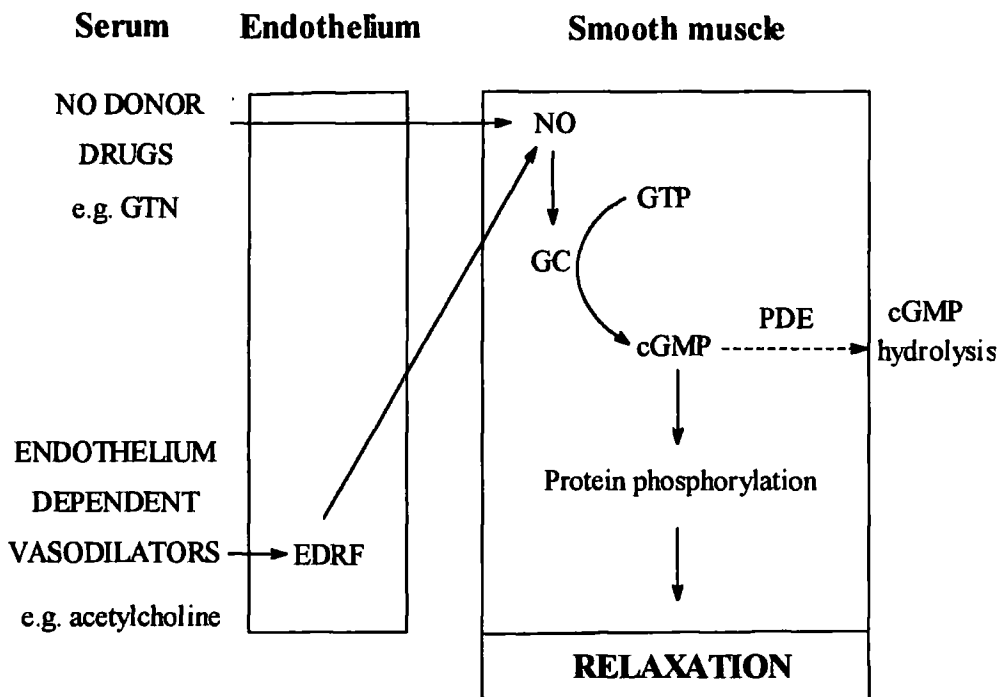


Although the debate over the EDRF's true identity continues nearly twenty years after its initial discovery, evidence still points to nitric oxide as the favoured candidate¹². Even so, species including S-nitrosothiols (section 1.2), dinitrosyl-iron-cysteine complexes, nitroxyl and hydroxylamine, have been suggested as alternatives.

Nitrovasodilators (section 1.1.5.1) activate guanylate cyclase by delivering NO directly to the smooth muscle without involving the endothelium and EDRF (figure 1.2).

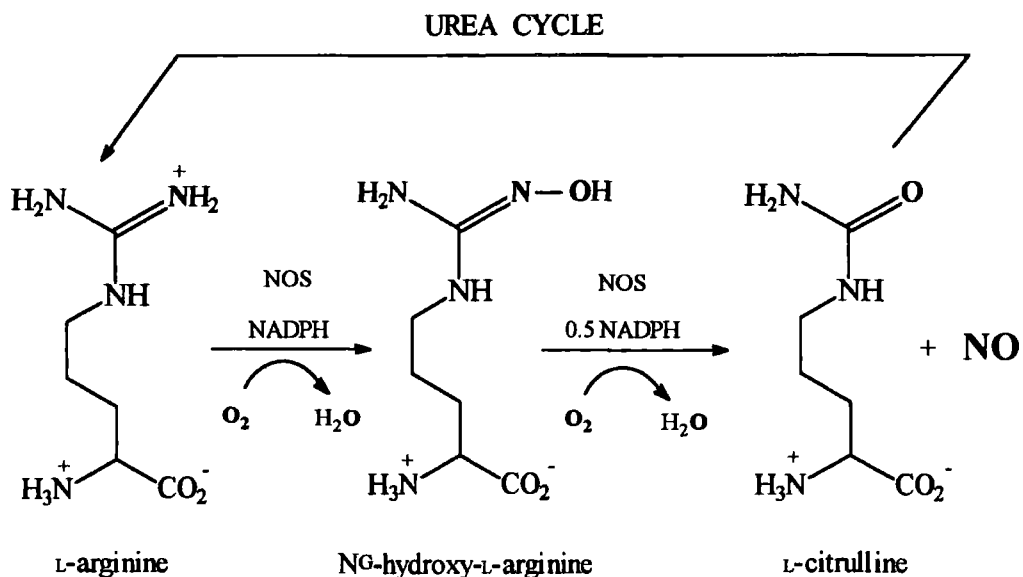
Viagra (Sildenafil) is a recent pharmaceutical drug developed to address the problem of impotence among some men³. This can be caused by a deficiency of NO. Sildenafil inhibits an enzyme called phosphodiesterase (PDE) which hydrolyses cGMP (figure 1.2). Such a compound can therefore be administered to raise the cGMP level within a patient and increase blood supply to the penile tissue.

Figure 1.2
Mechanism of action of vasodilators



1.1.4.2 Biosynthesis of NO

Nitric oxide synthase (NOS) is the enzyme responsible for the synthesis of nitric oxide *in vivo*¹³. Two different forms are believed to exist; one assigned as inducible and the other constitutive¹⁴. Both forms of NOS can catalyse the oxidation of a terminal guanidino nitrogen atom of the amino acid L-arginine. This produces NO and L-citrulline via a N^G-hydroxy-L-arginine intermediate (scheme 1.3). Oxygen atoms in both products derive from molecular oxygen, with any excess lost as water¹⁵. L-Citrulline can be converted back into L-arginine as part of the urea cycle.

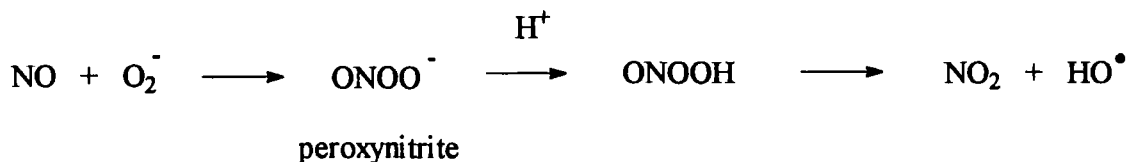


Scheme 1.3

1.1.4.3 Macrophage Cytotoxicity

In the immune system white blood cells known as macrophages non-selectively defend the body against foreign micro-organisms. There have been many precedents for the notion that NO is the cytotoxic substance used by macrophages to destroy any enveloped matter (phagocytosis)¹⁶.

The radical character of NO is one factor attributed as responsible for this potent toxicity. Superoxide ions are however common by-products in macrophages, and on reaction with NO can additionally generate biologically destructive hydroxyl radicals from a peroxynitrite precursor (scheme 1.4).



Scheme 1.4

Septic shock is a potentially fatal medical condition involving the over-production of NO by macrophages. This induces a dramatic decrease in patient blood

pressure. Treatments for this disorder will develop via a better understanding of the inducible variant of NOS which macrophages contain.

1.1.4.4 Neurotransmission

Extensive studies have been conducted concerning the roles that NO can assume within the peripheral and central nervous systems. Nitric oxide has been implicated as a factor in the dementia experienced by AIDS and Alzheimer's disease sufferers, as well as the neuronal damage linked to stroke victims, Parkinson's disease, and multiple sclerosis. In a better light NO is understood to operate as a neurotransmitter within the body - a chemical messenger that conveys impulses across the synapses or junctions between cells.

NO release from NOS within the brain has been characterised as potentially important in memory and learning¹⁷. Supplementary to functioning as a neurotransmitter, the NO manufactured in postsynaptic nerve cells can diffuse back into presynaptic neurones. A feedback loop between synapses is therefore completed, with NO acting as a "retrograde messenger"¹⁸.

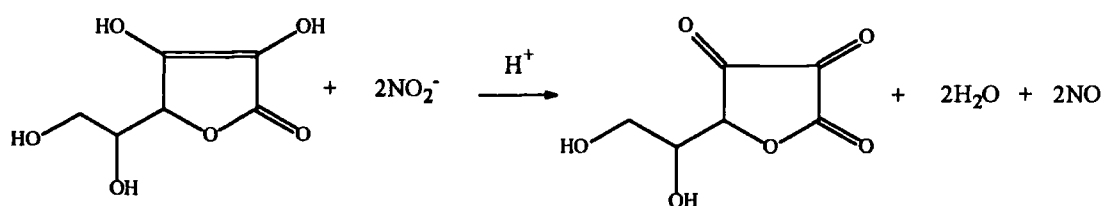
1.1.4.5 Platelet Aggregation

Blood coagulation leading to clotting, is one of the human body's primary defences against extensive blood loss after injury. Platelet aggregation is an intrinsic part of this process, whereby prostacyclin formation promotes cellular components of the blood plasma (platelets) to adhere to each other and the interior of the affected blood vessel. A barrier to prevent bleeding is therefore constructed. NO is known to inhibit this action¹⁹. As platelets (and endothelial cells they come into contact with) themselves contain enzymes capable of generating NO, its release can act as a negative feedback mechanism which impedes the platelet activation induced by other substances.

1.1.5 Nitric Oxide Donor Compounds

1.1.5.1 Nitrovasodilators

The reduction of nitric acid or solutions of nitrites and nitrates, offer the simplest methods for the preparation of nitric oxide in the laboratory. A convenient procedure involves the reaction of ascorbic acid (vitamin C) with sodium nitrite (equation 1.3)²⁰.



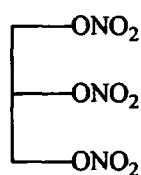
eqn 1.3

Compounds that can potentially release NO *in vivo* are called nitrovasodilators. These NO-storage and transport units can directly replenish a natural deficiency of nitric oxide within the body. To date only a limited number of compounds are known to exhibit such vasodilatory action.

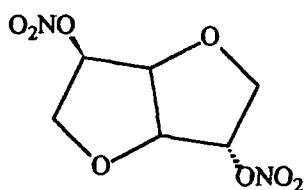
1.1.5.2 Organic Nitrates and Nitrites

For years medicine has relied upon the use of short-term treatments such as glyceryl trinitrate (GTN, 1.4) to successfully remedy cardiovascular problems in humans, even though tolerance can be developed by the sufferer. The symptoms of angina have been treated using GTN²¹, which can stimulate the widening of a patient's blood vessels within an affected area. Blood flow and oxygen levels in the heart thereby increase and ease chest pain. Even so, an understanding of the biological mechanism involved has not yet been reached. Only a decade ago did Feelisch *et al*²² identify that metabolism to NO (in the presence of certain thiols such as cysteine) actually plays a vital part in this process.

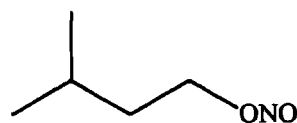
Other organic nitrates and nitrites such as isosorbide dinitrate¹³ (1.5) and amyl nitrite (1.6) have also proved to be effective NO donors.



1.4

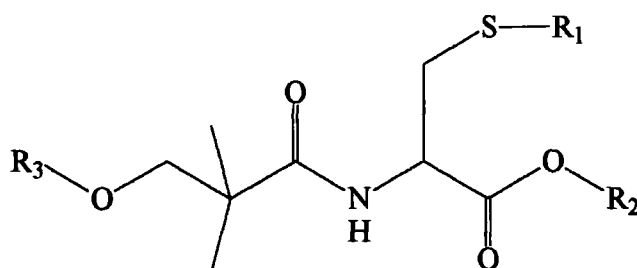


1.5



1.6

Innovative design strategies have enabled Bonn *et al*²³ to synthesise novel hybrid molecules combining the structural characteristics of organic nitrates with the pharmacological properties of chosen drugs. As mentioned previously, the presence of a thiol group is regarded as intrinsic to the mode of NO release from nitrates. One such combination (1.7) therefore involves the intramolecular coupling of cysteine to the nitrate ester of a fatty acid (nitratopivaloyl acid). The choice of the latter species enhances the lipophilic properties of the molecule.



1.7

where; a. $R_1 = \text{N}^{\text{Ac}}\text{-Gly}$, $R_2 = \text{C}_2\text{H}_5$, $R_3 = \text{NO}_2$

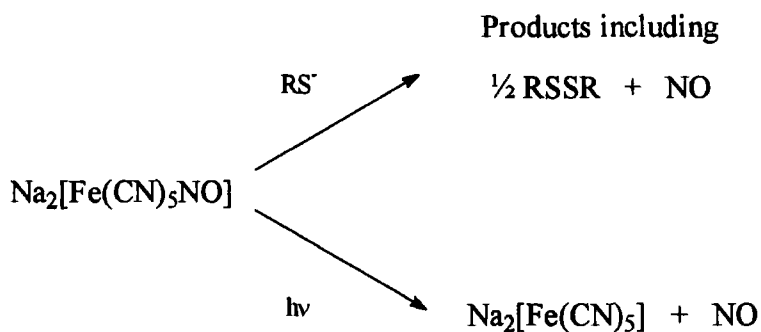
b. $R_1 = \text{H}$, $R_2 = \text{C}_2\text{H}_5$, $R_3 = \text{NO}_2$

c. $R_1 = R_2 = \text{H}$, $R_3 = \text{NO}_2$

Millar *et al*²⁴ have recently shown that xanthine oxidoreductase can also influence the therapeutic potential of organic nitrates. This complicated molybdoflavoprotein catalyses the reduction of GTN (and inorganic nitrates/nitrites) to nitric oxide under hypoxic conditions.

1.1.5.3 Metal Nitrosyls

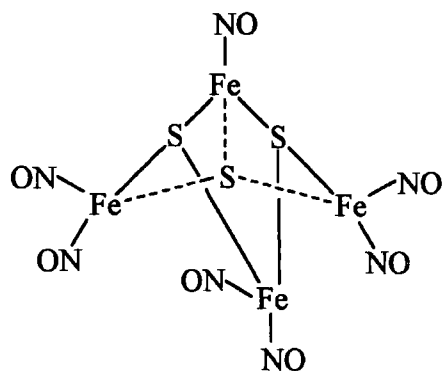
Photochemical decomposition of the iron-nitrosyl complex, sodium nitroprusside (SNP), can liberate NO (scheme 1.5). Reductive activation using a thiol²⁵ can have a similar albeit slower effect.



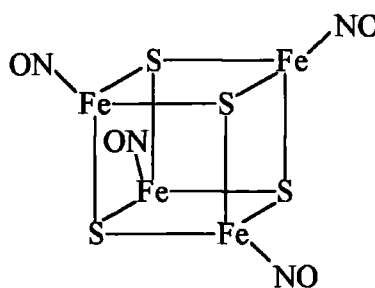
Scheme 1.5

Due to a favourable lipid solubility, heptanitrosyl- μ_3 -thioxotetraferrate (1-) (Roussin's black salt, RBS, 1.8) is a particularly effective example of a metal nitrosyl that can regulate the production of nitric oxide *in vivo*²⁶. Again the pathway is chemically or photochemically mediated.

Tetranitrosyltetra- μ_3 -sulphidotetrahydro-tetrairon (Cubane, 1.9) is another compound containing NO ligands that is an effective NO source. It can be synthesised from RBS via reaction with elemental sulfur.



1.8

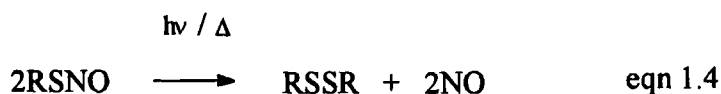


1.9

Interest has continued to grow in the area of metal nitrosyls, particularly dinitrosyl-dithiol-iron complexes that incorporate cysteine or the tripeptide glutathione into their structure²⁷. Such nitrosyls are now recognised as legitimate physiologic transport forms of NO, as they can be created *in vivo* on exposure of the relevant precursors to nitric oxide.

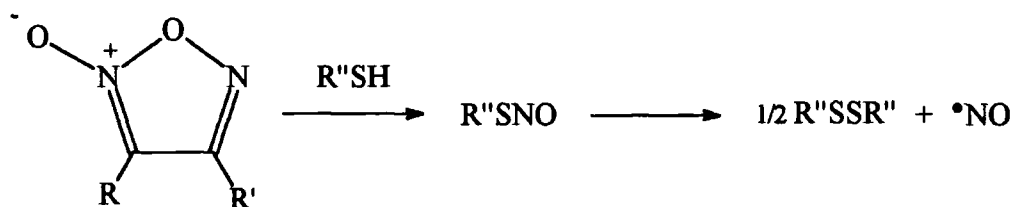
1.1.5.4 S-Nitrosothiols

S-Nitrosothiols (RSNO) are established vasodilators²⁸. They exhibit parallel biological properties to NO, e.g. the inhibition of platelet aggregation²⁹. Decomposition can occur via a number of recognised pathways that will be discussed in detail in section 1.3. NO and the corresponding disulfide can be generated via photochemically and thermally mediated routes³⁰ (equation 1.4). As yet it is not clear whether decomposition is necessary to induce a physiological response.



1.1.5.5 Furoxans

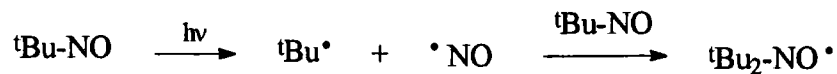
The furoxans (1,2,5-oxadiazole-2-oxides) are a family of heterocyclic compounds that can react with an added thiol to form NO via an unstable S-nitrosothiol intermediate³¹ (scheme 1.6).



Scheme 1.6

1.1.5.6 C-Nitroso Compounds

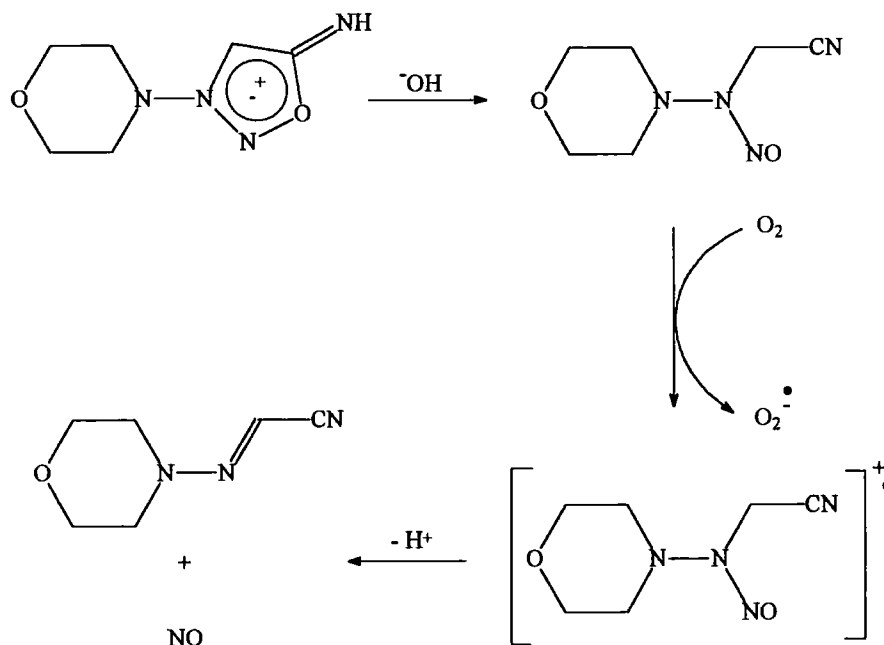
Facile homolytic cleavage of the C-N bond in C-nitroso species can free NO^{32} (scheme 1.7).



Scheme 1.7

1.1.5.7 Sydnonimines

Nucleophilic attack by a hydroxide ion cleaves the 5-membered ring of 3-morpholino-sydnonimine, and forms a carcinogenic nitrosamine. NO is evolved upon oxidation³³ (scheme 1.8). Harmful peroxyxynitrite by-products may be generated.



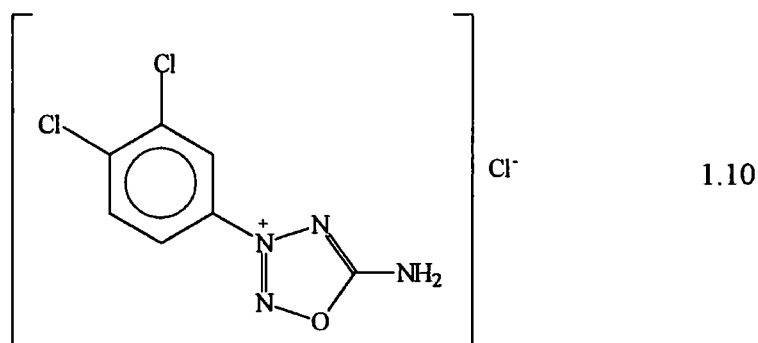
Scheme 1.8

Preliminary *in vitro* investigations now suggest that this sydnonimine can act as an exclusive NO donor³⁴, incurring negligible superoxide or peroxyxynitrite production. This is viable as one-electron oxidising agents have been used in preference to oxygen within the process. Nitronyl and imino nitroxides, together with

biologically relevant ferricytochrome c and haemproteins, have been implicated as suitable electron acceptors under anaerobic conditions.

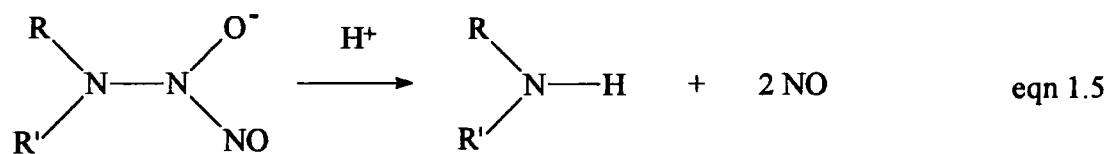
1.1.5.8 Oxatriazole-5-imine Derivatives

1,2,3,4-Oxatriazolium 5-amino-3-(dichlorophenyl)-chloride (1.10) is similar in structure to 3-morpholino-sydnonimine. Holm *et al*³⁵ have recently established that the oxatriazole-5-imine derivative is a superior NO donor in aqueous solution, and does not generate O_2^- or $ONOO^-$ when active. The S-nitrosothiol, S-nitroso-N-acetylpenicillamine, was the leading nitrovasodilator in all the tests performed.



1.1.5.9 NONOates

NONOates (diazoniumdiolates) are complexes of NO with nucleophiles (Y), and have the general formula $YN(O^-)NO$. Examples include water soluble solids which incorporate a secondary amine. These are capable of delivering controlled amounts of NO ³⁶ (equation 1.5).



One of the latest NONOates to be developed is a derivative of spermine³⁷ (1.11). It shows effective pulmonary vasorelaxant properties.

1.2 S-Nitrosothiols

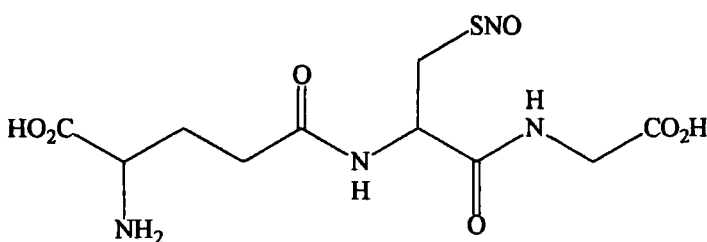
1.2.1 Introduction

S-Nitrosothiols (or thionitrites) have recently been highlighted as potentially useful compounds with regards to the release and transport of nitric oxide *in vivo*. They are known to occur naturally within the body ($\sim 7 \times 10^{-6} \text{ mol dm}^{-3}$ RSNO in plasma), predominantly as the S-nitroso adducts of the protein, human serum albumin, and the tripeptide, glutathione⁴¹. Some arguments have also been forwarded suggesting a S-nitrosothiol as a plausible candidate for the EDRF⁴² (section 1.1.4.1).

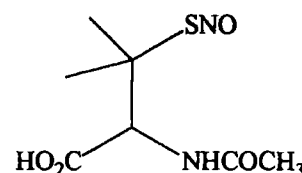
S-Nitrosothiols have the general formula RSNO and are usually less stable than their well studied oxygen analogues, the alkyl nitrites (RONO). The greater tendency of RSNOs to decompose is related to the fact that sulfur is considerably less electronegative than oxygen. The S-N bond is therefore more susceptible to homolytic fission than the O-N bond. For this reason only a limited number of S-nitrosothiols have been isolated and characterised in their stable pure form, although most can be readily generated *in situ*.

1.2.2 Physical Properties

Primary and secondary S-nitrosothiols are generally red or pink in colour (e.g. S-nitrosogluthathione, GSNO, 1.13), whereas tertiary S-nitrosothiols are green (e.g. S-nitroso-N-acetylpenicillamine, SNAP, 1.14)⁴³. The latter are usually more stable than the former due to an increase in the electron donating effect of 'R'. Solutions of S-nitrosoproteins tend to be orange or rose coloured⁴⁴.



1.13



1.14

Colour differences are reflected in the uv-visible spectra of RSNOs, which usually contain two characteristic absorption peaks. One maximum in the 330 - 350nm region ($\epsilon \sim 1000 \text{ mol}^{-1} \text{ dm}^3 \text{ cm}^{-1}$) is common to all S-nitrosothiols and is used as a reliable quantitative assessment of their decomposition. The absorption has been assigned to the $n_o \rightarrow \pi^*$ electronic transition⁴⁵. On the other hand the peak found at 540 - 600nm ($\epsilon \sim 10 \text{ mol}^{-1} \text{ dm}^3 \text{ cm}^{-1}$) is structure dependent, occurring at either 540nm (primary/secondary compounds) or 590nm (tertiary compounds). It is due to the $n_N \rightarrow \pi^*$ electronic transition.

Other physical techniques offer varied success when analysing S-nitrosothiols. IR spectroscopy enables the fingerprint stretching vibrations of the N=O (1480 - 1530 cm^{-1}) and C-S (600 - 730 cm^{-1}) bonds to be recognised⁴⁶. FAB-MS provides high enough resolution for a mass spectrum of the molecular ion to be attained. The best diagnostic tools however are ^1H and ^{13}C NMR spectroscopy. Spectra show a distinguishable downfield shift of both α -proton and α -carbon atom signals upon S-nitrosation⁴⁷. The signal observed for the S-H proton is also lost.

Field *et al*⁴⁸ were able to measure a melting point of 152 - 154°C for SNAP, but decomposition to the disulfide (section 1.3.2) usually prevents melting points from being recorded. The same group also managed to obtain a X-ray crystal structure for the molecule, which characterised the C-S bond (1.841Å) as rather long in relation to the S-N (1.771Å) and N=O (1.214Å) bonds.

Dipole moments of stable RSNOs are similar to the organic nitrite equivalents.

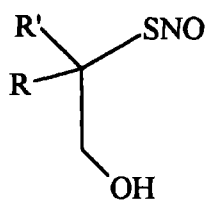
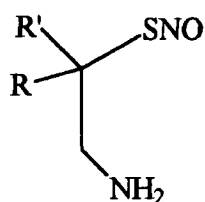
1.2.3 History of S-Nitrosothiols

S-Nitrosothiols were first synthesised over 150 years ago, when chemists observed that a bright red solution was produced on mixing a thiol with nitrous acid. It took a further 70 years until Tasker and Jones⁴⁹ eventually isolated genuine compounds containing the S-nitroso moiety, when they successfully prepared phenyl thionitrite (1.15) and ethyl thionitrite (1.16). Other early examples of RSNOs included triphenylmethyl thionitrite⁵⁰ (1.17) and ^tbutyl thionitrite⁵¹ (1.18). Both incorporated sterically bulky substituents into their structure to enhance stability.

PhSNO	EtSNO	Ph ₃ CSNO	(CH ₃) ₃ CSNO
1.15	1.16	1.17	1.18

Over recent decades the synthesis of SNAP (1.14) by Field *et al*⁴⁸ and the formation of GSNO (1.13) by Hart⁵², have proved invaluable in generating the biological interest associated with S-nitrosothiols. The fact that these two compounds are infinitely stable at room temperature when stored in the dark, has allowed *in vivo* testing to reveal the true relevance of their physiological action.

Present day efforts related to the synthesis of new S-nitrosothiols include a range of compounds based upon cysteamine (1.19) and mercaptoethanol (1.20). Roy *et al*⁴⁷ have fully characterised these products, and analysed the effects of different substituents within the molecule on NO donating capabilities.

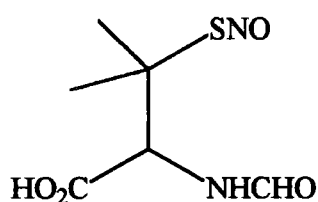


e.g. R = R' = H

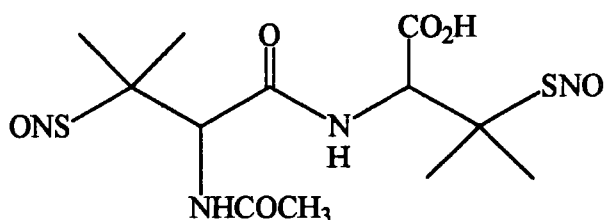
1.19

1.20

Moynihan and Roberts⁵³ have made progress towards an authentic sample of S-nitrosopenicillamine. Analogous S-nitrosothiols including N-formyl-S-nitrosopenicillamine (1.21) have been attained as pure solids, and unique S,S'-dinitrosodithiols also created. These penicillamine dipeptides contain the potential to release two equivalents of NO per molecule within the body, and only generate non-toxic cyclic disulfides as decomposition by-products. The dimer of SNAP, (N-acetyl-S-nitrosopenicillaminy)-S-nitrosopenicillamine (1.22), is an example.

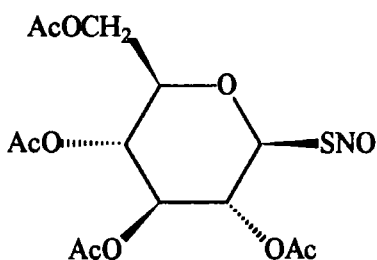


1.21

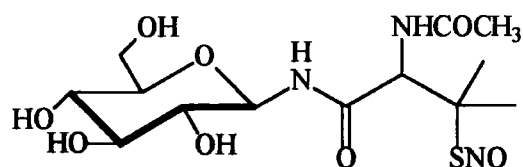


1.22

Butler *et al*⁵⁴ have synthesised unique RSNO compounds derived from 1-thiosugars (glucose, galactose, xylose, maltose, and lactose), e.g. S-nitroso-1-thiogluco-1-thioacetate (1.23). The glyco-S-nitrosothiols developed by Ramirez *et al*⁵⁵ are also based upon the skeletal configuration of a sugar, coupled with the structural features of SNAP (1.24). The carbohydrate fragment is beneficial to the biological activity of the drug as it assists the solubility in water. Transfer of the molecule through cell membranes is therefore easier and the quantity of NO that can be delivered is increased.

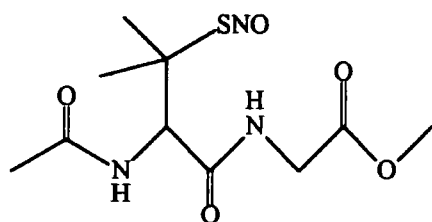


1.23

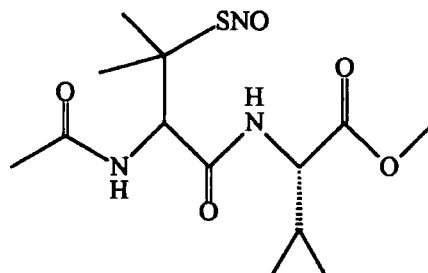


1.24

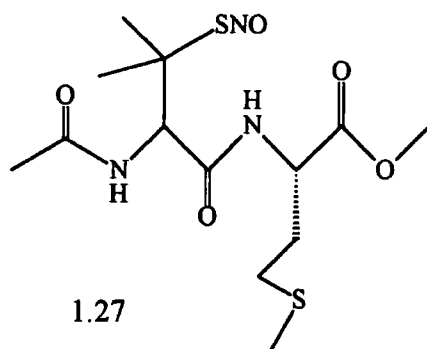
The structural characteristics of SNAP have been incorporated into a selection of S-nitrosated dipeptides. Within the last year the synthesis, decomposition, and effective vasodilatory action of these nitrosothiols (containing amino acid methyl ester components) have been reported⁵⁶. S-Nitroso-N-acetyl-D,L-β,β-dimethyl-cysteinylglycine methyl ester (1.25) is one such compound that has been isolated as a green solid. Other examples include the derivatives of valine (1.26) and methionine (1.27).



1.25

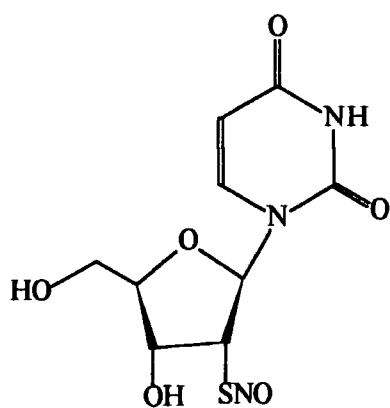


1.26

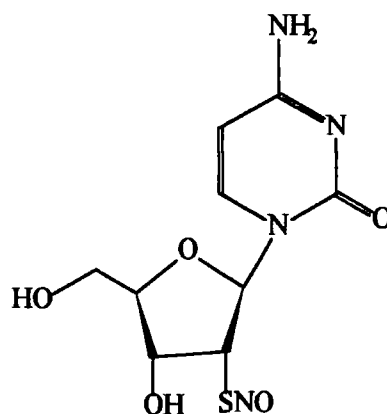


1.27

Nucleosidic nitrosothiols have been prepared in solution from 2'-thiouridine (1.28) and 2'-thiocytidine (1.29)⁵⁷. The thiol precursors were manufactured from nucleoside 5'-diphosphates via replacement of the 2'-hydroxy substituent with a -SH group. Apart from NO-related effects, these drugs are regarded as potential inhibitors of ribonucleotide reductase. This is the essential enzyme in the reduction of ribonucleotides to 2'-deoxyribonucleotides, which is the rate-limiting step in the biosynthesis of DNA.



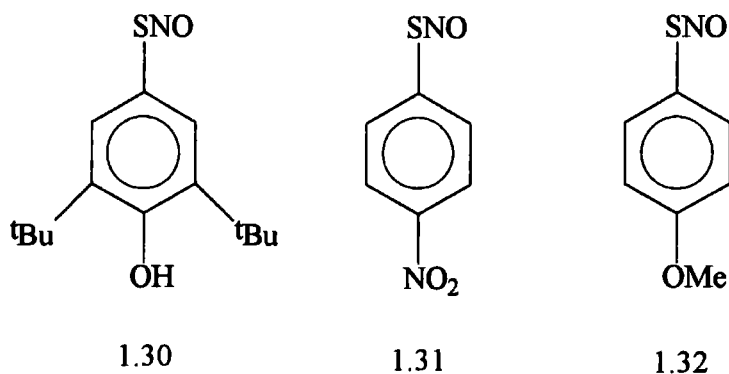
1.28



1.29

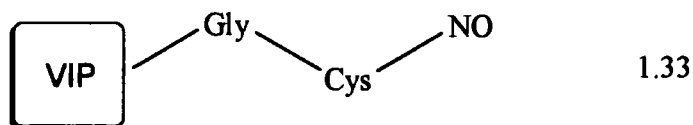
In the past attention has been primarily directed towards aliphatic RSNOs, and limited work has been conducted upon isolating new aromatic and heterocyclic

S-nitrosothiols. Petit *et al*⁵⁸ have however managed to synthesise and fully characterise an original collection of aromatic thionitrites in organic solution. S-Nitroso derivatives containing a 3,5-di-*tert*-butylphenol (1.30), *p*-nitrophenyl (1.31), and *p*-methoxyphenyl (1.32) aromatic portion, were stable enough to be analysed in EPR experiments.



The isolation of pure S-nitroso proteins is an area still in its infancy. Even so, the *in situ* S-nitroso adducts of albumin⁴⁴, cathepsin B, tissue plasminogen activator, and soybean extract, have been classified as more stable than amino acid and small peptide nitrosothiols at physiological pH. Favourable intramolecular interactions within the protein and steric inhibition of attack by reactive nucleophiles, have been suggested as reasonable explanations for this behaviour.

Jia and Stamler⁵⁹ have recently published details concerning the synthesis of the S-nitroso derivative (1.33) of vasoactive intestinal peptide (VIP). VIP is a 28 amino acid peptide that can act as a vasodilator and an inhibitory neurotransmitter in the central and peripheral nervous system. It has also been highlighted as a possible non-adrenergic non-cholinergic (NANC) transmitter.



The biological relevance of the possible S-nitrosation of peptides, proteins, and amino acids *in vivo*, is a topic receiving much attention in current research.

1.2.4 S-Nitrosothiol Formation

1.2.4.1 S-Nitrosation and Nitrosating Agents

The most convenient method for producing S-nitrosothiols is the electrophilic nitrosation of thiols³⁰. This procedure is an illustration of S-nitrosation and is analogous to O-nitrosation which yields alkyl nitrites from alcohols. Other categories of nitrosation include C-nitrosation. This involves the substitution of a nitroso group in place of a hydrogen atom at a carbon centre, which can lead to molecular rearrangement. N-Nitrosation can create species including nitrosamides, diazonium ions and N-nitrosamines, from amides and primary or secondary amines.

S-Nitrosation occurs rapidly in water or organic solvents using reagents (XNO) capable of transferring NO⁺ (equation 1.7). XNO species in which X is a good leaving group (i.e. X is a powerful electron-attracting group) tend to be more effective nitrosating agents.



Nitrous acid (HNO₂) is the most commonly used nitrosating agent in aqueous systems. It is readily produced from an acidified solution of sodium nitrite (equation 1.8).



HNO₂ has a pK_a value of 3.15 at 25°C⁶⁰. It is easily identified in solution by a characteristic 5-peak fingerprint uv-visible spectrum⁶¹ (340 - 390nm), and exists primarily as the more stable *trans* isomer at room temperature⁶² (figure 1.3).

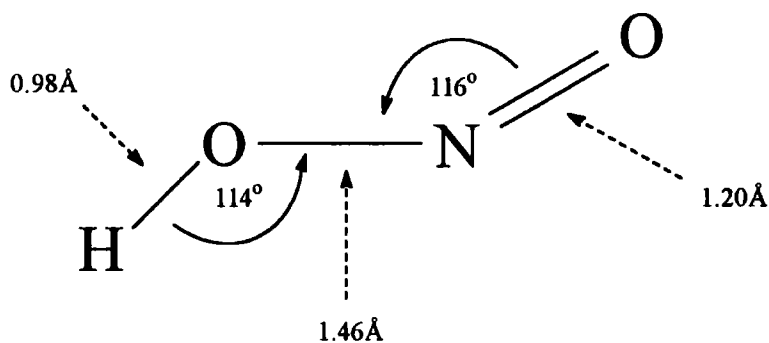
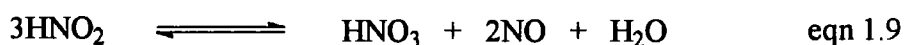
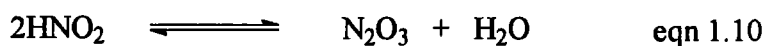


Figure 1.3

Nitrous acid can decompose on standing to form nitric acid and nitric oxide (equation 1.9).



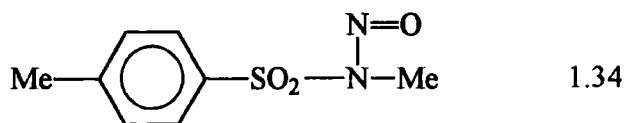
At high acid concentrations and low pH, an equilibrium can also exist between HNO_2 and dinitrogen trioxide (equation 1.10).



The majority of S-nitrosation reactions involving thiols are however performed at much lower nitrous acid concentrations and a higher pH. Under these conditions the levels of N_2O_3 produced are negligible.

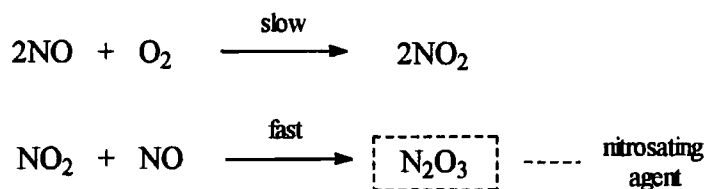
The nature of the actual nitrosating species and kinetics involved in S-nitrosothiol formation using HNO_2 will be discussed in section 1.2.4.2.

A range of other conventional nitrosating agents can generate S-nitrosothiols from thiol precursors in good yield. Typical examples are alkyl nitrites (e.g. ${}^t\text{BuONO}$ in chloroform⁶³) and N-nitrososulfonamides (e.g. N-methyl-N-nitrosotoluene-*p*-sulfonamide, MNTS, 1.34, in aqueous ethanol⁶⁴).



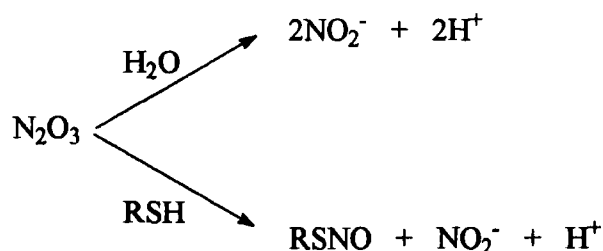
Gaseous nitrosyl halides⁶⁵ (nitrosyl fluoride, chloride and bromide) are convenient sources of NO^+ when dissolved in organic solvents (ether or chloroform). Some of the higher oxides of nitrogen including dinitrogen tetroxide⁶⁶ (N_2O_4) are also effective, particularly in inert solvents such as hexane, acetonitrile or carbon tetrachloride.

There has been much debate in the literature as to the capacity of nitric oxide as a nitrosating agent. Investigations have now established that nitric oxide will not nitrosate a thiol at physiological pH (7.4) unless oxygen is present. One set of studies concerning the kinetics and products of this reaction have identified dinitrogen trioxide (N_2O_3) as the likely nitrosating species⁶⁷. It is proposed that N_2O_3 is formed from NO , via oxidation to NO_2 . The rate-limiting step in the process is the reaction of NO with oxygen (scheme 1.9).



Scheme 1.9

Nitrosation competes with the hydrolysis of dinitrogen trioxide. The latter forms nitrite ions (scheme 1.10).



Scheme 1.10

Gow *et al*⁶⁸ have suggested another mechanism representing the possible *in vivo* formation of S-nitrosothiols from nitric oxide. It involves the oxidation of a radical intermediate, and therefore requires the presence of a suitable electron acceptor (such as oxygen). The reaction initially proceeds via a direct interaction between NO and the thiol (scheme 1.11).

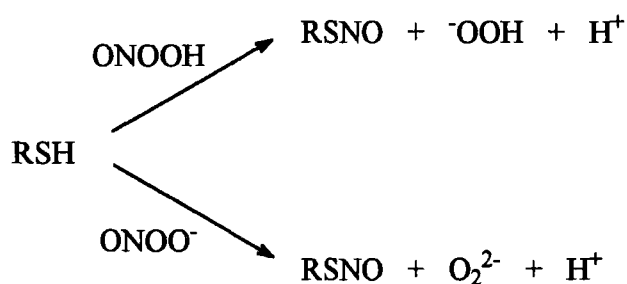


Scheme 1.11

A base-catalysed process reported by Pryor *et al*⁶¹ has however shown that in alkaline conditions and on complete **elimination** of oxygen, nucleophilic attack of RS⁻ towards NO can produce S-nitrosothiols.

As yet no evidence exists to support the formation of RSNOs from nitric oxide and thiyl radicals. It is known that thiols can be oxidised to the corresponding thiyl radical *in vivo*.

Confusion currently surrounds the issue of whether peroxyxynitrite and peroxyxynitrous acid can be classified as electrophilic nitrosating agents. Williams⁶⁹ has reviewed the subject, and scheme 1.12 highlights his theoretical opinion on how these reagents could react with a thiolate substrate. He implies that O₂²⁻ and ⁻OOH would be very poor leaving groups, and thus render the reaction thermodynamically and kinetically unfavourable. A protonated form of peroxyxynitrite (e.g. ONO⁺(H)OH) is suggested as a more suitable candidate, or even prior decomposition to NO. Interestingly, it has been shown that peroxyxynitrite-mediated vasorelaxation *in vivo* does not involve the formation of S-nitrosothiols⁷⁰.

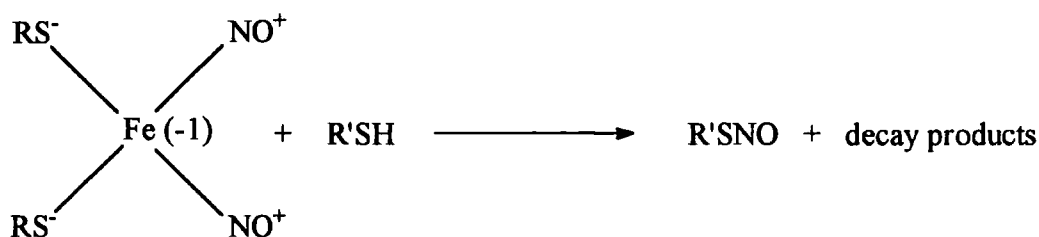


Scheme 1.12

Several independent groups^{71,72} have detected small quantities of GSNO (~1% yield) in the products of the reaction between GSH and peroxyntirite at pH 7.4. The mechanism proposed by van der Vliet *et al*⁷² proceeds via nucleophilic attack of the thiolate anion at the nitrogen atom of ONOOH. As a result HOO⁻ is eliminated and protonated to H₂O₂. It was confirmed that reaction did not involve the intermediate formation of S-nitrothiols (RSNO₂) as previously postulated.

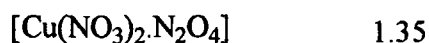
The whole issue of nitrosation via peroxyntirite awaits a thorough investigation.

A dinitrosyl-iron complex⁷³ has been used as a model to show that protein bound metal nitrosyls can potentially nitrosate thiols such as bovine serum albumin *in vivo*. Evidence indicates that S-nitrosoalbumin formation involves the direct transfer of NO⁺ (equation 1.11).



eqn 1.11

Recent innovations in metal nitrosyl mediated nitrosation include the synthesis of a dinitrogen tetroxide copper nitrate complex (1.35) by Iranpoor *et al*⁷⁴. It has been shown to be an effective nitrosating agent in acetone at room temperature. Essentially the complex exists as NO⁺[Cu(NO₃)₃], but suffers from drawbacks as it contains a Cu²⁺ ion. The reason for this will be explained in section 1.3.3.1.

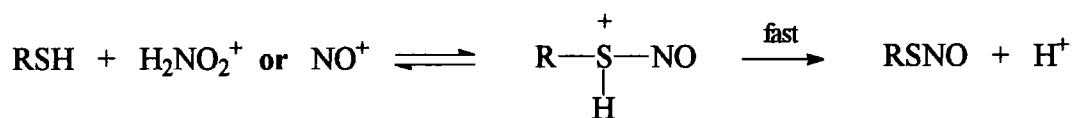
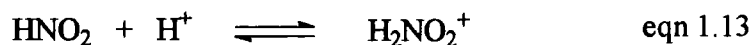


1.2.4.2 Kinetics of S-Nitrosation

Advanced instrumentation including stopped-flow spectrophotometry is required to accurately monitor S-nitrosation, which is generally an extremely rapid process. Kinetic measurements of the nitrosation of many aliphatic⁷⁵, aromatic and heterocyclic⁷⁶ thiols have been collected, using reagents such as nitrous acid under aqueous conditions. A standard rate equation has been established which is applicable to most aliphatic substrates (equation 1.12).

$$\text{Rate} = k_3[\text{HNO}_2][\text{RSH}][\text{H}^+] \quad \text{eqn 1.12}$$

Within the accepted mechanism of RSNO formation, the slow rate-determining step has been assigned as the attack of a positively charged nitrosating species at the sulfur atom of the thiol (scheme 1.13). In the case of an aqueous solution of acidified sodium nitrite, it is impossible to establish whether a nitrous acidium ion (H_2NO_2^+) (equation 1.13) or nitrosonium ion (NO^+) (equation 1.14) is the true agent involved.

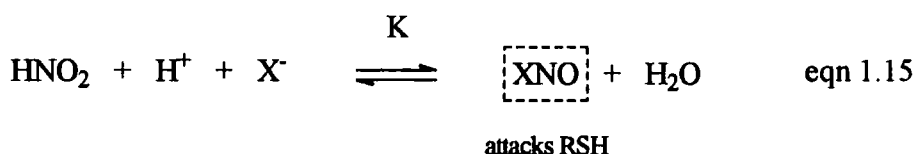


Scheme 1.13

The third order rate constant (k_3) is typically quite large (e.g. glutathione $\sim 1080 \text{ mol}^{-2} \text{ dm}^6 \text{ s}^{-1}$), and can reach an encounter-controlled limit ($k_3 \sim 7000 \text{ mol}^{-2} \text{ dm}^6 \text{ s}^{-1}$).

A rate-limiting process involving the interaction of a nitrosyl compound (XNO) with the thiol, is the reason why nucleophiles are recognised catalysts of S-nitrosation⁷⁷. The extent of this effect depends on the magnitude of the equilibrium

constant (K) that exists between the initial nitrosating species/nucleophile (X) and the subsequent nitrosyl formed from these reactants (equation 1.15).



The rate equation for this nitrosation pathway has also been derived (equation 1.16).

$$\text{Rate} = k_2[\text{RSH}][\text{XNO}] \quad \text{eqn 1.16}$$

The second order rate constant (k_2) exhibits a marked increase as the nucleophilicity of the added species increases (i.e. $\text{I}^- > \text{SCN}^- > \text{Br}^- > \text{Cl}^-$).

It has been known for a number of years that the nitrosation of alcohols to form alkyl nitrites in acidic media is a highly reversible process (equation 1.17).



It was also generally accepted that the nitrosation of thiols to form S-nitrosothiols was irreversible under similar conditions. These observations were explained by the apparent nucleophilicity ($\text{S} > \text{O}$) and basicity ($\text{O} > \text{S}$) differences important in the forward and reverse reactions respectively. Beloso and Williams⁷⁸ have recently shown that the S-nitrosation process is in fact sufficiently reversible in mildly acidic solution, to allow a small thiol concentration to be continually present at equilibrium (equation 1.18). Accordingly solid samples together with those created *in situ* (using even an excess of nitrous acid), all contain a low but significant thiol content. The important implications of this phenomenon in S-nitrosothiol decomposition will be examined later (section 1.3.3.1).



1.3 Reactions of S-Nitrosothiols

1.3.1 Introduction

Developments within the last seven years have prompted a reassessment of the categories of reaction in which S-nitrosothiols can be involved. The different pathways by which RSNOs can decompose are therefore only slowly becoming clear. A diverse spectrum of nitrogen containing products apart from nitric oxide are now understood to originate from S-nitrosothiol precursors, under *in vitro* conditions that mimic those which are common within the body.

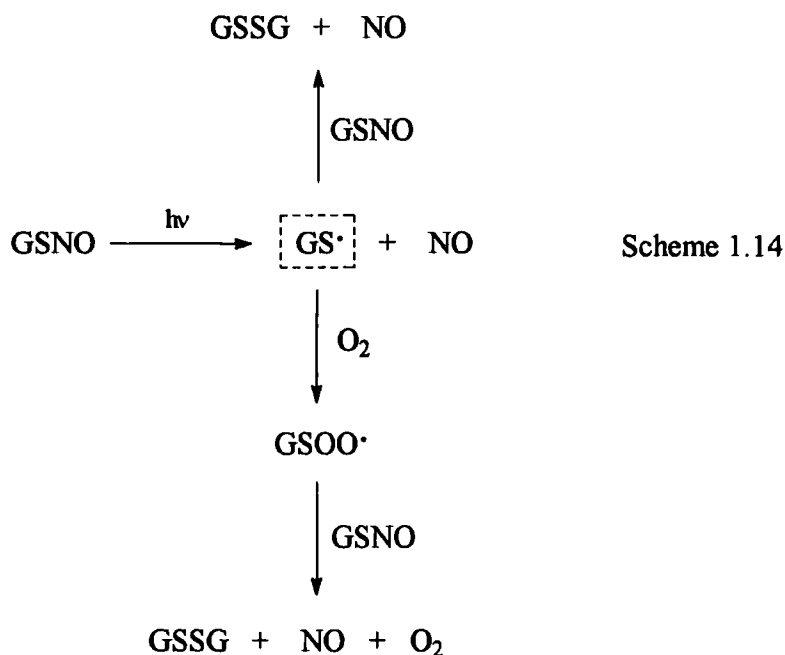
1.3.2 Thermal/Photochemical Decomposition

S-Nitrosothiols decompose both thermally and photochemically to yield the corresponding disulfide and nitric oxide³⁰ (equation 1.4). Both processes are thought to involve initial homolytic fission of the S-N bond.



The photochemical reaction has been studied via irradiation of a solution of GSNO at one of its absorption bands⁷⁹ ($\lambda_{\text{max}} = 340$ or 545nm). The mechanism involved is summarised in scheme 1.14. It describes how a thiyl radical generated in the first stage of the process, can combine with atmospheric oxygen to form a peroxy radical intermediate that may react further⁸⁰.

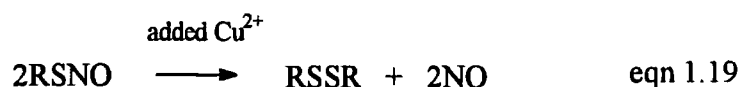
It has been noted that visible radiation increases the cytotoxic effect of GSNO⁷⁹. This is an observation consistent with the increased liberation of NO, which is the actual cytotoxic substance (section 1.1.4.3). Understandably therefore, GSNO has been labelled as a compound offering potential as a photochemotherapeutic agent. Experiments by Zhelyaskov *et al*⁸¹ have indeed indicated that a photolytic control can be implemented to regulate the NO concentrations released from GSNO (and SNAP).



1.3.3 Metal Ion Induced Decay

1.3.3.1 Copper Ion Catalysed Decomposition

Williams *et al*³⁰ have analysed the effect that metal ions⁸², in particular copper ions⁸³, have on the decomposition of RSNOs at physiological pH. In an analogous fashion to photolysis and thermolysis, the main products of this process are the disulfide and NO (equation 1.19).

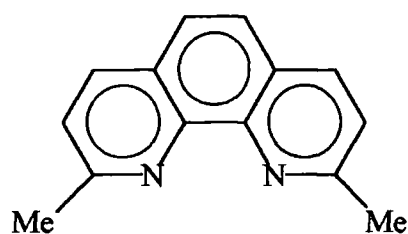


Nitric oxide has been detected using a NO-probe electrode system under anaerobic conditions, but in aerated phosphate buffer the oxidation/hydrolysis of NO to nitrite is quantitative (equation 1.20).



Adventitious levels of Cu^{2+} ions found naturally in aqueous solutions (typically $\sim 10^{-6}$ mol dm⁻³) are high enough to significantly affect the stability of RSNOs.

Cu^+ and not Cu^{2+} as first proposed, has now been identified as the catalytic reagent essential for RSNO decomposition⁸⁴. The addition of a Cu^+ chelator such as neocuproine (1.36) to the system has illustrated this fact, as the reaction can be progressively inhibited as [neocuproine] is increased and eventually stopped. UV-Visible spectrophotometric evidence has been obtained in the form of the spectrum of the Cu^+ /neocuproine adduct ($\lambda_{\text{max}} \sim 456\text{nm}$). An excess of the transition metal ion chelator, ethylene diamine tetraacetic acid (EDTA, 1.37), can also effectively halt the reaction, but it is non-specific and removes all copper ions. In either case only the thermal reaction is then evident, which in most cases is insignificant at room temperature.

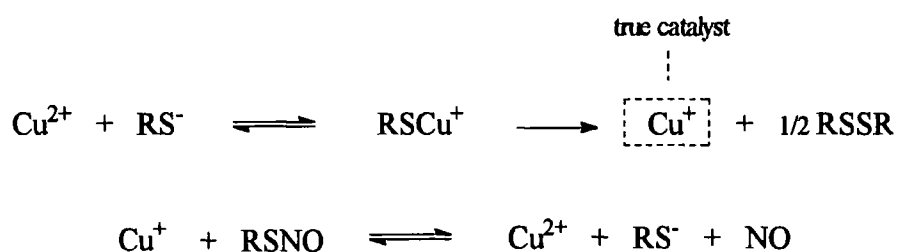


1.36



1.37

The mechanism describing RSNO decomposition revolves around a two step pathway and involves copper redox chemistry (scheme 1.15).



Scheme 1.15

The first step explains how Cu^+ is formed via the reduction of Cu^{2+} by thiolate ions (RS^-), sometimes creating a small induction period before reaction. Cu^+ is produced via an intermediate that is probably RSCu^+ . Thiyl radicals were not detected in EPR experiments, and radical traps did not influence the RSSR quantities obtained.

Trace amounts of thiolate ion present in solution can be accounted for by the reversibility of S-nitrosation (section 1.2.4.2), explained by partial hydrolysis of the RSNO. Adding RSH to a reaction mixture can reduce or even remove induction periods altogether, but at too high a concentration the Cu^{2+} is complexed out of solution⁸⁵. RSNO solutions are stabilised by using a large excess of HNO_2 in the *in situ* formation of S-nitrosothiols. This ensures that $[\text{RS}^-]$ levels are almost zero, as the nitrosation equilibrium (equation 1.18) is driven towards the products.

The second step describes the interaction of Cu^+ and RSNO to yield Cu^{2+} , NO and RS^- . Cu^{2+} is thus regenerated for use in the first step (hence the catalytic effect), and RS^- further oxidised to the disulfide.

Perhaps the most important discovery in relation to copper ion catalysis has been that the *in vitro* decomposition of S-nitrosothiols is possible using protein (e.g. human serum albumin), tripeptide (e.g. Gly-Gly-His) and amino acid bound Cu^{2+} sources⁸⁶. This could have major repercussions on NO generation within the body, even though the reaction is somewhat slower than that seen when free hydrated Cu^{2+} ions are used as the copper source.

The kinetics of decomposition of many S-nitrosothiols have been followed over a range of $[\text{Cu}^{2+}]$ ⁸³. The rate of copper promoted decay can be described by equation 1.21, which shows a first-order dependence on Cu^{2+} and RSNO.

$$\text{Rate} = k_2[\text{RSNO}][\text{Cu}^{2+}] + k'[\text{RSNO}] \quad \text{eqn 1.21}$$

Here;

$$\text{Rate} = k_{\text{obs}}[\text{RSNO}] \quad \text{eqn 1.22}$$

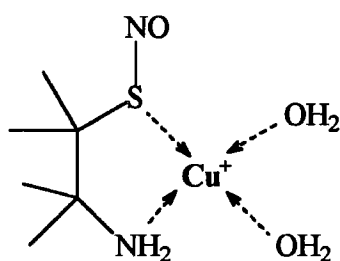
and;

$$k_{\text{obs}} = k_2[\text{Cu}^{2+}] + k' \quad \text{eqn 1.23}$$

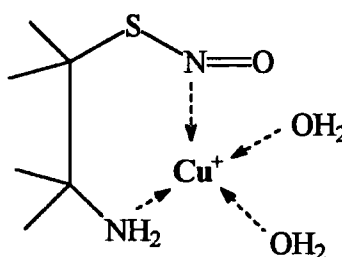
A plot of k_{obs} versus $[\text{Cu}^{2+}]$ produces a linear relationship with the gradient equal to the second order rate constant, k_2 . k' accounts for the portion of the rate due to spontaneous unimolecular decomposition of the RSNO (thermal reaction), and that caused by residual copper ions. It can be evident in a graph as a small positive intercept.

Zero-order kinetics were sometimes observed at particular $[\text{Cu}^{2+}]$ and $[\text{RS}^-]$ for the more reactive RSNOs. These were explained by an alteration in the rate-determining step, from the reaction of Cu^+ with RSNO to the generation of Cu^+ .

Structure-reactivity investigations revealed that the most reactive S-nitrosothiols (with higher k_2 values) could bidentately co-ordinate to Cu^+ as part of the decomposition procedure. Five- (1.38) or six-membered (1.39) ring structures were proposed as suitable representations of the intermediate created between the sulfur or the nitroso nitrogen atom, an electron donating substituent such as an amino group, and the complexed Cu^+ .



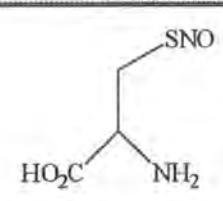
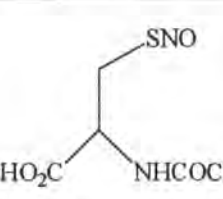
1.38



1.39

The k_2 values calculated for S-nitrosocysteine and S-nitroso-N-acetylcysteine (SNAC) are shown in table 1.1. It is clearly evident that N-acetylation of the amino group in SNAC (which results in delocalisation of the lone pair of electrons away from the nitrogen atom) greatly reduces its reactivity.

Table 1.1

S-Nitrosothiol	k_2 ($\text{mol}^{-1} \text{dm}^3 \text{s}^{-1}$)
 <p>S-nitrosocysteine</p>	24500
 <p>S-nitroso-N-acetylcysteine</p>	~ 0

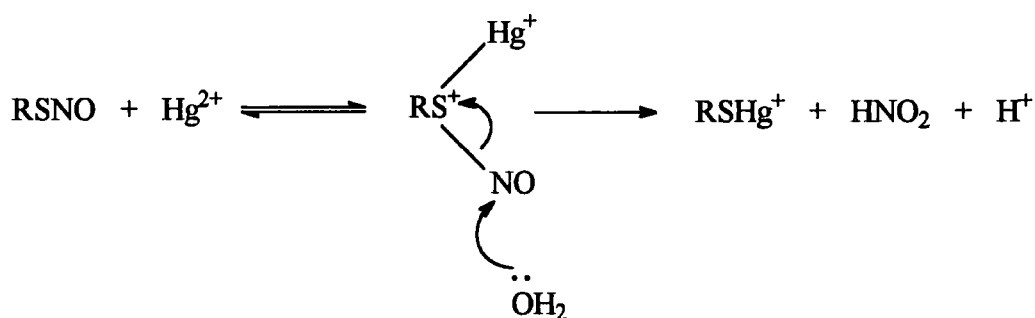
Articles published in the literature prior to 1993 do not take into account the copper catalysed decomposition of S-nitrosothiols. As $[\text{Cu}^{2+}]$ and $[\text{RS}^-]$ levels can vary considerably, the quantitative data reported in these documents in relation to RSNO work are not values that can be compared. Care must be taken that any direct reactions reported between RSNOs and other species, do not involve initial copper(I) catalysed release of NO, and its subsequent oxidation to a suitable nitrosating species, e.g. N_2O_3 .

1.3.3.2 Decomposition Induced by Mercury and Silver Salts

The mercuric ion (Hg^{2+}) promoted reduction of S-nitrosothiols to the corresponding thiol, is the basis of an established test for the mercapto group ($-\text{SH}$)⁸⁷. Swift and Williams⁸⁸ have examined the kinetic aspects of this procedure. The reaction was found to be first order in both S-nitrosothiol and Hg^{2+} (equation 1.24), and calculated second order decomposition rate constants exhibited little structural dependence.

$$\text{Rate} = k_2[\text{RSNO}][\text{Hg}^{2+}] \quad \text{eqn 1.24}$$

It was concluded that reactions initiated by Hg^{2+} proceed to completion on a much quicker time-scale than those catalysed by copper, e.g. S-nitroso-N-acetylcysteine, k_2 (Hg^{2+}) $\sim 3560 \text{ mol}^{-1} \text{ dm}^3 \text{ s}^{-1}$ and k_2 (Cu^+) $\sim 0 \text{ mol}^{-1} \text{ dm}^3 \text{ s}^{-1}$. Unlike the $\text{Cu}^{2+}/\text{Cu}^+$ system, reactions with Hg^{2+} have little biological significance and were stoichiometric as opposed to catalytic. Nitrous acid and the thiol (as the mercury complex) were identified as the products of the reaction, rather than nitric oxide and the disulfide as in copper-related RSNO degradation. The accepted reaction mechanism involves the rapid and reversible formation of a monodentate Hg-sulfur complex, which is then subject to attack by a water molecule at the nitrogen atom (scheme 1.16).



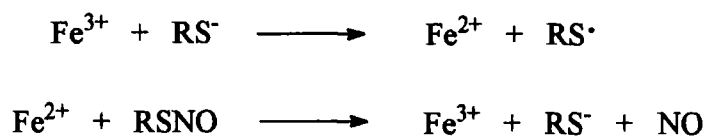
Scheme 1.16

Silver ions also have an affinity for sulfur sites, but co-ordinate less strongly than the mercuric ion. S-Nitrosothiol decomposition induced by Ag^+ is therefore slower in comparison to Hg^{2+} , but expected to proceed via an almost identical pathway. Difficulties were experienced in following the kinetics associated with this work due to the precipitation of the silver-thiol (RSAg) product.

1.3.3.3 Iron Ion Catalysed Decomposition

Ferrous ions (Fe^{2+}) are recognised as possible catalysts of S-nitrosothiol decomposition at neutral pH⁸². As the iron content within human cells and tissue exceeds that of any other metal (approximately two orders of magnitude greater than copper), any influence on RSNO stability and NO production is of paramount importance. Problems are created however, as apparently selective iron chelators such as *o*-phenanthroline also bind copper ions. It is therefore difficult to distinguish

between Fe^{2+} and $\text{Cu}^{2+}/\text{Cu}^+$ catalysis. Unless oxygen is rigorously excluded from the reaction vessel, Fe^{2+} is also easily oxidised to the redundant ferric iron (Fe^{3+}). Kinetic investigations can therefore offer inconsistent results⁸⁹. Vanin *et al*⁹⁰ are currently examining the concept of iron catalysed RSNO decomposition, and have forwarded complicated pathways to explain the action of Fe^{2+} . One of these routes is based upon the thiol-mediated formation, and sequential breakdown, of a dinitrosyl-iron complex (shown in equation 1.11) derived from two S-nitrosothiol molecules. Gorren *et al*⁹¹ have proposed a mechanism that is similar to the copper catalysed process, whereby Fe^{3+} is reduced to Fe^{2+} by RS^- (scheme 1.17).



Scheme 1.17

1.3.3.4 Decomposition Induced by Other Metal Ions

The stability of S-nitrosothiols in water at pH 7.4 was found to be unaffected by Ca^{2+} , Zn^{2+} , Mg^{2+} , Co^{2+} , Ni^{2+} , Mn^{2+} , Cr^{3+} , and Fe^{3+} ions⁸².

Results describing the influence of vanadium (III) ions on S-nitrosoglutathione decomposition are contained within the details of a biological assay specific to RSNO detection⁹² (equation 1.25). The reaction is interpreted as stoichiometric, and under anaerobic conditions is thought to proceed more readily at a neutral rather than acidic pH. V^{3+} ions were introduced into the reaction as the chloride salt and the nitrogen species present in GSNO accounted for by NO production. The inclusion of iron and copper ion chelators ensured that no component of decay was due to these metal contaminants, but the high temperatures (90°C) employed would have inevitably induced a large thermal reaction.

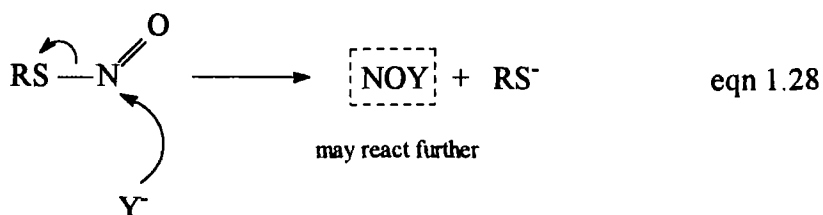


eqn 1.25

1.3.5 S-Nitrosothiols as a Source of NO⁺

1.3.5.1 Reactions with Nucleophiles

Alkyl nitrites (RONO)⁹⁴ and nitrosamines (e.g. RR'NNO)⁹⁵ are known to be susceptible to nucleophilic attack at the nitrogen atom of the nitroso group, resulting in the direct transfer of the -NO functionality between different molecules. Nitroso compounds can therefore serve as an effective source of NO⁺ (a species which to date has not been detected as the free entity in these reactions). In physiological terms one of the most relevant scenarios concerns the reactions involving S-nitrosothiols. It is understood that such processes concern a limited category of attacking nucleophiles (Y⁻), including thiols and to a lesser degree amines. Essentially RSNOs can act as electrophilic nitrosating agents, thus forming NOY which may be a stable species or decompose further. The other product is thiolate ion which may be oxidised to the disulfide (equation 1.28).



1.3.5.2 Reactions with Thiols (Transnitrosation)

Thiols can react with S-nitrosothiols in aqueous solution (particularly at pH > 8)⁹⁶. The reaction can be followed using stopped-flow techniques and proceeds so rapidly that the copper ion catalysed release of nitric oxide is not a factor. Although the reaction has been studied kinetically, it is not yet clear whether it involves only a one step or an addition-elimination process. In an analogous fashion to alkyl nitrite/thiol interactions⁹⁷, it is known that the mechanism involved incorporates an initial reversible reaction via the thiolate anion (R'S⁻) derived from the thiol⁹⁸ (equation 1.29).



A new S-nitrosothiol (R'SNO) and a mixture of symmetrical and unsymmetrical disulfides (RSSR, RSSR' and R'SSR') are the final products^{66,99}. The rate equation has been established as first order in both RSNO and R'S⁻ (equation 1.30).

$$\text{Rate} = k_2 [\text{RSNO}] [\text{R}'\text{S}^-] \quad \text{eqn 1.30}$$

Treatment of a RSNO such as S-nitrosoglutathione (which is relatively unreactive in terms of copper catalysed NO release) with a different thiol such as cysteine¹⁰⁰, can therefore produce S-nitrocysteine which is much more reactive and potentially a better nitric oxide donor *in vivo*. Meyer *et al*⁹⁸ have measured a k_2 value of $83 \text{ mol}^{-1} \text{ dm}^3 \text{ s}^{-1}$ for this GSNO/cysteine transnitrosation reaction at pH 7.4 and 37°C.

Structure-reactivity investigations using nitrosothiols and anions with bulky substituents such as *tert*-butyl or *gem*-dimethyl groups (figure 1.4), have clarified that steric rather than electronic limitations have a more profound effect in dictating reaction rates⁹⁶. Electron withdrawing groups situated on the carbon atoms adjacent to the -SNO moiety, are nevertheless recognised as factors likely to promote reaction.

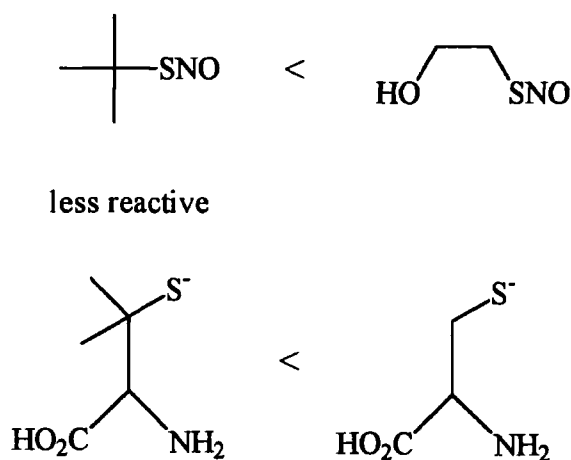


Figure 1.4

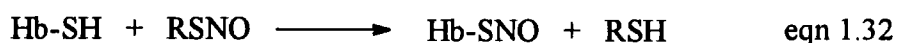
From a biological perspective, literature has been published describing how transnitrosation from simple nitrosothiols to the endogenous thiol ligands present in some proteins can be modelled¹⁰¹. As an example, S-nitrosocysteine is just one of a selection of RSNOs that have been utilised in experiments to nitrosate human serum albumin and bovine serum albumin (BSA)¹⁰² (equation 1.31). The latter contains a single Cys-34 thiol group.



eqn 1.31

The reverse exchange, namely the transfer of -NO from plasma protein bound nitrosothiol reservoirs to available low molecular weight thiol pools *in vivo*, has also been studied by Scharfstein *et al*¹⁰³.

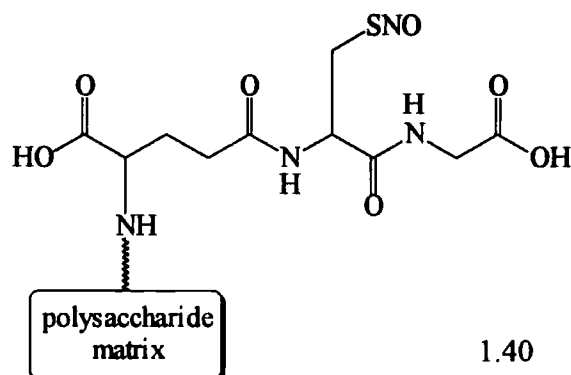
Similar transnitrosation reactions could account for the formation of S-nitrosohaemoglobin (Hb-SNO) within humans (equation 1.32). Hb-SNO ($3 - 30 \times 10^{-8}$ mol dm⁻³) has been detected in red blood cells¹⁰⁴.



This suggestion is feasible as haemoglobin is a tetramer, composed of two α - and two β -subunits. Each β -subunit contains highly reactive sulfhydryl residues (Cys β 93), which have been identified as capable of binding NO¹⁰⁵. Each subunit additionally contains one haem, and so the formation of haem-NO complexes is possible. These metal nitrosyls have been implicated in clinical conditions such as α -thalassaemia, which may itself lead to hypertension¹⁰⁵.

The enzyme creatine kinase¹⁰⁶, and the transcriptional activator OxyR¹⁰⁷ (which regulates gene expression), are two of the latest physiologically important -SH

containing species to be assigned as able to partake in transnitrosation reactions with RSNOs. Vice versa, S-nitroso-glutathionyl-sepharose 4B¹⁰⁸ (SNO-4B, 1.40) is one of the more recent nitrosothiols to be effectively incorporated with aliphatic thiols.



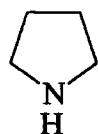
1.3.5.3 Reactions with Amines

Carcinogenic N-nitrosamines are potentially the products of treating nitrosothiols with secondary amines⁴³ (equation 1.33).

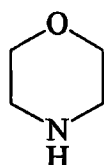


Nitrosamines are also understood to be highly toxic, mutagenic, and teratogenic¹⁰⁹. The possible formation of these compounds within the lower intestine region is therefore a serious health threat to humans, if one considers that secondary amines and amides are common in food, tobacco, and medicinal drugs. Surprisingly only a limited amount of research has been conducted upon this topic, and the exact mechanism and intermediates of the reaction have yet to be identified. Most RSNOs are too unreactive with amines to be studied conveniently, although there are a few exceptional examples^{66,110}.

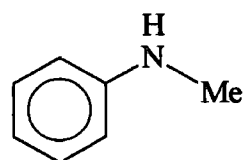
Dennis *et al*¹¹¹ have followed the interaction between S-nitrosocysteine and pyrrolidine (1.41), morpholine (1.42), and N-methylaniline (1.43), with reference to nitrosamine generation within cured meat.



1.41

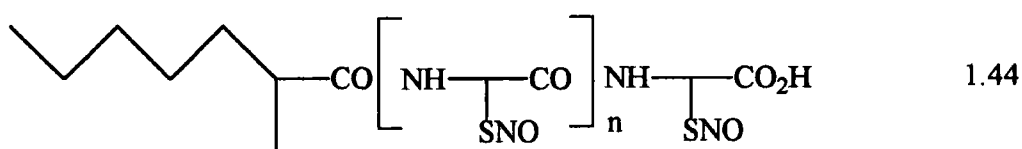


1.42



1.43

Results suggested that both strongly and weakly basic amines could react to form N-nitrosamines under acidic or alkaline conditions. The reaction rate appeared to decrease with amines of higher basicity, but the authors were unable to distinguish the kinetics or nature of the reaction pathway. A comparison with the nitrosation of the amines by nitrous acid was made and interestingly the RSNO characterised as a more effective nitrosating agent (if used at a slightly alkaline pH). In further tests a simulated macromolecular 'protein-bound nitrite' system (SPBN, 1.44) was utilised¹¹². It contained a carboxymethylated polysaccharide portion linked to a GSNO fragment, creating a mimic of the cysteine residues within meat. Transnitrosation to amines from this large molecule was found to be more sterically hindered than from S-nitrosocysteine.



1.44

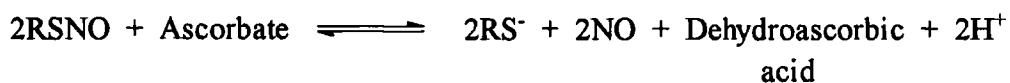
When evaluating these experiments one must appreciate that adventitious copper ions had not been removed from solution. To date no example has been illustrated whereby a nitrosothiol directly transfers its nitroso group to a secondary (or primary/tertiary) amine in the presence of a Cu^{2+} chelator, so eliminating intermediate NO production. Keshive *et al*¹¹³ have verified that in the absence of O_2 (which halts the oxidation of NO to the nitrosating agent N_2O_3), reactions in neutral buffer between morpholine and GSNO, SNAP, or SNAC, can be completely stopped.

1.3.5.4 Reactions with Ascorbate (Vitamin C)

At low concentrations (typically $< 1 \times 10^{-4}$ mol dm⁻³) ascorbate can act as a reducing agent⁸⁴. It can therefore adopt a parallel role to the thiolate anion in the generation of Cu⁺ from Cu²⁺ (scheme 1.15), and promote nitrosothiol decomposition in pH 7.4 buffer. Such copper catalysed reactions yield NO and disulfide.

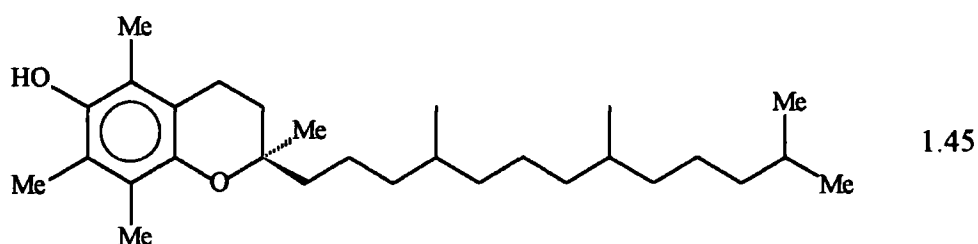
At higher concentrations however (typically $> 1 \times 10^{-3}$ mol dm⁻³), ascorbate can act as a nucleophile and is susceptible to electrophilic nitrosation by nitrosothiols¹¹⁴. The presence of EDTA or added Cu²⁺ in the system does not influence the reaction, and nitric oxide is again liberated. Thiol and not disulfide is detected as the main sulfur-containing product. Reactions performed with [ascorbate] \gg [RSNO] were found to show first order dependence on both reactants.

The pK_a values of ascorbic acid are 4.3 and 11.8, and so the reaction mechanism at pH 7.4 is thought to involve initial attack of the monoanion of ascorbic acid at the nitrogen atom of the -SNO moiety. This step mirrors that reported for the reactions of alkyl nitrites with ascorbate¹¹⁵. O-Nitrosation of the ascorbate ion and homolytic fission of O-N bonds to release NO and create dehydroascorbic acid, have been suggested as intermediate stages in the reaction (equation 1.34).



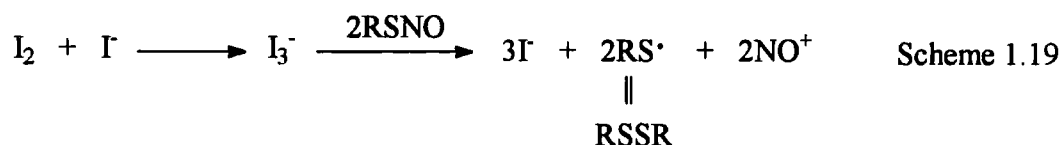
eqn 1.34

It has been claimed that α -Tocopherol¹¹⁶ (Vitamin E, 1.45) can perform a similar function to ascorbate in the formation of Cu⁺ from Cu²⁺. Perhaps this antioxidant can adopt the same 'dual role' in stimulating the breakdown of RSNOs.

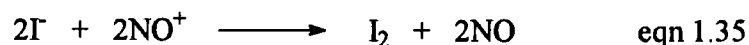


1.3.5.5 Reactions with Iodide/Iodine

Samouilov *et al*¹¹⁷ have developed a sensitive method of measuring S-nitrosothiol levels in blood plasma and biological buffer, incorporating treatment with an acidified solution (0.47 mol dm⁻³ HCl) of potassium iodide and dissolved free iodine. The I₃⁻ ion formed from these reagents can oxidise nitrosothiols, to produce thiyl radicals (hence the disulfide) and NO⁺ (scheme 1.19).



I⁻ can further reduce the nitrosonium ion, rapidly releasing NO and reforming I₂ (equation 1.35). A catalytic redox cycle is thus completed.

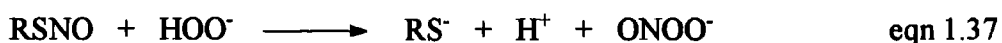


Copper ions were complexed out of solution in these assays using diethylenetriaminepentaacetic acid (DTPA). The addition of RSH retarded NO production, as iodine is destroyed by reducing agents such as thiols (equation 1.36). The reaction is therefore effectively quenched.



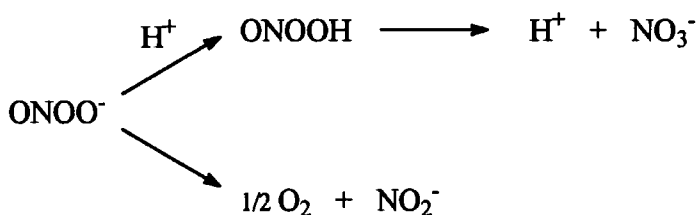
1.3.5.6 Reactions with Hydrogen Peroxide

Preliminary results have indicated that in the presence of EDTA, S-nitrosothiols slowly decompose if exposed to hydrogen peroxide in aqueous media¹¹⁸. The reaction appears to be quite general with regards to RSNO structure over the pH range 7 - 13, and peroxyxynitrite is ultimately formed (equation 1.37).



Kinetic experiments in which $[\text{H}_2\text{O}_2] \gg [\text{RSNO}]$ exhibited a good first order dependence on hydrogen peroxide and nitrosothiol. Observed pseudo-first order rate constants (k_{obs}) increased notably with pH, e.g. for the reaction of S-nitrosocysteine ($5 \times 10^{-3} \text{ mol dm}^{-3}$) with H_2O_2 ($5 \times 10^{-2} \text{ mol dm}^{-3}$) at 25°C , k_{obs} (pH 9.75) $\sim 8 \times 10^{-4} \text{ s}^{-1}$ and k_{obs} (pH 13.1) $\sim 5 \times 10^{-3} \text{ s}^{-1}$. The reaction mechanism is therefore thought to comprise rate-limiting nucleophilic attack of HOO^- (pK_a 11.5) at the nitroso group.

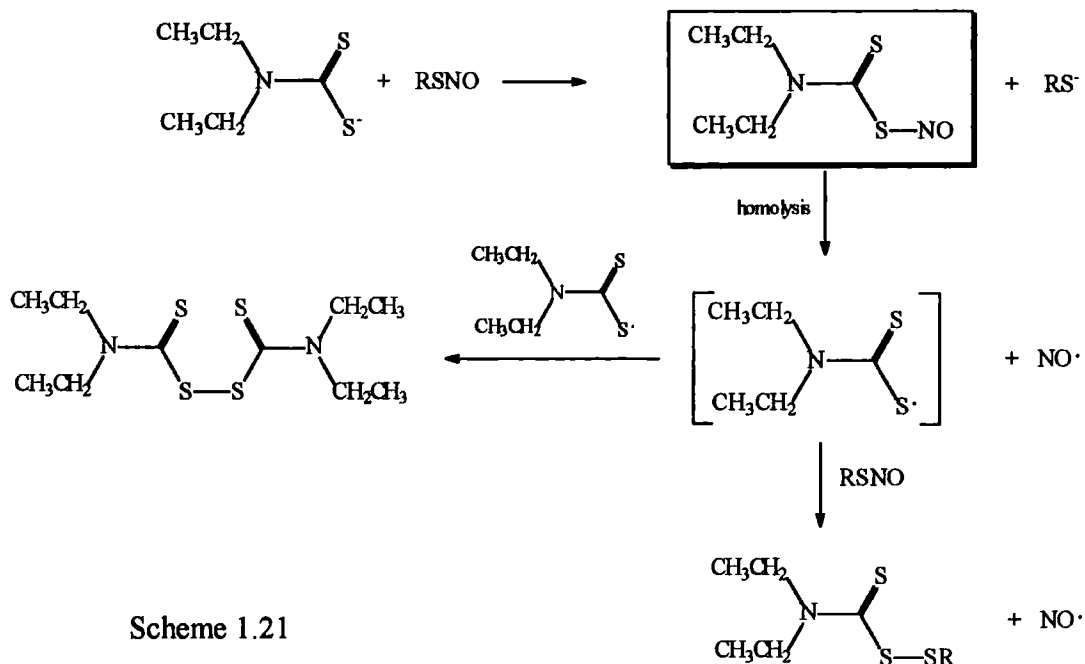
Peroxynitrite has been linked with cytotoxicity *in vivo* (section 1.1.4.3) and is of particular physiological interest. In solution it can decompose via peroxynitrous acid (pK_a 6.5) to give nitrate ion, or generate nitrite ion in alkaline conditions (scheme 1.20). Nevertheless, studies at very high pH (> 13) have characterised the peroxynitrite anion created from $\text{RSNO}/\text{H}_2\text{O}_2$ interactions as relatively stable.



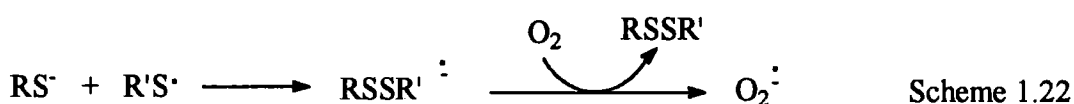
Scheme 1.20

1.3.5.7 Reactions with Diethyl Dithiocarbamate

Diethyl dithiocarbamate (DDC) possesses the ability to deactivate superoxide dismutase (SOD). SOD is an enzyme that catalyses the dismutation of superoxide to form H_2O_2 and O_2 . Millimolar quantities of DDC have been employed to regulate the production of O_2^- within human cells and tissue. Arnelle *et al*¹¹⁹ have ascertained that in the absence of Cu^{2+} ions, DDC will react with GSNO, SNAP and S-nitrosocysteine at pH 7.4, via a complicated radical chain mechanism (scheme 1.21).



The S-nitroso adduct of DDC is thought to be the crucial intermediate in this process. It is formed via rapid nitrosyl transfer (transnitrosation) from the $-SNO$ group, following attack by the nucleophilic sulfur centre in DDC (pK_a 4.7). Reaction conditions dictate the sequential pathway adopted. Homolytic cleavage for example can lead to the DDC thiyl radical, NO and symmetrical/mixed disulfides. Superoxide is also potentially created (scheme 1.22). The influence of DDC on O_2^- levels *in vivo* may therefore be due to interactions with RSNOs rather than only SOD inactivation.



1.3.5.8 Reactions with Phenolic Nucleophiles

As expected the reaction of phenol with SNAP in the pH range 2 - 9, generates 4-nitrosophenol when Cu^{2+} ions are not removed from solution¹²⁰. The direct reaction of a substituted phenolate ion (O-nucleophile) with a RSNO has not yet been studied. Analogous reactions with alkyl nitrites have been successfully performed in aqueous solution¹²¹, and perhaps this area is worthy of further study.

1.3.6 Decomposition Induced by Other Species

1.3.6.1 Reactions with Inorganic Complexes

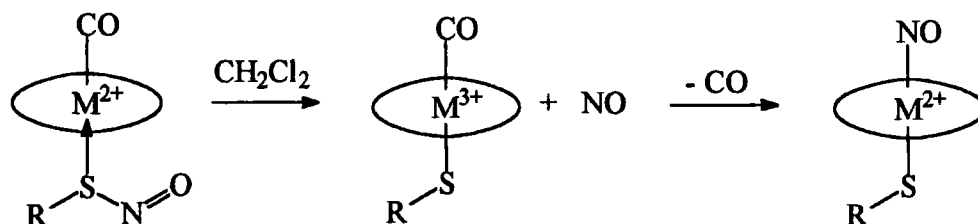
S-Nitrosothiols have been employed in the synthesis of metal nitrosyls for many years. *Trans*-addition of S-nitrosothiols to metalloporphyrin complexes derived from group 8 metals are a recent example¹²². These inorganic compounds contain structural features that are ideal models for the metal sites found *in vivo* in nitric oxide synthase (NOS), cytochrome P450, and the haem unit in guanylyl cyclase.

Reactions of this type have been successfully performed with both primary and tertiary nitrosothiols in dichloromethane, resulting in their decomposition. Strongly coloured five co-ordinate ($M = \text{Fe}$, equation 1.38) and six co-ordinate ($M = \text{Ru}$ or Os , equation 1.39) nitrosyl thiolate complexes are formed. These are stable crystalline solids at room temperature.



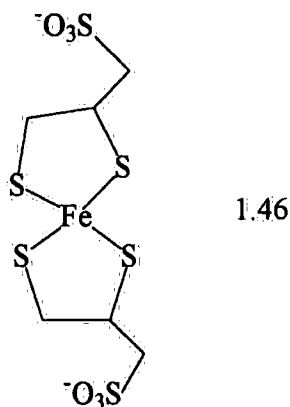
where; por = porphyrinato dianion

It is understood that the RSNO binds to the sixth co-ordination site of the metal via the sulfur (rather than nitrogen) atom in Ru and Os porphyrins. Homolysis of the S-N bond then results in substitution of CO by NO in the $(\text{por})\text{M}(\text{CO})(\text{SR})$ intermediate. This yields the nitrosyl product (scheme 1.23).



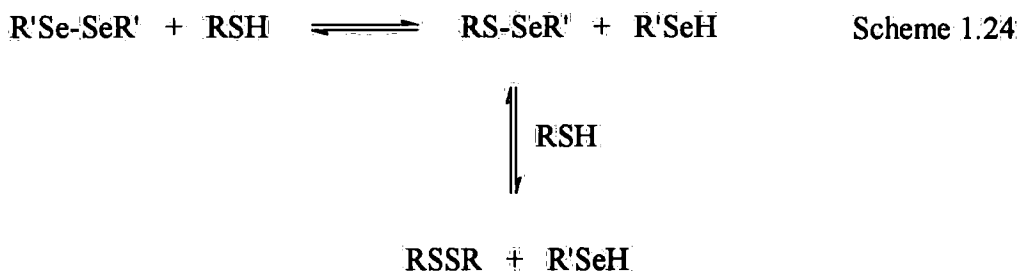
Scheme 1.23

Stopped-flow experiments in aqueous buffer (pH 7.4) have revealed that GSNO decomposition is rapidly induced by a novel iron-thiolate complex (1.46), itself generated *in situ*.¹²³ Tentative reaction mechanisms have been forwarded to account for these observations. They infer binding of the NO to the iron centre rather than the ligand sulfur atoms. Work is ongoing in this area.

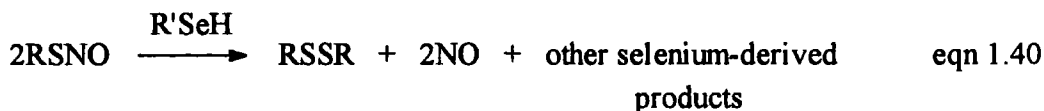


1.3.6.2 Reactions with Seleno Compounds and Glucose Peroxidase

Selenols (R'SeH) are the products of exchange reactions between diselenides and thiols (scheme 1.24). Transient selenosulfides (RS-SeR') have also been detected.



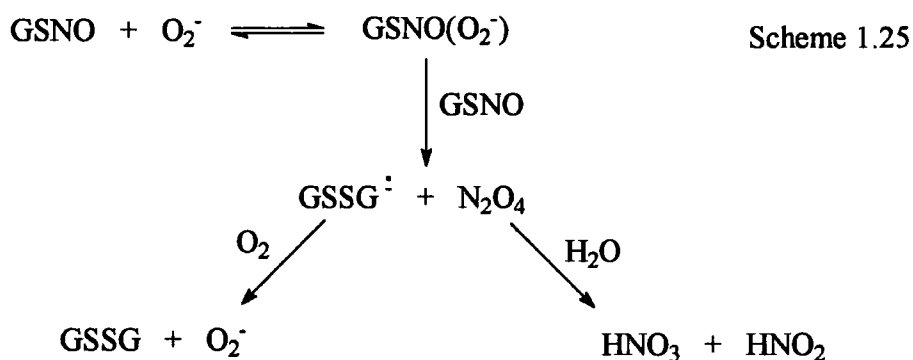
Selenols have been proposed as active intermediates that can stimulate the decomposition of S-nitrosothiols (e.g. GSNO) in EDTA treated, pH 7.4 phosphate buffer¹²⁴. Although mechanistic and kinetic details are as yet uncertain, disulfide and nitric oxide have been characterised within the products (equation 1.40).



Glutathione peroxidase (GSH-Px) is a selenium-based antioxidant enzyme that is capable of inducing S-nitrosogluthathione decomposition under the same conditions described for selenols¹²⁴. The metabolic effects of endogenous GSNO have actually been improved by the presence of GSH-Px, e.g. increased inhibition of platelet aggregation¹²⁵. This may simply be due to increased NO production (section 1.1.4.5).

1.3.6.3 Reactions with Superoxide

Superoxide (derived from xanthine/xanthine oxidase) is an oxygen metabolite that reacts with GSNO at pH 7.4 - 7.8 (trace metal ions chelated by DTPA). Jourdeuil *et al*¹²⁶ believe that this reaction can furnish GSSG, nitrite and nitrate, in a 1:1:1 stoichiometric ratio. Superoxide is catalytic in the mechanism devised to interpret results (scheme 1.25), and oxidising species such as dinitrogen tetroxide are perceived as intermediates.



Trujillo *et al*¹²⁷ favour the concept that GSH and NO are developed by O_2^- instigated reduction of GSNO (equation 1.41). Peroxynitrite generation is implied.



The kinetic details quoted by different authors are incompatible^{126,127,128}. RSNO degradation was however always proportional to $[O_2]$ and hindered by SOD.

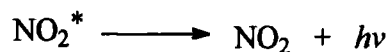
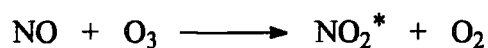
1.3.6.4 Enzymatic and Cell-Mediated Reactions

γ -Glutamyltransferase (γ -GTP)¹²⁹, thioredoxin¹³⁰, GSNO lyase¹³¹, and an unknown enzyme in *E. coli*¹⁰⁷, have all been linked in some manner to the cellular biotransformation of GSNO into NO. Due to the complex cell-mediated pathways involved, studies are still attempting to determine the exact relevance of these intracellular reactions.

1.3.7 Analytical Reactions

Sensitive and specific methods are commercially available to conveniently detect and measure S-nitrosothiols in biological systems.

Most reliable techniques have been developed around the principle of metal ion (Cu^{2+} or Hg^{2+}) catalysed¹³² or photolytic¹³³ RSNO decomposition, and subsequent accurate quantification of the NO released. For this purpose a vanadium (III) species has recently been used to reduce solution nitrite back to NO¹³⁴. Nitric oxide was then analysed by gas-phase chemiluminescence via its reaction with ozone (scheme 1.26).



Scheme 1.26

HPLC^{132,135}, electrochemical detection¹³⁶ (including the use of a Clark-type electrode¹³⁷), and colorimetric or fluorometric assays¹³⁸, are now all standard approaches in the determination of nitrosothiol quantities in solution.

References

- 1 E. Culotta and D.E. Koshland Jr, *Science*, 1992, **258**, 1862.
- 2 E.W. Ainscough and A.M. Brodie, *J. Chem. Ed.*, 1995, **72(8)**, 686.
- 3 R. Stevenson, *Chem. Br.*, 1998, **34** (11), 30.
- 4 J.S. Stamler, D.J. Singel and J. Loscalzo, *Science*, 1992, **258**, 1898.
- 5 K. Jones in *Comprehensive Inorganic Chemistry*, Vol. 2, Eds. J.C. Bailar, H.R. Emeleus, R. Nyholm and A.F. Trotman-Dickenson, Pergamon Press, New York, 1973, p.p. 329.
- 6 J.M. Beer, R.S. Benson, P. Gray, A.H. Lefebvre, E. Tyrrell and J.R.F. Hayes, *Combustion Generated Pollution*, Scientific Research Council, 1976.
- 7 R.F. Furchgott and J.V. Zawadzki, *Nature*, 1980, **288**, 373.
- 8 S. Moncada, R.M.J. Palmer and E.A. Higgs, *Pharmacol. Rev.*, 1991, **43**, 109.
- 9 R.F. Furchgott, *Mechanisms of Vasodilation (Vol. IV)*, Ed. P.M. Vanhoutte, Raven Press, 1987.
- 10 L.J. Ignarro, G.M. Buga, K.S. Wood, R.E. Byrns and G. Chaudhuri, *Proc. Natl. Acad. Sci., USA*, 1987, **84**, 9265.
- 11 R.M.J. Palmer, A.G. Ferrige and S. Moncada, *Nature*, 1987, **327**, 524.
- 12 M. Feelisch, M. te Poel, R. Zamora, A. Deussen and S. Moncada, *ibid.*, 1994, **368**, 62.
- 13 M.J. Palmer, D.S. Ashton and S. Moncada, *ibid.*, 1988, **333**, 664.
- 14 A.R. Butler and D.L.H. Williams, *Chem. Soc. Rev.*, 1993, 233.
- 15 P.L. Feldman, O.W. Griffith and D.J. Stuehr, *Chem. Eng. News.*, 1993, **20**, 26.
- 16 M.A. Marletta, P.S. Yoon, R. Iyengar, C.D. Leaf and J.S. Wishnok, *Biochemistry*, 1988, **27**, 8706.
- 17 D.S. Bredt and S.H. Snyder, *Proc. Natl. Acad. Sci., USA*, 1989, **86**, 9030.
- 18 M. Barinaga, *Science*, 1991, **254**, 1296.
- 19 R.M.J. Palmer, S. Moncada and M.W. Radomski, *Brit. J. Pharmacol.*, 1987, **92**, 181.
- 20 F.A. Cotton and G. Wilkinson, *Advanced Inorganic Chemistry*, 3rd ed., Interscience Publishers, New York, 1972.
- 21 D.A. Wink, J.F. Darbyshire, R.W. Nims, J.E. Saavedra and P.C. Ford, *Chem. Res. Toxicol.*, 1993, **6**, 23.
- 22 M. Feelisch and E. Noack, *Eur. J. Pharmacol.*, 1987, **139**, 19.

- 23 R. Bonn, U. Scharfenecker, H. Friehe and J. Gerloff, *Cardiovascular Drug Reviews*, 1998, **16**(3), 195.
- 24 T.M. Millar, C.R. Stevens, N. Benjamin, R. Eisenthal, R. Harrison and D.R. Blake, *FEBS Lett.*, 1998, **427**, 225.
- 25 A.R. Butler, A.M. Calsy-Harrison, C. Glidewell and P.E. Sørensen, *Polyhedron*, 1988, **7**, 1197.
- 26 F.W. Flitney, I.L. Megson, D.E. Flitney and A.R. Butler, *Brit. J. Pharmacol.*, 1992, **107**, 842.
- 27 M.A. Keese, M. Böse, A. Mülsch, R.H. Schirmer and K. Becker, *Biochem. Pharmacol.*, 1997, **54**, 1307.
- 28 W.R. Mathews and S.W. Kerr, *J. Pharmacol. Exp. Ther.*, 1993, **267**(3), 1529.
- 29 J. Loscalzo, D. Smick, N. Andon and J. Cooke, *ibid.*, 1989, **249**, 726.
- 30 D.L.H. Williams, *J. Chem. Soc., Chem. Commun.*, 1996, 1085.
- 31 W.A. Pryor, D.F. Church, C.K. Govindan and G. Crank, *J. Org. Chem.*, 1982, **47**, 156.
- 32 W. Chamulitrat, S.J. Jordan, R.P. Mason, K. Saito and R.G. Cutler, *J. Biol. Chem.*, 1993, **268**, 11520.
- 33 M. Feelisch, *J. Cardiovasc. Pharmacol.*, 1991, **17**(suppl. 3), 25.
- 34 R.J. Singh, N. Hogg, J. Joseph, E. Konorev and B. Kalyanaraman, *Arch. Biochem. Biophys.*, 1999, **361**(2), 331.
- 35 P. Holm, H. Kankaanranta, T. Metsä-Ketelä and E. Moilanen, *Eur. J. Pharmacol.*, 1998, **346**, 97.
- 36 J.A. Hrabie, J.R. Klose, D.A. Wink and L.K. Keefer, *J. Org. Chem.*, 1993, **58**, 1472.
- 37 K. Homer and J. Wanstall, *Eur. J. Pharmacol.*, 1998, **356**, 49.
- 38 J.M. Fukuto, G.C. Wallace, R. Hszieh and G. Chaudhuri, *Biochem. Pharmacol.*, 1992, **43**(3), 607.
- 39 G.J. Southan, A. Srinivasan, C. George, H.M. Fales and L.K. Keefer, *J. Chem. Soc., Chem. Commun.*, 1998, 1191.
- 40 N.B. Grigor'ev, V.I. Levina, S.A. Shevelev, I.L. Dalinger and V.G. Granik, *Mendeleev Commun.*, 1996, **1**, 11.
- 41 J.S. Stamler, O. Jaraki, J. Osborne, D.I. Simon, J. Keaney, J. Vita, D. Singel, C.R. Valeri and J. Loscalzo, *Proc. Natl. Acad. Sci., USA*, 1992, **89**, 7674.
- 42 P.R. Myers, R.L. Minor, R. Guerra, J.N. Bates and D.G. Harrison, *Nature*, 1990, **345**, 161.

- 43 S. Oae and K. Shinhama, *Org. Prep. Proc. Int.*, 1983, **15**(3), 165.
- 44 J.S. Stamler, D.I. Simon, J.A. Osborne, M.E. Mullins, O. Joraki, T. Michael, D.J. Singel and J. Loscalzo, *Proc. Natl. Acad. Sci., USA*, 1992, **89**, 444.
- 45 J. Barrett, D.F. Debenham and J. Glauser, *J. Chem. Soc., Chem. Commun.*, 1965, 248.
- 46 J. Mason, *J. Chem. Soc. (A)*, 1969, 1587.
- 47 B. Roy, A. du Moulinet d'Hardemare and M. Fontecave, *J. Org. Chem.*, 1994, **59**, 7019.
- 48 L. Field, R.V. Dilts, R. Ravichandran, P.G. Lenhert and G.E. Carnahan, *J. Chem. Soc., Chem. Commun.*, 1978, 249.
- 49 H.S. Tasker and H.O. Jones, *J. Chem. Soc.*, 1909, **95**, 1910, 1917.
- 50 H. Rheinboldt, *Ber.*, 1926, **59**, 1311.
- 51 G. Kresze and U. Uhlich, *Chem. Ber.*, 1959, **92**, 1048.
- 52 T.W. Hart, *Tet. Lett.*, 1985, **26**, 2013.
- 53 H.A. Moynihan and S.M. Roberts, *J. Chem. Soc., Perkin Trans. 1*, 1994, 797.
- 54 A.R. Butler, R.A. Field, I.R. Greig, F.W. Flitney, S.K. Bisland, F. Khan and J.J.F. Belch, *Nitric Oxide; Biology and Chemistry*, 1997, **1**(3), 211.
- 55 J. Ramirez, L. Yu, J. Li, P.G. Braunschweiger and P.G. Wang, *Bioorganic & Medicinal Chemistry Letters*, 1996, **6**(21), 2575.
- 56 A.R. Butler, H.H. Al-Sa'doni, I.L. Megson and F.W. Flitney, *Nitric Oxide; Biology and Chemistry*, 1998, **2**(3), 193.
- 57 L.L.H. de Fallois, J-L. Décout and M. Fontecave, *J. Chem. Soc., Perkin Trans. 1*, 1997, 2587.
- 58 C. Petit, P. Hoffmann, J-P. Souchard and S. Labidalle, *Phosphorus, Sulfur, and Silicon*, 1997, **129**, 59.
- 59 L. Jia and J.S. Stamler, *Eur. J. Pharmacol.*, 1999, **366**, 79.
- 60 J. Tummavuori and P. Lumme, *Acta Chem. Scand.*, 1968, **22**(6), 2003, P. Lumme, P. Lahermo and J. Tummavuori, *ibid.*, 1965, **19**(9), 2175, P. Lumme and J. Tummavuori, *ibid.*, 1965, **19**(3), 617.
- 61 K. Singer and P.A. Vamplew, *J. Chem. Soc.*, 1956, 3971.
- 62 Reference 5, p.p. 368.
- 63 M.P. Doyle, J.W. Terpstra, R.A. Pickering and D.M. LePoire, *J. Org. Chem.*, 1983, **48**, 3379.
- 64 S.M.N.Y.F. Oh and D.L.H. Williams, *J. Chem. Soc., Perkin Trans. 2*, 1989, 755.

- 65 L.J. Beckman, W.A. Fessler and M.A. Kise, *Chem. Rev.*, 1951, **48**, 319.
- 66 S. Oae, Y.H. Kim, D. Fukushima and K. Shinhama, *J. Chem. Soc., Perkin Trans. 1*, 1978, 913.
- 67 S. Goldstein and G. Czapski, *J. Am. Chem. Soc.*, 1996, **118**, 3419, V.G. Kharitonov, A.R. Sundquist and V.S. Sharma, *J. Biol. Chem.*, 1995, **270**(47), 28158.
- 68 A.J. Gow, D.G. Buerk and H. Ischiropoulos, *ibid.*, 1997, **272**(5), 2841.
- 69 D.L.H. Williams, *Nitric Oxide; Biology and Chemistry*, 1997, **1**(6), 522.
- 70 J.E. Graves, S.J. Lewis and N.W. Kooy, *Am. J. Physiol.*, 1998, **274**, H1001.
- 71 B. Mayer, A. Schrammel, P. Klatt, D. Koesling and K. Schmidt, *J. Biol. Chem.*, 1995, **270**, 17355, M.A. Moro, V.M. Darley-Usmar, D.A. Goodwin, N.G. Read, R. Zamora-Pino, M. Feelisch, M.W. Radomski and S. Moncada, *Proc. Natl. Acad. Sci., USA*, 1994, **91**, 6702.
- 72 A. van der Vliet, P.A. Chr. 't Hoen, P.S.-Y. Wong, A. Bast and C.E. Cross, *J. Biol. Chem.*, 1998, **273**(46), 30255.
- 73 M. Boese, P.I. Mordvintcev, A.F. Vanin, R. Busse and A. Mülsch, *ibid.*, 1995, **270**(49), 29244.
- 74 N. Iranpoor, H. Firouzabadi and M.A. Zolfigol, *Synth. Commun.*, 1998, **28**(2), 367.
- 75 D.L.H. Williams, *Nitrosation*, Cambridge University Press, 1988, Ch. 7.
- 76 S. Amado, A.P. Dicks and D.L.H. Williams, *J. Chem. Soc., Perkin Trans. 2*, 1998, 1869.
- 77 P.A. Morris and D.L.H. Williams, *ibid.*, 1988, 513.
- 78 P.H. Beloso and D.L.H. Williams, *J. Chem. Soc., Chem. Commun.*, 1997, 89.
- 79 D.J. Sexton, A. Muruganandam, D.J. McKenney and B. Mutus, *Photochem. Photobiol.*, 1994, **59**(4), 463.
- 80 P.D. Wood, B. Mutus and R.W. Redmond, *ibid.*, 1996, **64**(3), 518.
- 81 V.R. Zhelyaskov, K.R. Gee and D.W. Godwin, *ibid.*, 1998, **67**(3), 282.
- 82 D.L.H. Williams, *Methods in Enzymology*, 1996, **268**, 299, J. McAninly, D.L.H. Williams, S.C. Askew, A.R. Butler and C. Russell, *J. Chem. Soc., Chem. Commun.*, 1993, 1758.
- 83 S.C. Askew, D.J. Barnett, J. McAninly and D.L.H. Williams, *J. Chem. Soc., Perkin Trans. 2*, 1995, 741.
- 84 A.P. Dicks, H.R. Swift, D.L.H. Williams, A.R. Butler, H.H. Al-Sa'doni and B.G. Cox, *ibid.*, 1996, 481.

- 85 A.P. Dicks, P.H. Beloso and D.L.H. Williams, *ibid.*, 1997, 1429.
- 86 D. Jourdeuil, F.S. Laroux, A.M. Miles, D.A. Wink and M.B. Grisham, *Arch. Biochem. Biophys.*, 1999, **361**(2), 323, A.P. Dicks and D.L.H. Williams, *Chemistry & Biology*, 1996, **3**, 655.
- 87 B. Saville, *Analyst*, 1958, **83**, 670.
- 88 H.R. Swift and D.L.H. Williams, *J. Chem. Soc., Perkin Trans. 2*, 1997, 1933.
- 89 H.R. Swift, Ph.D. Thesis, University of Durham, 1996.
- 90 A.F. Vanin, *Biochemistry (Moscow)*, 1998, **63**(7), 782, A.F. Vanin, I.V. Malenkova and V.A. Serezhenkov, *Nitric Oxide; Biology and Chemistry*, 1997, **1**(3), 191, A.F. Vanin, *Biochemistry (Moscow)*, 1995, **60**(4), 441.
- 91 A.C.F. Gorren, A. Schrammel, K. Schmidt and B. Mayer, *Arch. Biochem. Biophys.*, 1996, **330**(2), 219.
- 92 K. Fang, N.V. Ragsdale, R.M. Carey, T. MacDonald and B. Gaston, *Biochem. Biophys. Res. Commun.*, 1998, **252**, 535.
- 93 S.S. Al-Kaabi, D.L.H. Williams, R. Bonnett and S.L. Ooi, *J. Chem. Soc., Perkin Trans. 2*, 1982, 227.
- 94 S. Oae, N. Asai and K. Fujimori, *ibid.*, 1978, 1124.
- 95 C.L. Bumgardner, K.S. McCallum and J.P. Freeman, *J. Am. Chem. Soc.*, 1961, **83**, 4417.
- 96 D.J. Barnett, A. Ríos and D.L.H. Williams, *J. Chem. Soc., Perkin Trans. 2*, 1995, 1279, D.J. Barnett, J. McAninly and D.L.H. Williams, *ibid.*, 1994, 1131.
- 97 H.M. Patel and D.L.H. Williams, *ibid.*, 1990, 37.
- 98 D.J. Meyer, H. Kramer, N. Özer, B. Coles and B. Ketterer, *FEBS Lett.*, 1994, **345**, 177.
- 99 D.R. Arnelle and J.S. Stamler, *Arch. Biochem. Biophys.*, 1995, **318**(2), 279, J.W. Park, *Biochem. Biophys. Res. Commun.*, 1988, **152**, 916.
- 100 S.C. Askew, A.R. Butler, F.W. Flitney, G.D. Kemp and I.L. Megson, *Bioorganic & Medicinal Chemistry*, 1995, **3**(1), 1.
- 101 Y. Ji, T.P.M. Akerboom, H. Sies and J.A. Thomas, *Arch. Biochem. Biophys.*, 1999, **362**(1), 67, M. Tannous, N. Labbe, R.W. Redmond and B. Mutus, *J. Photochem. Photobiol.*, 1997, **41**, 249, S. Mohr, J.S. Stamler and B. Brüne, *FEBS Lett.*, 1994, **348**, 223.
- 102 M.S. Studebaker, H. Zhang and G.E. Means, *Anal. Biochem.*, 1996, **237**, 193, H. Zhang and G.E. Means, *ibid.*, 1996, **237**, 141.

- 103 J.S. Scharfstein, J.F. Keaney Jr, A. Slivka, G.N. Welch, J.A. Vita, J.S. Stamler and J. Loscalzo, *J. Clin. Invest.*, 1994, **94**, 1432.
- 104 L. Jia, C. Bonaventura, J. Bonaventura and J.S. Stamler, *Nature*, 1996, **380**, 221.
- 105 P.L. Reddy, L.J. Bowie and S. Callistein, *Clinical Chemistry*, 1997, **43(8)**, 1442.
- 106 M.A. Arstall, C. Bailey, W.L. Gross, M. Bak, J-L. Balligand and R.A. Kelly, *J. Mol. Cell Cardiol.*, 1998, **30**, 979.
- 107 A. Hausladen, C.T. Privalle, T. Keng, J. DeAngelo and J.S. Stamler, *Cell*, 1996, **86**, 719.
- 108 Z. Liu, M.A. Rudd, J.E. Freedman and J. Loscalzo, *J. Pharm. Exp. Ther.*, 1998, **284(2)**, 526.
- 109 Reference 75, Ch. 5.
- 110 S. Oae, D. Fukushima and Y.H. Kim, *J. Chem. Soc., Chem. Commun.*, 1977, 407.
- 111 M.J. Dennis, R. Davies and D.J. McWeeny, *J. Sci. Food Agric.*, 1979, **30**, 639.
- 112 M.J. Dennis, R.C. Massey and D.J. McWeeny, *ibid.*, 1980, **31**, 1195.
- 113 M. Keshive, S. Singh, J.S. Wishnok, S.R. Tannenbaum and W.M. Deen, *Chem. Res. Toxicol.*, 1996, **9**, 988.
- 114 A.J. Holmes and D.L.H. Williams, *J. Chem. Soc., Chem. Commun.*, 1998, 1171.
- 115 J.R. Leis and A. Ríos, *ibid.*, 1995, 169.
- 116 J.G. De Man, B.Y. De Winter, T.G. Moreels, A.G. Herman and P.A. Pelckmans, *Br. J. Pharmacol.*, 1998, **123**, 1039.
- 117 A. Samouilov and J.L. Zweier, *Anal. Biochem.*, 1998, **258**, 322.
- 118 P.J. Coupe and D.L.H. Williams, *J. Chem. Soc, Perkin Trans. 2*, 1999, 1057.
- 119 D.R. Arnelle, B.J. Day and J.S. Stamler, *Nitric Oxide; Biology & Chemistry*, 1997, **1(1)**, 56.
- 120 S.M.N.Y.F. Oh and D.L.H. Williams, *J. Chem. Soc., Perkin Trans. 2*, 1991, 685.
- 121 J.R. Leis, A. Ríos and L. Rodríguez-Sánchez, *ibid.*, 1998, 2729.
- 122 L. Chen, M.A. Khan and G.B. Richter-Addo, *Inorg. Chem.*, 1998, **37**, 533, G-B. Yi, M.A. Khan, D.R. Powell and G.B. Richter-Addo, *ibid.*, 1998, **37**, 208, G-B. Yi, L. Chen, M.A. Khan and G.B. Richter-Addo, *ibid.*, 1997, **36**, 3876.
- 123 A.R. Butler, unpublished results.

- 124 Y. Hou, Z. Guo, J. Li and P.G. Wang, *Biochem. Biophys. Res. Commun.*, 1996, **228**, 88.
- 125 J.E. Freedman, B. Frei, G.N. Welch and J. Loscalzo, *J. Clin. Invest.*, 1995, **96**, 394.
- 126 D. Jourdeuil, C.T. Mai, F.S. Laroux, D.A. Wink and M.B. Grisham, *Biochem. Biophys. Res. Commun.*, 1998, **244**, 525.
- 127 M. Trujillo, M.N. Alvarez, G. Peluffo, B.A. Freeman and R. Radi, *J. Biol. Chem.*, 1998, **273**(14), 7828.
- 128 S. Aleryani, E. Milo, Y. Rose and P. Kostka, *ibid.*, 1998, **273**(11), 6041.
- 129 M. Kashiba, E. Kasahara, K.C. Chien and M. Inoue, *Arch. Biochem. Biophys.*, 1999, **363**(2), 213.
- 130 D. Nikitovic and A. Holmgren, *J. Biol. Chem.*, 1996, **271**(32), 19180.
- 131 M.P. Gorge, P. Addis, A.A. Noronha-Dutra and J.S. Hothersall, *Biochem. Pharmacol.*, 1998, **55**, 657.
- 132 T. Akaike, K. Inoue, T. Okamoto, H. Nishino, M. Otagiri, S. Fujii and H. Maeda, *J. Biochem.*, 1997, **122**, 459.
- 133 C. Alpert, N. Ramdev, D. George and J. Loscalzo, *Anal. Biochem.*, 1997, **245**, 1.
- 134 J.F. Ewing and D.R. Janero, *Free Radical Biology & Medicine*, 1998, **25**(4/5), 621.
- 135 R.K. Goldman, A.A. Vlessis and D.D. Trunkey, *Anal. Biochem.*, 1998, **259**, 98.
- 136 D.V. Vukomanovic, A. Hussain, D.E. Zoutman, G.S. Marks, J.F. Brien and K. Nakatsu, *J. Pharm. Toxicol. Meth.*, 1998, **39**, 235, Y. Hou, J. Wang, F. Arias, L. Echegoyen and P.G. Wang, *Bioorganic & Medicinal Chemistry Letters*, 1998, **8**, 3065.
- 137 S. Pfeiffer, A. Schrammel, K. Schmidt and B. Mayer, *Anal. Biochem.*, 1998, **258**, 68.
- 138 J.A. Cook, S.Y. Kim, D. Teague, M.C. Krishna, R. Pacelli, J.B. Mitchell, Y. Vodovotz, R.W. Nims, D. Christodoulou, A.M. Miles, M.B. Grisham and D.A. Wink, *ibid.*, 1996, **238**, 150.

Chapter 2

The Reaction of S-Nitrosothiols with Thiols at High Thiol Concentration

Chapter 2 : The Reaction of S-Nitrosothiols with Thiols at High Thiol Concentration

2.1 Introduction

The role that thiols (RSH) play in S-nitrosothiol decomposition is a topic that has received little attention in the published literature. Of the investigations conducted within this area, each has afforded rather inconsistent results. On the one hand Oae *et al*¹ and Kowaluk *et al*² have independently stated that N-acetylpenicillamine (NAP) promotes the decomposition of GSNO and SNAP to yield NO. Alternatively, Feelisch *et al*³ have inferred that cysteine prolongs the lifetime of S-nitrosocysteine in a concentration dependent fashion. These discrepancies can however be reconciled in terms of the mechanism involved in copper catalysed RSNO decomposition. Increasing the thiol concentration can initially advance nitrosothiol decay by increasing the rate of Cu^{2+} reduction to Cu^+ , but then retard reaction due to metal-ion chelation by the thiol⁴ (section 1.3.3.1).

A recent report by Komiyama and Fujimori⁵ has highlighted that a different, copper independent reaction can occur when S-nitrosocysteine is reacted with L-cysteine, at high L-cysteine concentration (> 10 fold excess). This discovery verifies preliminary findings by Singh *et al*⁶ and those made within this laboratory. Swift⁷ originally noted a similar trend during the reaction of GSNO and SNAC with their corresponding thiols. The fact that *thiol induced decomposition of S-nitrosothiols* has not previously received more interest is surprising, if one considers that the thiol concentration in living mammalian cells *in vivo* is relatively high (~ 0.5 - 10 mmol dm^{-3})⁸. Here the tripeptide glutathione (GSH) is the predominant thiol⁹, but several other amino acids and proteins also exhibit free -SH groups. The relative intracellular S-nitrosothiol content is believed to be much lower (~ 1 - 10 $\mu\text{mol dm}^{-3}$)¹⁰, so leaving an excess of thiol approaching several hundred fold.

Thiols may therefore exhibit the potential to influence RSNO breakdown to NO, and possibly regulate the biological action of nitrosothiols within the body. The aim of this chapter of work was to first clarify the generality and kinetics of the reaction of high concentrations of thiols with S-nitrosothiols, and secondly set about identifying the products and verifying the mechanism of reaction.

2.2 Thiol Induced S-Nitrosothiol Decomposition

2.2.1 Kinetic Studies

All S-nitrosothiols were generated in solution via the nitrosation of RSH using an equimolar amount of acidic sodium nitrite, and then immediately used in experiments. The RSNO concentration was taken to be the concentration of thiol and sodium nitrite used. S-Nitrosothiol decomposition in pH 7.4 phosphate buffer at 25°C was recorded spectrophotometrically by monitoring the disappearance of the absorbance peak at 340nm as a function of time. Unless stated otherwise, EDTA (usually $1 \times 10^{-4} \text{ mol dm}^{-3}$) was added before reaction to prevent any component of RSNO decomposition catalysed by Cu^+ ions.

In each case excellent first order plots were obtained for the individual kinetic runs performed at $[\text{RSH}] \gg [\text{RSNO}]$. The pH (7.4) of the reaction solution was kept constant using diluted NaOH, as $[\text{RSH}]$ typically ranged from 10 - 100 fold excess. The rate equation was established for the reaction of S-nitrosocysteine with L-cysteine as⁵ -

$$\text{Rate} = k'[\text{RSNO}] + k_2[\text{RSNO}][\text{RSH}] \quad \text{eqn 2.1}$$

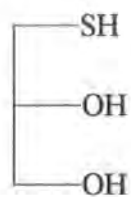
In conditions where $[\text{RSH}] \gg [\text{RSNO}]$, $[\text{RSH}]$ can be assumed as constant -

$$\text{Rate} = k_{\text{obs}}[\text{RSNO}] \quad \text{eqn 2.2}$$

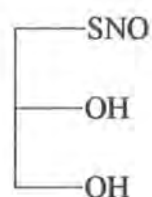
Therefore,

$$k_{\text{obs}} = k' + k_2[\text{RSH}] \quad \text{eqn 2.3}$$

Plotting the pseudo-first order rate constant (k_{obs}) against $[\text{RSH}]$ should produce a straight line, with the slope indicative of the second order rate constant, k_2 . Such a graph representing the 1-thioglycerol (2.1) induced decay of S-nitroso-1-thioglycerol (2.2) is demonstrated in figure 2.1 (data summarised in table 2.1). A small positive intercept is quite common at $[\text{RSH}] = 0 \text{ mol dm}^{-3}$. This corresponds to the thermal reaction (k'). In the case of 2.2 however it appears to be too slow to measure.



2.1



2.2

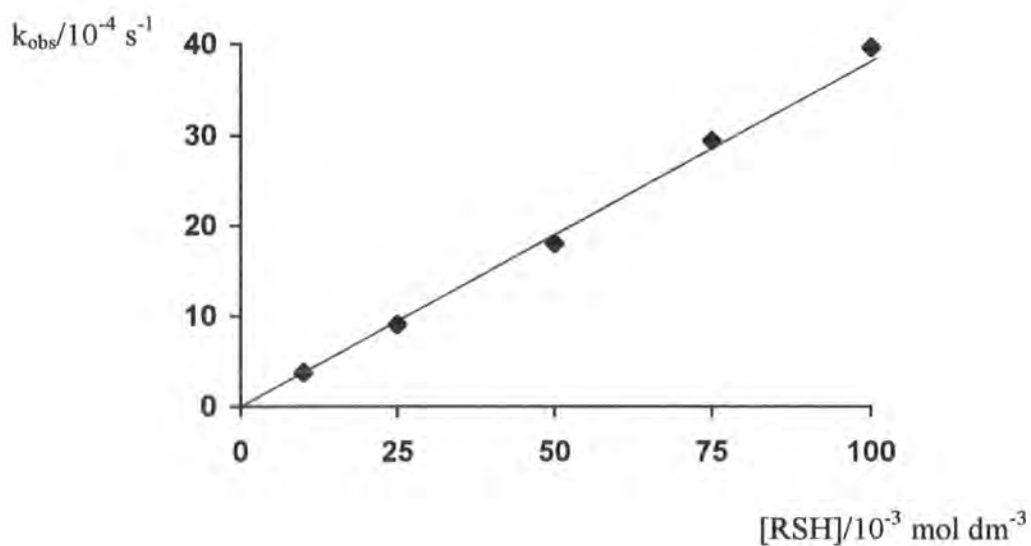
Table 2.1

Kinetic data for the 1-thioglycerol induced decomposition of S-nitroso-1-thioglycerol ($1 \times 10^{-3} \text{ mol dm}^{-3}$) in pH 7.4 buffer, with $[\text{EDTA}] = 1 \times 10^{-4} \text{ mol dm}^{-3}$

$[\text{RSH}]/10^{-3} \text{ mol dm}^{-3}$	$k_{\text{obs}}/10^{-4} \text{ s}^{-1}$
10	3.76 ± 0.03
25	9.08 ± 0.01
50	18.0 ± 0.1
75	29.5 ± 0.2
100	39.7 ± 0.2

Figure 2.1

Plot of k_{obs} against $[\text{RSH}]$ for the thiol induced decay of S-nitroso-1-thioglycerol



An experiment was performed in which the quantity of EDTA added prior to reaction was systematically varied for kinetic runs at fixed [RSNO], [RSH] and added [Cu²⁺]. Calculated rate constants for the L-cysteine promoted decay of S-nitrosocysteine are shown in table 2.2.

Table 2.2

Kinetic data for the reaction of L-cysteine ($2.5 \times 10^{-2} \text{ mol dm}^{-3}$) and S-nitrosocysteine ($1 \times 10^{-3} \text{ mol dm}^{-3}$) in pH 7.4 buffer, with added Cu²⁺ ($1 \times 10^{-5} \text{ mol dm}^{-3}$) and varying [EDTA]

[EDTA]/ $10^{-5} \text{ mol dm}^{-3}$	$k_{\text{obs}}/10^{-4} \text{ s}^{-1}$
0	2.63 ± 0.04
5	2.69 ± 0.08
10	2.68 ± 0.11
25	2.62 ± 0.09
50	2.57 ± 0.05

It can be deduced from the negligible change in k_{obs} that the rate of decomposition of S-nitrosocysteine via this pathway is unchanged upon EDTA introduction. Added Cu²⁺ (with no added EDTA) also has no effect. In either instance it can be concluded that the reaction taking place is inherently different to the Cu⁺ catalysed process, and thiol is present in sufficient quantity to efficiently complex copper out of solution.

2.2.2 Reactions of S-Nitrosothiols with the Parent Thiol

To test the generality of the reaction of S-nitrosothiols with a large excess of the parent thiol (the RSNO/RSH system), a wider spectrum of nitrosothiols was examined. One could then establish if any significant structure/reactivity relationship was evident. The results obtained with regards to the S-nitrosocysteine/L-cysteine reaction are shown as an example in table 2.3. Table 2.4 contains a summary of the RSH structures investigated and the calculated values of k_2 .

Table 2.3

Kinetic data for the L-cysteine induced decomposition of S-nitrosocysteine ($1 \times 10^{-3} \text{ mol dm}^{-3}$) in pH 7.4 buffer, with $[\text{EDTA}] = 1 \times 10^{-4} \text{ mol dm}^{-3}$

$[\text{RSH}]/10^{-3} \text{ mol dm}^{-3}$	$k_{\text{obs}}/10^{-4} \text{ s}^{-1}$
10	3.76 ± 0.03
25	9.08 ± 0.01
50	18.0 ± 0.1
75	29.5 ± 0.2
100	39.7 ± 0.2

Calculated value of $k_2^a = (1.09 \pm 0.01) \times 10^{-2} \text{ mol}^{-1} \text{ dm}^3 \text{ s}^{-1}$

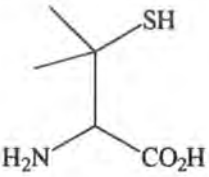
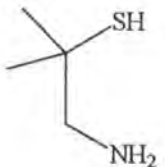
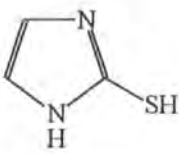
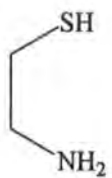
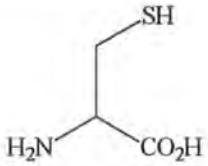
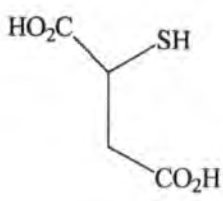
(a. Komiyama and Fujimori⁵ calculated a value of $1.11 \times 10^{-2} \text{ mol}^{-1} \text{ dm}^3 \text{ s}^{-1}$ at 37°C)

It is immediately apparent from table 2.4 that the two tertiary thiol systems studied (penicillamine and 1-amino-2-methyl-2-propanethiol) are considerably more reactive than the analogous primary compounds (L-cysteine and cysteamine). On the whole the thiol induced reaction is very slow compared to the copper(I) catalysed process (table 2.5). Nitrosothiols containing two methyl substituents attached to the carbon atom adjacent to the S-nitroso functionality, are known to exhibit an enhanced rate of reaction in copper mediated RSNO decomposition (table 2.5). This is commonly referred to as the 'gem-dimethyl effect' and is attributed to the electron donating ability of the methyl groups¹¹. Perhaps therefore, the resulting increased electron density upon the sulfur atom of the RSH, may be of importance when considering the make-up of the thiol based reaction mechanism.

It would appear from the enhanced reactivity of 2-mercaptoimidazole, that delocalisation of a lone pair of electrons on one of the nitrogen atoms next to the α -carbon atom, has an inductive effect comparable to that of methyl groups. At the other extreme, the electron withdrawing ability of the carboxylic acid groups present in mercaptosuccinic acid substantially reduce its reactivity.

Table 2.4

Values of k_2 for the reaction of S-nitrosothiols ($1 \times 10^{-3} \text{ mol dm}^{-3}$) and their respective thiols (RSH) in pH 7.4 buffer, with $[\text{EDTA}] = 1 \times 10^{-4} \text{ mol dm}^{-3}$

RSH	Structure	k_2 $/10^{-4} \text{ mol}^{-1} \text{ dm}^3 \text{ s}^{-1}$
Penicillamine		2590 ± 30
1-Amino-2-methyl-2-propanethiol		1639 ± 82
2-Mercaptoimidazole (measured in distilled water)		1152 ± 17
Cysteamine		119 ± 1^a
L-Cysteine		109 ± 1
Mercaptosuccinic acid		6.0 ± 0.5

a. Value obtained by A.P. Dicks, Ph.D. Thesis, University of Durham, 1997.

Table 2.5

Comparison of k_2 values for the copper(I) catalysed and thiol induced decomposition of S-nitrosopenicillamine and S-nitrosocysteine in pH 7.4 buffer at 25°C

S-Nitrosothiol	Cu ⁺ Reaction ^a k_2 /mol ⁻¹ dm ³ s ⁻¹	Thiol Reaction ^b k_2 /10 ⁻⁵ mol ⁻¹ dm ³ s ⁻¹
S-Nitrosopenicillamine (<i>tertiary RSNO</i>)	67000 ^c	25900
S-Nitrosocysteine (<i>primary RSNO</i>)	24500 ^c	1090

a. k_2 in rate = $k_2[\text{RSNO}][\text{Cu}^{2+}]$, b. k_2 in rate = $k_2[\text{RSNO}][\text{RSH}]$,

c. Values obtained by D.J. Barnett, Ph.D. Thesis, University of Durham, 1994.

Within the range of primary species analysed (table 2.6), k_2 values were of a similar size with no obvious trend. The decreased reactivity of glutathione may be related to steric effects, due to the larger size of this molecule.

Table 2.6

Values of k_2 for the reaction of primary S-nitrosothiols (1×10^{-3} mol dm⁻³) and their respective thiols (RSH) in pH 7.4 buffer, with [EDTA] = 1×10^{-4} mol dm⁻³

RSH	k_2 /10 ⁻⁴ mol ⁻¹ dm ³ s ⁻¹
1-Thioglycerol	389 ± 7
2-Mercaptoethane sulfonic acid	306 ± 2
Captopril	273 ± 12 ^a
N-Acetylcysteine	93 ± 3 ^a
Glutathione	48 ± 2

a. Values obtained by A.P. Dicks, Ph.D. Thesis, University of Durham, 1997.

Dithiols that contain closely located or vicinal -SH groups are regarded as more suitable models of the free thiol sites available within proteins¹². It was therefore of interest to study the dithiol promoted decomposition of the S,S-dinitroso derivatives of such precursors (table 2.7). For this purpose S,S-dinitrosodithiothreitol ($\epsilon_{\text{calc}} \sim 1594 \text{ mol}^{-1} \text{ dm}^3 \text{ cm}^{-1}$ at 333nm) and S,S-dinitrosodithioerythritol were synthesised in solution using a 2:1 excess of sodium nitrite to dithiol, to ensure complete nitrosation of both sulfur atoms.

Table 2.7

Values of k_2 and k' for the reaction of S,S-dinitrosodithiols ($5 \times 10^{-4} \text{ mol dm}^{-3}$) and their respective dithiols in pH 7.4 buffer, with $[\text{EDTA}] = 1 \times 10^{-4} \text{ mol dm}^{-3}$

Dithiol	Structure	k_2 / $10^{-4} \text{ mol}^{-1} \text{ dm}^3 \text{ s}^{-1}$	k' / 10^{-4} s^{-1}
Dithiothreitol (DTT)	<p style="text-align: center;"><i>threo</i></p>	2728 ± 68^a	10.5 ± 1.0
Dithioerythritol (DTE)	<p style="text-align: center;"><i>erythro</i></p>	1345 ± 26^b	7.6 ± 0.5

a. Le *et al*¹² have since obtained a value of $7.8 \times 10^{-1} \text{ mol}^{-1} \text{ dm}^3 \text{ s}^{-1}$ at 37°C.

b. Le *et al*¹² have since obtained a value of $4.2 \times 10^{-1} \text{ mol}^{-1} \text{ dm}^3 \text{ s}^{-1}$ at 37°C.

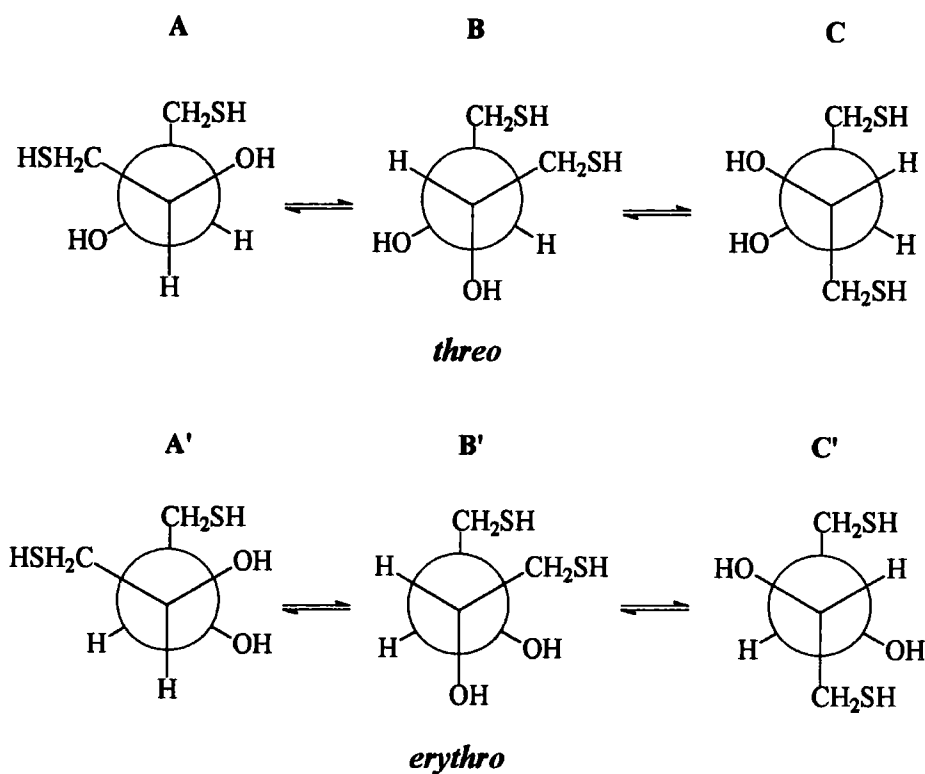
Dithiols are generally more reactive than structurally similar mono thiols, as they exhibit an extra -SH moiety and react via intramolecular pathways¹². This was found to be true in the above case. The DTT system studied was nearly an order of

magnitude more reactive than 1-thioglycerol, and equivalent to the most reactive aliphatic thiol, penicillamine. The thermal reaction (k') was also found to be more prominent for S,S-dinitrosodithiols relative to simple S-nitrosothiols.

The difference in reactivity between the dithiothreitol and dithioerythritol systems can be explained using the Newman projection formulas that represent the rotamers of these dithiols (figure 2.2). The *erythro* diastereomer has at least one rotamer in which all the similar groups are eclipsed, when viewed along the bond connecting the two adjacent asymmetric carbon atoms¹³. The *threo* diastereomer does not have any rotamers in which all the similar groups are eclipsed. The fact that the k_2 value for DTT is approximately twice that for DTE, could therefore be related to the substituent crowding and increased steric hindrance within the *erythro* diastereomer.

Figure 2.2

Staggered rotamers of dithiothreitol and dithioerythritol



A, B & C = Rotamers of the *threo* diastereomer

A', B' & C' = Rotamers of the *erythro* diastereomer

2.2.3 Reactions of S-Nitrosothiols with Thiols other than the Parent Thiol

Some experiments were conducted in which the thiol added in excess was different to the parent thiol from which the S-nitrosothiol originated (the RSNO/R'SH system, where $R \neq R'$). Nitrosothiol decomposition was still seen to occur. The results for such a reaction are given in table 2.8.

Table 2.8

Kinetic data for the 1-thioglycerol induced decomposition of S-nitrosopenicillamine ($1 \times 10^{-3} \text{ mol dm}^{-3}$) in pH 7.4 buffer, with $[\text{EDTA}] = 1 \times 10^{-4} \text{ mol dm}^{-3}$

$[\text{R'SH}]/10^{-3} \text{ mol dm}^{-3}$	$k_{\text{obs}}/10^{-4} \text{ s}^{-1}$
10	2.81 ± 0.01
25	6.84 ± 0.03
50	14.0 ± 0.1
75	22.0 ± 0.1
100	28.2 ± 0.1

$$k_2 = (2.85 \pm 0.03) \times 10^{-2} \text{ mol}^{-1} \text{ dm}^3 \text{ s}^{-1}$$

Table 2.9 offers a comparison of the rate data collected from a number of RSNO/RSH and RSNO/R'SH systems. The relevant thiol structures and abbreviations are highlighted in table 2.10.

The results of the reaction taking place between RSNO and R'SH are consistent with a large degree of initial rapid transnitrosation¹⁴ (section 1.3.5.2). This process generates R'SNO (scheme 2.1). As R'SH is present in such high concentration the equilibrium is driven towards the products. What is then observed can be qualitatively accounted for by slow R'SH induced decomposition of R'SNO (and to a much lesser extent decay of RSNO). An averaged form of the rate constants from the competing pathways is therefore measured.

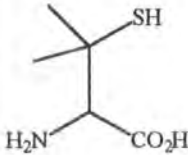
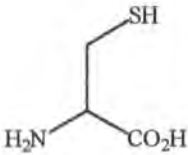
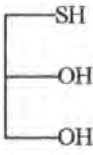
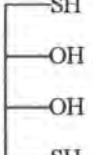
Table 2.9

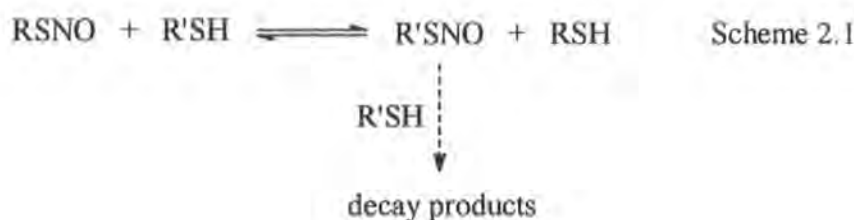
Values of k_2 for the reaction of S-nitrosothiols ($1 \times 10^{-3} \text{ mol dm}^{-3}$) and the parent (RSH) or a different thiol (R'SH) in pH 7.4 buffer, with $[\text{EDTA}] = 1 \times 10^{-4} \text{ mol dm}^{-3}$

RSNO	RSH	k_2 $/10^{-4} \text{ mol}^{-1} \text{ dm}^3 \text{ s}^{-1}$
Pen	Pen	2590 ± 30
TG	TG	389 ± 7
Cys	Cys	109 ± 1
DTT	DTT	2728 ± 68
DTE	DTE	1345 ± 26
RSNO	R'SH	k_2 $/10^{-4} \text{ mol}^{-1} \text{ dm}^3 \text{ s}^{-1}$
Pen	TG	285 ± 3
TG	Pen	1312 ± 90
Pen	Cys	100 ± 6
TG	DTT	2779 ± 52
DTT	TG	277 ± 7

Table 2.10

Thiols used in RSNO/R'SH reactions

Thiol	Penicillamine (Pen)	L-Cysteine (Cys)	1-Thioglycerol (TG)	Dithiothreitol (DTT) & Dithioerythritol (DTE)
Structure				

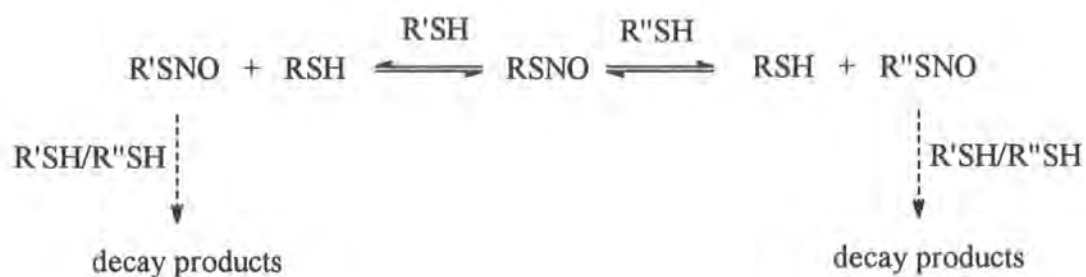


As an example the rate constant for the reaction of penicillamine with S-nitrosopenicillamine ($2590 \times 10^{-4} \text{ mol}^{-1} \text{ dm}^3 \text{ s}^{-1}$) is much reduced (to $285 \times 10^{-4} \text{ mol}^{-1} \text{ dm}^3 \text{ s}^{-1}$) when the thiol is changed to 1-thioglycerol, i.e. behaviour is closer to that of the reaction of S-nitroso-1-thioglycerol with 1-thioglycerol ($389 \times 10^{-4} \text{ mol}^{-1} \text{ dm}^3 \text{ s}^{-1}$). It is not immediately evident why the value is actually lower than this. Vice versa, when S-nitroso-1-thioglycerol is reacted with penicillamine, the rate constant is increased (to $1312 \times 10^{-4} \text{ mol}^{-1} \text{ dm}^3 \text{ s}^{-1}$) relative to the value for its reaction with 1-thioglycerol.

The choice of added thiol ultimately determines the S-nitrosothiol decomposition kinetics recorded. Identical transnitrosation characteristics were noticed when L-cysteine was reacted with S-nitrosopenicillamine, dithiothreitol reacted with S-nitroso-1-thioglycerol, and 1-thioglycerol reacted with S,S-dinitroso-dithiothreitol.

2.2.4 Reactions of S-Nitrosothiols with Mixed Thiols

In more complex tests S-nitrosothiols were exposed to a large excess of two "mixed" thiols, both different from the parent thiol (the RSNO/R'SH & R''SH system, where $R \neq R' \neq R''$). Each thiol was added in equal quantity. The total amount of thiol present was taken to be the sum of the individual thiol concentrations, i.e. $[\text{Thiol}]_{\text{total}} = [\text{R'SH}] + [\text{R''SH}]$. Reference to the k_2 values calculated for RSNO/RSH systems (table 2.9), could then help deduce which S-nitrosothiol decay characteristics (i.e. RSNO, R'SNO or R''SNO) the observed rate measurements resembled most closely (scheme 2.2). These results would clearly indicate to which thiol species transfer of the -NO group was favoured, prior to thiol promoted nitrosothiol decomposition.



Scheme 2.2

Nitrosation¹⁵ and transnitrosation^{14,16} reactions are dictated by steric as well as electronic effects. Accordingly the reaction of S,S-dinitrosodithiothreitol with penicillamine and L-cysteine (table 2.11) can be used as an example to display how transnitrosation from a S-nitrosothiol to a primary thiol (L-cysteine), is preferred over that to a tertiary thiol (penicillamine). This can be argued as the k_2 value ($139 \times 10^{-4} \text{ mol}^{-1} \text{ dm}^3 \text{ s}^{-1}$) determined in this experiment, resembles that for the reaction of L-cysteine and S-nitrosocysteine ($109 \times 10^{-4} \text{ mol}^{-1} \text{ dm}^3 \text{ s}^{-1}$) rather than penicillamine and S-nitrosopenicillamine ($2590 \times 10^{-4} \text{ mol}^{-1} \text{ dm}^3 \text{ s}^{-1}$). The reaction of S,S-dinitrosodithiothreitol with 1-thioglycerol and penicillamine was similar (table 2.12).

Table 2.11

Kinetic data for the reaction of S,S-dinitrosodithiothreitol ($5 \times 10^{-4} \text{ mol dm}^{-3}$) and equimolar quantities of penicillamine and L-cysteine in pH 7.4 buffer, with $[\text{EDTA}] = 1 \times 10^{-4} \text{ mol dm}^{-3}$

$[\text{Thiol}]_{\text{total}}/10^{-3} \text{ mol dm}^{-3}$	$k_{\text{obs}}/10^{-4} \text{ s}^{-1}$
10	5.54 ± 0.23
25	7.42 ± 0.22
50	10.9 ± 0.2
75	14.6 ± 0.2
100	17.9 ± 0.2

$$k_2 = (1.39 \pm 0.02) \times 10^{-2} \text{ mol}^{-1} \text{ dm}^3 \text{ s}^{-1}$$

Table 2.12

Values of k_2 for the reaction of S-nitrosothiols ($5 \times 10^{-4} \text{ mol dm}^{-3}$) and two different thiols (R'SH and R''SH) in pH 7.4 buffer, with $[\text{EDTA}] = 1 \times 10^{-4} \text{ mol dm}^{-3}$

RSNO ^a	R'SH ^a	R''SH ^a	k_2 / $10^{-4} \text{ mol}^{-1} \text{ dm}^3 \text{ s}^{-1}$
DTT	Cys	Pen	139 ± 2
DTT	TG	Pen	237 ± 1
DTT	Cys	TG	215 ± 5
DTT	DTE	TG	719 ± 6
TG	DTT	DTE	1782 ± 14

a. Structures and abbreviations shown in table 2.10.

Table 2.12 also presents rate information for the reaction of S-nitrosothiols with two thiols that are both primary structures, e.g. the reaction of S,S-dinitrosodithiothreitol with L-cysteine and 1-thioglycerol. The observed k_2 value ($215 \times 10^{-4} \text{ mol}^{-1} \text{ dm}^3 \text{ s}^{-1}$) is some average almost midway between those calculated for the reactions of L-cysteine with S-nitrosocysteine ($109 \times 10^{-4} \text{ mol}^{-1} \text{ dm}^3 \text{ s}^{-1}$) and 1-thioglycerol with S-nitroso-1-thioglycerol ($389 \times 10^{-4} \text{ mol}^{-1} \text{ dm}^3 \text{ s}^{-1}$). In this instance (as well as the reactions of S,S-dinitrosodithiothreitol with dithioerythritol and 1-thioglycerol, and S-nitroso-1-thioglycerol with dithiothreitol and dithioerythritol) transnitrosation to neither thiol is favoured over the other.

2.3 Determination of Reactive Species

Komiyama and Fujimori⁵ have studied the relationship between pH and reactivity within a RSNO/RSH system, by following the reaction of L-cysteine and S-nitrosocysteine within the pH range 4.9 - 9.4 at 37°C. Limited conclusions could be drawn from the results obtained however, as only a small pH effect was apparent with no distinguishable trend. The maximum k_2 value at pH 8.2 ($371 \times 10^{-4} \text{ mol}^{-1} \text{ dm}^3 \text{ s}^{-1}$)

was merely twice as large as the minimum at pH 4.9 ($185 \times 10^{-4} \text{ mol}^{-1} \text{ dm}^3 \text{ s}^{-1}$). It was therefore our intention to perform an independent pH investigation at 25°C , using aqueous buffers over the wider pH range 1.0 - 13.3. The same S-nitrosocysteine /cysteine system was analysed, but substantially larger thiol quantities than used by Komiyama and Fujimori⁵ were introduced into the reaction (in some cases a 200:1 ratio of RSH:RSNO). The rate constants calculated at pH 6.0 and 7.0 are tabulated as examples below (table 2.13), and all the values attained during the study summarised in table 2.14. The pH-rate profile that can be constructed is provided (figure 2.3).

Table 2.13

Kinetic data for the L-cysteine induced decomposition of S-nitrosocysteine ($1 \times 10^{-3} \text{ mol dm}^{-3}$) at pH 6.0 and 7.0, with $[\text{EDTA}] = 1 \times 10^{-4} \text{ mol dm}^{-3}$

[RSH] / $10^{-3} \text{ mol dm}^{-3}$	$k_{\text{obs}}/10^{-4} \text{ s}^{-1}$ pH 6.0	$k_{\text{obs}}/10^{-4} \text{ s}^{-1}$ pH 7.0
10	1.48 ± 0.04	1.28 ± 0.01
25	2.70 ± 0.02	2.59 ± 0.01
50	4.75 ± 0.02	4.99 ± 0.01
75	6.77 ± 0.02	7.58 ± 0.01
100	8.70 ± 0.01	10.3 ± 0.1

$$k_2 (\text{pH } 6.0) = (8.04 \pm 0.05) \times 10^{-3} \text{ mol}^{-1} \text{ dm}^3 \text{ s}^{-1}$$

$$k_2 (\text{pH } 7.0) = (1.00 \pm 0.02) \times 10^{-2} \text{ mol}^{-1} \text{ dm}^3 \text{ s}^{-1}$$

Figure 2.3 clearly depicts a broadly S-shaped curve, which levels off at high pH (ca. pH 13). The k_2 value observed at pH 13.3 ($320 \times 10^{-4} \text{ mol}^{-1} \text{ dm}^3 \text{ s}^{-1}$) is nearly 30 times greater than that at pH 1.0 ($11.9 \times 10^{-4} \text{ mol}^{-1} \text{ dm}^3 \text{ s}^{-1}$). Reactivity is therefore strictly dependent upon the pH of the buffer solution. The marked increase in the magnitude of k_2 above pH 8 is linked to thiol deprotonation and reveals that RS^- is intrinsic in controlling the rate of reaction. The thiolate anion can therefore be assigned as the **more** reactive species. The precise form of Cys^- involved may be established from the equilibria laid out in scheme 2.3.

Table 2.14

Dependence of k_2 on pH for the L-cysteine induced decomposition of S-nitrosocysteine ($1 \times 10^{-3} \text{ mol dm}^{-3}$), with $[\text{EDTA}] = 1 \times 10^{-4} \text{ mol dm}^{-3}$

pH	k_2 $/10^{-4} \text{ mol}^{-1} \text{ dm}^3 \text{ s}^{-1}$	pH	k_2 $/10^{-4} \text{ mol}^{-1} \text{ dm}^3 \text{ s}^{-1}$
1.0	11.9 ± 0.4	8.0	119 ± 3
2.0	24.2 ± 0.4	8.6	162 ± 7
3.0	36.5 ± 0.8	9.0	167 ± 8
4.0	53.4 ± 2.2	9.6	225 ± 8
5.0	78.9 ± 2.0	10.0	276 ± 15
6.0	80.4 ± 0.5	10.5	303 ± 17
7.0	100 ± 2	13.3	320 ± 15
7.4	109 ± 1	-----	-----

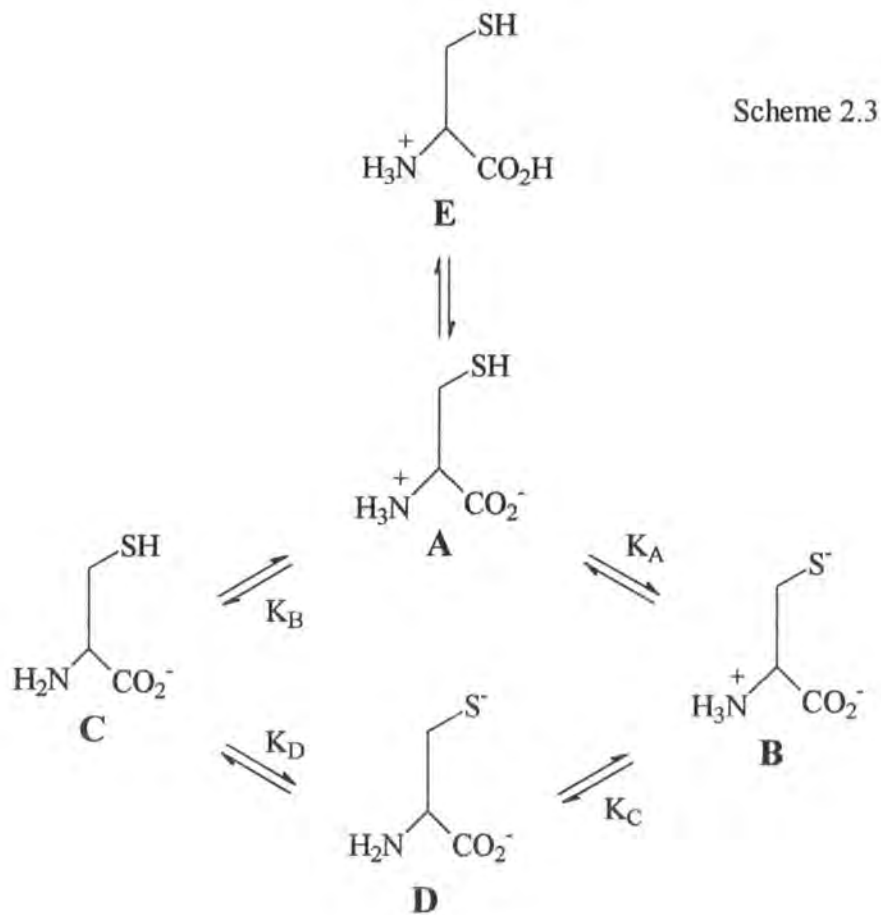
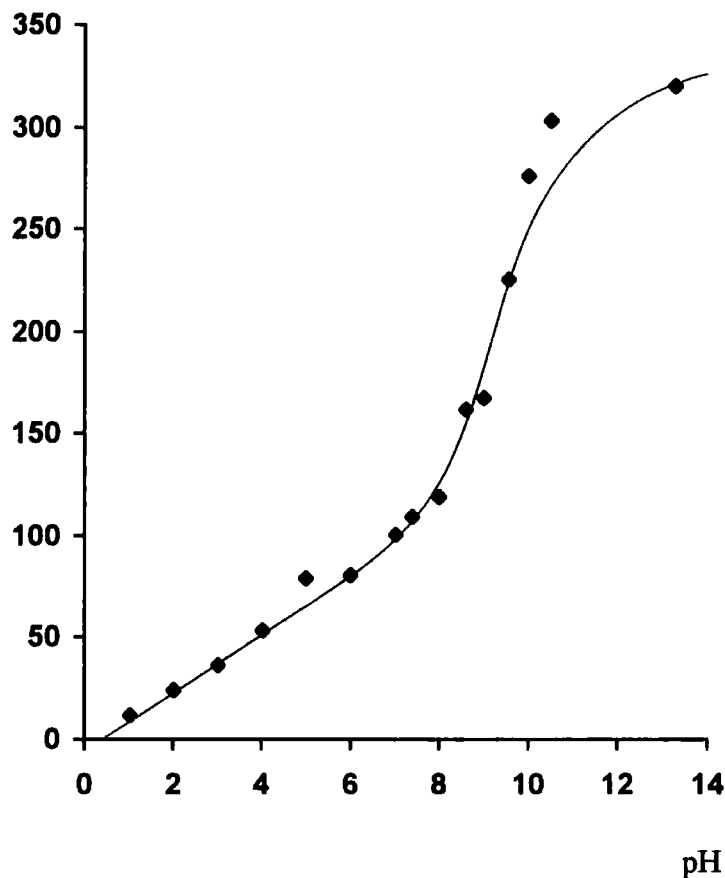


Figure 2.3

Plot of k_2 versus pH for the reaction of L-cysteine and S-nitrosocysteine
 ($1 \times 10^{-3} \text{ mol dm}^{-3}$), with $[\text{EDTA}] = 1 \times 10^{-4} \text{ mol dm}^{-3}$

$k_2/10^{-4} \text{ mol}^{-1} \text{ dm}^3 \text{ s}^{-1}$



There are four published pK_a values for L-cysteine¹⁷, which are complicated due to overlapping ionisations of $-\text{NH}_3^+$ and $-\text{SH}$. In figure 2.3 a sudden escalation in the size of k_2 is particularly clear within the pH 8 - 10 region. If one considers interactions at the thiol substituent, this increase does indeed coincide well with the values of pK_A (8.20) and pK_D (9.56) quoted in the literature¹⁸. It can therefore be assumed that B and D are the types of anion largely affecting RSNO decomposition.

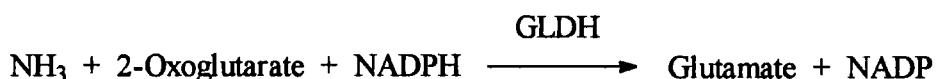
At higher acidity the rate of L-cysteine promoted S-nitrosocysteine decay slows significantly. The protonated form of the thiol (RSH) may still be able to initiate reaction, albeit to a lesser extent than RS^- . Species involving unionised carboxylic acid groups (E) would also have to be considered under these conditions.

2.4 Product Analysis

The unusual discovery that ammonia (and not nitric oxide) is the major nitrogenous product in the reaction of S-nitrosoglutathione and glutathione in pH 7.4 phosphate buffer, was made by Singh *et al*⁶ in 1996. Nitrite anion (NO₂⁻) and nitrous oxide (N₂O) were classified as by-products under aerobic conditions. Following our comprehensive investigation into the reaction kinetics of thiol induced S-nitrosothiol decomposition, the next objective was to confirm the identity of the end products within the systems studied.

2.4.1 Detection of Ammonia

A standard diagnostic kit acquired from Sigma-Aldrich Co. Ltd. was used to measure the ammonia content within the decay products. The principles behind this technique revolve around a kinetic method originally implemented by van Anken and Schiphorst¹⁹, which has been developed to detect accurately NH₃ levels as low as 0.2 µg/ml (1.2 x 10⁻⁵ mol dm⁻³) in assays. The enzymes, glutamate dehydrogenase (GLDH) and coenzyme reduced nicotinamide adenine dinucleotide phosphate (NADPH), are utilised in this procedure, which is based upon a reductive amination (equation 2.4).

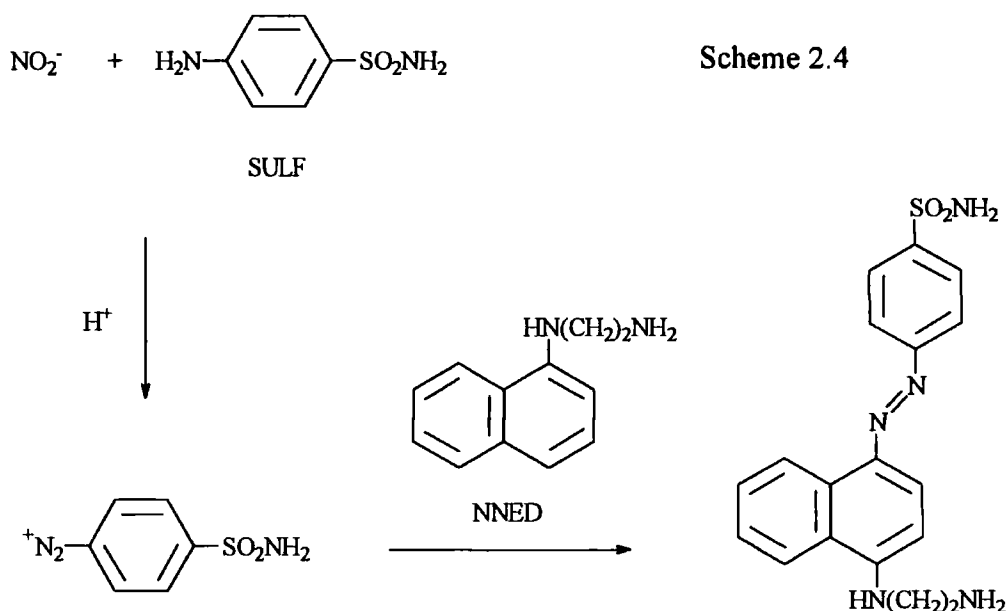


eqn 2.4

If 2-oxoglutarate and NADPH are used in excess, the reaction becomes pseudo-first order and the rate is only related to the activity of GLDH and [ammonia]. As the quantity of GLDH introduced is substantially greater than the residual amount in solution, the reaction rate is therefore directly proportional to the concentration of ammonia. The test involves monitoring the absorbance (340nm) corresponding to NADPH, before and after the addition of GLDH (see also section 6.2.1.1).

2.4.2 Detection of Nitrite

The Griess method²⁰ was the most convenient technique allowing a quantitative assessment of the nitrite ions present in reaction products. This test is described in scheme 2.4.



The diazotisation of sulfanilamide (SULF) by nitrous acid (generated from nitrite) constitutes the basis of this process. Subsequent coupling of the diazonium ion to N-1-naphthylethylenediamine (NNED) yields a purple azo dye that has an absorption maximum at 540nm. Standard solutions of nitrite ion can therefore be used to construct a suitable calibration curve. The gradient indicates the molar extinction coefficient ($\epsilon_{540\text{nm}}$) of the purple species at this wavelength (table 2.15), which can be used to evaluate nitrite concentrations (see also section 6.2.1.2).

As a rule, reaction mixtures were left for > 24 hours before NH_3 or NO_2^- analyses were performed, to ensure as near as possible, complete decay of the S-nitrosothiol. The calculated levels of ammonia and nitrite were then expressed as a percentage of the theoretical maximum quantity of nitrogen derived products, that could be generated from $1 \times 10^{-3} \text{ mol dm}^{-3}$ S-nitrosothiol.

Table 2.15

Calibration data used in the calculation of $\epsilon_{540\text{nm}}$

$[\text{NO}_2]/10^{-6} \text{ mol dm}^{-3}$	Absorbance (540nm)
5	0.314
10	0.548
15	0.806
20	1.048
25	1.316

$$\epsilon_{540\text{nm}} = 50080 \pm 621 \text{ mol}^{-1} \text{ dm}^3 \text{ cm}^{-1} \text{ (no lit. value available)}$$

2.4.3 Detection of Nitrous Oxide

GC-MS⁶ is one of the limited number of analytical techniques offering the resolution to study the production of gaseous N₂O, if the mass spectrometer is programmed to detect selected ions at m/z 44 and 30. The procedure is complicated as any CO₂ leaking into the vessel can induce misleading signals at m/z 44. Isotopic labelling in unison with millimetre-wave spectroscopy²¹ has also been successfully employed to distinguish N₂O, via recognition of part of its rotational spectrum.

2.4.4 Detection of Disulfide

As expected, oxidised glutathione (GSSG) has been characterised by Singh *et al*⁶ as the principal organic product in the GSNO/GSH system. HPLC can be used for RSSR quantification, although ¹H NMR and IR spectroscopy are also viable approaches. The latter are more applicable if a solid disulfide sample can be attained as a precipitate from aqueous solution. Even though disulfides show no measurable uv-visible absorption, the addition of copper ions upon reaction completion may enable the distinctive uv spectrum of the Cu²⁺-disulfide complex²² to be recognised, e.g. a shoulder at 250 - 260nm in the case of GSSG⁷ (see also section 5.3.1.4).

2.4.5 Composition of Reaction Products

The products of the decay of S-nitroso-1-thioglycerol as a function of added 1-thioglycerol are outlined in table 2.16 and graphically represented in figure 2.4.

Table 2.16

Ammonia/nitrite yields from the reaction of 1-thioglycerol and S-nitroso-1-thioglycerol ($1 \times 10^{-3} \text{ mol dm}^{-3}$) in pH 7.4 buffer, with $[\text{EDTA}] = 1 \times 10^{-4} \text{ mol dm}^{-3}$

[RSH] / $10^{-3} \text{ mol dm}^{-3}$	% NH_3	% NO_2^-	% N
0	3	43	46
10	71	26	97
25	79	20	99
50	80	17	97
75	82	15	97
100	83	13	96

Results indicate that the ammonia content within the final products increases sharply to 70 - 80%, as the concentration of 1-thioglycerol introduced into the reaction exceeds 0.01 mol dm^{-3} . The production of NH_3 is then dominant at the expense of nitrite at high [RSH]. Ammonia and nitrite ($[\text{NH}_3] + [\text{NO}_2^-]$) collectively account for > 96% of the "nitrogen" products. These findings support those made by Singh *et al*⁶. Nitrous oxide may constitute the missing fraction.

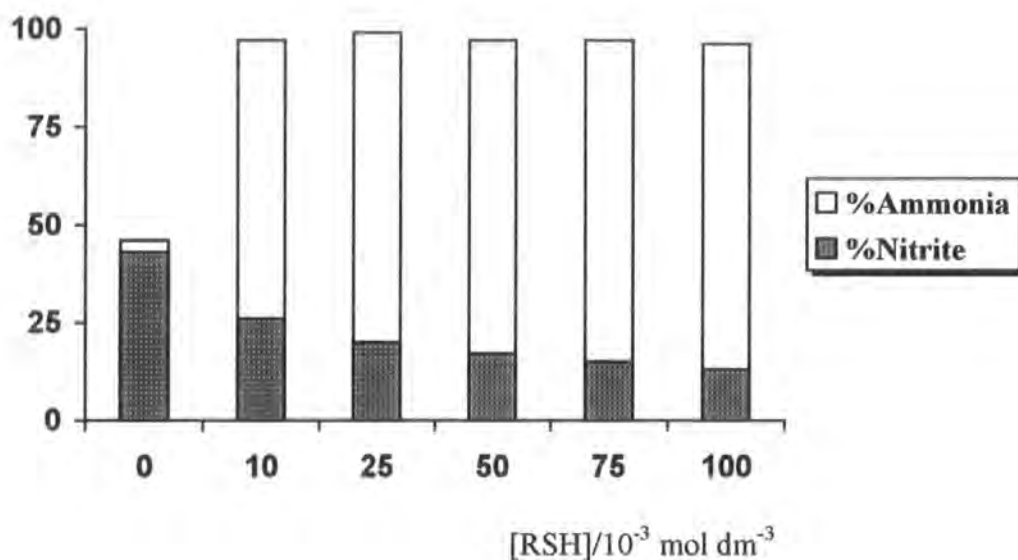
The total nitrogen content detected is low (< 50%) if no 1-thioglycerol is added, as S-nitroso-1-thioglycerol is relatively stable in a solution from which Cu^{2+} ions have been removed. Nitrite only originates from the hydrolysis of NO, which is released via thermal or photochemical decomposition of the RSNO (section 1.3.2).

The described product distribution seems to be indicative of most RSNO/RSH systems, as similar patterns were revealed in the reactions of S-nitrosocysteine and S-nitrosopenicillamine with their respective thiol precursors.

Figure 2.4

Product distribution for the reaction of 1-thioglycerol and S-nitroso-1-thioglycerol ($1 \times 10^{-3} \text{ mol dm}^{-3}$) in pH 7.4 buffer, with $[\text{EDTA}] = 1 \times 10^{-4} \text{ mol dm}^{-3}$

% Nitrogenous Product



An acidic pH has been shown to promote ammonia formation in the reaction between L-cysteine and S-nitrosocysteine (table 2.17). Alternatively, an alkaline buffer increases nitrite quantities. If the unknown nitrogen portion is indeed N_2O , then its production is almost unchanged at pH 1.0 (3%) or pH 13.3 (1%).

Table 2.17

Ammonia/nitrite yields from the reaction of L-cysteine ($3.75 \times 10^{-2} \text{ mol dm}^{-3}$) and S-nitrosocysteine ($1 \times 10^{-3} \text{ mol dm}^{-3}$) at varied pH, with $[\text{EDTA}] = 1 \times 10^{-4} \text{ mol dm}^{-3}$

pH	% NH_3^a	% $\text{NO}_2^-^a$	% N
1.0	88	9	97
13.3	31	68	99

a. Analysis performed following neutralisation of the test solution to pH 7.4.

2.5 Anaerobic Reaction

Anaerobic experiments were carried out using N_2 -purged solutions in conjunction with the glucose/glucose oxidase method devised by Gorren *et al*²³ (see also section 6.2.2). When the reaction of S-nitroso-1-thioglycerol and 1-thioglycerol was performed in deaerated rather than aerated buffer at pH 7.4, there was no change (within experimental error) in the measured second-order rate constant (table 2.18).

Table 2.18

Values of k_2 for the aerobic/anaerobic reactions of S-nitroso-1-thioglycerol (1×10^{-3} mol dm⁻³) and 1-thioglycerol in pH 7.4 buffer, with [EDTA] = 1×10^{-4} mol dm⁻³

RSH	Aerobic k_2 / 10^{-4} mol ⁻¹ dm ³ s ⁻¹	Anaerobic k_2 / 10^{-4} mol ⁻¹ dm ³ s ⁻¹
1-Thioglycerol	389 ± 7	391 ± 6

The product distribution (table 2.19 and figure 2.5) was however modified according to whether the reaction was conducted in O_2 deficient or O_2 rich media. The ammonia yield in anaerobic tests appears to be a little higher than in aerobic work, e.g. at [RSH] = 5×10^{-2} mol dm⁻³, NH_3 (anaerobic) = 91% whilst NH_3 (aerobic) = 80%. On the other hand nitrite levels are significantly lower anaerobically, e.g. at [RSH] = 5×10^{-2} mol dm⁻³, NO_2^- (anaerobic) = 1% whilst NO_2^- (aerobic) = 17%. The liberation of nitric oxide was confirmed using a NO-specific electrode (section 6.1.8), and its oxidation explains one potential source of NO_2^- . The yield of the undetected product grows if O_2 is rigorously excluded from the system, and therefore NO may account for some of the missing nitrogen species. It is more likely that increased N_2O generation is responsible, as over many hours, NO is converted to (and detected as) nitrite, by slow leakage of O_2 into the reaction vessel.

The results described provide evidence for the existence of a complex set of oxygen dependent reaction pathways following the rate-determining step.

Table 2.19

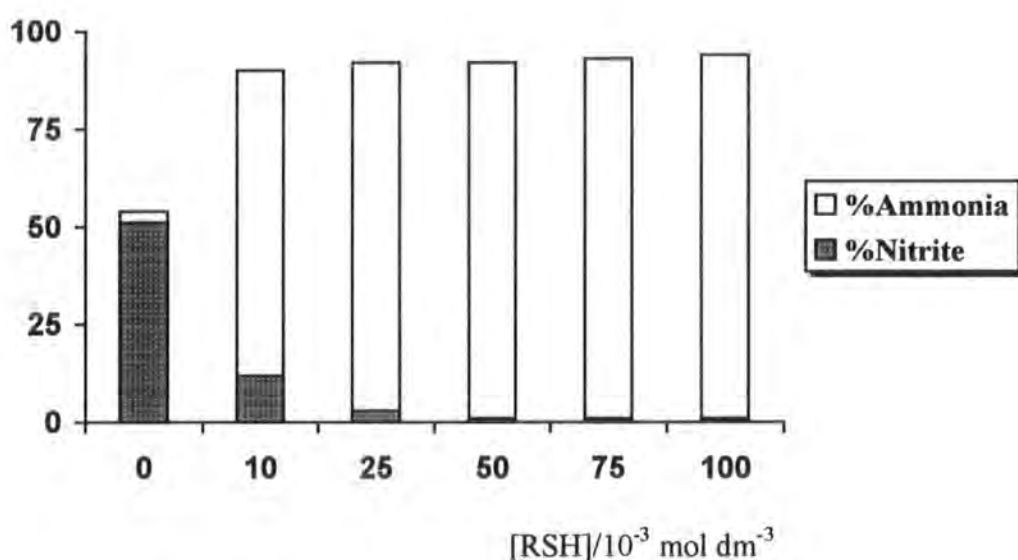
Ammonia/nitrite yields from the anaerobic reaction of 1-thioglycerol and S-nitroso-1-thioglycerol ($1 \times 10^{-3} \text{ mol dm}^{-3}$) in pH 7.4 buffer, with $[\text{EDTA}] = 1 \times 10^{-4} \text{ mol dm}^{-3}$

[RSH] / $10^{-3} \text{ mol dm}^{-3}$	% NH_3	% NO_2^-	% N
0	3	51	54
10	78	12	90
25	89	3	92
50	91	1	92
75	92	1	93
100	93	1	94

Figure 2.5

Product distribution for the anaerobic reaction of 1-thioglycerol and S-nitroso-1-thioglycerol ($1 \times 10^{-3} \text{ mol dm}^{-3}$) in pH 7.4 buffer, with $[\text{EDTA}] = 1 \times 10^{-4} \text{ mol dm}^{-3}$

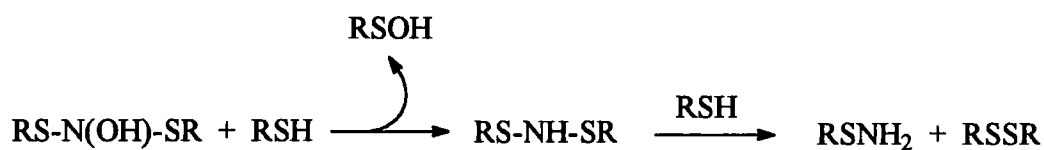
% Nitrogenous Product



Spectral evidence (not shown) verified that RSSR formation was quantitative (> 90%) and unchanged in aerobic or anaerobic conditions (see section 5.3.1.4).

The increased reactivity of systems derived from thiols exhibiting gem-dimethyl groups (e.g. penicillamine), and reduced reactivity of mercaptosuccinic acid, can be reasoned in terms of the inductive effects of the -Me and -CO₂H substituents respectively, intensifying or depleting the nucleophilic activity of RS⁻. Investigations support the notion of RS⁻ attack at the nitroso nitrogen rather than sulfur atom, as an increased electron density upon the sulfur within a RSNO would in theory impede (not promote) nucleophilic interactions. Displacements at the sulfur atom have been postulated in some reports²⁵, and are thought to afford NO⁻ ^{12,26}.

A N-hydroxysulfenamide compound (RS-N(OH)-SR) has been proposed as the pivotal intermediate formed from this first step. This RSH conjugate is capable of accommodating transnitrosation and can dictate how reaction products are furnished according to the conditions utilised. Sequential reductions of this species by the large quantity of RSH present, can for example yield ammonia and disulfide via a sulfenamide (RS-NH-SR) (scheme 2.6 and equation 2.5). Thiolate mediated reduction of the -NO group also offers a valid route to NH₃, following the generation of amines such as hydroxylamine²⁷.



Scheme 2.6



Homolytic fission of the S-N bond in the N-hydroxysulfenamide can generate N-hydroxyl (RS-N[•]-OH) and thiyl (RS[•]) radicals. The ultimate fate of these species is primarily governed by the oxygen levels within the system. Dimerisation of the N-hydroxyl radical can produce an unstable dihydroxyhydrazine (RS-N(OH)-N(OH)-SR), which develops gaseous N₂O via hyponitrous acid (HO-N=N-OH). Disulfide and water are the other possible products from this path.

In aerobic solution, an excess of thiol can assist in the conversion of the N-hydroxyl radical into sulfenic acid (RSOH) and nitrous acid (HNO₂). This complex reaction sequence involves hydrogen atom abstraction from the RSH to form RS-N(OH)-OOH. Further molecular rearrangements lead to nitrite and disulfide.

Thiyl radicals can react with oxygen or RSNO (to give NO). The former process encompasses extensive thiol oxidation, but both involve RSSR formation.

The illustrated scheme explains the relative amounts of nitrogenous product obtained from aerobic or anaerobic reactions. In the presence of O₂, a higher concentration of thiol or an acidic pH (i.e. the thiol is fully protonated) will increase the reduction of RS-N(OH)-SR by RSH, and produce a larger quantity of NH₃. This is to the detriment of nitrite. Alkaline buffers have the reverse effect, as a greater proportion of the reaction can now pass via radical species. A basic pH also assists the hydrolysis of NO to NO₂⁻. Finally, heightened anaerobic levels of N₂O and NH₃ stem from the redundancy of the O₂ dependent pathways that supply NO₂⁻ and RSSR.

Schulz and McCalla²⁸ noted that NH₃, N₂O, NO₂⁻ and RSSR, are products of the reaction of N-nitrosamines and cysteine. Sodium nitroprusside and glutathione also interact to afford N₂O²⁹. A similar reaction to that outlined for RSNOs and RSH, may therefore be general for thiols and any molecule containing a -NO group.

2.7 Conclusion

At high thiol concentration there is a reaction between S-nitrosothiols and thiols, which is not catalysed by Cu⁺ and forms NH₃ (and not NO) as the main nitrogen product. Under physiological conditions the parent thiol, a different thiol or a mixture of thiols, are all effective at inducing RSNO decomposition. The degradation mechanism is complicated due to the nature of the multiple secondary reactions that can take place via RSH conjugates and free radicals. These paths determine the other products. Results are of particular relevance, considering that the NO-releasing capabilities of nitrosothiols such as GSNO which are present *in vivo* in micromolar quantities, may be modified by the millimolar concentrations of thiol present.

References

- 1 S. Oae, D. Fukushima and Y.H. Kim, *J. Chem. Soc., Chem. Commun.*, 1977, 407.
- 2 E.A. Kowaluk and H.L. Fung, *J. Pharm. Exp. Ther.*, 1990, **255**(3), 1256.
- 3 M. Feelisch, M. te Poel, R. Zamora, A. Deussen and S. Moncada, *Nature*, 1994, **368**, 62.
- 4 A.P. Dicks, P.H. Beloso and D.L.H. Williams, *J. Chem. Soc., Perkin Trans. 2*, 1997, 1429.
- 5 T. Komiyama and K. Fujimori, *Bioorganic & Medicinal Chemistry Letters*, 1997, **7**(2), 175.
- 6 S.P. Singh, J.S. Wishnok, M. Keshive, W.M. Deen and S.R. Tannenbaum, *Proc. Natl. Acad. Sci., USA*, 1996, **93**, 14428.
- 7 H.R. Swift, Ph.D. Thesis, University of Durham, 1996.
- 8 A. Meister and M.E. Anderson, *Ann. Rev. Biochem.*, 1983, **52**, 711.
- 9 S. Oae and K. Shinhama, *Org. Prep. Proc. Int.*, 1983, **15**(3), 165.
- 10 J.S. Stamler, D.I. Simon, J.A. Osborne, M.E. Mullins, O. Joraki, T. Michael, D.J. Singel and J. Loscalzo, *Proc. Natl. Acad. Sci., USA*, 1992, **89**, 444.
- 11 W.P. Jencks, *Catalysis in Chemistry and Enzymology*, Dover Publications Inc., 1987, p.p. 12.
- 12 M. Le, H. Zhang and G.E. Means, *Bioorganic & Medicinal Chemistry Letters*, 1997, **7**(11), 1393.
- 13 S.H. Pine, *Organic Chemistry*, 5th ed., McGraw-Hill Inc., Singapore, 1987, p.p. 481.
- 14 D.J. Barnett, A. Ríos and D.L.H. Williams, *J. Chem. Soc., Perkin Trans. 2*, 1995, 1279.
- 15 S. González-Mancebo, E. Calle, M.P. García-Santos and J. Casado, *J. Agric. Food Chem.*, 1997, **45**, 334.
- 16 D.J. Barnett, J. McAninly and D.L.H. Williams, *J. Chem. Soc., Perkin Trans. 2*, 1994, 1131.
- 17 H.M.S. Patel and D.L.H. Williams, *ibid.*, 1990, 37.
- 18 D.M.E. Reuben and T.C. Bruice, *J. Am. Chem. Soc.*, 1976, **98**, 114.
- 19 H.C. van Anken and M.E. Schiphorst, *Clin. Chim. Acta*, 1974, **56**, 151.
- 20 *Vogel's Textbook of Quantitative Inorganic Analysis*, 4th ed., Longman, 1978, p.p. 755.

- 21 J. Haider, M.N.S. Hill, I.D. Menneer, H. Maskill and J.G. Smith, *J. Chem. Soc., Chem. Commun.*, 1997, 1571.
- 22 S.C. Askew, D.J. Barnett, J. McAninly and D.L.H. Williams, *J. Chem. Soc., Perkin Trans. 2*, 1995, 741.
- 23 A.C.F. Gorren, A. Schrammel, K. Schmidt and B. Mayer, *Arch. Biochem. Biophys.*, 1996, **330**(2), 219.
- 24 A.P. Dicks, E. Li, A.P. Munro, H.R. Swift and D.L.H. Williams, *Can. J. Chem.*, 1998, **76**, 789.
- 25 D.R. Arnelle and J.S. Stamler, *Arch. Biochem. Biophys.*, 1995, **318**(2), 279.
- 26 P.S.-Y. Wong, J. Hyun, J.M. Fukuto, F.N. Shirota, E.G. DeMaster, D.W. Shoeman and H.T. Nagasawa, *Biochemistry*, 1998, **37**, 5362, N. Hogg, R.J. Singh and B. Kalyanaraman, *FEBS Lett.*, 1996, **382**, 223.
- 27 J.H. Boyer in *The Chemistry of the Nitro and Nitroso Groups (Part 1)*, Ed. H. Feuer, Wiley-Interscience, 1969, p.p. 260.
- 28 U. Schulz and D.R. McCalla, *Can. J. Chem.*, 1969, **47**, 2021.
- 29 V.Sampath, D.L. Rousseau and W.S. Caughey in *Methods in Nitric Oxide Research*, Eds. M. Feelisch and J.S. Stamler, Wiley, 1996, p.p. 415.

Chapter 3

Reactivity of Nitrogen Nucleophiles Towards S-Nitrosopenicillamine

Chapter 3 : Reactivity of Nitrogen Nucleophiles

Towards S-Nitrosopenicillamine

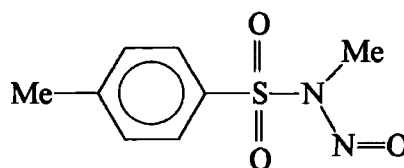
3.1 Introduction

The question of whether S-nitrosothiols can efficiently nitrosate nitrogen nucleophiles (such as amines) in trace metal ion free aqueous solution, still remains unanswered. Studies that have attempted to address this notion (section 1.3.5.3) have neglected the initial Cu^{2+} catalysed liberation of NO from RSNOs. Due to the long time scale necessary for reaction completion, any possible copper-independent direct interaction between these species has previously been dismissed as irrelevant.

The electrophilic nitrosation of nitrogen nucleophiles by nitroso compounds is however common in the literature. Examples relate to alkyl nitrites¹, N-nitrosamines² and sodium nitroprusside³. A diverse number of solvents have been utilised for this purpose, and in most instances an alkaline medium is required. Conditions generally contrast with the low pH and requisite solvents essential for nitrosation via the standard reagents, nitrous acid and nitrosyl halides. The work conducted by Leis *et al*⁴ within this topic is worthy of particular attention. It incorporates comprehensive mechanistic investigations into the attack of an extensive range of structurally varied nitrogen nucleophiles at the N=O group of the alkyl nitrite, 2-ethoxyethyl nitrite (3.1, EEN), and the N-nitrososulfonamide, N-methyl-N-nitrosotoluene-*p*-sulfonamide (3.2, MNTS).

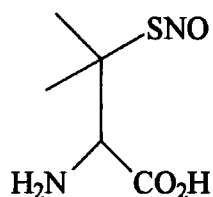


3.1



3.2

Our experiments regarding the reaction of thiols with S-nitrosothiols at high thiol concentration⁵ (chapter 2), enabled us to classify S-nitrosopenicillamine (3.3, SPEN) as the most reactive substrate within the aliphatic RSNOs tested (20 in total).



3.3

As the behaviour of SPEN was equivalent to that of heterocyclic and di-nitroso species, it was considered reactive enough to allow a thorough kinetic analysis of transnitrosation between a S-nitrosothiol and nitrogen nucleophiles at high pH. Comparisons could then be made with the analogous reactions of other -NO derived molecules described above.

Although SPEN could not be isolated as a pure solid, a sample was easily prepared and used *in situ* via nitrosation of the thiol precursor, D,L-penicillamine, using an equimolar amount of acidic sodium nitrite. This amino acid is of particular biological interest. The D-isomer has been utilised in the treatment of Wilson's disease (hepatolenticular degeneration) in humans for more than 40 years⁶. This disorder is linked to an abnormally high copper metabolism. D-Penicillamine is known to be a most effective chelator of copper ions as a result of clinical trials⁷, and initiates their eventual urinary excretion. On the other hand the L-isomer is highly toxic to mammals, as it diminishes levels of the coenzyme, pyridoxal phosphate⁸.

3.2 Reactions of Secondary Amines

3.2.1 Effect of Amine Concentration on S-Nitrosopenicillamine Decomposition

The dependence of the rate of SPEN decomposition on added amine concentration was analysed using ten different secondary amines (R'RNH). Each experiment involved following the disappearance of the SPEN ($2.5 \times 10^{-4} \text{ mol dm}^{-3}$) absorbance peak ($\lambda \sim 340\text{nm}$) as a function of time at 25°C . Total absorbance changes during the course of the reaction corresponded approximately with the known molar extinction coefficient of SPEN⁹, $\epsilon \sim 860 \text{ mol}^{-1} \text{ dm}^3 \text{ cm}^{-1}$. The nitrosothiol sample was freshly prepared *in situ* for all kinetic runs, diluted with distilled water, and then used immediately. EDTA ($1 \times 10^{-4} \text{ mol dm}^{-3}$) was also introduced into the reaction systems, to halt any component of decay promoted by copper(I) ions.

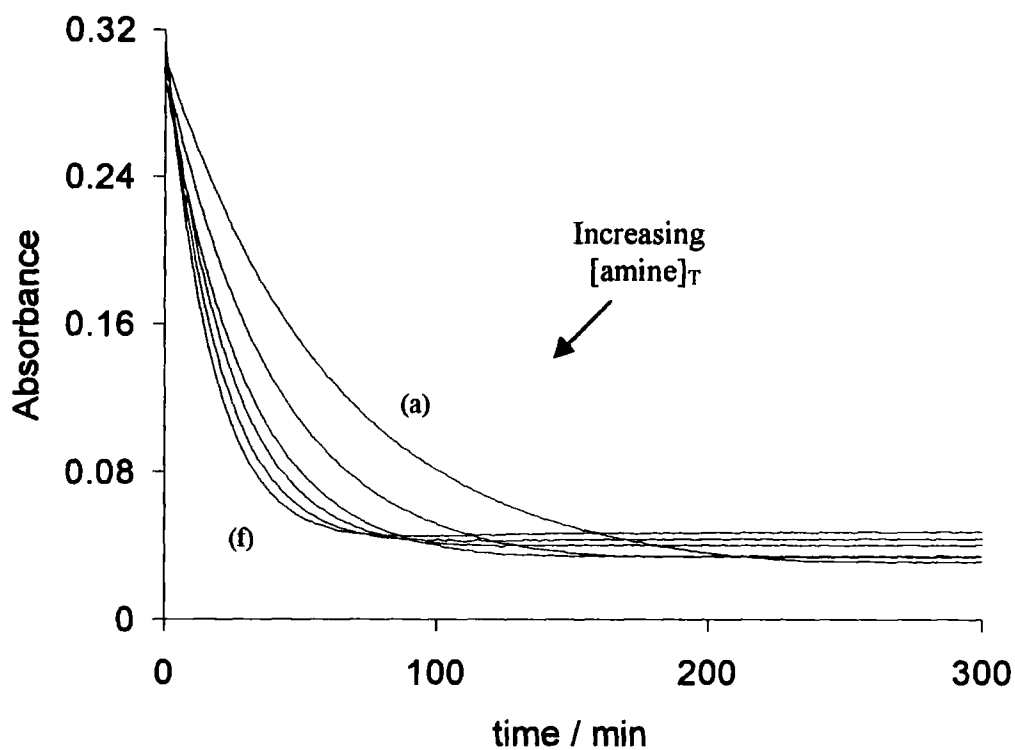
Pyrrolidine, piperidine, sarcosine, N-methylbenzylamine, N-methylpiperazine, piperazine, 4-hydroxy-L-proline, D,L-proline, morpholine, and N-methylaniline, were each reacted separately with SPEN at an uniformly maintained pH. Experiments were performed with a large excess (> 20 fold) of nitrogen nucleophile over nitrosothiol. Phosphate buffer (pH 7.4) was rendered useless due to the high amine concentrations needed, and so buffer solutions were composed of the nucleophile itself. These conditions were employed by carefully manipulating the amine/ammonium salt buffer ratio present in aqueous solution (equation 3.1), via the addition of known quantities of acid (HClO_4 or HCl) or alkali (NaOH). In each instance pH measurements were taken before and after reaction, and were found to be close to the pK_a of the protonated amine, and consistent, when the ionic strength (I) was kept constant via the use of NaClO_4 or NaCl . Unless otherwise stated, $I = 0.105 \text{ mol dm}^{-3}$.



With $[\text{amine}] \gg [\text{SPEN}]$ to ensure pseudo-first order conditions, excellent first-order decay characteristics were observed at each amine concentration studied. The time-dependent spectra resulting from such a reaction involving pyrrolidine are shown in figure 3.1.

Figure 3.1

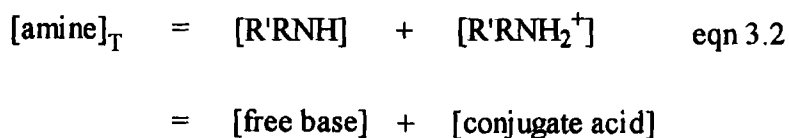
Kinetic traces showing the reaction of SPEN ($2.5 \times 10^{-4} \text{ mol dm}^{-3}$) and pyrrolidine at pH 11.57, with $[\text{EDTA}] = 1 \times 10^{-4} \text{ mol dm}^{-3}$



N.B. $[\text{amine}]_T =$ see below

(a) $[\text{amine}]_T = 0.06 \text{ mol dm}^{-3}$, (b) $[\text{amine}]_T = 0.09 \text{ mol dm}^{-3}$, (c) $[\text{amine}]_T = 0.12 \text{ mol dm}^{-3}$,
(d) $[\text{amine}]_T = 0.15 \text{ mol dm}^{-3}$, (e) $[\text{amine}]_T = 0.18 \text{ mol dm}^{-3}$ and (f) $[\text{amine}]_T = 0.21 \text{ mol dm}^{-3}$.

A linear relationship between the observed pseudo-first order rate constant (k_{obs}) and total stoichiometric amine concentration, $[\text{amine}]_T$ (equation 3.2), was evident for each amine studied.



The results for pyrrolidine (corresponding to figure 3.1) and piperidine are presented in tables 3.1 – 3.2 and figure 3.2. This clarified the reaction as first order in amine.

Table 3.1

Kinetic data for the reaction of SPEN ($2.5 \times 10^{-4} \text{ mol dm}^{-3}$) and pyrrolidine at pH 11.57, with $[\text{EDTA}] = 1 \times 10^{-4} \text{ mol dm}^{-3}$

$[\text{amine}]_T / \text{mol dm}^{-3}$	$k_{\text{obs}} / 10^{-4} \text{ s}^{-1}$
0.06	2.67 ± 0.01
0.09	4.12 ± 0.01
0.12	5.58 ± 0.01
0.15	7.01 ± 0.02
0.18	8.45 ± 0.02
0.21	10.0 ± 0.1

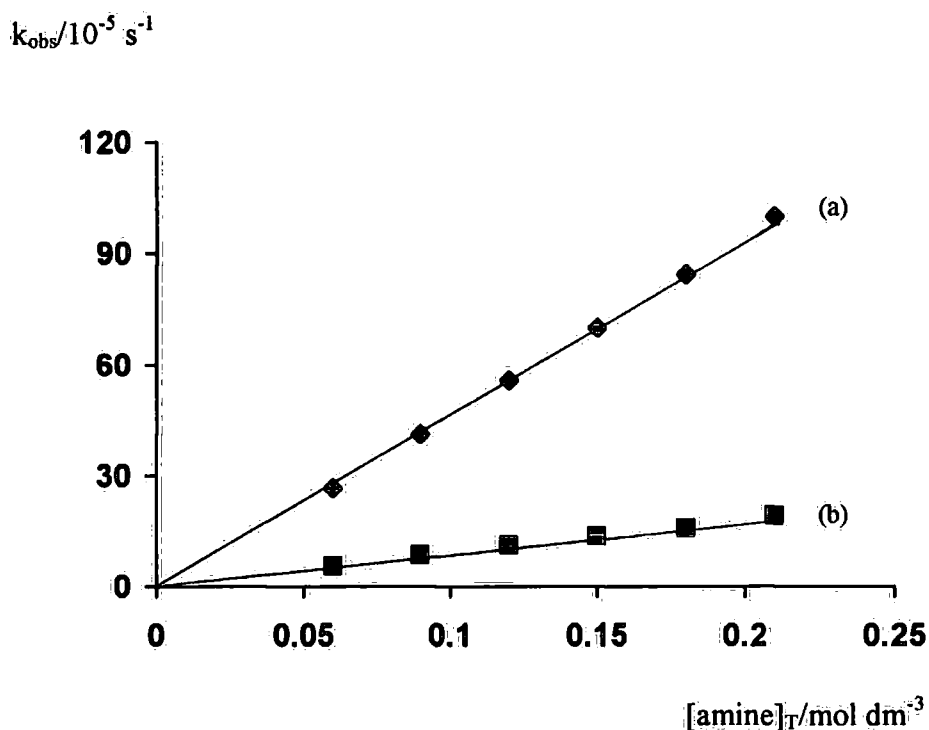
Table 3.2

Kinetic data for the reaction of SPEN ($2.5 \times 10^{-4} \text{ mol dm}^{-3}$) and piperidine at pH 11.21, with $[\text{EDTA}] = 1 \times 10^{-4} \text{ mol dm}^{-3}$

$[\text{amine}]_T / \text{mol dm}^{-3}$	$k_{\text{obs}} / 10^{-5} \text{ s}^{-1}$
0.06	5.59 ± 0.09
0.09	8.59 ± 0.13
0.12	11.3 ± 0.2
0.15	13.6 ± 0.3
0.18	15.8 ± 0.3
0.21	19.4 ± 0.3

Figure 3.2

Plot of k_{obs} against $[\text{amine}]_{\text{T}}$ for the reaction of SPEN ($2.5 \times 10^{-4} \text{ mol dm}^{-3}$) and pyrrolidine or piperidine, with $[\text{EDTA}] = 1 \times 10^{-4} \text{ mol dm}^{-3}$



(a) Pyrrolidine and (b) Piperidine.

The full rate equation can be expressed as follows, if one assumes that reaction takes place via the free base form of the amine (see section 3.2.2):

$$\text{Rate} = k_2[\text{SPEN}][\text{R}'\text{RNH}] \quad \text{eqn 3.3}$$

Where k_2 = second order rate constant for the reaction of SPEN with free amine, and $[\text{R}'\text{RNH}]$ = concentration of free amine.

For fixed $[\text{SPEN}]$, $[\text{R}'\text{RNH}]$ is constant and hence equation 3.4 is applicable.

$$\text{Rate} = k_{\text{obs}}[\text{SPEN}] \quad \text{eqn 3.4}$$

Furthermore, the substituted form of the pseudo-first order rate constant can then be derived (equation 3.5).

$$k_{\text{obs}} = k_2[\text{R}'\text{RNH}] \quad \text{eqn 3.5}$$

Here,

$$[\text{R}'\text{RNH}] = \frac{K_a [\text{amine}]_T}{K_a + [\text{H}^+]} \quad \text{eqn 3.6}$$

Where K_a = acidity constant for the protonated amine.

Equation 3.7 can now be established. In theory it should relate k_{obs} and acidity.

$$k_{\text{obs}} = \frac{k_2 K_a [\text{amine}]_T}{K_a + [\text{H}^+]} \quad \text{eqn 3.7}$$

3.2.2 Active Form of the Amine

To confirm that transnitrosation reactions between SPEN and secondary amines did indeed proceed via direct nucleophilic attack of the basic form of the amine, alterations in k_{obs} induced by a change in solution pH (within one unit above or below the amine $\text{p}K_a$) were monitored at constant $[\text{amine}]_T$. Pyrrolidine and piperidine were chosen for this purpose. In both instances an incremental change in k_{obs} was observed as the buffer pH increased. Table 3.3 contains the relevant data corresponding to piperidine, and figure 3.3 offers a graphical representation of the pseudo-first order rate constants versus pH. The plot is a S-shaped (sigmoid) curve with an inflexion point in the vicinity of the $\text{p}K_a$ value, which is consistent with the rate-determining step involving $\text{R}'\text{RNH}$ as the reactive species.

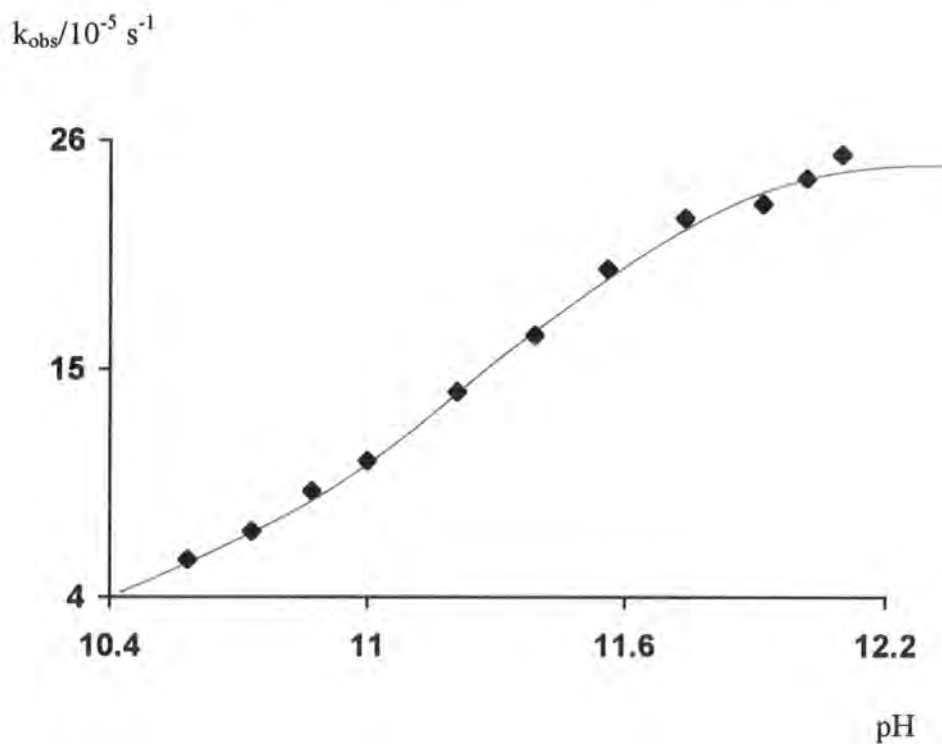
Table 3.3

Influence of buffer pH on k_{obs} for the reaction of SPEN ($2.5 \times 10^{-4} \text{ mol dm}^{-3}$) and piperidine. $[\text{EDTA}] = 1 \times 10^{-4} \text{ mol dm}^{-3}$ and $[\text{amine}]_{\text{T}} = 0.20 \text{ mol dm}^{-3}$

pH	$k_{\text{obs}} / 10^{-5} \text{ s}^{-1}$	pH	$k_{\text{obs}} / 10^{-5} \text{ s}^{-1}$
10.58	5.82 ± 0.03	11.56	19.8 ± 0.2
10.73	7.17 ± 0.02	11.74	22.3 ± 0.3
10.87	9.12 ± 0.01	11.92	23.0 ± 0.3
11.00	10.6 ± 0.1	12.02	24.2 ± 0.3
11.21	13.9 ± 0.2	12.10	25.3 ± 0.3
11.39	16.6 ± 0.1	----	----

Figure 3.3

Plot of k_{obs} versus pH for the reaction of SPEN ($2.5 \times 10^{-4} \text{ mol dm}^{-3}$) and piperidine. $[\text{EDTA}] = 1 \times 10^{-4} \text{ mol dm}^{-3}$ and $[\text{amine}]_{\text{T}} = 0.20 \text{ mol dm}^{-3}$



The reciprocal form of equation 3.7 can be translated into equation 3.8. Table 3.4 contains the necessary data points that enable $1/k_{\text{obs}}$ to be plotted against $[\text{H}^+]$ (figure 3.4). This should yield a straight line, the positive gradient (m) and intercept (c) of which can be used to estimate the K_a of the amine (equations 3.9 - 3.11).

$$\frac{1}{k_{\text{obs}}} = \frac{1}{k_2 [\text{amine}]_{\text{T}}} + \frac{[\text{H}^+]}{k_2 K_a [\text{amine}]_{\text{T}}} \quad \text{eqn 3.8}$$

Where,

$$c = \frac{1}{k_2 [\text{amine}]_{\text{T}}} \quad \text{eqn 3.9}$$

and,

$$m = \frac{1}{k_2 K_a [\text{amine}]_{\text{T}}} \quad \text{eqn 3.10}$$

$$\therefore \frac{c}{m} = K_a \quad \text{eqn 3.11}$$

For piperidine, $m = 5.29 \times 10^{14} \text{ mol}^{-1} \text{ dm}^3 \text{ s}$

and $c = 3738 \text{ s}$

$$\therefore K_a = 7.07 \times 10^{-12} \text{ mol dm}^{-3}$$

The $\text{p}K_a$ values of the protonated forms of piperidine and pyrrolidine that are determined using equation 3.11 are summarised in table 3.5. They agree with their respective literature values. Similar results were noticed for all the other secondary amines considered (see later).

Table 3.4

Values of $1/k_{\text{obs}}$ against $[\text{H}^+]$ for the reaction of SPEN ($2.5 \times 10^{-4} \text{ mol dm}^{-3}$) and piperidine. $[\text{EDTA}] = 1 \times 10^{-4} \text{ mol dm}^{-3}$ and $[\text{amine}]_{\text{T}} = 0.20 \text{ mol dm}^{-3}$

$[\text{H}^+]$ $/10^{-13} \text{ mol dm}^{-3}$	$1/k_{\text{obs}}$ $/10^3 \text{ s}$	$[\text{H}^+]$ $/10^{-13} \text{ mol dm}^{-3}$	$1/k_{\text{obs}}$ $/10^3 \text{ s}$
7.94	3.95	61.7	7.19
9.55	4.13	100	9.43
12.0	4.35	135	11.0
18.2	4.48	186	14.0
27.5	5.05	263	17.2
40.7	6.02	----	----

Figure 3.4

Plot of $1/k_{\text{obs}}$ versus $[\text{H}^+]$ for the reaction of SPEN ($2.5 \times 10^{-4} \text{ mol dm}^{-3}$) and piperidine. $[\text{EDTA}] = 1 \times 10^{-4} \text{ mol dm}^{-3}$ and $[\text{amine}]_{\text{T}} = 0.20 \text{ mol dm}^{-3}$

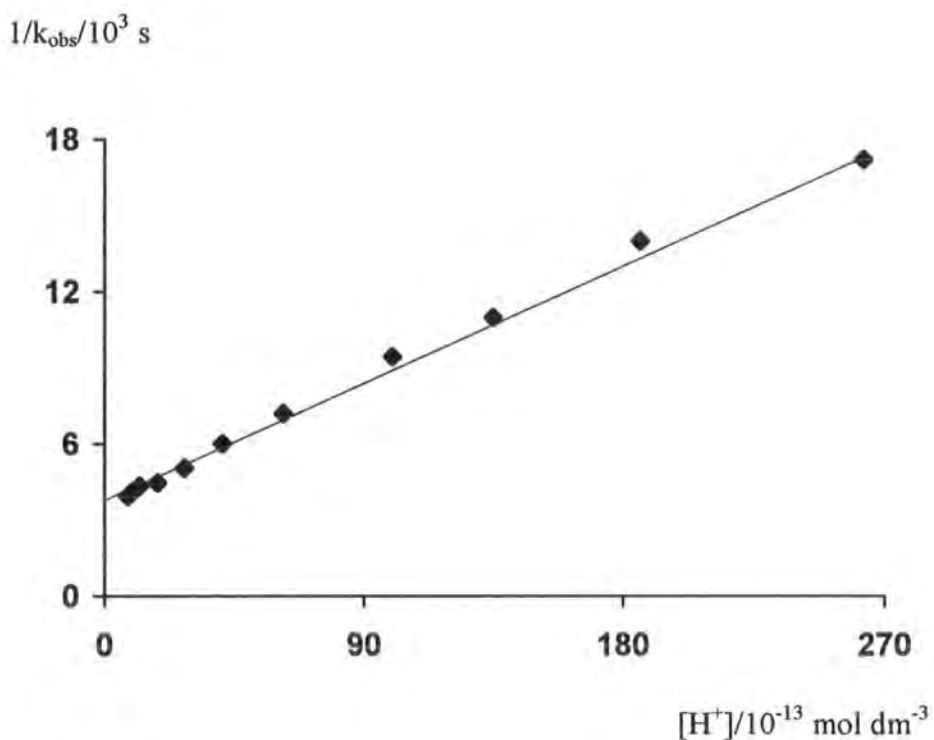


Table 3.5

Amine pK_a values calculated from the reaction of SPEN ($2.5 \times 10^{-4} \text{ mol dm}^{-3}$) with piperidine or pyrrolidine. $[\text{EDTA}] = 1 \times 10^{-4} \text{ mol dm}^{-3}$ and $[\text{amine}]_T = 0.20 \text{ mol dm}^{-3}$

Amine	Calculated pK_a	Literature $pK_a^{10, a}$
Piperidine	11.15	11.12
Pyrrolidine	11.55	11.30

a. Measured in water at 25°C.

3.2.3 Second Order Rate Constants

The relative magnitudes of the second order rate constants (k_2) for the reactions of deprotonated amines with SPEN, could be approximated using equation 3.7 if the gradient (m') of the $k_{\text{obs}} \text{ v } [\text{amine}]_T$ graph was known. This value would afford a true interpretation of the reactivity of the different nucleophiles towards the nitrosothiol. The pH of the reaction medium and amine pK_a had to be known for this purpose. Calculations for piperidine are written as an example in equation 3.12 below.

$$m' = 9.13 \times 10^{-4} \text{ mol}^{-1} \text{ dm}^3 \text{ s}^{-1} = \frac{k_2 K_a}{K_a + [\text{H}^+]} = \frac{k_2 10^{-11.12}}{10^{-11.12} + 10^{-\text{pH}}} \quad \text{eqn 3.12}$$

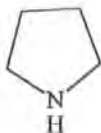
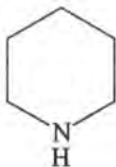
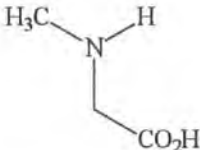
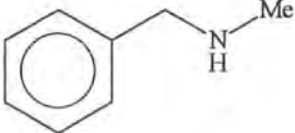
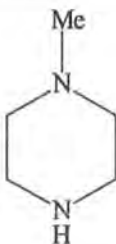
Where $\text{pH} = 11.21$ and $pK_a = 11.12^{10}$

$$\therefore k_2 \sim 1.7 \times 10^{-3} \text{ mol}^{-1} \text{ dm}^3 \text{ s}^{-1}$$

Table 3.6 lists the structures and pK_a values of the selection of amines analysed during this investigation, together with their appropriate rate constants. The estimates of k_2 for pyrrolidine and piperidine were found to complement those derived from the intercept of the $1/k_{\text{obs}} \text{ v } [\text{H}^+]$ plot (equation 3.9).

Table 3.6

Values of k_2 (from equation 3.7) for the reaction of SPEN ($2.5 \times 10^{-4} \text{ mol dm}^{-3}$) and various secondary amines, with $[\text{EDTA}] = 1 \times 10^{-4} \text{ mol dm}^{-3}$

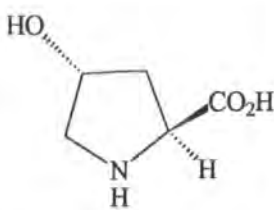
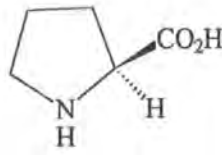
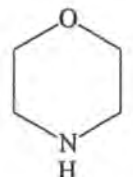
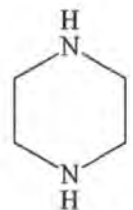
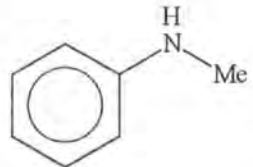
Amine	Structure	pK_a^{10}	k_2 $/\text{mol}^{-1} \text{ dm}^3 \text{ s}^{-1}$	$\log k_2$
Pyrrolidine		11.30	7.2×10^{-3} $7.0 \times 10^{-3}^a$	- 2.14
Piperidine		11.12	1.7×10^{-3} $1.4 \times 10^{-3}^a$	- 2.77
Sarcosine		10.20	1.3×10^{-3}	- 2.89
N-Methyl- benzylamine (measured in 23% v/v 1,4-dioxane ^b)		9.71^4	7.1×10^{-4}	- 3.15
N-Methyl- piperazine		8.98	6.3×10^{-4}	- 3.20

a. Calculated from the reciprocal plot of $1/k_{\text{obs}} \text{ v } [\text{H}^+]$ (equation 3.9).

b. Necessary due to a poor solubility in water.

Table 3.6 (continued)

Values of k_2 (from equation 3.7) for the reaction of SPEN ($2.5 \times 10^{-4} \text{ mol dm}^{-3}$) and various secondary amines, with $[\text{EDTA}] = 1 \times 10^{-4} \text{ mol dm}^{-3}$

Amine	Structure	pK_a^{10}	k_2 / $\text{mol}^{-1} \text{ dm}^3 \text{ s}^{-1}$	$\log k_2$
4-Hydroxy-L-proline		9.66	6.1×10^{-4}	- 3.21
D,L-Proline		10.64	5.8×10^{-4}	- 3.24
Morpholine		8.49	3.8×10^{-4}	- 3.42
Piperazine		9.73	$3.5 \times 10^{-4} \text{ }^c$	- 3.46
N-Methylaniline		4.85	Too slow to measure	----

c. Statistically amended value (due to two identical nucleophilic sites).

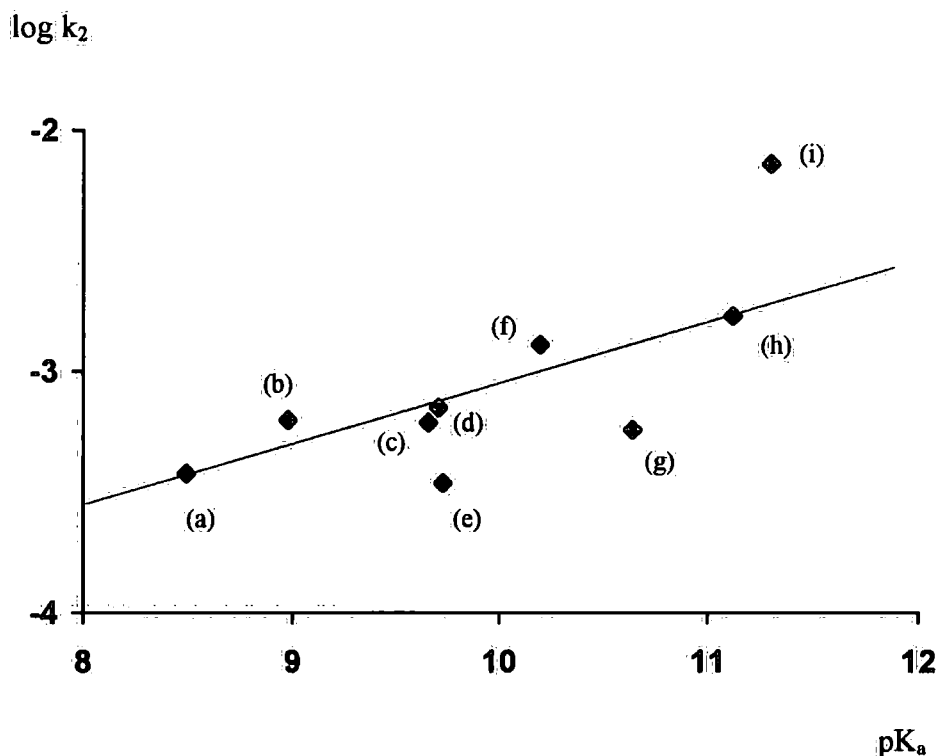
Table 3.6 also states the logarithms of these k_2 values (referred to in section 3.2.4).

3.2.4 Reactivity

The Brønsted plot ($\log k_2$ versus pK_a) that can be constructed for the reaction of SPEN with secondary amines is illustrated in figure 3.5. It is assembled using the $\log k_2$ values tabulated in table 3.6.

Figure 3.5

Brønsted diagram for the reaction between SPEN and secondary amines



(a) Morpholine, (b) N-Methylpiperazine, (c) 4-Hydroxy-L-proline, (d) N-Methylbenzylamine, (e) Piperazine, (f) Sarcosine, (g) D,L-Proline, (h) Piperidine and (i) Pyrrolidine.

A clear relationship between amine basicity and the rate of SPEN decomposition is apparent, with progressively basic amines attacking the S-nitrosothiol more readily. Fitting a straight line to these points gives a Brønsted coefficient (β) of ~ 0.2 , which is numerically smaller than the value of ~ 0.6 revealed for the parallel reactions of secondary amines with MNTS⁴. This parameter indicates on a qualitative scale, that the degree of charge transfer in the activated complexes

(transition states) of the SPEN reactions is less extensive. Such a fact is probably attributable to the strong electron-withdrawing ability of the sulfonyl substituent within the N-nitrososulfonamide.

Pyrrolidine ($k_2 \sim 7.2 \times 10^{-3} \text{ mol}^{-1} \text{ dm}^3 \text{ s}^{-1}$) is distinctly more reactive than any of the other amines in the series examined. This can be reasoned in terms of its smaller molecular size (i.e. a 5-membered heterocyclic ring with no other substituents), and the associated decreased steric hindrance of the nucleophile. Increased steric effects are known to be intrinsic in the inhibition of nitrosation reactions involving amines^{4,11}. Accordingly, the reactivity of D,L-proline ($k_2 \sim 5.8 \times 10^{-4} \text{ mol}^{-1} \text{ dm}^3 \text{ s}^{-1}$) is markedly suppressed, presumably due to the bulky carboxylic acid group adjacent to the amino functionality.

The reaction of SPEN with N-methylaniline (NMA) was far too slow to permit accurate rate measurements. This finding reinforces the notion that there is no direct interaction between SPEN (and therefore S-nitrosothiols) and such a weakly basic amine (delocalisation of the nitrogen lone pair into the aromatic ring greatly reduces basicity). It also substantiates claims by Askew *et al*¹² that when NMA and SNAP react at neutral pH without added EDTA, the oxidised species created via the Cu^{2+} catalysed generation of NO from the RSNO is accountable. Understandably, they found that the removal of O_2 stopped the reaction.

3.2.5 Reaction under Anaerobic Conditions

The reaction between SPEN and pyrrolidine was carried out in deaerated solution¹³ (sections 2.5 and 6.2.2), to offer an experimental insight into whether nitric oxide production was fundamental to the mechanism concerned. This could be inferred if reaction was somehow prevented or hindered in any way (compared to that under normal conditions) by the exclusion of O_2 from the system. The appropriate rate constants are quoted in table 3.7. It is evident that the aerobic ($k_2 \sim 7.2 \times 10^{-3} \text{ mol}^{-1} \text{ dm}^3 \text{ s}^{-1}$) and anaerobic ($k_2 \sim 7.9 \times 10^{-3} \text{ mol}^{-1} \text{ dm}^3 \text{ s}^{-1}$) values are consistent and within experimental error. They conclusively indicate that dissolved molecular oxygen is not a pivotal part of transnitrosation between SPEN and pyrrolidine.

Table 3.7

Comparison of k_2 values for the aerobic/anaerobic reactions of SPEN ($2.5 \times 10^{-4} \text{ mol dm}^{-3}$) and pyrrolidine, with $[\text{EDTA}] = 1 \times 10^{-4} \text{ mol dm}^{-3}$

Amine	Aerobic ^a $k_2/\text{mol}^{-1} \text{ dm}^3 \text{ s}^{-1}$	Anaerobic ^b $k_2/\text{mol}^{-1} \text{ dm}^3 \text{ s}^{-1}$
Pyrrolidine	7.2×10^{-3}	7.9×10^{-3}

a. Calculated at pH 11.57.

b. Calculated at pH 11.68.

3.2.6 Identification of Decomposition Products

3.2.6.1 Nitrogen-Derived Species

Carcinogenic N-nitrosamines (R'RNNNO) are the usual products of the nitrosation of secondary amines by MNTS^{4,14} and other nitrosating agents¹⁵. The different spectroscopic properties of these stable N-nitroso compounds enable their appearance to be distinguished from RSNO decay within the uv region. Nitrosamines exhibit a characteristic absorption peak (λ_{max}) at 230 - 240nm, corresponding to a $\pi \rightarrow \pi^*$ electronic transition within the N=O bond¹⁶. In a similar fashion to RSNOs they also have an absorption maximum at 330 - 350nm due to a $n \rightarrow \pi^*$ transition. Extinction coefficient values are far smaller than those for nitrosothiols at this wavelength however, so allowing the behaviour of SPEN to be monitored at 340nm. Aromatic, alkyl, and aryl substituents influence the nature of these nitrosamine absorption wavelengths and intensities. A few examples are contained in table 3.8.

A series of repeat scan spectra were recorded within the wavelength range 225 - 475nm (time interval = 15 minutes) for the reaction of SPEN and pyrrolidine at $[\text{amine}]_{\text{T}} = 0.06 \text{ mol dm}^{-3}$. The resulting traces (figure 3.6) clearly depict an increase in the large N-nitrosopyrrolidine peak at $\sim 230 - 240\text{nm}$ ($\epsilon \sim 8128 \text{ mol}^{-1} \text{ dm}^3 \text{ cm}^{-1}$), to the expense of the RSNO signal. The rate of formation at 230nm and final absorbance of the reaction mixture (not shown), were further incorporated to prove that nitrosamine creation was quantitative relative to the transfer of $-\text{NO}$ from SPEN.

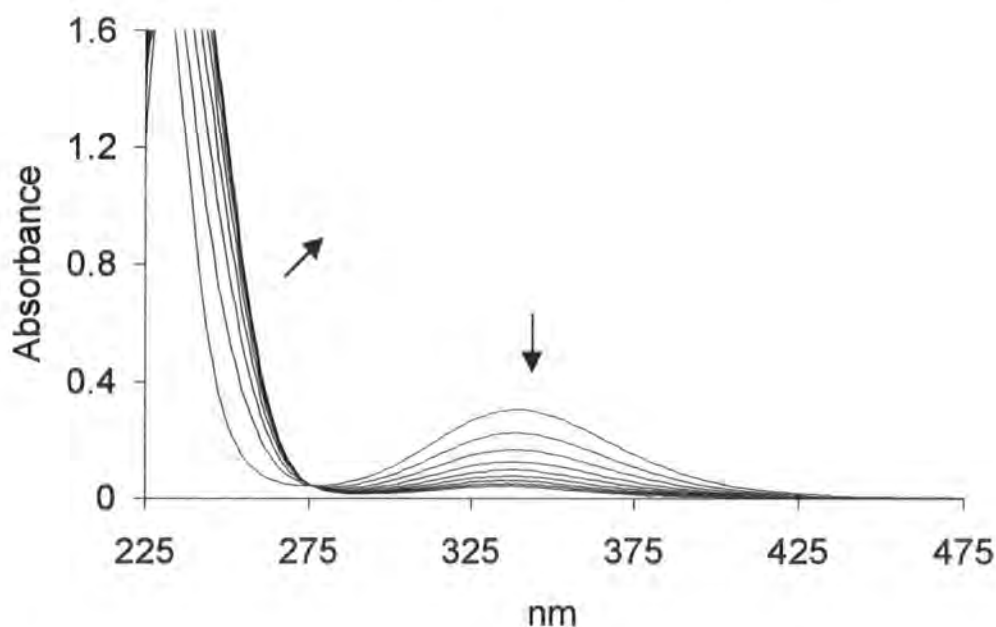
Table 3.8

UV spectral characteristics of some N-nitroso¹⁶ and S-nitroso⁹ compounds in water

Compound	$\lambda_{\text{max}}/\text{nm}$	$\epsilon/\text{mol}^{-1} \text{ dm}^3 \text{ cm}^{-1}$
N-Nitroso- sarcosine pyrrolidine piperidine morpholine	234, 337	5888, 78
	230, 333	8128, 107
	235, 337	9550, 83
	237, 346	7943, 85
S-Nitroso- penicillamine (SPEN)	339, 594	858, 15

Figure 3.6

Repeat scan spectra^a (time interval = 15 minutes) for the reaction of SPEN ($2.5 \times 10^{-4} \text{ mol dm}^{-3}$) and pyrrolidine at pH 11.59. $[\text{EDTA}] = 1 \times 10^{-4} \text{ mol dm}^{-3}$ and $[\text{amine}]_{\text{T}} = 0.06 \text{ mol dm}^{-3}$



a. Unchanged when the reaction is performed under anaerobic conditions.

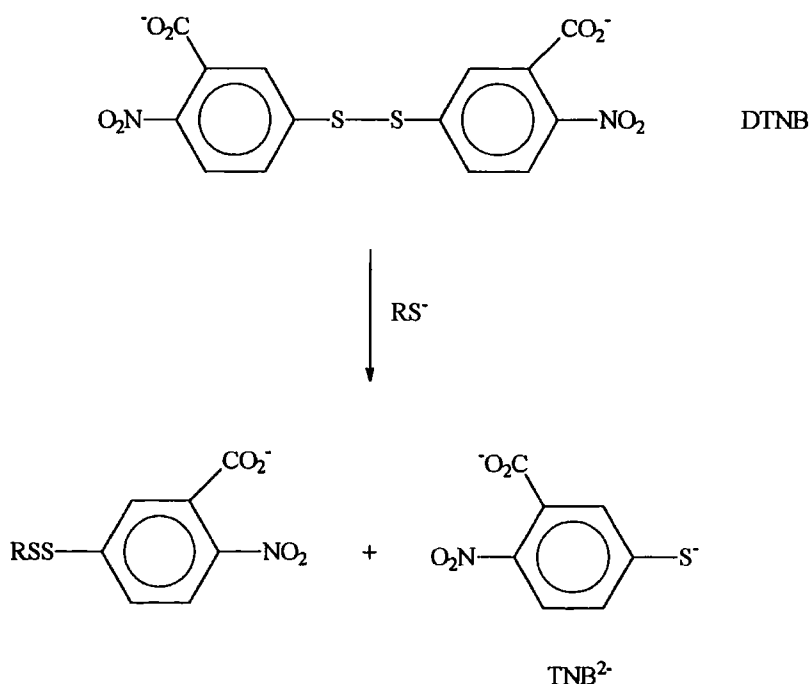
The process does not appear to include any complex kinetics, as an isosbestic point is seen at $\sim 275\text{nm}$.

The reaction of SPEN with pyrrolidine highlighted in figure 3.6 was further analysed in order to evaluate whether NO and NO₂⁻ were developed. Nitric oxide was not detected using a NO-probe during an O₂ deficient reaction (section 6.1.8), and only small amounts of nitrite (< 10%) were found by the conventional diazotisation-azo dye method¹⁷ (sections 2.4.2 and 6.2.1.2). This NO₂⁻ can be explained by another factor that will be described in more detail in section 3.2.9.

Similar spectral changes and product distributions were always seen when test samples involving secondary amines were assayed.

3.2.6.2 Sulfur-Derived Species

Ellman's reagent¹⁸ (5,5'-dithiobis(2-nitrobenzoic acid), DTNB) was employed to establish the final thiolate content within the reaction mixture referred to in figure 3.6. This diagnostic procedure involves reacting DTNB with any free thiol, to give the 2-nitro-5-mercaptobenzoate dianion (TNB²⁻) and a mixed disulfide (equation 3.13).



eqn 3.13

TNB²⁻ has an intense yellow colour and exhibits a λ_{max} at 412nm in the visible spectrum. This is a quantitative measure of thiol concentration. Consequently, authentic solutions of RSH (D,L-penicillamine) can be used to ascertain the molar extinction coefficient ($\epsilon_{412\text{nm}}$) of TNB²⁻ at this wavelength in pH 7.4 buffer (table 3.9).

Table 3.9
Calibration data used in the calculation of $\epsilon_{412\text{nm}}$

[RSH]/10 ⁻⁵ mol dm ⁻³	Absorbance (412nm)
2.0	0.353
3.0	0.502
4.0	0.657
5.0	0.784
6.0	0.921

$$\epsilon_{412\text{nm}} = 14180 \pm 299 \text{ mol}^{-1} \text{ dm}^3 \text{ cm}^{-1}$$

A calculated $\epsilon_{412\text{nm}}$ of 14180 mol⁻¹ dm³ cm⁻¹ is in accordance with the values cited in the chemical literature¹⁹ ($\epsilon_{412\text{nm}} \sim 11000 - 14200 \text{ mol}^{-1} \text{ dm}^3 \text{ cm}^{-1}$ at 25°C).

One could apply $\epsilon_{412\text{nm}}$ to an assessment of [RSH] in the reaction products (see also section 6.2.1.3). Alkaline solutions had to be standardised for this purpose, via neutralisation of excess/free amine and pH adjustment to 7.4. The extent and change of the thiolate yield over time is reported in table 3.10.

Penicillamine does not immediately appear to be a major constituent of the end products. The quantity detected also seems to be inversely proportional to the time elapsed. It is however reasonable to expect that a large proportion of any RSH manufactured is oxidised to disulfide over the lengthy time period between reaction initiation and testing. It is well known that a basic pH promotes the conversion of thiols (e.g. glutathione²⁰) into RSSR.

Table 3.10

Thiol produced as a function of time from the reaction of SPEN
 ($2.5 \times 10^{-4} \text{ mol dm}^{-3}$) and pyrrolidine at pH 11.59.
 $[\text{EDTA}] = 1 \times 10^{-4} \text{ mol dm}^{-3}$ and $[\text{amine}]_{\text{T}} = 0.06 \text{ mol dm}^{-3}$

Time/hours ^a	%RS ^b
24	24.1
48	14.2
72	9.9

a. Time after reaction started.

b. A percentage of the maximum concentration of D,L-penicillamine that can yield from SPEN.

Disulfide (~ 70%) was characterised via the spectrophotometric technique of Cu^{2+} -complexation defined in sections 2.4.4 and 5.3.1.4. A commercial sample of D-penicillamine disulfide was purchased (Sigma-Aldrich) as a reference.

3.2.7 Activation Parameters of Reaction

It was hoped that a knowledge of the fundamental thermodynamics involved in the reaction between SPEN and a secondary amine, would enable further mechanistic information to be derived. Thermodynamic details can be interpreted from rate data via incorporation of the Arrhenius relationship (equation 3.14).

$$\ln k = \ln A - \frac{E_a}{RT} \quad \text{eqn 3.14}$$

Where k = rate constant and R (gas constant) = $8.3145 \text{ J K}^{-1} \text{ mol}^{-1}$

A plot of $\ln k$ against $1/T$ should give a straight line (or a curve for more complicated processes), from which the activation energy (E_a) and pre-exponential factor (A) of reaction can be determined (equations 3.15 – 3.16).

$$\text{slope} = -\frac{E_a}{R} \quad \text{eqn 3.15}$$

$$\text{y-axis intercept} = \ln A \quad \text{eqn 3.16}$$

For this reason a series of second order rate constants (k_2) representing nitrosothiol decomposition were collected, via the treatment of SPEN ($2.5 \times 10^{-4} \text{ mol dm}^{-3}$) with pyrrolidine at 32, 36, 40 and 44°C (table 3.11). The temperature range studied was limited, as thermal RSNO decay becomes significant at $> 44^\circ\text{C}$.

Table 3.11

k_2 as a function of temperature (T) for the reaction of SPEN ($2.5 \times 10^{-4} \text{ mol dm}^{-3}$) and pyrrolidine, with $[\text{EDTA}] = 1 \times 10^{-4} \text{ mol dm}^{-3}$

T/K	pH ^a	pK _a ¹⁰	m ¹ b /10 ⁻³ mol ⁻¹ dm ³ s ⁻¹	k ₂ /mol ⁻¹ dm ³ s ⁻¹
305	11.14	11.08	5.21 ± 0.04	9.7 × 10 ⁻³
309	11.07	10.96	7.09 ± 0.03	1.3 × 10 ⁻²
313	10.93	10.84	8.77 ± 0.05	1.6 × 10 ⁻²
317	10.82	10.73	10.4 ± 0.1	1.9 × 10 ⁻²

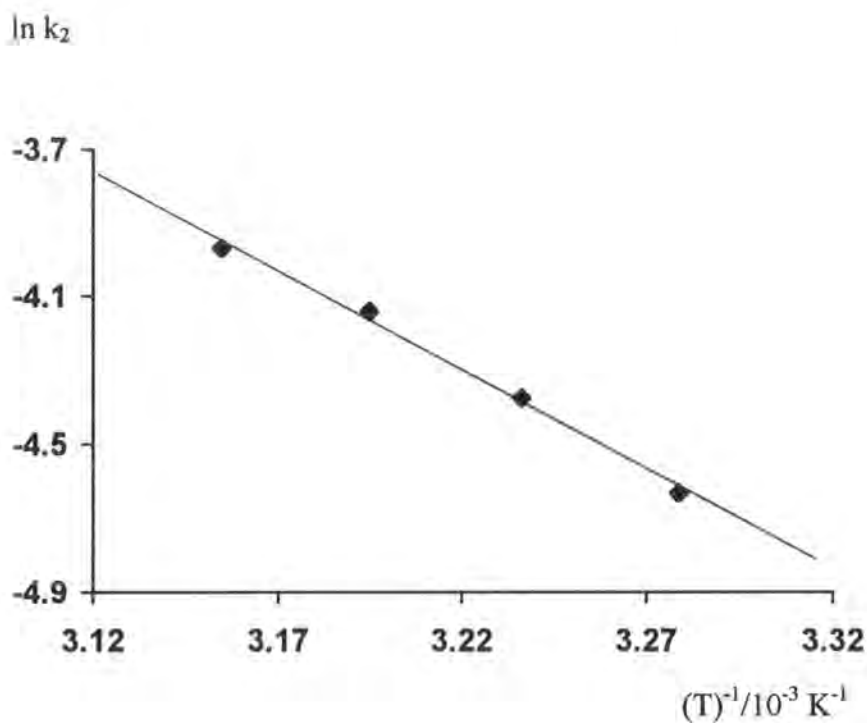
a. pH of reaction mixture.

b. Gradient of $k_{\text{obs}} \nu [\text{amine}]_T$ plot.

Figure 3.7 shows the relevant Arrhenius diagram. It appears that the temperature dependence of the reaction of SPEN and pyrrolidine does not deviate too much from simple Arrhenius behaviour.

Figure 3.7

Arrhenius plot for the reaction of SPEN and pyrrolidine



Extrapolation of the data points indicates that $k_2 \sim 6.6 \times 10^{-3} \text{ mol}^{-1} \text{ dm}^3 \text{ s}^{-1}$ at 25°C . This conforms with the k_2 value of $7.2 \times 10^{-3} \text{ mol}^{-1} \text{ dm}^3 \text{ s}^{-1}$ obtained for pyrrolidine during the separate structure-reactivity study summarised in table 3.6.

Calculated values of E_a and A (a measure of collision frequency) for this reaction are quite small (table 3.12).

Table 3.12

 E_a and A for the reaction of SPEN and pyrrolidine

E_a /kJ mol ⁻¹	A /10 ⁵ mol ⁻¹ dm ³ s ⁻¹
44.9	4.9

The application of transition state theory and substitution of these parameters into mathematical expressions such as the Eyring equation (equation 3.17), means that more thermodynamic quantities can be calculated for this transnitrosation reaction at 298K (equations 3.18 – 3.19). These terms include the enthalpy (ΔH^\ddagger) and entropy of activation (ΔS^\ddagger), as well as the Gibbs energy of activation (ΔG^\ddagger_{298K}) (table 3.13).

$$k = \frac{k_B T}{h} e^{\Delta S^\ddagger/R} e^{-\Delta H^\ddagger/RT} \quad \text{eqn 3.17}$$

$$\Delta H^\ddagger = E_a - RT \quad \text{eqn 3.18}$$

$$\Delta G^\ddagger_{298K} = \Delta H^\ddagger - T\Delta S^\ddagger \quad \text{eqn 3.19}$$

Where k_B (Boltzmann constant) = $1.381 \times 10^{-23} \text{ J K}^{-1}$
 h (Planck constant) = $6.626 \times 10^{-34} \text{ J s}$
 $k = k_2$ (pyrrolidine) at 298K = $6.6 \times 10^{-3} \text{ mol}^{-1} \text{ dm}^3 \text{ s}^{-1}$

Table 3.13

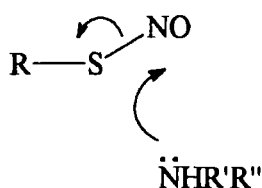
ΔH^\ddagger , ΔS^\ddagger , and ΔG^\ddagger_{298K} for the reaction of SPEN and pyrrolidine

ΔH^\ddagger /kJ mol ⁻¹	ΔS^\ddagger /J K ⁻¹ mol ⁻¹	ΔG^\ddagger_{298K} /kJ mol ⁻¹
42.4	- 144	85.3

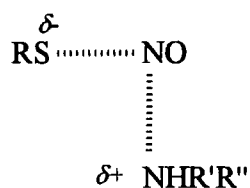
Only limited conclusions can be drawn from these empirical results. One point of note is that ΔS^\ddagger is negative and relatively large. This suggests that the reaction mechanism may resemble a S_N2 type process, in which the transition state involves a high degree of association during the accommodation of both reactants.

3.2.8 Deduced Reaction Mechanism

On the basis of the experimental data gathered using an array of secondary amines, there is little doubt that the nucleophilic sites of these neutral molecules directly attack the nitroso nitrogen atom of SPEN (3.4) via a pathway that precludes NO production. At this stage we have no evidence for the existence of a discrete intermediate. A purely hypothetical representation of the intermediate/transition state that could be involved is given below (3.5), but additional work is needed to clarify the exact nature of this species.

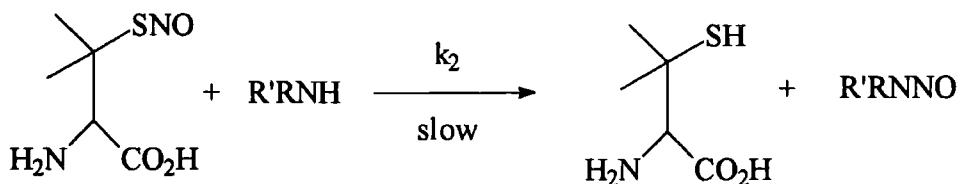


3.4

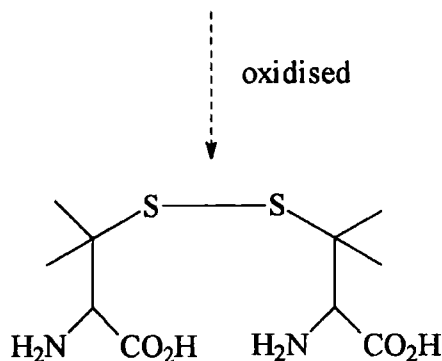


3.5

Exchange of the $-NO$ substituent to the amine furnishes a stable N-nitrosamine (scheme 3.1). Penicillamine also originates from the breakdown of SPEN, but at pH 8 - 12 is most likely transformed into the corresponding disulfide.



Scheme 3.1



3.2.9 Alkaline Hydrolysis

When k_{obs} was plotted versus $[\text{amine}]_{\text{T}}$ to obtain the k_2 values discussed in section 3.2.3, the lines of best fit through the data acquired from the less reactive nucleophiles (tables 3.14 – 3.16) did not pass through the origin (cf. pyrrolidine and piperidine). Instead, a significant positive intercept (c) on the y-axis was noticeable at $[\text{amine}]_{\text{T}} = 0 \text{ mol dm}^{-3}$ (figure 3.8 and table 3.17).

Table 3.14

Kinetic data for the reaction of SPEN ($2.5 \times 10^{-4} \text{ mol dm}^{-3}$) and morpholine at pH 8.73, with $[\text{EDTA}] = 1 \times 10^{-4} \text{ mol dm}^{-3}$

$[\text{amine}]_{\text{T}}/\text{mol dm}^{-3}$	$k_{\text{obs}}/10^{-5} \text{ s}^{-1}$
0.09	5.20 ± 0.07
0.12	5.87 ± 0.06
0.18	7.33 ± 0.03
0.21	8.05 ± 0.03

Table 3.15

Kinetic data for the reaction of SPEN ($2.5 \times 10^{-4} \text{ mol dm}^{-3}$) and piperazine at pH 9.91, or 4-hydroxy-L-proline at pH 9.77, with $[\text{EDTA}] = 1 \times 10^{-4} \text{ mol dm}^{-3}$

$[\text{amine}]_{\text{T}}/\text{mol dm}^{-3}$	Piperazine $k_{\text{obs}}/10^{-5} \text{ s}^{-1}$	4-Hydroxy-L-proline $k_{\text{obs}}/10^{-4} \text{ s}^{-1}$
0.06	5.34 ± 0.06	1.04 ± 0.02
0.09	7.13 ± 0.06	1.23 ± 0.02
0.12	7.71 ± 0.06	1.31 ± 0.02
0.15	9.40 ± 0.09	1.40 ± 0.02
0.21	11.7 ± 0.2	1.57 ± 0.02

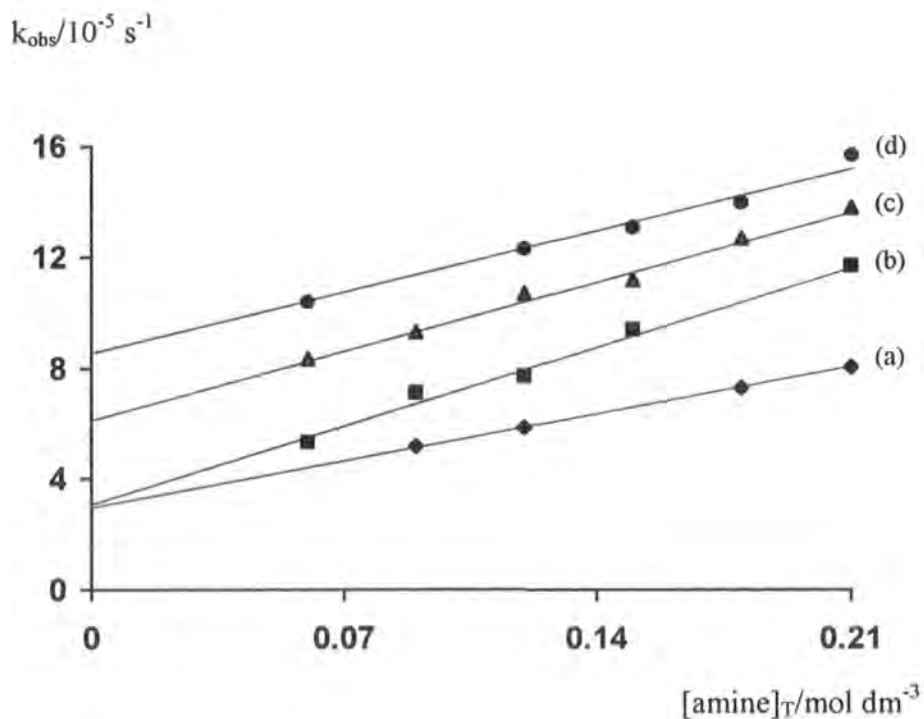
Table 3.16

Kinetic data for the reaction of SPEN ($2.5 \times 10^{-4} \text{ mol dm}^{-3}$) and D,L-proline at pH 10.86, with $[\text{EDTA}] = 1 \times 10^{-4} \text{ mol dm}^{-3}$

$[\text{amine}]_{\text{T}}/\text{mol dm}^{-3}$	$k_{\text{obs}}/10^{-5} \text{ s}^{-1}$
0.06	8.34 ± 0.10
0.09	9.30 ± 0.13
0.12	10.7 ± 0.2
0.15	11.2 ± 0.2
0.18	12.7 ± 0.2
0.21	13.8 ± 0.2

Figure 3.8

Y-axis intercepts evident when plotting k_{obs} against $[\text{amine}]_{\text{T}}$ for the reactions of SPEN ($2.5 \times 10^{-4} \text{ mol dm}^{-3}$) and some secondary amines, with $[\text{EDTA}] = 1 \times 10^{-4} \text{ mol dm}^{-3}$



(a) Morpholine, (b) Piperazine, (c) D,L-Proline and (d) 4-Hydroxy-L-proline.



To date however the alkaline hydrolysis of S-nitrosothiols has not been examined. A set of independent experiments were therefore devised to inspect the true effect of OH^- upon the stability of $2.5 \times 10^{-4} \text{ mol dm}^{-3}$ SPEN in water ($1 \times 10^{-4} \text{ mol dm}^{-3}$ EDTA present). This involved analysing the influence of $[\text{OH}^-]$ upon the observed pseudo-first order rate constant (k_{obs}) accounting for RSNO decay (table 3.18). For this purpose, added NaOH was systematically varied between 0.058 - 0.202 mol dm^{-3} , but ionic strength kept constant at $0.202 \text{ mol dm}^{-3}$. Kinetically, the reaction was very clean and strictly first order in SPEN.

Table 3.18

Kinetic data for the reaction of SPEN ($2.5 \times 10^{-4} \text{ mol dm}^{-3}$) and sodium hydroxide, with $[\text{EDTA}] = 1 \times 10^{-4} \text{ mol dm}^{-3}$

$[\text{OH}^-]/10^{-2} \text{ mol dm}^{-3}$	$k_{\text{obs}}/10^{-4} \text{ s}^{-1}$
5.8	1.67 ± 0.01
8.7	2.30 ± 0.01
11.5	2.97 ± 0.01
14.4	3.62 ± 0.01
17.3	4.22 ± 0.03
20.2	4.79 ± 0.03

The rate equation can now be written as;

$$\text{Rate} = k_{\text{OH}}[\text{SPEN}][\text{OH}^-] + k'[\text{SPEN}] \quad \text{eqn 3.21}$$

As $[\text{OH}^-] \gg [\text{SPEN}]$;

$$\text{Rate} = k_{\text{obs}} [\text{SPEN}] \quad \text{eqn 3.22}$$

Therefore,

$$k_{\text{obs}} = k_{\text{OH}} [\text{OH}^-] + k' \quad \text{eqn 3.23}$$

A graph of k_{obs} against $[\text{OH}^-]$ was linear as expected (figure 3.9), with the gradient denoting the second order (hydrolysis) rate constant of SPEN (k_{OH}) (table 3.19). It is likely that the thermal reaction partly contributes to the slight intercept (k').

Figure 3.9

Effect of $[\text{OH}^-]$ on k_{obs} in the alkaline hydrolysis of SPEN ($2.5 \times 10^{-4} \text{ mol dm}^{-3}$),
with $[\text{EDTA}] = 1 \times 10^{-4} \text{ mol dm}^{-3}$

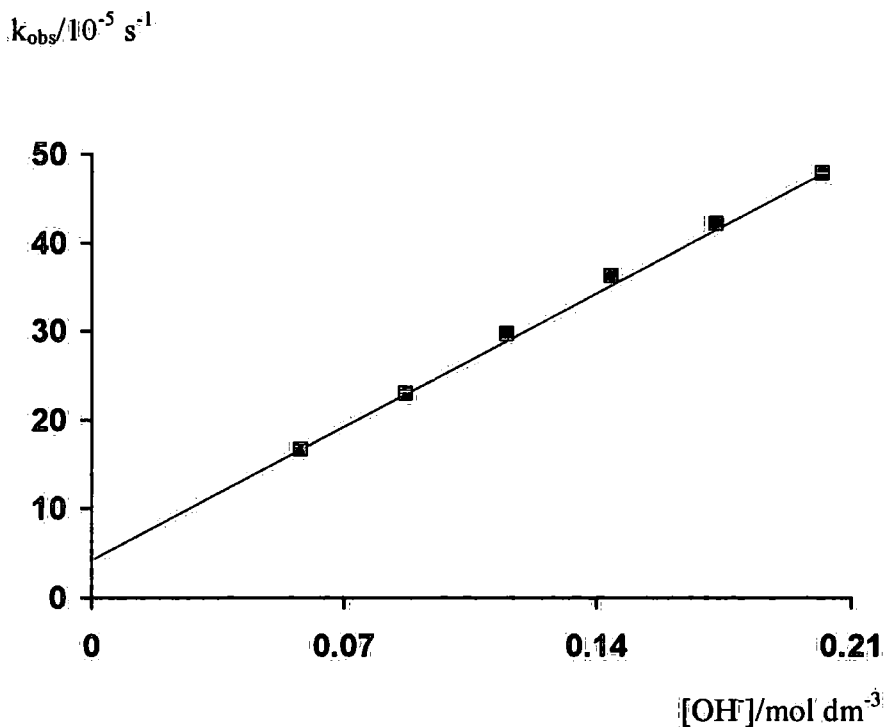


Table 3.19
Value of k_{OH} determined for SPEN

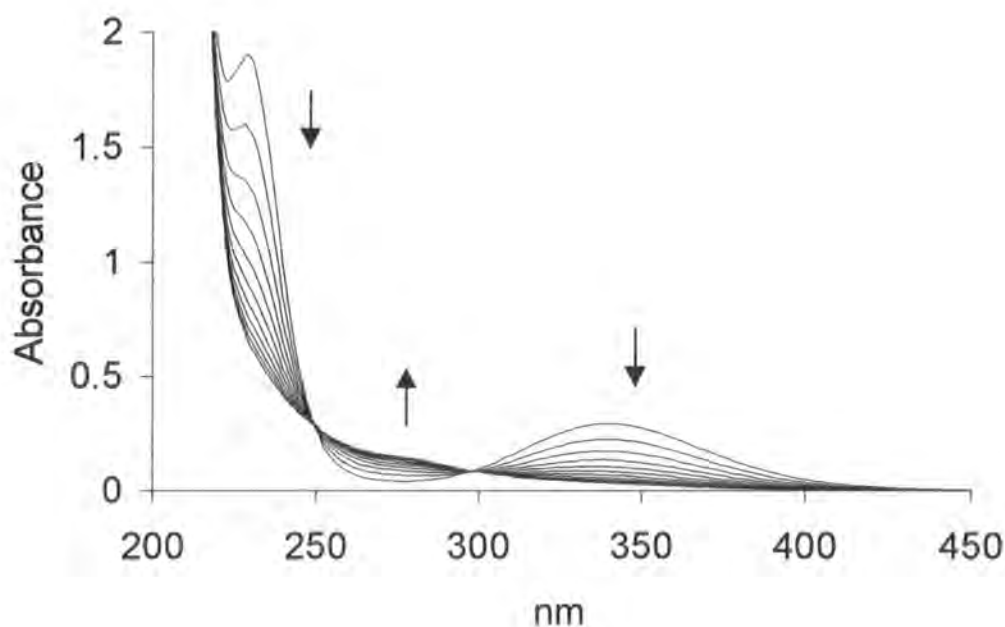
k_{OH} $/10^{-3} \text{ mol}^{-1} \text{ dm}^3 \text{ s}^{-1}$
2.18 ± 0.04

The size of k_{OH} suggests that base hydrolysis is a significant component of the decomposition of SPEN in amine buffers at 25°C. Together with thermal effects, it is responsible for the intercepts witnessed.

The time-dependent uv-visible spectra of the reaction at $[OH^-] = 0.115 \text{ mol dm}^{-3}$ are indicated in figure 3.10. Decreases in the SPEN absorbance peaks at 340 and 230nm are obvious (the latter maximum is not recognisable when amines are used at high concentration, as they absorb too strongly within this uv region).

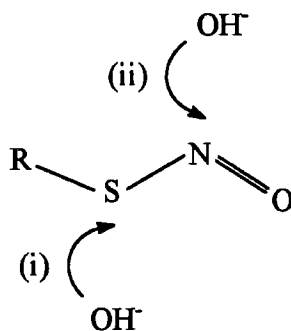
Figure 3.10

Repeat scan spectra (time interval = 15 minutes) of the reaction between SPEN ($2.5 \times 10^{-4} \text{ mol dm}^{-3}$) and OH^- ($0.115 \text{ mol dm}^{-3}$), with $[EDTA] = 1 \times 10^{-4} \text{ mol dm}^{-3}$



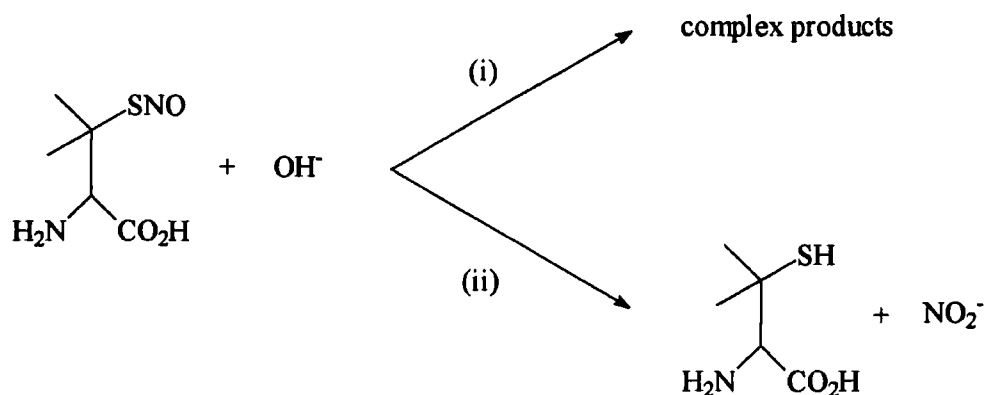
Isosbestic points are found at 250 and 298nm, but more intriguingly an appreciable absorbance increase seen at $\lambda \sim 275\text{nm}$. Thorough investigations were unable to confirm the identity of this species. Many products that could be formed from penicillamine, disulfide, NaOH and NaCl, were considered.

Typically, only $\sim 50\%$ NO_2^- was detected in the final test mixtures following alkaline hydrolysis. It is conceivable that further complex chemistry accounts for the missing nitrogen content and the previously mentioned spectral change. Pearson's classification of Lewis bases²² can be applied to offer a plausible explanation of these findings. It is possible that unlike the so-called 'softer' amine nucleophiles, which interact with what is imagined as a relatively 'soft' nitroso-nitrogen atom, the 'harder' OH nucleophile can attack the comparatively 'hard' sulfur atom of SPEN. This is a common feature of reactions involving OH^- or OEt^- and MNTS^{4,23}. Some nucleophiles are however capable of interacting with the two electrophilic sites in MNTS. SPEN could perhaps therefore act as an ambidentate electrophile, exhibiting both S- and N-sites that can partake in exchanges with the hydroxide ion (3.6).



3.6

Reaction via path (i) might lead to nitroxyl anion (NO^-) and nitrous oxide (N_2O), i.e. the absent nitrogenous molecules. It seems logical though, that the main hydrolysis reaction passes via route (ii). In an analogous fashion to alkyl nitrites this would create thiol and nitrite (scheme 3.3). Penicillamine was measured at 15%, but extensive oxidation to RSSR would be anticipated in pH 13 - 14 solution (as stated in section 3.2.6.2).



Scheme 3.3

3.3 Reactions of Primary Amines

3.3.1 Interactions at Low Amine Concentration

3.3.1.1 Effect of pH and Amine Basicity upon Reactivity

SPEN was reacted with a range of primary aliphatic amines (RNH_2) via the method defined for secondary amines in section 3.2. Reaction conditions were otherwise unchanged ([EDTA], ionic strength etc.). The nucleophiles chosen were isobutylamine, propylamine, ethylamine, ethylenediamine, *sec*-butylamine, isopropylamine, and *tert*-butylamine.

The behaviour of the primary amines was very similar to that of their secondary equivalents. In each instance a plot of $1/k_{\text{obs}}$ versus $[\text{H}^+]$ (not included) distinguished the free amine as the reactive species. Estimated pK_a values of the protonated amines were close to those given in the literature (table 3.20).

At lower concentrations of added primary amine ($[\text{amine}]_{\text{T}} \leq 0.09 \text{ mol dm}^{-3}$), the usual linear dependence of k_{obs} on $[\text{amine}]_{\text{T}}$ was observed (e.g. tables 3.21 – 3.23). As before, second order rate constants could then be evaluated using equation 3.7 (table 3.24).

Table 3.20

Amine pK_a values calculated from the reaction of SPEN ($2.5 \times 10^{-4} \text{ mol dm}^{-3}$) with ethylamine or isobutylamine. $[\text{EDTA}] = 1 \times 10^{-4} \text{ mol dm}^{-3}$ and $[\text{amine}]_T = 0.06 \text{ mol dm}^{-3}$

Amine	Calculated pK_a	Literature pK_a^{10}
Ethylamine	10.49	10.64
Isobutylamine	10.28	10.48

Table 3.21

Kinetic data for the reaction of SPEN ($2.5 \times 10^{-4} \text{ mol dm}^{-3}$) and isopropylamine at pH 10.70, with $[\text{EDTA}] = 1 \times 10^{-4} \text{ mol dm}^{-3}$

$[\text{amine}]_T/10^{-2} \text{ mol dm}^{-3}$	$k_{\text{obs}}/10^{-5} \text{ s}^{-1}$
3.0	3.49 ± 0.04
4.5	3.78 ± 0.05
7.5	4.30 ± 0.05
9.0	4.47 ± 0.10

Table 3.22

Kinetic data for the reaction of SPEN ($2.5 \times 10^{-4} \text{ mol dm}^{-3}$) and *tert*-butylamine at pH 10.71, with $[\text{EDTA}] = 1 \times 10^{-4} \text{ mol dm}^{-3}$

$[\text{amine}]_T/10^{-2} \text{ mol dm}^{-3}$	$k_{\text{obs}}/10^{-5} \text{ s}^{-1}$
3.0	1.04 ± 0.10
6.0	1.32 ± 0.13
7.5	1.48 ± 0.13
9.0	1.57 ± 0.14

Table 3.23

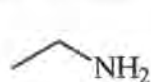
Kinetic data for the reaction of SPEN ($2.5 \times 10^{-4} \text{ mol dm}^{-3}$) and ethylamine at pH 10.82, with $[\text{EDTA}] = 1 \times 10^{-4} \text{ mol dm}^{-3}$

$[\text{amine}]_{\text{T}}/10^{-2} \text{ mol dm}^{-3}$	$k_{\text{obs}}/10^{-5} \text{ s}^{-1}$
1.5	2.92 ± 0.09
3.0	3.25 ± 0.10
4.5	3.86 ± 0.08
6.0	4.00 ± 0.08
7.5	4.52 ± 0.09
9.0	5.24 ± 0.08

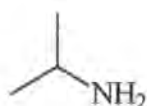
Primary and secondary amines of comparable basicity are almost equally reactive towards SPEN, e.g. k_2 of isobutylamine (pK_a 10.48) = $8.9 \times 10^{-4} \text{ mol}^{-1} \text{ dm}^3 \text{ s}^{-1}$ and k_2 of sarcosine (pK_a 10.20) = $1.3 \times 10^{-3} \text{ mol}^{-1} \text{ dm}^3 \text{ s}^{-1}$. The Brønsted plot (figure 3.11) that can be drawn for primary amines discloses however, that there is no straightforward connection between $\log k_2$ and pK_a (although only a small pK_a range was covered). The lack of a relationship contrasts the correlation that is prominent in the study using secondary amines. Leis *et al*⁴ obtained matching results using MNTS.

Within the primary amine structures examined, reactivity is dependent upon the nature of the α -carbon atom next to the $-\text{NH}_2$ group. Molecules in which this is a primary centre tend to be more reactive than those of a similar basicity in which it is secondary, which in turn are more reactive than those in which it is tertiary, e.g. k_2 of ethylamine > isopropylamine > *tert*-butylamine (figure 3.12). Such observations during the N-nitrosation of amines¹¹ and transnitrosation between nitrosothiols and thiols²⁴ (section 1.3.5.2), have been explained by steric effects.

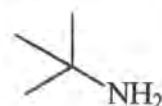
more reactive



>



>

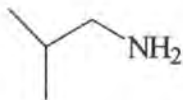

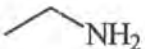
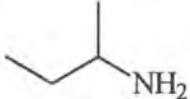
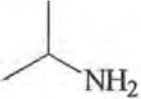

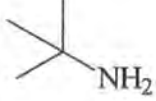


less reactive

Figure 3.12

Table 3.24

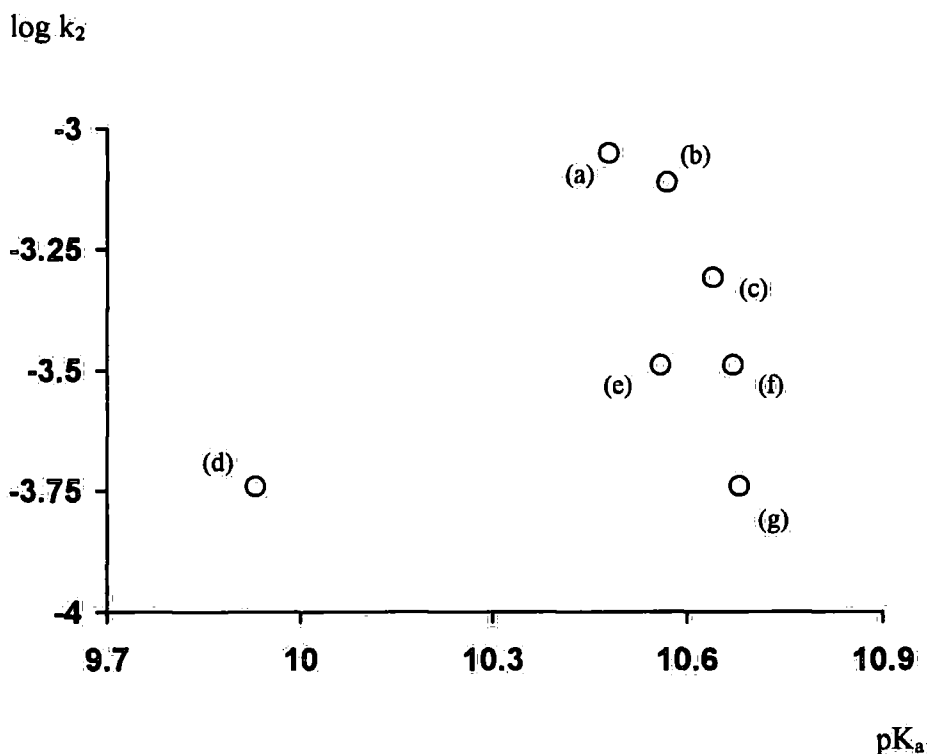
Values of k_2 (from equation 3.7) for the reaction of SPEN ($2.5 \times 10^{-4} \text{ mol dm}^{-3}$) and various primary amines, with $[\text{EDTA}] = 1 \times 10^{-4} \text{ mol dm}^{-3}$

Amine	Structure	pK_a^{10}	k_2 / $\text{mol}^{-1} \text{ dm}^3 \text{ s}^{-1}$	$\log k_2$
Isobutylamine		10.48	8.9×10^{-4}	- 3.05
Propylamine		10.57	7.8×10^{-4}	- 3.11
Ethylamine		10.64	4.9×10^{-4}	- 3.31
<i>sec</i> -Butylamine		10.56	3.2×10^{-4}	- 3.49
Isopropylamine		10.67	3.2×10^{-4}	- 3.49
Ethylenediamine		9.93	1.8×10^{-4} ^a	- 3.74
<i>tert</i> -Butylamine		10.68	1.8×10^{-4}	- 3.74

a. Statistically amended value (due to two identical nucleophilic sites).

Figure 3.11

Brønsted diagram for the reaction between SPEN and primary amines



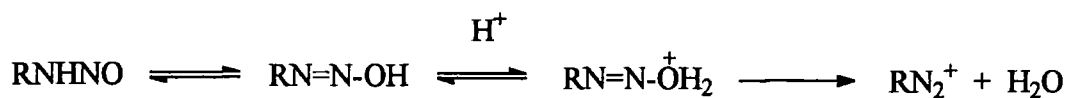
(a) Isobutylamine, (b) Propylamine, (c) Ethylamine, (d) Ethylenediamine, (e) *sec*-Butylamine, (f) Isopropylamine and (g) *tert*-Butylamine.

3.3.1.2 End Products

The quantities of nitrite, nitric oxide, thiol, and disulfide, found in the decay products of the reaction between SPEN and primary amines, were unchanged relative to those created from the corresponding reactions involving secondary amines (section 3.2.6). Nevertheless, a major difference was immediately conspicuous as the reactions were monitored spectrophotometrically (spectra not shown). The N-nitrosamine absorbance maximum at $\lambda \sim 230 - 240\text{nm}$ was not formed when ethylamine (at pH 10.72), isobutylamine (at pH 10.60), and propylamine (at pH 10.82), were introduced at $[\text{amine}]_T = 0.06 \text{ mol dm}^{-3}$ to induce the decomposition of $2.5 \times 10^{-4} \text{ mol dm}^{-3}$ SPEN. No other species were detected.

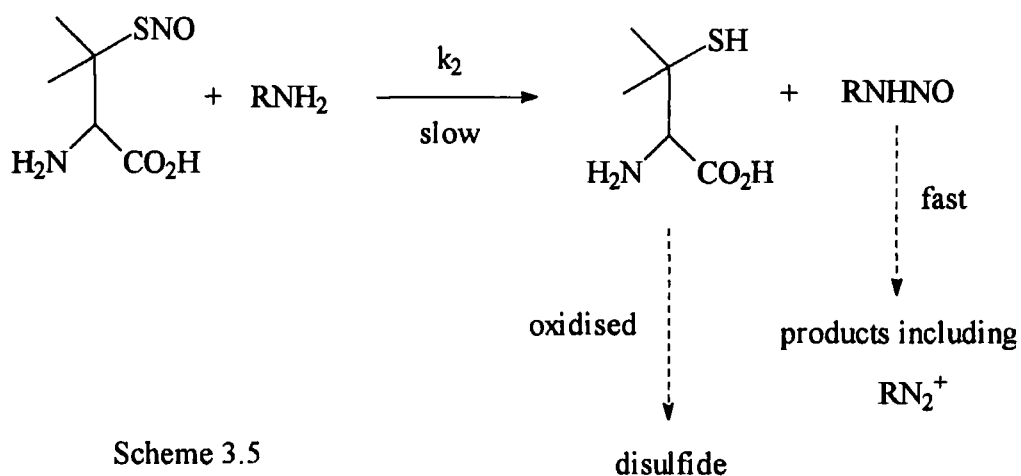
3.3.1.3 Proposed Mechanism of Deamination

The nitrosation of primary aliphatic amines using nitrous acid leads to a number of deamination products²⁵. Primary nitrosamines (RNHNO) that arise from the initial rate-limiting step normally decompose to diazonium ions (RN_2^+), via a succession of fast reactions that comprise proton transfer and loss of a water molecule (scheme 3.4). Secondary nitrosamines are unreactive (as considered earlier), as the absence of a α -hydrogen atom prohibits proton transfer.



Scheme 3.4

A version of scheme 3.4 has been interpreted as a legitimate route to the final products in the reactions of MNTS/alkyl nitrites with primary amines at a basic pH^4 . Our own product inspection, although not performed in any depth, supports this concept. The reactions of SPEN and RNH_2 (at low concentration) possibly pass via the path outlined in scheme 3.5. The only amendment to the reaction postulated for secondary amines, is the ultimate fate of RNHNO.



3.3.2 Interactions at High Amine Concentration

3.3.2.1 Kinetic Characteristics

At $[\text{amine}]_T \geq 0.09 \text{ mol dm}^{-3}$ every plot of $k_{\text{obs}} \text{ v } [\text{amine}]_T$ for the reaction of primary amines and SPEN, became curved and levelled off at a limiting k_{obs} value. Lines of best fit were now no longer linear. The reaction of SPEN with propylamine is an example that demonstrates this tendency of the rate constant to plateau (at $k_{\text{obs}} \sim 7 \times 10^{-5} \text{ s}^{-1}$ in this case) (table 3.25 and figure 3.13). Secondary amines did not show this feature.

Table 3.25

Kinetic data for the reaction of SPEN ($2.5 \times 10^{-4} \text{ mol dm}^{-3}$) and propylamine at pH 10.90, with $[\text{EDTA}] = 1 \times 10^{-4} \text{ mol dm}^{-3}$

$[\text{amine}]_T/\text{mol dm}^{-3}$	$k_{\text{obs}}/10^{-5} \text{ s}^{-1}$
0.06	3.88 ± 0.04
0.09	5.63 ± 0.04
0.12	6.68 ± 0.04
0.15	6.90 ± 0.05
0.18	7.06 ± 0.05
0.21	7.55 ± 0.05

Replacement of the primary amines by ammonia (i.e. RNH_2 where $\text{R} = \text{H}$, $\text{pK}_a \sim 9.24^{26}$) caused a considerable increase in the relative rate of SPEN decomposition (a ten fold increase in k_{obs}). Despite this, all k_{obs} values calculated for the reaction of this nucleophile with SPEN were approximately constant ($k_{\text{obs}} \sim 5 \times 10^{-4} \text{ s}^{-1}$) and independent of added amine concentration (table 3.26, where $[\text{NH}_3]_T \equiv [\text{amine}]_T$). Presumably therefore, the curvature of the k_{obs} vs $[\text{NH}_3]_T$ graph is even more pronounced for NH_3 . The size of k_2 could not be assessed, even at $[\text{NH}_3]_T \leq 0.09 \text{ mol dm}^{-3}$.

Figure 3.13

Plot of k_{obs} against $[\text{amine}]_{\text{T}}$ for the reaction of SPEN ($2.5 \times 10^{-4} \text{ mol dm}^{-3}$) and propylamine, with $[\text{EDTA}] = 1 \times 10^{-4} \text{ mol dm}^{-3}$

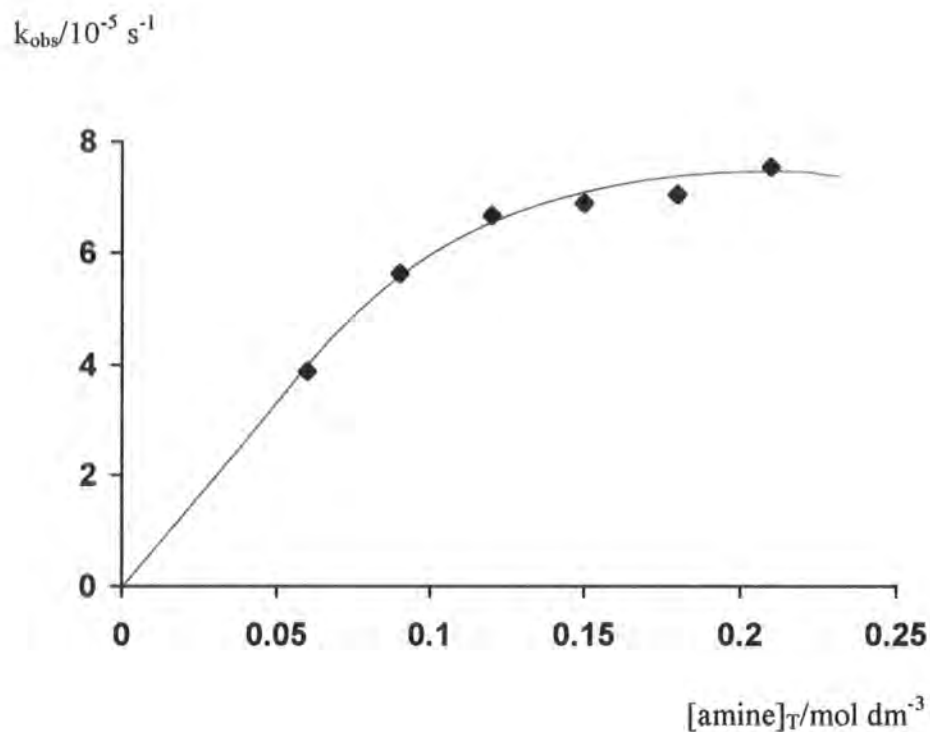


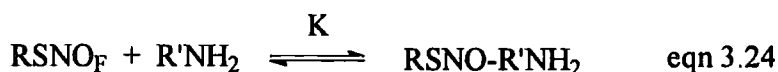
Table 3.26

Kinetic data for the reaction of SPEN ($2.5 \times 10^{-4} \text{ mol dm}^{-3}$) and ammonia at pH 9.43, with $[\text{EDTA}] = 1 \times 10^{-4} \text{ mol dm}^{-3}$

$[\text{NH}_3]_{\text{T}} / \text{mol dm}^{-3}$	$k_{\text{obs}} / 10^{-4} \text{ s}^{-1}$
0.03	5.13 ± 0.05
0.06	5.63 ± 0.03
0.09	4.92 ± 0.02
0.12	4.38 ± 0.03
0.15	5.73 ± 0.05
0.18	5.54 ± 0.03

3.3.2.2 Nitrosothiol-Amine Complex Formation

A possible explanation for the rate of reaction reaching a finite limit, is that a non-reactive RSNO-R'NH_2 complex is rapidly generated from SPEN and the amine at high $[\text{amine}]_T$ (equation 3.24), prior to rate-determining attack of the nucleophile at the nitrosothiol (equations 3.25 - 3.26).



$$\text{Rate} = k_2[\text{RSNO}]_F[\text{R'NH}_2] \quad \text{eqn 3.26}$$

RSNO_F represents the free RSNO that is not bound by the complex, and R'NH_2 the free amine. The equilibrium constant (K) for the formation of this complex can therefore be described by equation 3.27.

$$K = \frac{[\text{RSNO-R'NH}_2]}{[\text{RSNO}]_F[\text{R'NH}_2]} \quad \text{eqn 3.27}$$

Using the total concentration of nitrosothiol ($[\text{RSNO}]_T$) and the expression for K above, it is now possible to derive $[\text{RSNO}]_F$;

$$[\text{RSNO}]_T = [\text{RSNO}]_F + [\text{RSNO-R'NH}_2] \quad \text{eqn 3.28}$$

Here,

$$[\text{RSNO}]_T = [\text{RSNO}]_F + K[\text{RSNO}]_F[\text{R}'\text{NH}_2] \quad \text{eqn 3.29}$$

and so,

$$[\text{RSNO}]_F = \frac{[\text{RSNO}]_T}{1 + K[\text{R}'\text{NH}_2]} \quad \text{eqn 3.30}$$

One can substitute for $[\text{RSNO}]_F$ in equation 3.26. At uniform $[\text{RSNO}]_T$ this can then be re-written as;

$$\text{Rate} = \frac{k_2[\text{RSNO}]_T[\text{R}'\text{NH}_2]}{1 + K[\text{R}'\text{NH}_2]} = k_{\text{obs}}[\text{RSNO}]_T \quad \text{eqn 3.31}$$

Consequently, the observed pseudo-first order rate constant is now equal to;

$$k_{\text{obs}} = \frac{k_2[\text{R}'\text{NH}_2]}{1 + K[\text{R}'\text{NH}_2]} \quad \text{eqn 3.32}$$

The free form of the amine is given by equation 3.33.

$$[\text{R}'\text{NH}_2] = \frac{K_a[\text{R}'\text{NH}_2]_T}{K_a + [\text{H}^+]} \quad \text{eqn 3.33}$$

Incorporating this into equation 3.32 leads to;

$$k_{\text{obs}} = \frac{k_2 K_a [\text{R}'\text{NH}_2]_T}{(K_a + [\text{H}^+]) + K K_a [\text{R}'\text{NH}_2]_T} \quad \text{eqn 3.34}$$

At high $[R'NH_2]_T$, $[R'NH_2]_T \gg K_a$ or $[H^+]$. As a result of this, equation 3.34 can be abbreviated to;

$$k_{obs} \approx \frac{k_2 K_a [R'NH_2]_T}{K K_a [R'NH_2]_T} \approx \frac{k_2}{K} \quad \text{eqn 3.35}$$

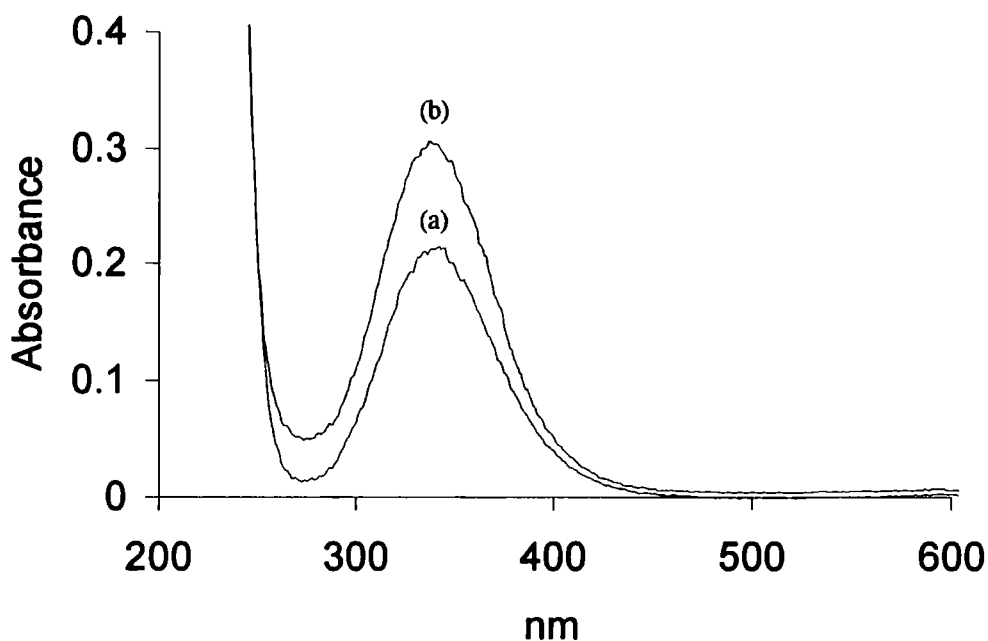
According to this equality, k_{obs} should be unchanged regardless of $[R'NH_2]_T$ under the conditions discussed. This is the precise outcome that has been witnessed. If k_2 ($7.8 \times 10^{-4} \text{ mol}^{-1} \text{ dm}^3 \text{ s}^{-1}$) and the limiting value of k_{obs} ($\sim 7 \times 10^{-5} \text{ s}^{-1}$) for the reaction of SPEN and propylamine are inserted into equation 3.35, they afford $K \approx 11 \text{ mol}^{-1} \text{ dm}^3$ for the appropriate complex.

The subsequent objective was to clarify if the development of the RSNO- $R'NH_2$ species was linked to a spectral change. For this reason, two uv-visible spectra were recorded between 200 – 600nm (figure 3.14). Spectrum (a) is indicative of $2.5 \times 10^{-4} \text{ mol dm}^{-3}$ SPEN in distilled water, with $[EDTA] = 1 \times 10^{-4} \text{ mol dm}^{-3}$. Alternatively, spectrum (b) corresponds to an identical reaction mixture in which ammonia at $[NH_3]_T = 0.20 \text{ mol dm}^{-3}$ has been added. Both spectra were acquired immediately after the introduction of the reagents.

Spectrum (b) displays a 50% increase in the absorbance at $\lambda \sim 340\text{nm}$. This modification could well be due to the presence of the inactive complex, considering that ammonia alone does not absorb within this region.

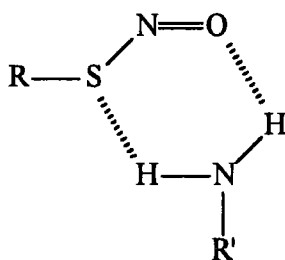
Figure 3.14

Spectra of SPEN ($2.5 \times 10^{-4} \text{ mol dm}^{-3}$) in distilled water,
with/without added ammonia and $[\text{EDTA}] = 1 \times 10^{-4} \text{ mol dm}^{-3}$



(a) $[\text{NH}_3]_{\text{T}} = 0 \text{ mol dm}^{-3}$ and (b) $[\text{NH}_3]_{\text{T}} = 0.20 \text{ mol dm}^{-3}$ (pH 9.55).

If RSNO-R'NH_2 is a 1:1 complex, its structure (3.7) may comprise a six-membered ring system composed of two hydrogen-bonding interactions between the oxygen and sulfur atoms of the $-\text{SNO}$ moiety in SPEN, and the hydrogen atoms of the primary amine. This structure would substantiate the experimental data, as ammonia would be a particularly effective molecule for integration into this complex due to the enhanced number of H-atoms (hence marked curvature of the k_{obs} vs $[\text{NH}_3]_{\text{T}}$ plots). At the opposite extreme, secondary amines would be unable to form the complex due to a lack of H-atoms (hence zero curvature).



3.7

3.4 Reactions of Tertiary Amines

Tertiary amines (R^1R^2RN) are recognised as poor nucleophiles towards nitroso compounds²⁷. They have also been categorised as substrates that are difficult to nitrosate under acidic conditions, and to this day a mechanistic understanding of many of these reactions is still confused. It was of particular relevance to our work, to ascertain if tertiary amines, like their secondary and primary counterparts, were sufficiently nucleophilic to react with SPEN at basic pH.

The procedure followed was that which is comprehensively reviewed for the secondary amines in section 3.2. The results obtained did certify that SPEN decomposition is initiated by the tertiary amines, quinuclidine (table 3.27), trimethylamine, 1,4-diazabicyclo[2,2,2]octane (DABCO), and *N,N*-diethylmethylamine, at a rate (table 3.28) not dissimilar to the secondary/primary amines studied.

Table 3.27


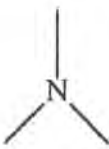
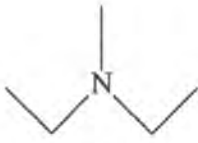

Kinetic data for the reaction of SPEN ($2.5 \times 10^{-4} \text{ mol dm}^{-3}$) and quinuclidine at pH 11.42, with $[\text{EDTA}] = 1 \times 10^{-4} \text{ mol dm}^{-3}$

$[\text{amine}]_T / 10^{-2} \text{ mol dm}^{-3}$	$k_{\text{obs}} / 10^{-5} \text{ s}^{-1}$
1.5	3.10 ± 0.11
3.0	3.87 ± 0.12
4.5	4.42 ± 0.13
6.0	5.02 ± 0.11
7.5	5.87 ± 0.10
9.0	6.63 ± 0.11

Reaction once more took place through the unprotonated amine, without any complications (details not specified). Graphs of k_{obs} vs $[\text{amine}]_T$ were still linear at high $[\text{amine}]_T$, thus endorsing the proposed configuration of the $\text{RSNO-R}^1\text{NH}_2$ complex (3.7) (as tertiary amines cannot H-bond to RSNO).

Table 3.28

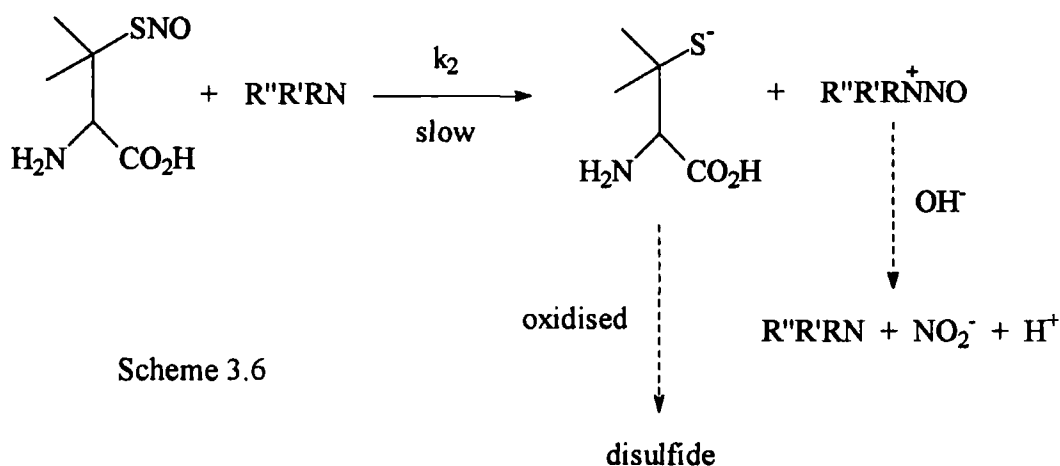
Values of k_2 (from equation 3.7) for the reaction of SPEN ($2.5 \times 10^{-4} \text{ mol dm}^{-3}$) and various tertiary amines, with $[\text{EDTA}] = 1 \times 10^{-4} \text{ mol dm}^{-3}$

Amine	Structure	pK_a^{10}	k_2 $/\text{mol}^{-1} \text{ dm}^3 \text{ s}^{-1}$	$\log k_2$
Quinuclidine		11.15	7.1×10^{-4}	- 3.15
Trimethylamine		9.80	3.6×10^{-4}	- 3.44
N,N-Diethylmethylamine		10.54 ⁴	2.2×10^{-4}	- 3.66
DABCO		8.82 ²⁶	1.8×10^{-4} ^a	- 3.74

a. Statistically amended value (due to two identical nucleophilic sites).

As only four tertiary amines were used in these experiments, the range is too limited to pinpoint any meaningful association between reactivity and nucleophile basicity. Table 3.28 does however re-emphasise the influence of steric effects within this class of reaction^{11,24}, i.e. k_2 (trimethylamine) $>$ k_2 (N,N-diethylmethylamine), even though the former amine is less basic.

Products of the reaction of SPEN ($2.5 \times 10^{-4} \text{ mol dm}^{-3}$) and DABCO ($[\text{amine}]_{\text{T}} = 0.06 \text{ mol dm}^{-3}$) at pH 8.96 with $[\text{EDTA}] = 1 \times 10^{-4} \text{ mol dm}^{-3}$, were not the same as those from the SPEN/primary amine interactions (section 3.3.1.2). The exception was that the $-\text{NO}$ group was recovered quantitatively as nitrite (92%). This discovery immediately suggests a comparison to the reactions of alkyl nitrites¹ and MNTS⁴ with $\text{R}''\text{R}'\text{RN}$. Here it is thought that a nitrosated tertiary amine intermediate ($\text{R}''\text{R}'\text{RN}^+\text{NO}$) is hydrolysed to NO_2^- at high pH. $\text{R}''\text{R}'\text{RN}$ is thereby regenerated. Pathways involving this species are however known to be highly complex²⁸. Adapting this knowledge to the reaction of SPEN and a tertiary amine, yields the feasible reaction laid out in scheme 3.6. The other steps are unchanged relative to the mechanism forwarded for secondary amines and SPEN.



3.5 Reactions of Other Nitrogen Nucleophiles

Until now, only the reactions of SPEN with an amine have been considered. To gain a more general insight into the reactivity of this S-nitrosothiol, several other nitrogen nucleophiles of lower basicity were examined. Hydroxylamine (table 3.29), semicarbazide (table 3.30), hydrazine (table 3.31), azide ion, and methoxyamine, were chosen for this study, which concentrated purely upon determining the rate of transnitrosation. No attempts were made to characterise the reaction products.

Table 3.29

Kinetic data for the reaction of SPEN ($2.5 \times 10^{-4} \text{ mol dm}^{-3}$) and hydroxylamine at pH 6.12, with $[\text{EDTA}] = 1 \times 10^{-4} \text{ mol dm}^{-3}$

$[\text{nucleophile}]_{\text{T}}/\text{mol dm}^{-3}$	$k_{\text{obs}}/10^{-5} \text{ s}^{-1}$
0.06	4.21 ± 0.16
0.09	6.40 ± 0.18
0.12	7.85 ± 0.18
0.15	9.69 ± 0.21
0.18	11.3 ± 0.3
0.21	13.3 ± 0.3

a. $[\text{nucleophile}]_{\text{T}} = [\text{amine}]_{\text{T}}$.

Table 3.30

Kinetic data for the reaction of SPEN ($2.5 \times 10^{-4} \text{ mol dm}^{-3}$) and semicarbazide at pH 3.57, with $[\text{EDTA}] = 1 \times 10^{-4} \text{ mol dm}^{-3}$ ($I = 0.50 \text{ mol dm}^{-3}$)

$[\text{nucleophile}]_{\text{T}}/\text{mol dm}^{-3}$	$k_{\text{obs}}/10^{-6} \text{ s}^{-1}$
0.6	8.57 ± 0.11
0.7	10.5 ± 0.1
0.8	12.0 ± 0.2
0.9	13.5 ± 0.2
1.0	15.3 ± 0.2

Table 3.32 presents the appropriate second order rate constants, calculated as usual by using equation 3.7. Plots of k_{obs} against $[\text{nucleophile}]_{\text{T}}$ were not subject to curvature as $[\text{nucleophile}]_{\text{T}}$ was increased.

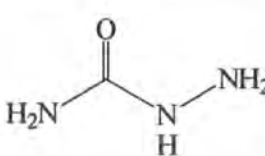
Table 3.31

Kinetic data for the reaction of SPEN ($2.5 \times 10^{-4} \text{ mol dm}^{-3}$) and hydrazine at pH 8.17, with $[\text{EDTA}] = 1 \times 10^{-4} \text{ mol dm}^{-3}$

$[\text{nucleophile}]_T / \text{mol dm}^{-3}$	$k_{\text{obs}} / 10^{-3} \text{ s}^{-1}$
0.06	3.11 ± 0.03
0.09	4.31 ± 0.03
0.12	5.38 ± 0.03
0.21	9.07 ± 0.08

Table 3.32

Values of k_2 (from equation 3.7) for the reaction of SPEN ($2.5 \times 10^{-4} \text{ mol dm}^{-3}$) and various nitrogen nucleophiles, with $[\text{EDTA}] = 1 \times 10^{-4} \text{ mol dm}^{-3}$

Nucleophile	Structure/Formula	pK_a^{10}	$k_2 / \text{mol}^{-1} \text{ dm}^3 \text{ s}^{-1}$	$\log k_2$
Hydrazine	NH_2NH_2	7.96 ²⁶	$3.3 \times 10^{-2} \text{ a}$	- 1.48
Azide ion	N_3^-	4.69 ²⁹	$1.1 \times 10^{-2} \text{ a}$	- 1.96
Hydroxylamine	NH_2OH	5.95	9.9×10^{-4}	- 3.00
Semicarbazide		3.86 ³⁰	4.4×10^{-5}	- 4.36
Methoxyamine	MeONH_2	4.60	1.5×10^{-5}	- 4.82

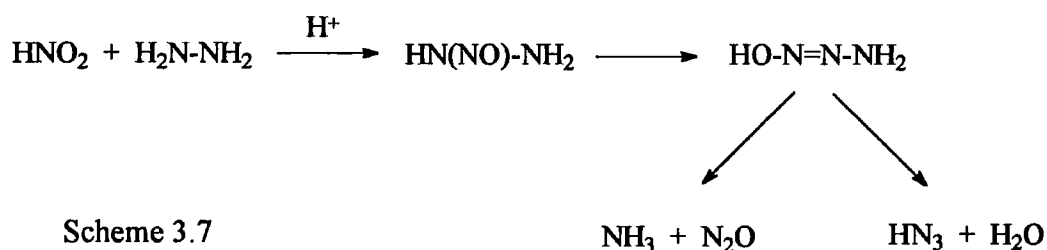
a. Statistically amended value (due to two identical nucleophilic sites).

Hydrazine ($k_2 \sim 3.3 \times 10^{-2} \text{ mol}^{-1} \text{ dm}^3 \text{ s}^{-1}$) and azide ion ($k_2 \sim 1.1 \times 10^{-2} \text{ mol}^{-1} \text{ dm}^3 \text{ s}^{-1}$) are exceptionally reactive towards SPEN (an order of magnitude more so than primary amines). In addition, the reactivity of hydroxylamine ($k_2 \sim 9.9 \times 10^{-4} \text{ mol}^{-1} \text{ dm}^3 \text{ s}^{-1}$) is tantamount to that of isobutylamine ($k_2 \sim 8.9 \times 10^{-4} \text{ mol}^{-1} \text{ dm}^3 \text{ s}^{-1}$), which is the most reactive RNH₂. Behaviour of this kind could be ascribed to the reduced molecular size of NH₂NH₂, N₃⁻, and NH₂OH. A more conceivable answer however, is that these nucleophiles exhibit a considerable α -effect³¹, i.e. there is at least one lone pair of electrons on the atom α to the nucleophilic site. These species often show heightened reactivity, relative to nucleophiles of equivalent basicity that are deprived of this structural attribute. The reasons behind this effect have been frequently addressed in the literature³², but opinions still remain divided on the topic. Reduced solvation, destabilisation of the ground-state of the nucleophile, and stabilisation of the transition-state or reaction products, have been put forward. All these factors are inherently related to the adjacent unshared electrons.

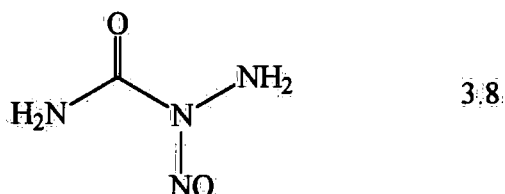
Semicarbazide and methoxyamine display a minor α -effect, and so reactions with SPEN still proceed at pH 3 - 5 (albeit at a much slower rate). Under these conditions the reaction between SPEN and amines is negligible.

There are many examples of the facile nitrosation of α -nucleophiles³³. Some of these are worthy of a brief mention, as they are hypothetical illustrations of reactions that may arise from the treatment of such species with a S-nitrosothiol.

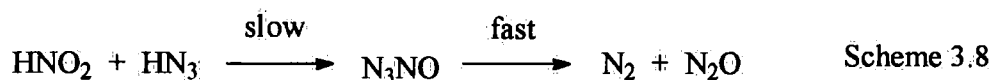
Hydrazine initially forms N-nitrosohydrazine (HN(NO)-NH₂) when reacted with nitrous acid. This compound subsequently decomposes to create ammonia and nitrous oxide, or hydrazoic acid (HN₃) (scheme 3.7). The acidity of the medium influences the product distribution³⁴.



Hydroxylamine and HNO_2 react to liberate N_2O ³⁵ (equation 3.36), and the nitrosation of semicarbazide yields a stable nitrosamide³⁶ (3.8).

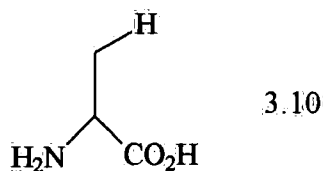
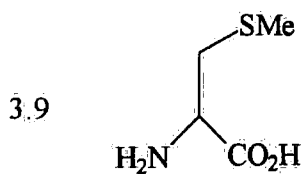


Interactions between nitrous acid and the azide ion at low pH, generate nitrogen and nitrous oxide via the short-lived intermediate, nitrosyl azide (N_3NO)³⁷ (scheme 3.8). The same products derive from a N-nitrosamine and N_3^- ³⁸.

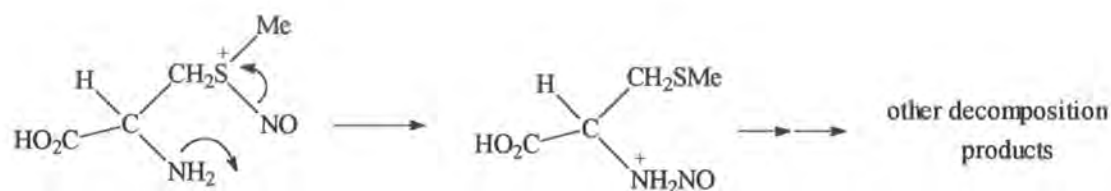


3.6 Reactions of Ambident Nucleophiles

Thiomorpholine³⁹, S-methyl-L-cysteine (3.9)⁴⁰, and thioproline⁴¹, are ambident substrates that can undergo nitrosation at either the S- or N-atom. In acid, these reactions are considerably more rapid than those of the corresponding amines in which the -SR functionality is absent, i.e. morpholine, alanine (3.10), and proline.



Reaction initiates S-nitrosation at the more nucleophilic and energetically favoured⁴² sulfur site. This is superseded by a quick intramolecular rearrangement of -NO (a 1,4- or 1,5-shift), to leave the N-nitroso species. Scheme 3.9 portrays this “migration” of the nitroso group within S-methyl-L-cysteine.



Scheme 3.9

Naturally, our attention was drawn to distinguishing whether ambident nucleophiles continue to show amplified reactivity in nitrosation reactions, if the nitrosating agent embodies a nitrosothiol in basic media. SPEN was therefore reacted separately with S-methyl-L-cysteine (table 3.33) and thiomorpholine (table 3.34), and k_2 (table 3.35) measured via the method highlighted earlier.

Table 3.33

Kinetic data for the reaction of SPEN ($2.5 \times 10^{-4} \text{ mol dm}^{-3}$) and S-methyl-L-cysteine at pH 8.80, with $[\text{EDTA}] = 1 \times 10^{-4} \text{ mol dm}^{-3}$

$[\text{nucleophile}]_T / 10^{-2} \text{ mol dm}^{-3}$	$k_{\text{obs}} / 10^{-3} \text{ s}^{-1}$
1.5	3.22 ± 0.04
4.5	3.68 ± 0.02
6.0	3.90 ± 0.02
7.5	4.15 ± 0.03

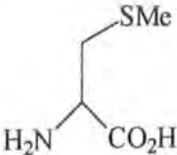
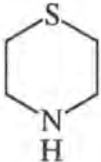
Table 3.34

Kinetic data for the reaction of SPEN ($2.5 \times 10^{-4} \text{ mol dm}^{-3}$) and thiomorpholine at pH 9.02, with $[\text{EDTA}] = 1 \times 10^{-4} \text{ mol dm}^{-3}$

$[\text{nucleophile}]_T / \text{mol dm}^{-3}$	$k_{\text{obs}} / 10^{-4} \text{ s}^{-1}$
0.06	6.63 ± 0.07
0.09	9.63 ± 0.23
0.12	10.7 ± 0.6
0.15	13.6 ± 0.7
0.18	15.5 ± 0.6

Table 3.35

Values of k_2 (from equation 3.7) for the reaction of SPEN ($2.5 \times 10^{-4} \text{ mol dm}^{-3}$) and ambident nucleophiles, with $[\text{EDTA}] = 1 \times 10^{-4} \text{ mol dm}^{-3}$

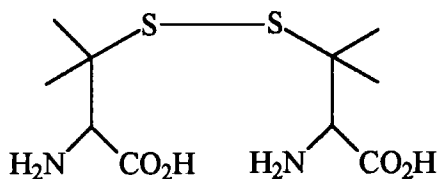
Nucleophile	Structure	pK_a^{10}	$k_2 / \text{mol}^{-1} \text{ dm}^3 \text{ s}^{-1}$	$\log k_2$
S-Methyl-L-cysteine		8.97	3.8×10^{-2}	- 1.42
Thiomorpholine		9.06^4	1.5×10^{-2}	- 1.82

As imagined, the rate constant for the reaction of thiomorpholine with SPEN ($k_2 \sim 1.5 \times 10^{-2} \text{ mol}^{-1} \text{ dm}^3 \text{ s}^{-1}$) is emphatically larger than that for the reaction of morpholine and SPEN ($k_2 \sim 3.8 \times 10^{-4} \text{ mol}^{-1} \text{ dm}^3 \text{ s}^{-1}$) (table 3.6). Similarly, the value

for S-methyl-L-cysteine ($k_2 \sim 3.8 \times 10^{-2} \text{ mol}^{-1} \text{ dm}^3 \text{ s}^{-1}$) is 80 times greater than the average k_2 value for simple primary amines (table 3.24). Unfortunately, no comparison could be made to alanine itself, due to the irregular and unexpected kinetics of its reaction with SPEN (not mentioned).

The situation is not so clear-cut for reactions of MNTS and ambident nucleophiles⁴. Here, equivalent rate constants were obtained for thiomorpholine and morpholine, implying direct nitrosation at the nitrogen rather than sulfur atom. SPEN and MNTS must somehow differentiate between these potential locations.

As the nucleophilic sites within the disulfide of an amino acid mimic those exhibited by S-methyl-L-cysteine, a reaction between SPEN and RSSR could not be dismissed. Denitrosation of nitrosothiols by this route would be of relevance *in vivo*, as disulfides are crucial components of the structural make-up of extracellular proteins/enzymes, and have an intracellular role⁴³. Although disulfides are relatively unreactive substances, they are susceptible to cleavage at the S-S or C-S bonds. D-Penicillamine disulfide ($\text{pK}_a \sim 8.72^{10}$, 3.11) was chosen for a test reaction with SPEN (figure 3.15), as this RSSR possesses a molecular configuration that is highly resistant to breakdown by alkali⁴⁴ (it is also the oxidation product of SPEN).

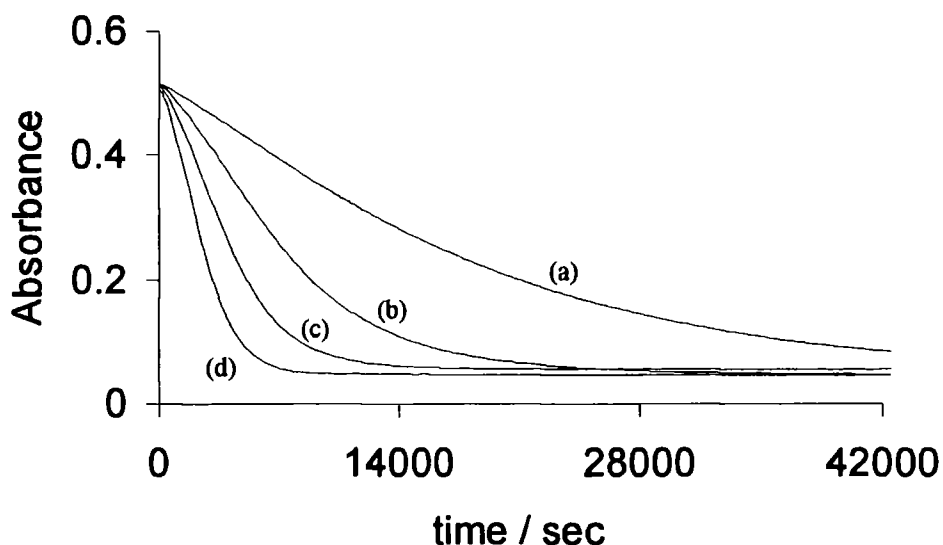


3.11

Induction periods in the resultant time-dependent traces hampered the measurement of k_{obs} and k_2 , but the rate of reaction definitely increases in proportion to added $[\text{RSSR}]_T$. This signals that an ambident disulfide is effective at inducing quantitative SPEN decay.

Figure 3.15

Absorbance-time spectra showing the reaction of SPEN ($5 \times 10^{-4} \text{ mol dm}^{-3}$) and D-penicillamine disulfide at pH 7.42, with $[\text{EDTA}] = 1 \times 10^{-4} \text{ mol dm}^{-3}$



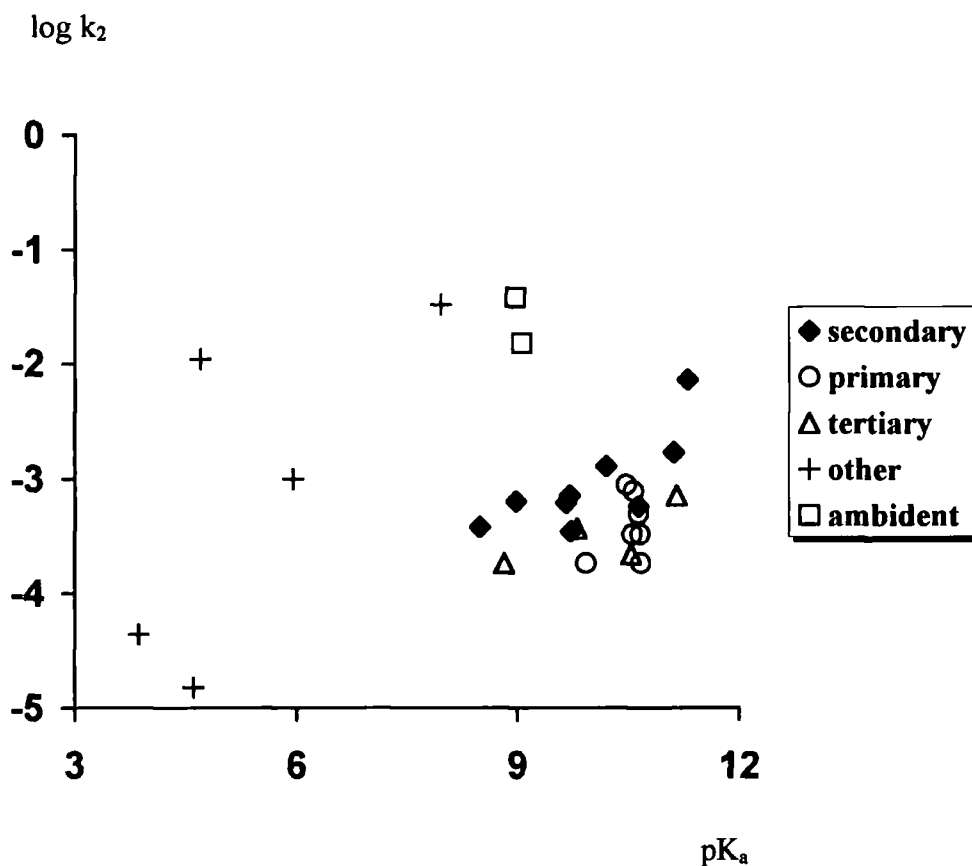
(a) $[\text{RSSR}]_{\text{T}} = 0.011 \text{ mol dm}^{-3}$, (b) $[\text{RSSR}]_{\text{T}} = 0.021 \text{ mol dm}^{-3}$, (c) $[\text{RSSR}]_{\text{T}} = 0.032 \text{ mol dm}^{-3}$ and (d) $[\text{RSSR}]_{\text{T}} = 0.042 \text{ mol dm}^{-3}$ (where $[\text{RSSR}]_{\text{T}} \equiv [\text{amine}]_{\text{T}}$).

NB. Preliminary experiments revealed that D-penicillamine disulfide can also react with S-nitrosocysteine, S-nitrosocysteamine, S-nitrosotiopronin, and S-nitroso-1-thio- β -D-glucose (at pH ~ 7.4).

3.7 Correlation and Discussion of Kinetic Results

The relationship that exists between $\log k_2$ and pK_a for the reactions of secondary amines and SPEN, has been discussed in section 3.2.4. If the reactions of SPEN and nitrogen nucleophiles are viewed in a wider context, there is no general trend evident (figure 3.16). The α -nucleophiles and ambident molecules are a particular cause of this data dispersion.

Figure 3.16
Brønsted diagram for the reaction between SPEN and
nucleophilic nitrogen compounds



There is no perceivable correlation between reactivity and the Pearson²² nucleophilicity index (n) (table 3.36). This can be concluded as the values of n (an indication of nucleophilicity, standardised relative to nucleophilic substitution in CH_3I) cited for hydrazine ($n = 6.61$) and azide ($n = 5.78$), are lower than or equal to those for hydroxylamine ($n = 6.60$) and piperidine ($n = 7.30$). This would suggest that the former two are not superior nucleophiles, whereas in actual fact, k_2 values show them to be many more times reactive towards SPEN than the latter pair.

Ritchie's^{45,46} scale of nucleophilicity (N_+) better correlates our results (table 3.36). Plotting $\log k_2$ (sections 3.2 – 3.6) against N_+ (an indication of nucleophilicity, standardised relative to nucleophilic interactions with carbocations of the form, Ar_3C^+ , e.g. malachite green), yields a distribution to which a straight line of gradient ~ 0.75 can be fitted (figure 3.17). This is quite close to the theoretical slope of 1.0 that is

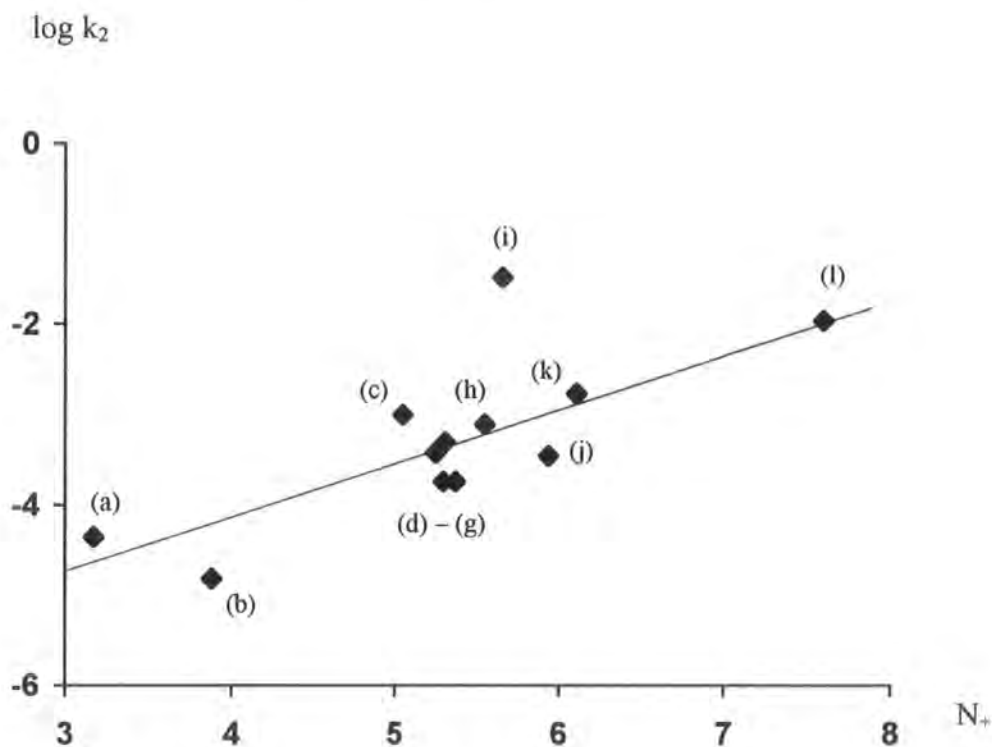
Table 3.36

Pearson (n) and Ritchie (N_+) parameters for nitrogen nucleophiles

Nucleophile	n^{22}	N_+^{45}	N_+^{46}	Nucleophile	n^{22}	N_+^{45}	N_+^{46}
Semicarbazide	---	3.17	3.73	Ethylenediamine	---	5.37	5.44
Methoxyamine	---	3.88	4.37	Propylamine	---	5.55	---
Hydroxylamine	6.60	5.05	5.05	Hydrazine	6.61	5.66	6.01
Morpholine	---	5.25	6.99	Piperazine	---	5.94	---
DABCO	---	5.30	---	Piperidine	7.30	6.11	7.58
Ethylamine	---	5.31	5.28	Azide	5.78	7.60	7.54

Figure 3.17

Plot of $\log k_2$ vs N_+ (from reference 45) for the reactions
of SPEN and nitrogen nucleophiles



(a) Semicarbazide, (b) Methoxyamine, (c) Hydroxylamine, (d) Morpholine, (e) DABCO,
(f) Ethylamine, (g) Ethylenediamine, (h) Propylamine, (i) Hydrazine, (j) Piperazine, (k) Piperidine
and (l) Azide.

predicted from Ritchie's original equation. Hydrazine is the only species that deviates significantly from the linear regression.

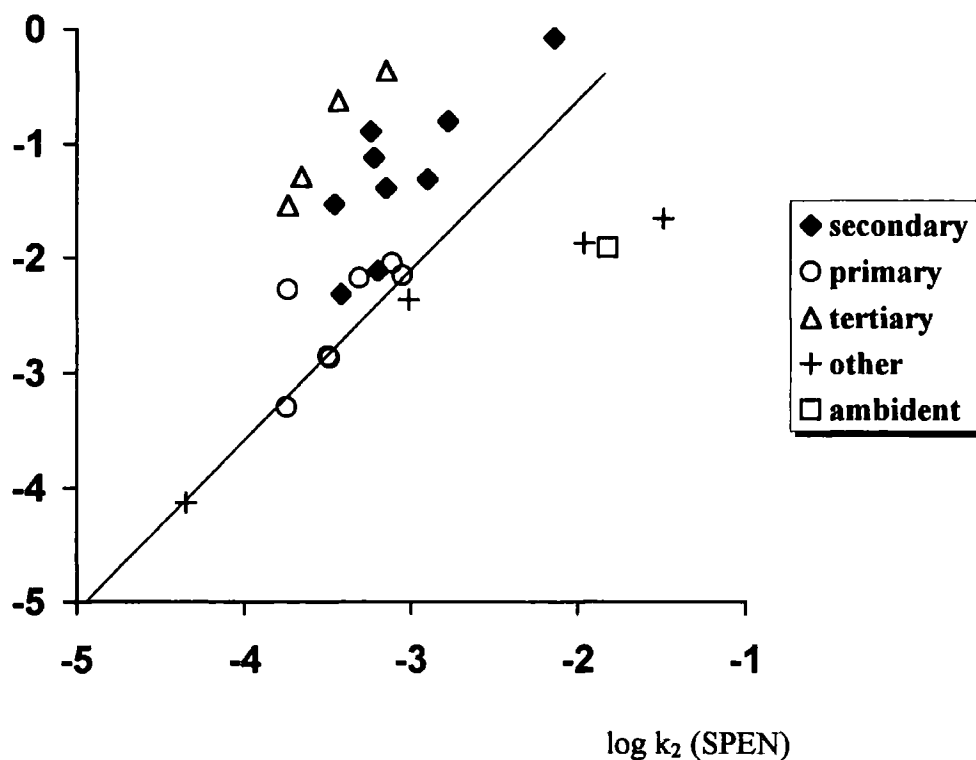
Reactivity is also closely related to N_+ , but not n , in the reactions of nitrogen nucleophiles with MNTS^{4,23}. Hoz⁴⁷ and Shaik⁴⁸ believe that these findings are indicative of a Klopman⁴⁹ frontier-controlled reaction, in which there is ready electron transfer between the nucleophile and electrophile, leading to a diradical transition state. This conjecture may also therefore extend to the reactions of SPEN.

Figure 3.18 is a log-log diagram ($\log k_2$ values) that demonstrates a tangible link between the relative reactivities of nitrogen nucleophiles towards SPEN and MNTS. The regression line has a slope of ~ 1.6 (cf. a theoretical value of unity). This disparity could be due to the fact that the MNTS work is conducted in mixed aqueous - organic systems.

Figure 3.18

log-log plot for the reaction of SPEN and MNTS⁴ with nitrogen nucleophiles

$\log k_2$ (MNTS)



3.8 Conclusion

This chapter has presented a thorough appraisal of the kinetics involved in the first examples of (a) the alkaline hydrolysis of a S-nitrosothiol, but more importantly, (b) direct nitrosation reactions between a RSNO and nucleophilic nitrogen compounds. It has been duly shown that this nitrosothiol, SPEN, can donate its nitroso group to primary, secondary (hence creating carcinogenic nitrosamines), and tertiary amines, in basic aqueous solution. This exchange emanates from nucleophilic attack by the free amine at the nitrogen atom of -SNO, and does not involve the prior formation of nitric oxide. Ambident and alpha-nucleophiles are especially effective at instigating SPEN decomposition. Most aspects of reaction parallel those that are prevalent in the reactions of nitrogen nucleophiles with MNTS/alkyl nitrites.

References

- 1 J. Casado, A. Castro, F.M. Lorenzo and F. Meijide, *Monatsh. Chem.*, 1986, **117**(3), 335, S. Oae, N. Asai and K. Fujimori, *J. Chem. Soc., Perkin Trans. 2*, 1978, 1124.
- 2 S.S. Singer, *J. Org. Chem.*, 1978, **43**(24), 4612, J.T. Thompson and D.L.H. Williams, *J. Chem. Soc., Perkin Trans. 2*, 1977, 1932, C.L. Bumgardner, K.S. McCallum and J.P. Freeman, *J. Am. Chem. Soc.*, 1961, **83**, 4417.
- 3 H. Maltz, M.A. Grant and M.C. Navaroli, *J. Org. Chem.*, 1971, **36**(2), 363.
- 4 L. García-Río, E. Iglesias, J.R. Leis, M.E. Peña and A. Ríos, *J. Chem. Soc., Perkin Trans. 2*, 1993, 29, A. Castro, J.R. Leis and M.E. Peña, *ibid.*, 1989, 1861.
- 5 A.P. Dicks, E. Li, A.P. Munro, H.R. Swift and D.L.H. Williams, *Can. J. Chem.*, 1998, **76**, 789.
- 6 J.M. Walshe, *Am. J. Med.*, 1956, **21**, 487.
- 7 J. Peisach and W.E. Blumberg, *Mol. Pharmacol.*, 1969, **5**, 200.
- 8 P.C. Jocelyn, *Biochemistry of the SH Group*, Academic Press, 1972, Ch. 16, p.p. 346.
- 9 D.J. Barnett, Ph.D. Thesis, University of Durham, 1994.
- 10 A.E. Martell and R.M. Smith, *Critical Stability Constants*, Plenum Press, New York, 1974, Vols. 1, 2 and 5, D.D. Perrin, *Dissociation Constants of Organic Bases in Aqueous Solution*, Butterworths, London, 1965.
- 11 S. González-Mancebo, E. Calle, M.P. García-Santos and J. Casado, *J. Agric. Food Chem.*, 1997, **45**, 334.
- 12 S.C. Askew, D.J. Barnett, J. McAninly and D.L.H. Williams, *J. Chem. Soc., Perkin Trans. 2*, 1995, 741.
- 13 A.C.F. Gorren, A. Schrammel, K. Schmidt and B. Mayer, *Arch. Biochem. Biophys.*, 1996, **330**(2), 219.
- 14 J. Garcia, J. González, R. Segura, F. Urpi and J. Vilarrasa, *J. Org. Chem.*, 1984, **49**, 3322.
- 15 D.L.H. Williams, *Nitrosation*, Cambridge University Press, 1988, Ch. 4, p.p. 95.
- 16 W. Lijinsky, *Chemistry and Biology of N-Nitroso Compounds*, Cambridge University Press, 1992, Ch. 3, p.p. 60.

- 17 *Vogel's Textbook of Quantitative Inorganic Analysis*, 4th ed., Longman, 1978, p.p. 755.
- 18 G.L. Ellman, *Arch. Biochem. Biophys.*, 1959, **82**, 70.
- 19 P.W. Riddles, R.L. Blakeley and B. Zerner, *Anal. Biochem.*, 1979, **94**, 75.
- 20 W.A. Pryor, D.F. Church, C.K. Govindan and G. Crank, *J. Org. Chem.*, 1982, **47**, 156.
- 21 Reference 15, Ch. 6, p.p. 163.
- 22 R.G. Pearson, H. Sobel and J. Songstad, *J. Am. Chem. Soc.*, 1968, **90**, 319.
- 23 J.R. Leis, M.E. Peña and A.M. Ríos, *J. Chem. Soc., Perkin Trans. 2*, 1995, 587.
- 24 D.J. Barnett, A. Ríos and D.L.H. Williams, *ibid.*, 1995, 1279, D.J. Barnett, J. McAninly and D.L.H. Williams, *ibid.*, 1994, 1131.
- 25 Reference 15, Ch. 4, p.p. 77.
- 26 J.J. Christensen, R.M. Izatt, D.P. Wrathall and L.D. Hansen, *J. Chem. Soc. (A)*, 1969, 1212.
- 27 Reference 15, Ch. 4, p.p. 98 and references therein.
- 28 P.A.S. Smith and R.N. Loeppky, *J. Am. Chem. Soc.*, 1967, **89**, 1147.
- 29 G. Stedman, *J. Chem. Soc.*, 1959, 2943.
- 30 W.P. Jencks and M. Gilchrist, *J. Am. Chem. Soc.*, 1968, **90**, 2622.
- 31 R.G. Pearson, *Advances in Linear Free Energy Relationships*, Eds. N. Chapman and J. Shorter, Plenum Press, New York, 1972, Ch. 6, W.P. Jencks and J. Carriuolo, *J. Am. Chem. Soc.*, 1960, **82**, 675, 1778.
- 32 J. March, *Advanced Organic Chemistry*, 4th ed., Wiley-Interscience, 1992, Ch. 10, p.p. 351 and references therein.
- 33 Reference 15, Ch. 4, p.p. 105.
- 34 J.R. Perrott, G. Stedman and N. Uysal, *J. Chem. Soc., Dalton Trans.*, 1976, 2058.
- 35 M.N. Hughes and G. Stedman, *J. Chem. Soc.*, 1963, 2824.
- 36 A. Castro, E. Iglesias, J.R. Leis, M.E. Peña and J.V. Tato, *J. Chem. Soc., Perkin Trans. 2*, 1986, 1725, G. Hallett and D.L.H. Williams, *ibid.*, 1980, 1372.
- 37 G. Stedman, *J. Chem. Soc.*, 1960, 1702, C.A. Bunton and G. Stedman, *ibid.*, 1959, 3466, G. Stedman, *ibid.*, 1959, 2949.
- 38 T.A. Meyer, D.L.H. Williams, R. Bonnett and S.L. Ooi, *J. Chem. Soc., Perkin Trans. 2*, 1982, 1383.

- 39 A. Coello, F. Meijide and J.V. Tato, *ibid.*, 1989, 1677.
- 40 T.A. Meyer and D.L.H. Williams, *J. Chem. Soc., Chem. Commun.*, 1983, 1067.
- 41 A. Castro, E. Iglesias, J.R. Leis, J.V. Tato, F. Meijide and M.E. Peña, *J. Chem. Soc., Perkin Trans. 2*, 1987, 651, T. Tahira, M. Tsuda, K. Wakabayashi, M. Nagao and T. Sugimura, *Gann.*, 1984, 75(10), 889.
- 42 K.A. Jørgensen, *J. Org. Chem.*, 1985, 50, 4758.
- 43 Reference 8, Ch. 1, p.p. 1.
- 44 J.M. Swan, *Nature*, 1957, 179, 965.
- 45 C.D. Ritchie, *J. Am. Chem. Soc.*, 1975, 97, 1170.
- 46 C.D. Ritchie, *Can. J. Chem.*, 1986, 64, 2239.
- 47 S. Hoz, *Acc. Chem. Res.*, 1993, 26(2), 69.
- 48 S.S. Shaik, *J. Org. Chem.*, 1987, 52, 1563.
- 49 G. Klopman, *J. Am. Chem. Soc.*, 1968, 90, 223.

Chapter 4

Reactivity of Sulfur Nucleophiles Towards S-Nitrosothiols

Chapter 4 : Reactivity of Sulfur Nucleophiles Towards S-Nitrosothiols

4.1 Introduction

In the Ritchie (N_+)¹ and Pearson (n)² classifications, sulfur nucleophiles such as thiosulfate ($S_2O_3^{2-}$) and sulfite (SO_3^{2-}) are found to be more reactive than nitrogen nucleophiles (table 4.1).

Table 4.1
Comparison of N_+ and n for S- and N-nucleophiles

Nucleophile	N_+	n
$S_2O_3^{2-}$	---	8.95
SO_3^{2-}	7.90	8.53
N_3^-	7.60	5.78
NH_2NH_2	5.66	6.61

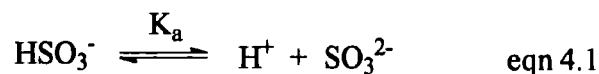
Higher nucleophilicity
↓
Lower nucleophilicity

Having previously ascertained in chapter 3 that 'soft' N-nucleophiles can react directly with a S-nitrosothiol (SPEN), the next rational step was an assessment of whether a similar process could encompass 'soft' S-nucleophiles. Known reactions of this type are few and far between, excepting transnitrosation to thiols³ (section 1.3.5.2) and a complex mechanism concerning diethyl dithiocarbamate⁴ (section 1.3.5.7). Quite why this selection is so limited is puzzling, as an abundance of kinetic data has been accumulated for the reactions of inorganic/organic sulfur species with N- and O-nitroso compounds⁵. One could argue that Harvey and Nelsestuen⁶ discovered another relevant example, when they noted that sulfite heightened S-nitroso bovine serum albumin and GSNO decay in pH 7.4 aqueous buffer. Sulfites are moderately strong reducing agents however⁷, and can generate Cu^+ from residual Cu^{2+} ions in solution. The reaction observed was actually copper catalysed decomposition of the RSNO (in unison with SO_3^{2-} mediated division of the S-S bonds in albumin).

4.2 Reactions of S-Nitrosothiols with Sulfites

4.2.1 Kinetic Analysis and Procedure

Sulfite (SO_3^{2-}) was deemed a suitable S-nucleophile with which to commence our study. Initial tests using SO_3^{2-} entailed an examination of its effect upon the stability of S-nitrosogluthathione. Thus, GSNO ($2.5 \times 10^{-4} \text{ mol dm}^{-3}$) was made *in situ* from GSH and acidified sodium nitrite, and reacted with a freshly prepared sample of NaHSO_3 (0.01 mol dm^{-3}) in pH 7.4 buffer. Sodium bisulfite could be used as the source of sulfite, as SO_3^{2-} exists as the principal S^{IV} form in a solution of this pH (pK_a^8 of $\text{HSO}_3^- \sim 7.0$) (equation 4.1). However, as the pH of the buffer was quite close to the pK_a of HSO_3^- , the relative amounts of sulfite and bisulfite had to be considered in any kinetic discussions.



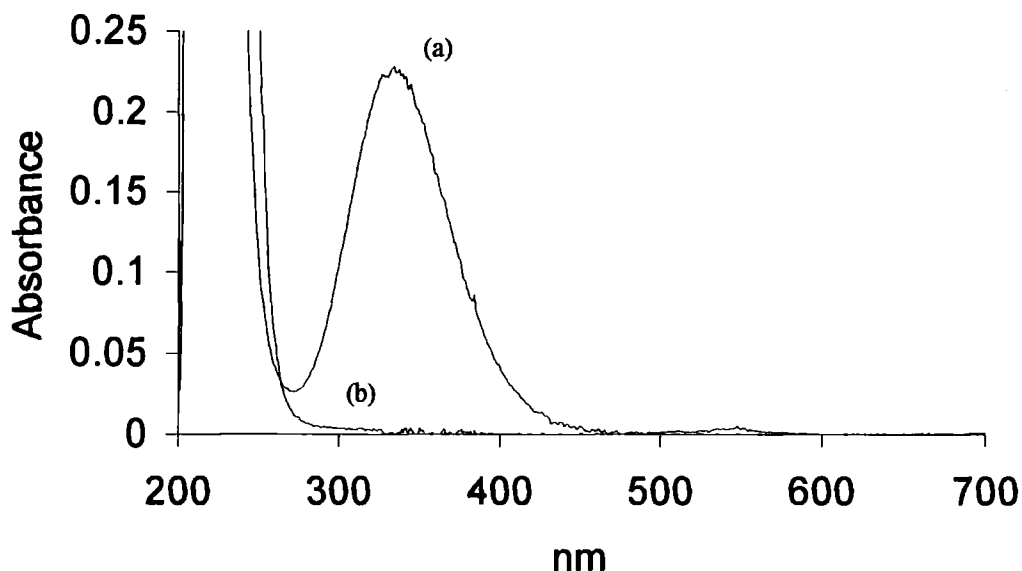
EDTA ($2.5 \times 10^{-4} \text{ mol dm}^{-3}$) was present to eliminate Cu^+ promoted decay of GSNO. Figure 4.1 shows the uv-visible spectrum of this reaction mixture in comparison to that of GSNO alone.

Spectrum (b) in figure 4.1 indicates that the denitrosation of GSNO via NaHSO_3 is extremely rapid and completed within a matter of seconds. No other species are formed that have a measurable absorption within this wavelength region.

The above result prompted an investigation into the interactions of sulfites with several S-nitrosothiols (produced *in situ*) at physiological pH. Reactions were monitored using a stopped-flow spectrophotometer, by following the decrease in the RSNO peak at 340nm and 25°C over time. Experiments were carried out with $[\text{EDTA}] = 2.5 \times 10^{-4} \text{ mol dm}^{-3}$ and a total stoichiometric sulfite concentration, i.e. $[\text{SO}_3^{2-}]_{\text{T}}$ (equation 4.2), in large excess over $[\text{RSNO}]$. Usually $[\text{SO}_3^{2-}]_{\text{T}}$ ranged from $2.5 - 8.75 \times 10^{-3} \text{ mol dm}^{-3}$ at a constant ionic strength ($I = 0.18 \text{ mol dm}^{-3}$).

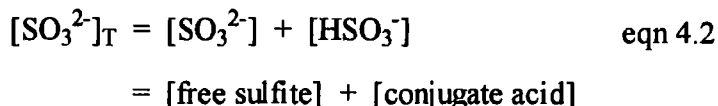
Figure 4.1

Spectra of GSNO ($2.5 \times 10^{-4} \text{ mol dm}^{-3}$) in pH 7.4 buffer with/without added sodium bisulfite, and $[\text{EDTA}] = 2.5 \times 10^{-4} \text{ mol dm}^{-3}$



(a) $[\text{NaHSO}_3] = 0 \text{ mol dm}^{-3}$ and

(b) $[\text{NaHSO}_3] = 0.01 \text{ mol dm}^{-3}$ (spectrum acquired 30 seconds after the introduction of substrate).



Good first-order behaviour was observed in each kinetic run, and rate constants (k_{obs}) obtained using the integrated form of the first order rate equation. Quoted k_{obs} values are the means of at least five determinations, in which the standard error was generally $< 2\%$. Tables 4.2 – 4.4 contain the rate information for the reactions of S-nitroso-N-acetylcysteine (SNAC), GSNO, S-nitrosotiopronin (SNTP), S-nitroso-2-aminoethanethiol (SNAE), and S-nitrosopenicillamine (SPEN) (structures displayed in table 4.8). A plot of k_{obs} versus $[\text{SO}_3^{2-}]_{\text{T}}$ was linear for every RSNO analysed (figure 4.2), thus identifying the reaction as having a first order dependence upon $[\text{SO}_3^{2-}]_{\text{T}}$. All lines passed through the origin because the reactions were too fast for any thermal component of RSNO decomposition to be seen.

Table 4.2

Kinetic data for the reaction of SNAC or GSNO ($2.5 \times 10^{-4} \text{ mol dm}^{-3}$) and sulfite in pH 7.4 buffer, with $[\text{EDTA}] = 2.5 \times 10^{-4} \text{ mol dm}^{-3}$

$[\text{SO}_3^{2-}]_r$ $/10^{-3} \text{ mol dm}^{-3}$	SNAC $k_{\text{obs}}/10^{-2} \text{ s}^{-1}$	GSNO $k_{\text{obs}}/10^{-1} \text{ s}^{-1}$
2.50	4.71 ± 0.04	2.38 ± 0.03
3.75	7.30 ± 0.07	3.60 ± 0.01
5.00	10.1 ± 0.1	5.07 ± 0.02
6.25	12.5 ± 0.2	5.83 ± 0.05
7.50	15.2 ± 0.1	6.92 ± 0.05
8.75	18.0 ± 0.3	7.98 ± 0.04

Table 4.3

Kinetic data for the reaction of SNTP or SNAE ($2.5 \times 10^{-4} \text{ mol dm}^{-3}$) and sulfite in pH 7.4 buffer, with $[\text{EDTA}] = 2.5 \times 10^{-4} \text{ mol dm}^{-3}$

$[\text{SO}_3^{2-}]_r$ $/10^{-3} \text{ mol dm}^{-3}$	SNTP $k_{\text{obs}}/10^{-1} \text{ s}^{-1}$	SNAE $k_{\text{obs}}/10^{-1} \text{ s}^{-1}$
2.50	3.63 ± 0.03	6.36 ± 0.05
3.75	5.57 ± 0.02	9.97 ± 0.02
5.00	7.68 ± 0.06	13.9 ± 0.1
6.25	9.68 ± 0.10	17.8 ± 0.1
7.50	11.5 ± 0.1	21.4 ± 0.2
8.75	13.6 ± 0.1	25.0 ± 0.3

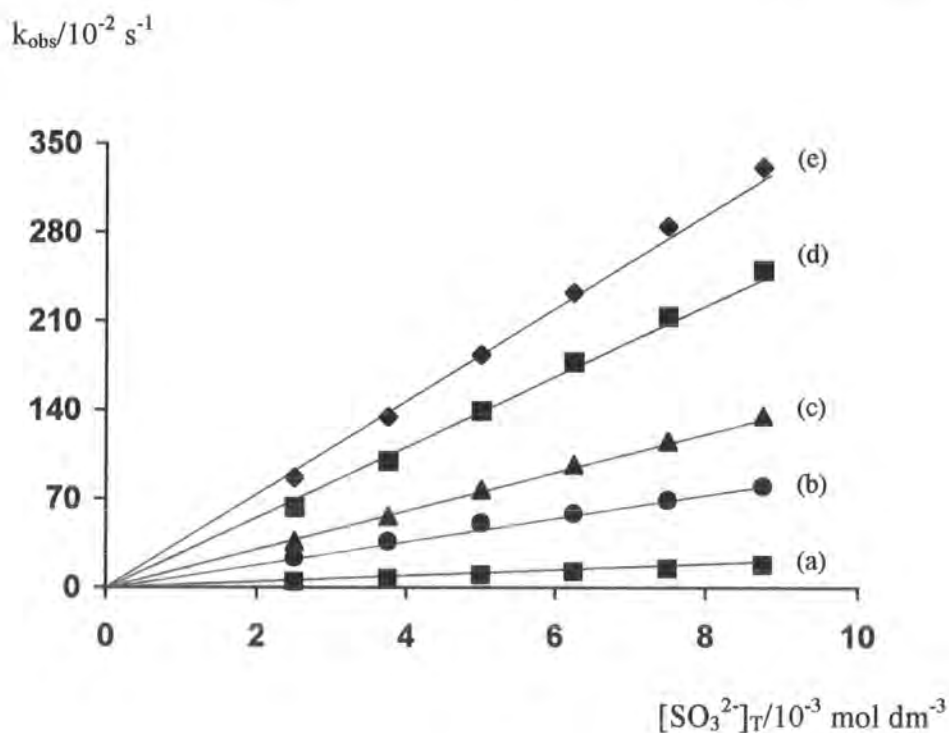
Table 4.4

Kinetic data for the reaction of SPEN ($2.5 \times 10^{-4} \text{ mol dm}^{-3}$) and sulfite in pH 7.4 buffer, with $[\text{EDTA}] = 2.5 \times 10^{-4} \text{ mol dm}^{-3}$

$[\text{SO}_3^{2-}]_T$ $/10^{-3} \text{ mol dm}^{-3}$	SPEN $k_{\text{obs}}/10^{-1} \text{ s}^{-1}$
2.50	8.68 ± 0.03
3.75	13.5 ± 0.1
5.00	18.4 ± 0.1
6.25	23.3 ± 0.3
7.50	28.5 ± 0.2
8.75	33.2 ± 0.3

Figure 4.2

Plot of k_{obs} against $[\text{SO}_3^{2-}]_T$ for the reaction of S-nitrosothiols ($2.5 \times 10^{-4} \text{ mol dm}^{-3}$) and sulfite at pH 7.4, with $[\text{EDTA}] = 2.5 \times 10^{-4} \text{ mol dm}^{-3}$



(a) SNAC, (b) GSNO, (c) SNTP, (d) SNAE and (e) SPEN.

If each reaction proceeded via the free form of the nucleophile as expected (see section 4.2.2), then the rate equation could be given by:

$$\text{Rate} = k_2[\text{RSNO}][\text{SO}_3^{2-}] \quad \text{eqn 4.3}$$

In which, k_2 = second order rate constant for the reaction of a RSNO with sulfite, and $[\text{SO}_3^{2-}]$ = concentration of free sulfite.

As $[\text{SO}_3^{2-}] \gg [\text{RSNO}]$, $[\text{SO}_3^{2-}]$ is constant and so,

$$\text{Rate} = k_{\text{obs}}[\text{RSNO}] \quad \text{eqn 4.4}$$

Here,

$$k_{\text{obs}} = k_2[\text{SO}_3^{2-}] \quad \text{eqn 4.5}$$

Substituting for $[\text{SO}_3^{2-}]$ (equation 4.6, where K_a = acidity constant for bisulfite) into equation 4.5 therefore yields equation 4.7. In principle it relates k_{obs} and pH.

$$[\text{SO}_3^{2-}] = \frac{K_a[\text{SO}_3^{2-}]_T}{K_a + [\text{H}^+]} \quad \text{eqn 4.6}$$

$$k_{\text{obs}} = \frac{k_2 K_a [\text{SO}_3^{2-}]_T}{K_a + [\text{H}^+]} \quad \text{eqn 4.7}$$

4.2.2 pH Dependence

It was believed that fluctuations in k_{obs} relative to $[\text{H}^+]$ at a uniform $[\text{SO}_3^{2-}]_{\text{T}}$, would help distinguish whether free SO_3^{2-} was the active form of the nucleophile. Figure 4.3 shows how k_{obs} for the reactions involving SPEN and S-nitrosocysteine (SNCys) depended upon pH (table 4.5). The rate constants at the higher pH limit are 100 times the size of those at the lower reaches, and each sigmoidal curve exhibits a sharp rate increase at $\text{pH} > 6$, i.e. near the pK_a of bisulfite. The rate slows and levels off as the pH is decreased to below 5. This drop in k_{obs} is connected to the increasing fraction of HSO_3^- that is produced at the expense of SO_3^{2-} . The pK_a^8 of $\text{H}_2\text{SO}_3 \sim 1.8$ (equation 4.8) and so no significant $[\text{H}_2\text{SO}_3]$ will be present at these pH values.

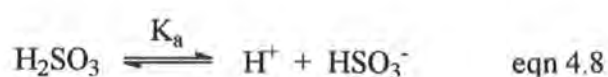


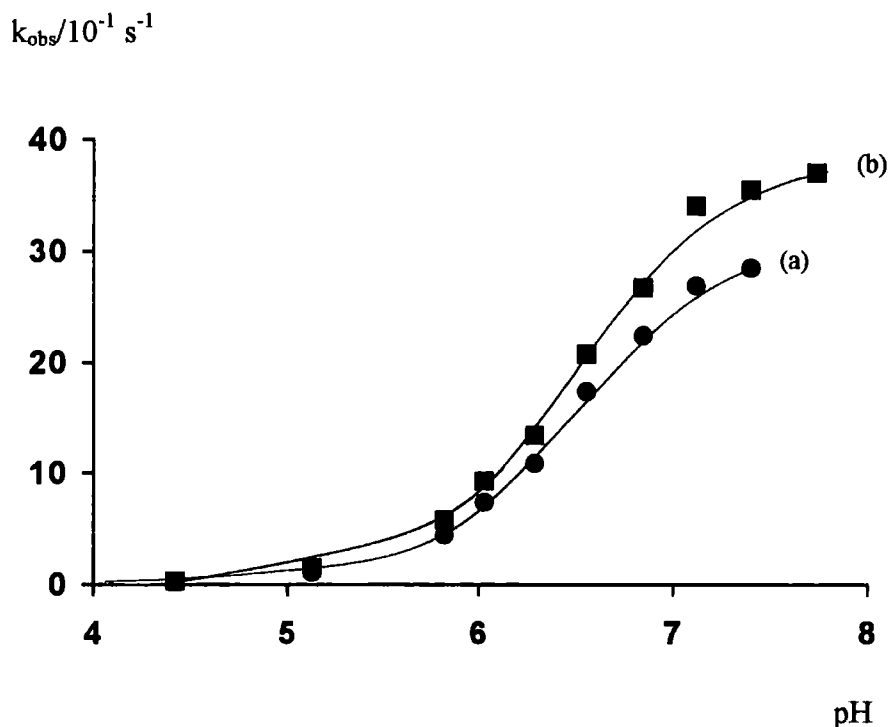
Table 4.5

Influence of buffer pH on k_{obs} for the reaction of SPEN or SNCys ($2.5 \times 10^{-4} \text{ mol dm}^{-3}$) and sulfite. $[\text{EDTA}] = 2.5 \times 10^{-4} \text{ mol dm}^{-3}$ and $[\text{SO}_3^{2-}]_{\text{T}} = 7.5 \times 10^{-3} \text{ mol dm}^{-3}$

pH	SPEN $k_{\text{obs}}/10^{-1} \text{ s}^{-1}$	SNCys $k_{\text{obs}}/10^{-1} \text{ s}^{-1}$
4.42	0.21 ± 0.01	0.31 ± 0.01
5.13	1.10 ± 0.01	1.52 ± 0.02
5.82	4.41 ± 0.02	5.74 ± 0.06
6.03	7.38 ± 0.02	9.29 ± 0.05
6.29	10.9 ± 0.1	13.4 ± 0.1
6.56	17.4 ± 0.1	20.7 ± 0.1
6.85	22.4 ± 0.1	26.7 ± 0.2
7.12	26.9 ± 0.2	34.1 ± 0.3
7.40	28.5 ± 0.2	35.5 ± 0.2
7.74	---	37.0 ± 0.4

Figure 4.3

Plot of k_{obs} versus pH for the reaction of SPEN or SNCys ($2.5 \times 10^{-4} \text{ mol dm}^{-3}$) and sulfite. $[\text{EDTA}] = 2.5 \times 10^{-4} \text{ mol dm}^{-3}$ and $[\text{SO}_3^{2-}]_{\text{T}} = 7.5 \times 10^{-3} \text{ mol dm}^{-3}$



(a) SPEN and (b) SNCys.

The reciprocal plot of equation 4.7 (table 4.6, figure 4.4, equation 4.9) results in a straight line (as did that for the SPEN/secondary amine reactions in section 3.2.2).

$$\frac{1}{k_{\text{obs}}} = \frac{[\text{H}^+]}{k_2 K_a [\text{SO}_3^{2-}]_{\text{T}}} + \frac{1}{k_2 [\text{SO}_3^{2-}]_{\text{T}}} \quad \text{eqn 4.9}$$

The $\text{p}K_a$ of HSO_3^- can be calculated from the gradient (m) and y -axis intercept (c) (equation 4.10). Estimates using SPEN and SNCys at various $[\text{SO}_3^{2-}]_{\text{T}}$ were similar to the value listed in the literature (table 4.7), and confirmed SO_3^{2-} as the reactive species.

$$\frac{c}{m} = K_a \quad \text{eqn 4.10}$$

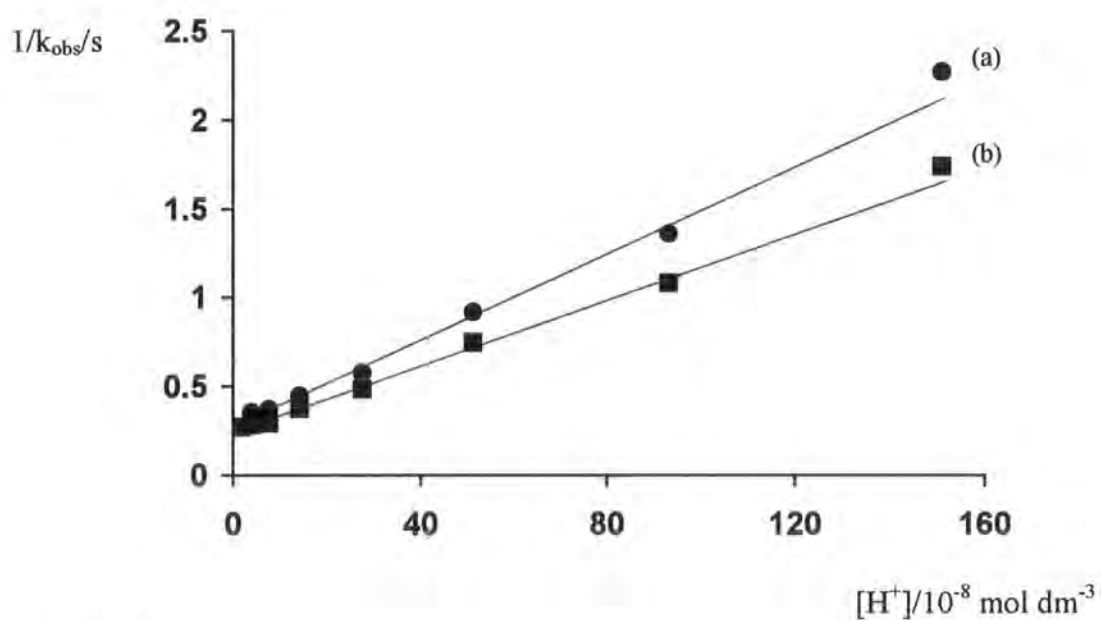
Table 4.6

Values of $1/k_{\text{obs}}$ against $[H^+]$ for the reaction of SPEN or SNCys ($2.5 \times 10^{-4} \text{ mol dm}^{-3}$) and sulfite. $[EDTA] = 2.5 \times 10^{-4} \text{ mol dm}^{-3}$ and $[SO_3^{2-}]_T = 7.5 \times 10^{-3} \text{ mol dm}^{-3}$

$[H^+]$ $/10^{-8} \text{ mol dm}^{-3}$	SPEN $1/k_{\text{obs}}/10^{-1} \text{ s}$	SNCys $1/k_{\text{obs}}/10^{-1} \text{ s}$
1.82	---	2.70
3.98	3.51	2.82
7.59	3.72	2.93
14.1	4.46	3.75
27.5	5.75	4.83
51.3	9.17	7.46
93.3	13.6	10.8
151	22.7	17.4

Figure 4.4

Plot of $1/k_{\text{obs}}$ versus $[H^+]$ for the reaction of SPEN or SNCys ($2.5 \times 10^{-4} \text{ mol dm}^{-3}$) and sulfite. $[EDTA] = 2.5 \times 10^{-4} \text{ mol dm}^{-3}$ and $[SO_3^{2-}]_T = 7.5 \times 10^{-3} \text{ mol dm}^{-3}$



(a) SPEN and (b) SNCys.

Table 4.7

pK_a values (for HSO_3^-) calculated from the reaction of SPEN or SNCys ($2.5 \times 10^{-4} \text{ mol dm}^{-3}$) and sulfite, with $[\text{EDTA}] = 2.5 \times 10^{-4} \text{ mol dm}^{-3}$

$[\text{SO}_3^{2-}]_T$ / $10^{-3} \text{ mol dm}^{-3}$	Calculated pK_a using SPEN	Calculated pK_a using SNCys
8.75	6.70	6.63
7.50 (figure 4.4)	6.70	6.63
6.25	6.71	6.64
5.00	6.73	6.63
Average (lit.⁸ $pK_a \sim 7$)	6.71	6.63

4.2.3 Structure/Reactivity Investigation

A second order rate constant (k_2) accounting for the $\text{RSNO}/\text{SO}_3^{2-}$ interaction could be derived by incorporating the slope (m') of the k_{obs} vs $[\text{SO}_3^{2-}]_T$ plot (figure 4.2) into equation 4.11 (composed from equation 4.7), e.g. k_2 (GSNO) $\sim 134 \text{ mol}^{-1} \text{ dm}^3 \text{ s}^{-1}$ as $m' = 95.7 \pm 1.7 \text{ mol}^{-1} \text{ dm}^3 \text{ s}^{-1}$. Table 4.8 summarises the k_2 values obtained for the reaction of twenty-four structurally varied S-nitrosothiols and SO_3^{2-} . These were checked for SPEN and SNCys using the intercept of the reciprocal plot in figure 4.4 (equation 4.9).

$$k_2 = \frac{m' (K_a + [\text{H}^+])}{K_a} \quad \text{eqn 4.11}$$

Where $[\text{H}^+] = 10^{-\text{pH}} = 10^{-7.4} \text{ mol dm}^{-3}$ and $K_a = 10^{-7} \text{ mol dm}^{-3}$

Table 4.8

Values of k_2 (from equation 4.11) for the reaction of S-nitrosothiols ($2.5 \times 10^{-4} \text{ mol dm}^{-3}$) and sulfite in pH 7.4 buffer, with $[\text{EDTA}] = 2.5 \times 10^{-4} \text{ mol dm}^{-3}$

S-Nitrosothiol	Structure	k_2 / $\text{mol}^{-1} \text{ dm}^3 \text{ s}^{-1}$
2-Acetamido-2-deoxy-S-nitroso-1-thio- β -D-glucopyranose 3,4,6-triacetate (GPSNO)		12100 ± 40
S-Nitroso-1-thio- β -D-glucose (SNTG)		3400 ± 50
S-Nitroso-2-dimethylaminoethanethiol (SDMA)		954 ± 7
S-Nitroso-2-diethylaminoethanethiol (SDEA)		769 ± 11
S-Nitrosocysteine (SNCys)		654 ± 10 577^a
S-Nitrosopenicillamine (SPEN)		527 ± 4 521^a

a. Calculated from the reciprocal plot of $1/k_{\text{obs}} \text{ v } [\text{H}^+]$ (equation 4.9).

Table 4.8 (continued)

Values of k_2 (from equation 4.11) for the reaction of S-nitrosothiols ($2.5 \times 10^{-4} \text{ mol dm}^{-3}$) and sulfite in pH 7.4 buffer, with $[\text{EDTA}] = 2.5 \times 10^{-4} \text{ mol dm}^{-3}$

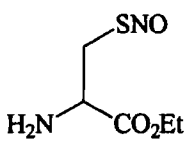
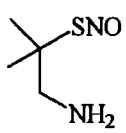
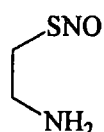
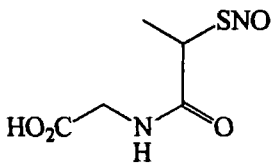
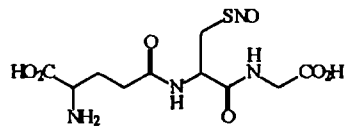
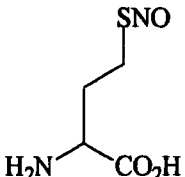
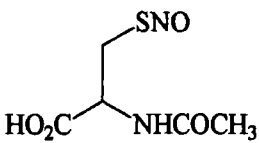
S-Nitrosothiol	Structure	k_2 / $\text{mol}^{-1} \text{ dm}^3 \text{ s}^{-1}$
S-Nitrosocysteine ethyl ester		502 ± 10
S-Nitroso-1-amino-2-methyl-2-propanethiol (SNMP)		467 ± 4
S-Nitroso-2-aminoethanethiol (SNAE)		396 ± 3
S-Nitrosotiopronin (SNTP)		215 ± 2
S-Nitrosoglutathione (GSNO)		134 ± 3
S-Nitrosohomocysteine		31.2 ± 0.6
S-Nitroso-N-acetylcysteine (SNAC)		28.4 ± 0.2

Table 4.8 (continued)

Values of k_2 (from equation 4.11) for the reaction of S-nitrosothiols
($2.5 \times 10^{-4} \text{ mol dm}^{-3}$) and sulfite in pH 7.4 buffer, with $[\text{EDTA}] = 2.5 \times 10^{-4} \text{ mol dm}^{-3}$

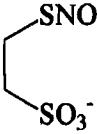
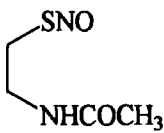
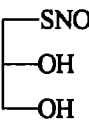
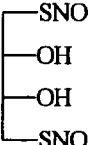
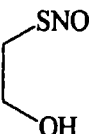
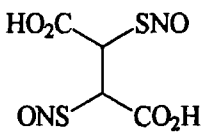
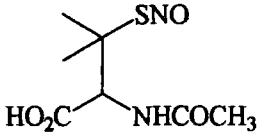
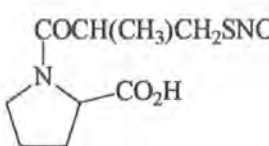
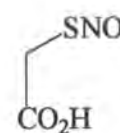
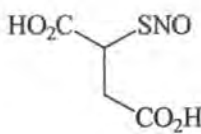
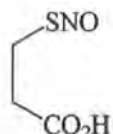
S-Nitrosothiol	Structure	k_2 / $\text{mol}^{-1} \text{dm}^3 \text{s}^{-1}$
S-Nitroso-2-mercaptoethane sulfonic acid		23.5 ± 0.2
S-Nitroso-N-acetylcysteamine (SNCA)		22.4 ± 0.3
S-Nitroso-1-thioglycerol (TGSNO)		20.0 ± 0.3
S,S-Dinitrosodithiothreitol		18.7 ± 0.6
S-Nitroso-2-mercaptoethanol		15.0 ± 0.2
S,S-Dinitroso-2,3-dimercaptosuccinic acid		14.7 ± 0.7
S-Nitroso-N-acetylpenicillamine (SNAP)		7.59 ± 0.07

Table 4.8 (continued)

Values of k_2 (from equation 4.11) for the reaction of S-nitrosothiols ($2.5 \times 10^{-4} \text{ mol dm}^{-3}$) and sulfite in pH 7.4 buffer, with $[\text{EDTA}] = 2.5 \times 10^{-4} \text{ mol dm}^{-3}$

S-Nitrosothiol	Structure	k_2 / $\text{mol}^{-1} \text{ dm}^3 \text{ s}^{-1}$
S-Nitrosocaptopril (SNOCAP)		7.12 ± 0.10
S-Nitroso-2-mercaptoacetic acid		6.88 ± 0.16
S-Nitrosomercaptosuccinic acid (SMSA)		6.63 ± 0.23
S-Nitroso-3-mercapto-propionic acid		3.52 ± 0.06

The most striking aspect uncovered by this survey, is that S-nitroso-1-thiosugars (referred to in chapter 5) are far more reactive towards sulfite than simple aliphatic RSNOs, e.g. GPSNO ($k_2 \sim 12100 \text{ mol}^{-1} \text{ dm}^3 \text{ s}^{-1}$) has 3400 times the reactivity of S-nitroso-3-mercapto-propionic acid ($k_2 \sim 3.52 \text{ mol}^{-1} \text{ dm}^3 \text{ s}^{-1}$). This means that for the reaction of GPSNO ($2.5 \times 10^{-4} \text{ mol dm}^{-3}$) and $[\text{SO}_3^{2-}]_T = 2 \times 10^{-2} \text{ mol dm}^{-3}$, the half-life is a mere 4×10^{-3} seconds. An interpretation of this behaviour is difficult, but the enhanced rate of reaction seems to be coupled to the presence of the main carbohydrate fragment and not the nature of the ring substituents.

No major structure/reactivity relationship is obvious within the other nitrosothiols.

N-Acetylation of the amino group at the β -position with respect to $-\text{SNO}$, reduces the reactivity of a RSNO in relation to another that exhibits a free $-\text{NH}_2$ group. This can be deduced as $k_2(\text{SNCys}) > k_2(\text{SNAC})$, $k_2(\text{SPEN}) > k_2(\text{SNAP})$, and $k_2(\text{SNAE}) > k_2(\text{SNCA})$. Increased steric hindrance due to the bulkier $-\text{COCH}_3$ functionality could of course be a factor. It is unlikely that the promotion of reaction is attributable to the availability of the lone pair of electrons on the nitrogen atom of the free amine, as S-nitroso-2-mercaptoethanol (with a lone pair on the $-\text{OH}$ at the β -position) has a k_2 value of only $15.0 \text{ mol}^{-1} \text{ dm}^3 \text{ s}^{-1}$. At pH 7.4 the amino groups are fully protonated ($\text{pK}_a \sim 8$). It is possible that reaction is assisted by favourable electrostatic interactions between the $-\text{NH}_3^+$ cation and the nucleophile anion, and maybe the N-acetyl group depresses this attractive force. On the other hand, repulsive electrostatic forces between a completely ionised carboxylic acid or $-\text{SO}_3^-$ group and the attacking nucleophile, could explain why the rate of reaction of a nitrosothiol such as S-nitrosomercaptosuccinic acid ($k_2 \sim 6.63 \text{ mol}^{-1} \text{ dm}^3 \text{ s}^{-1}$) or S-nitroso-2-mercaptoethane sulfonic acid ($k_2 \sim 23.5 \text{ mol}^{-1} \text{ dm}^3 \text{ s}^{-1}$) is suppressed. If this theory is true, the attractive force involving $-\text{NH}_3^+$ is dominant over the repulsion due to $-\text{CO}_2^-$, as SNCys and SPEN still have quite large k_2 values despite containing both groups. When the $-\text{NH}_2$ group is at the γ -position it has no positive influence on reactivity, i.e. $k_2(\text{S-nitrosohomocysteine}) \sim 31.2 \text{ mol}^{-1} \text{ dm}^3 \text{ s}^{-1}$. Research by Holmes⁹ using an ascorbate anion as the nucleophile, has identified an exactly similar trend in nitrosothiol reactivity as described above. The correlation could be consistent for most RSNO/nucleophile reactions.

Electron donating methyl groups at the α -position within the nitrosothiol would be expected to decrease the electrophilicity of the nitroso moiety and impede reactivity. The gem-dimethyl effect is almost negligible within our study, as $k_2(\text{SPEN}) \sim k_2(\text{SNCys})$, $k_2(\text{SNMP}) \sim k_2(\text{SNAE})$, and $k_2(\text{SNAP}) \sim k_2(\text{SNAC})$. Curiously, di-nitrosated species such as S,S-dinitrosodithiothreitol ($k_2 \sim 18.7 \text{ mol}^{-1} \text{ dm}^3 \text{ s}^{-1}$) do not demonstrate their usual amplified reactivity in these reactions.

4.2.4 Reaction using Different Forms of Sulfite

Sodium sulfite (Na_2SO_3), potassium sulfite (K_2SO_3), and sodium metabisulfite ($\text{Na}_2\text{S}_2\text{O}_5$), were exchanged in place of NaHSO_3 as the substrate (used to provide SO_3^{2-} ions). The impact upon the rate of SPEN and SNCys decomposition was then evaluated (table 4.9). All other reaction conditions were kept the same (section 4.2.1).

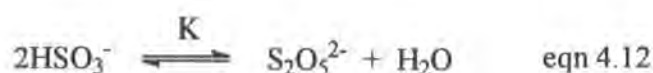
Table 4.9

Values of k_2 (from equation 4.11) for the reaction of SPEN or SNCys ($2.5 \times 10^{-4} \text{ mol dm}^{-3}$) and sulfites at pH 7.4, with $[\text{EDTA}] = 2.5 \times 10^{-4} \text{ mol dm}^{-3}$

Sulfite	SPEN $k_2/\text{mol}^{-1} \text{ dm}^3 \text{ s}^{-1}$	SNCys $k_2/\text{mol}^{-1} \text{ dm}^3 \text{ s}^{-1}$
NaHSO_3	527 ± 4	654 ± 10
Na_2SO_3	510 ± 9	629 ± 7
K_2SO_3	452 ± 5	600 ± 3

If we treat the results achieved for SNCys as an example, rate constants are somewhat independent of whether NaHSO_3 ($k_2 \sim 654 \text{ mol}^{-1} \text{ dm}^3 \text{ s}^{-1}$), Na_2SO_3 ($k_2 \sim 629 \text{ mol}^{-1} \text{ dm}^3 \text{ s}^{-1}$), or K_2SO_3 ($k_2 \sim 600 \text{ mol}^{-1} \text{ dm}^3 \text{ s}^{-1}$) are utilised. This consistency in k_2 endorses our proposal that SO_3^{2-} is the true nucleophile.

Metabisulfite ions ($\text{S}_2\text{O}_5^{2-}$) deliver a gradient (e.g. $m' \sim 696 \text{ mol}^{-1} \text{ dm}^3 \text{ s}^{-1}$ for SPEN) which is roughly twice as large as that measured using SO_3^{2-} (e.g. $m' \sim 365 \text{ mol}^{-1} \text{ dm}^3 \text{ s}^{-1}$ for SPEN using Na_2SO_3), if k_{obs} is plotted against $[\text{S}_2\text{O}_5^{2-}]_{\text{T}}$ (not shown) ($[\text{S}_2\text{O}_5^{2-}]_{\text{T}}$ is the total stoichiometric metabisulfite concentration). Such an outcome is logical, bearing in mind the known stoichiometry of the equilibrium between $\text{S}_2\text{O}_5^{2-}$ and HSO_3^- (and hence SO_3^{2-}) in water¹⁰ (equation 4.12). The value of K specifies that the latter species is favoured¹¹. As the metabisulfite dianion contains **two** sulfur atoms, it would be naive to rule out $\text{S}_2\text{O}_5^{2-}$ as a highly efficient S-nucleophile itself.



$$K \sim 7 \times 10^{-2} \text{ mol}^{-1} \text{ dm}^3 \text{ (at } 22^\circ\text{C)}$$

4.2.5 Denitrosation Products

Nitric oxide (section 6.1.8) and nitrite ion¹² (sections 2.4.2 and 6.2.1.2) were not recognised as products of the reaction between GSNO ($2.5 \times 10^{-4} \text{ mol dm}^{-3}$) and $0.01 \text{ mol dm}^{-3} \text{ NaHSO}_3$ at pH 7.4, where $[\text{EDTA}] = 2.5 \times 10^{-4} \text{ mol dm}^{-3}$. No new signals (except perhaps a small increase in the total absorbance $< 260\text{nm}$) could be singled out in the uv-visible spectrum of this final mixture (figure 4.1).

Quantitative levels of RS^- were discovered¹³ (sections 3.2.6.2 and 6.2.1.3) in test solutions derived from the SO_3^{2-} induced denitrosation of GSNO (table 4.10). For calibration purposes, $\epsilon_{412\text{nm}}$ was determined using GSH as $13420 \text{ mol}^{-1} \text{ dm}^3 \text{ cm}^{-1}$.

Table 4.10

Thiolate ion produced in the reaction of GSNO ($2.5 \times 10^{-4} \text{ mol dm}^{-3}$) and SO_3^{2-} at pH 7.4, with $[\text{EDTA}] = 2.5 \times 10^{-4} \text{ mol dm}^{-3}$

$[\text{SO}_3^{2-}]_{\text{T}}/10^{-4} \text{ mol dm}^{-3}$	% RS^- ^{a,b}
3.75	94.4
5.00	96.0

a. % of $[\text{RS}^-]_{\text{max}}$ that can be generated from GSNO.

b. Measured after 2 hours.

Low $[\text{SO}_3^{2-}]_{\text{T}}$ were necessary as the nucleophile reacted with DTNB to form some species that absorbed at $\lambda \sim 412\text{nm}$. This residual absorbance was thus subtracted from the $\text{Abs}_{412\text{nm}}$ recorded for each sample.

4.2.6 Reaction over a Temperature Range

We also established the temperature dependence of the reaction of a RSNO and sulfite. Second order rate constants were suitably acquired for the decomposition of SPEN, SNCys, SNTP, and S-nitroso-2-dimethylaminoethanethiol (SDMA), at regular intervals between 24 - 33°C (table 4.11). These values were then plotted in accordance with the Arrhenius equation (figure 4.5). Every graph was linear, meaning that the activation parameters (e.g. ΔS^\ddagger , ΔH^\ddagger) for the reactions could be calculated via Eyring analysis (table 4.12). The thermodynamic principles that were applied in this work are explained in more detail in section 3.2.7.

Table 4.11

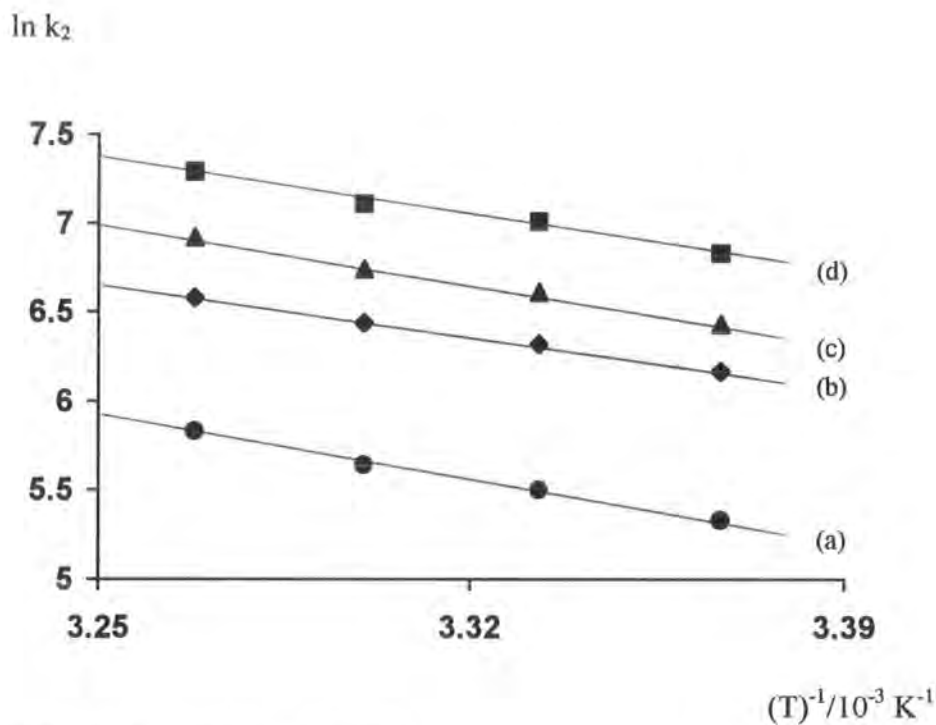
k_2^a as a function of temperature (T) for the reaction of S-nitrosothiols ($2.5 \times 10^{-4} \text{ mol dm}^{-3}$) and SO_3^{2-} at pH ~ 7.4, with [EDTA] = $2.5 \times 10^{-4} \text{ mol dm}^{-3}$

T/K	SPEN $k_2/\text{mol}^{-1} \text{ dm}^3 \text{ s}^{-1}$	SNCys $k_2/\text{mol}^{-1} \text{ dm}^3 \text{ s}^{-1}$	SNTP $k_2/\text{mol}^{-1} \text{ dm}^3 \text{ s}^{-1}$	SDMA $k_2/\text{mol}^{-1} \text{ dm}^3 \text{ s}^{-1}$
297	478 ± 6	621 ± 6	206 ± 2	927 ± 8
300	554 ± 9	740 ± 9	245 ± 3	1111 ± 16
303	626 ± 12	846 ± 7	281 ± 3	1229 ± 18
306	717 ± 14	1016 ± 16	341 ± 6	1468 ± 27

a. Calculated using equation 4.11 – not amended for the slight changes in K_a and pH with temperature.

Table 4.12 underlines that the entropic factors are moderately large and negative for all four S-nitroso compounds. These data give the impression that the activated (transition state) complex in each reaction has a high degree of order. SPEN in particular shows a much lower (more negative) ΔS^\ddagger than the others (i.e. $-89 \text{ J K}^{-1} \text{ mol}^{-1}$), but this is counteracted by the smaller activation energy (33.7 kJ mol^{-1}). The Gibbs energies of activation ($\Delta G_{298\text{K}}^\ddagger$) and enthalpy factors are otherwise comparatively unchanged between species.

Figure 4.5

Arrhenius plot for the reaction of S-nitrosothiols and SO_3^{2-} 

(a) SNTP, (b) SPEN, (c) SNCys and (d) SDMA.

Table 4.12

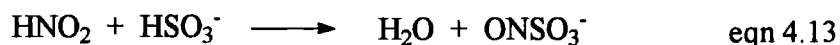
Kinetic/activation parameters for the reaction
of S-nitrosothiols and SO_3^{2-}

Parameter	SPEN	SNCys	SNTP	SDMA
$k_2^a/\text{mol}^{-1} \text{ dm}^3 \text{ s}^{-1}$ (298K)	502	656	217	982
$E_a/\text{kJ mol}^{-1}$	33.7	40.6	41.5	37.3
$A/10^9 \text{ mol}^{-1} \text{ dm}^3 \text{ s}^{-1}$	0.4	8.7	4.1	3.4
$\Delta H^\ddagger/\text{kJ mol}^{-1}$	31.2	38.1	39.0	34.8
$\Delta S^\ddagger/\text{J K}^{-1} \text{ mol}^{-1}$	-89	-63	-69	-71
$\Delta G^\ddagger_{298\text{K}}/\text{kJ mol}^{-1}$	57.7	56.9	59.6	56.0

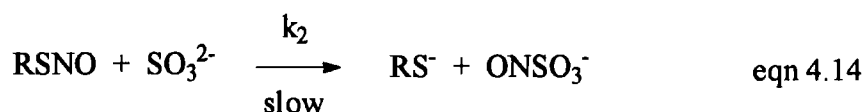
a. Calculated from figure 4.5 – within $\pm 5\%$ of the corresponding values quoted in table 4.8.

4.2.7 Mechanistic Interpretations

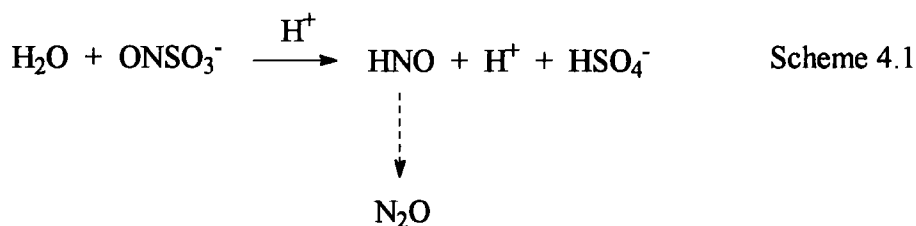
The nitrosation of SO_3^{2-} (as HSO_3^-) using nitrous acid is a fundamental step in the industrial synthesis of hydroxylamine¹⁴ (Raschig process). It is also intrinsic to the 'lead chamber' commercial manufacture of sulfuric acid¹⁵ and the purification of gaseous waste emissions, e.g. flue-gas desulfurisation/scrubbers¹⁶. The first stage of the reaction in aqueous acidic media furnishes an unstable nitrososulfonic acid intermediate^{11,17} (ONSO_3^-) (equation 4.13).



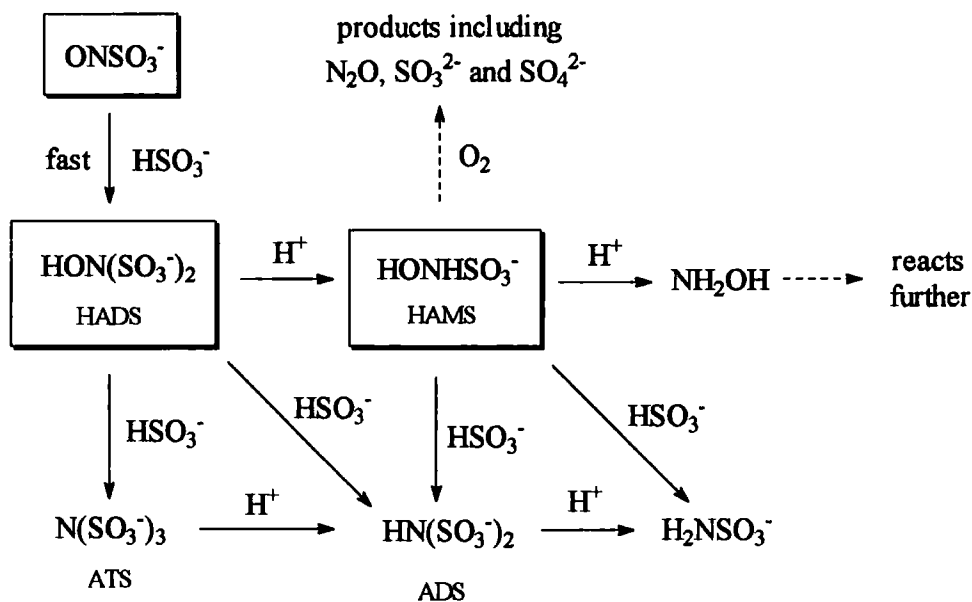
In the same way, it is assumed that ONSO_3^- and thiolate anion (as detected) are derived from rate-limiting attack of the SO_3^{2-} nucleophile at the nitrogen atom of the -SNO group within a nitrosothiol (equation 4.14). This is a comparable interaction to the one proposed for the reactions of SPEN and nitrogen nucleophiles in the previous chapter.



It has been reported that the ONSO_3^- adduct can form nitrous oxide in the $\text{HNO}_2/\text{HSO}_3^-$ system^{17,18} (scheme 4.1).



Nitrososulfonic acid is also unique in the way that it can act as a 'secondary' nitrosating agent, i.e. it can rapidly react with more substrate to give hydroxylamine disulfonate (HADS) (scheme 4.2).



Scheme 4.2

The reaction we are studying may therefore continue along a complex set of pathways that are similar to those known at $\text{pH} < 5$ (scheme 4.2);

- (i) Sulfonation of HADS leads to amine trisulfonate (ATS) and amine disulfonate (ADS), the latter of which is hydrolysed to sulfamate¹⁹ (H_2NSO_3^-).
- (ii) Hydrolysis of HADS delivers hydroxylamine-N-sulfonate (HAMS). This can be sulfonated, oxidised²⁰, or converted to hydroxylamine²¹. Sulfamic acid (NH_2HSO_3) and ammonium bisulfate (NH_4HSO_4), are however created upon the reaction of NH_2OH with bisulfite in water²².

The applicability of the reviewed mechanism will undoubtedly be affected by the fact that our experiments were performed in a buffer of physiological pH. Seel and Degener²³ have nevertheless measured the kinetics of formation of HADS at neutral pH.

Dissolved nitric oxide²⁴ in aerated solution ($\text{pH} 4 - 10$), iron nitrosyl complexes²⁵, MNTS⁵, and alkyl nitrites⁵, are some of the other reagents that have been successfully employed to nitrosate $\text{HSO}_3^-/\text{SO}_3^{2-}$ ions.

4.3 Reactions of S-Nitrosothiols with Thiourea, Thiocyanate, Thiosulfate, and Thiomethoxide

Thiosulfate²⁶ ($S_2O_3^{2-}$), thiourea²⁷ ($SC(NH_2)_2$), and thiocyanate²⁸ (SCN^-), are sulfur-based molecules that are easily nitrosated by standard methods. A nitrosothiosulfate anion (O_3SSNO^-), a nitrososulfonium ion ($ON^+SC(NH_2)_2$), and nitrosyl thiocyanate ($ONSCN$), are the initial outcome. Our next goal was to gauge the affinity between a S-nitrosothiol (SPEN or SNCys) and these nucleophiles. This was done with a view to comparing and contrasting performances with that of the SO_3^{2-} ion. Thiomethoxide (MeS^-) was regarded as an additional sulfur species worthy of inclusion in these trials.

Minor modifications were made to the experimental routine described for the RSNO/sulfite reactions in section 4.2.1. Table 4.13 discloses that these were; (i) the nature of the fresh substrate solution, (ii) the limits of the total stoichiometric nucleophile concentration ($[nucleophile]_T$), and (iii) the ionic strength (fixed for each series, but not uniform to all series).

Table 4.13

Kinetic details for the reaction of SPEN or SNCys ($2.5 \times 10^{-4} \text{ mol dm}^{-3}$) and S-nucleophiles in pH 7.4 buffer, with $[EDTA] = 2.5 \times 10^{-4} \text{ mol dm}^{-3}$

Nucleophile	Substrate	$[nucleophile]_T$ / $10^{-3} \text{ mol dm}^{-3}$	I / $10^{-1} \text{ mol dm}^{-3}$
Thiosulfate ^a	$Na_2S_2O_3$	170 – 230	8.40
Thiomethoxide ^b	MeSNa	15.0 – 25.0	1.75
Thiourea ^b	$SC(NH_2)_2^c$	500 – 1000	1.50
Thiocyanate ^b	$NaSCN^c$	200 – 400	5.50

a. Monitored using stopped-flow spectrophotometry.

b. Monitored using conventional uv-visible spectrophotometry.

c. Strictly speaking, thiourea/thiocyanate are ambident (S- and N-) nucleophiles (section 3.6) - for the purpose of this study they are categorised as S-nucleophiles.

Under the pseudo-first order conditions employed, a plot of k_{obs} against $[\text{nucleophile}]_{\text{T}}$ was again a straight line. Overall (as for the reactions with sulfite), our results satisfied the kinetic expressions in equations 4.15 – 4.17, where $[\text{nucleophile}]$ is the concentration of 'free' nucleophile.

$$\text{Rate} = k_2[\text{RSNO}][\text{nucleophile}] \quad \text{eqn 4.15}$$

$$\text{Rate} = k_{\text{obs}}[\text{RSNO}] \quad \text{eqn 4.16}$$

$$k_{\text{obs}} = k_2[\text{nucleophile}] \quad \text{eqn 4.17}$$

The pK_{a} values of these nucleophiles (e.g. $\text{pK}_{\text{a}}^{29}$ of $\text{HSCN} \leq 1$) meant that at pH 7.4, $[\text{nucleophile}] = [\text{nucleophile}]_{\text{T}}$, and so no correction had to be made when calculating k_2 (table 4.14) from the slope (m') of a $k_{\text{obs}} \text{ v } [\text{nucleophile}]_{\text{T}}$ plot, i.e. $m' = k_2$.

Table 4.14

Values of k_2 for the reaction of SPEN or SNCys ($2.5 \times 10^{-4} \text{ mol dm}^{-3}$) and various sulfur nucleophiles, with $[\text{EDTA}] = 2.5 \times 10^{-4} \text{ mol dm}^{-3}$

Nucleophile	SPEN $k_2/\text{mol}^{-1} \text{ dm}^3 \text{ s}^{-1}$	SNCys $k_2/\text{mol}^{-1} \text{ dm}^3 \text{ s}^{-1}$
SO_3^{2-}	$527 \pm 4^{\text{a}}$	$654 \pm 10^{\text{a}}$
$\text{S}_2\text{O}_3^{2-}$	2.29 ± 0.07	1.86 ± 0.02
MeS^-	$(3.00 \pm 0.42) \times 10^{-2}$	$(2.91 \pm 0.26) \times 10^{-2}$
$\text{SC}(\text{NH}_2)_2$	$(13.3 \pm 1.1) \times 10^{-4}$	$(6.26 \pm 0.21) \times 10^{-4}$
SCN^-	$(2.53 \pm 0.06) \times 10^{-4}$	$(2.11 \pm 0.09) \times 10^{-4}$

a. Determined in section 4.2.3.

A y-axis intercept was apparent in the graph of k_{obs} vs $[\text{nucleophile}]_{\text{T}}$ for the system involving thiosulfate (not shown). This is perplexing because the rate of RSNO decomposition ($k_2 \sim 2.29 \text{ mol}^{-1} \text{ dm}^3 \text{ s}^{-1}$ for SPEN/ $\text{S}_2\text{O}_3^{2-}$) is surely too rapid for it to be excused as a thermal element. The term could be linked to the reversibility of the reaction (common to the nitrosation of alcohols³⁰) or be of photochemical origin. Inorganic sulfur compounds generate free radicals on exposure to light⁵ (e.g. $\text{S}_2\text{O}_3^{\cdot-}$), and so a radical may then compete with the nucleophile for reaction at -SNO.

Reactions of S-nucleophiles with S-nitrosothiols do not correlate to the Pearson² nucleophilicity index (n) (table 4.15). This point is illustrated as sulfite ($k_2 \sim 527 \text{ mol}^{-1} \text{ dm}^3 \text{ s}^{-1}$) is ca. 230 times more reactive than thiosulfate ($k_2 \sim 2.29 \text{ mol}^{-1} \text{ dm}^3 \text{ s}^{-1}$) with SPEN, even though $n = 8.53$ and 8.95 respectively. The contrast is even stronger for SNCys. Unfortunately, the literature only lists a Ritchie parameter (N_+) for SO_3^{2-} . It is thus impossible to tell whether the behaviour imitates that of the N-nucleophiles, in coinciding well with N_+ and not n (section 3.7). Thiourea is reflected as a mildly better nucleophile than thiocyanate in our grouping. This has been remarked upon in earlier research referring to nitroso electrophiles^{5,16}.

Table 4.15
Reactivity of sulfur nucleophiles

Classification	Reactivity Rating
RSNO/S-nucleophile ^a	$\text{SO}_3^{2-} > \text{S}_2\text{O}_3^{2-} > \text{MeS}^- > \text{SC}(\text{NH}_2)_2 > \text{SCN}^-$
Pearson ^b	$\text{S}_2\text{O}_3^{2-} > \text{SO}_3^{2-} > \text{SC}(\text{NH}_2)_2 > \text{SCN}^-$

a. Ranked according to the k_2 values in table 4.14.

b. A value of n is not available for thiomethoxide.

The gem-dimethyl substituents within SPEN surprisingly promote a reaction that is faster than that of SNCys, with all of the S-nucleophiles except sulfite (table 4.14). This is the reverse of what is electronically predicted (see section 4.2.3), but duplicates the pattern found by Holmes⁹ using the ascorbate nucleophile.

Thiourea was reacted with four extra S-nitrosothiols to assess if the RSNO structural criteria understood to retard reactivity with sulfite in section 4.2.3, extended to reactions that engaged a different S-nucleophile (table 4.16).

Table 4.16

Values of k_2 for the reaction of S-nitrosothiols ($2.5 \times 10^{-4} \text{ mol dm}^{-3}$) and thiourea, with $[\text{EDTA}] = 2.5 \times 10^{-4} \text{ mol dm}^{-3}$

S-Nitrosothiol	$k_2/10^{-4} \text{ mol}^{-1} \text{ dm}^3 \text{ s}^{-1}$
SNMP	3.13 ± 0.22
SNAE	1.75 ± 0.08
SNAC and SNAP	Too slow to measure

The attenuation of the reaction rate that is influenced by a $\beta\text{-NHCOCH}_3$ group within a RSNO, is dominant enough to mean that SNAC and SNAP remain intact when exposed to thiourea. On the other hand their non-acetylated analogues decompose, i.e. SNCys and SPEN (table 4.14). Here also, $k_2(\text{SNMP}) > k_2(\text{SNAE})$, so reaffirming the bizarre rate-accelerating effect of methyl groups upon the α -carbon atom of the electrophile. Table 4.17 differentiates how the reactivity of a nitrosothiol varies, in line with whether the attacking nucleophile is $\text{SC}(\text{NH}_2)_2$ or SO_3^{2-} .

Table 4.17

Reactivity of S-nitrosothiols with sulfite and thiourea

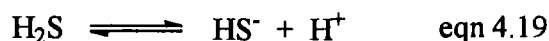
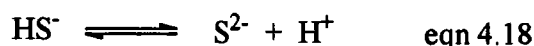
Nucleophile	Reactivity Rating
SO_3^{2-} ^a	SNCys > SPEN > SNMP > SNAE > SNAC > SNAP
$\text{SC}(\text{NH}_2)_2$ ^b	SPEN > SNCys > SNMP > SNAE > SNAC/SNAP

a. Ranked by the k_2 values in table 4.8 and b. Ranked by the k_2 values in tables 4.14 and 4.16.

4.4 Reactions of S-Nitrosothiols with Sulfides

4.4.1 Denitrosation of S-Nitrosoglutathione

The hydrosulfide ion (HS^-) is advocated as a potent nucleophile². Sodium sulfide hydrate ($\text{NaHS}\cdot x\text{H}_2\text{O}$) and sodium sulfide nonahydrate ($\text{Na}_2\text{S}\cdot 9\text{H}_2\text{O}$) are both convenient sources of HS^- , as the sulfide ion (S^{2-}) is completely protonated in aqueous solutions other than in concentrated NaOH (pK_a^{31} of $\text{HS}^- \sim 14.2$) (equation 4.18). The lethal gas, hydrogen sulfide (H_2S), is evolved at too low a pH (pK_a^{31} of $\text{H}_2\text{S} \sim 6.9$) (equation 4.19), and so extreme care has to be taken when handling these chemicals.

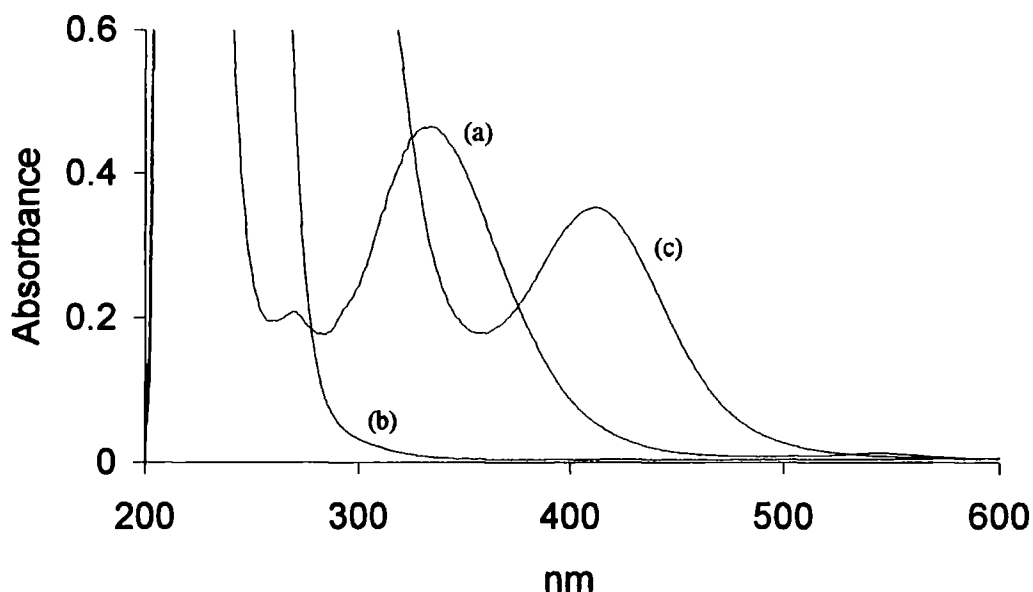


Each hydrate (0.10 mol dm^{-3} , $I = 0.30 \text{ mol dm}^{-3}$) was reacted with GSNO ($5 \times 10^{-4} \text{ mol dm}^{-3}$) in distilled water containing EDTA ($1 \times 10^{-4} \text{ mol dm}^{-3}$). Phosphate buffer (pH 7.4) was discarded on this occasion, as it was ineffective at such a high $[\text{HS}^-]$. The reaction spectra one minute after mixing highlight that the denitrosation of GSNO is the only spectral permutation to follow $\text{NaHS}\cdot x\text{H}_2\text{O}$ addition (pH 9.72, spectrum (b) in figure 4.6). However, a new absorbance peak at 410nm (λ_{max}) is immediately visible when $\text{Na}_2\text{S}\cdot 9\text{H}_2\text{O}$ is used (pH 12.70, spectrum (c) in figure 4.6). This change was accompanied by the development of a bright orange-yellow colour in the reaction mixture. The coloration and absorption maximum then simultaneously disappeared over 6 hours.

The absorbance-time traces (not shown) representing the decomposition of GSNO at 340nm in spectrum (b), or the formation of the maximum at 410nm in spectrum (c), were too confusing for rate analysis. The latter time-drive spectrum demonstrated the existence of many successive kinetic processes with a duration of less than 40 seconds.

Figure 4.6

Spectra of GSNO ($5 \times 10^{-4} \text{ mol dm}^{-3}$) in distilled water, with/without added sulfide and $[\text{EDTA}] = 1 \times 10^{-4} \text{ mol dm}^{-3}$



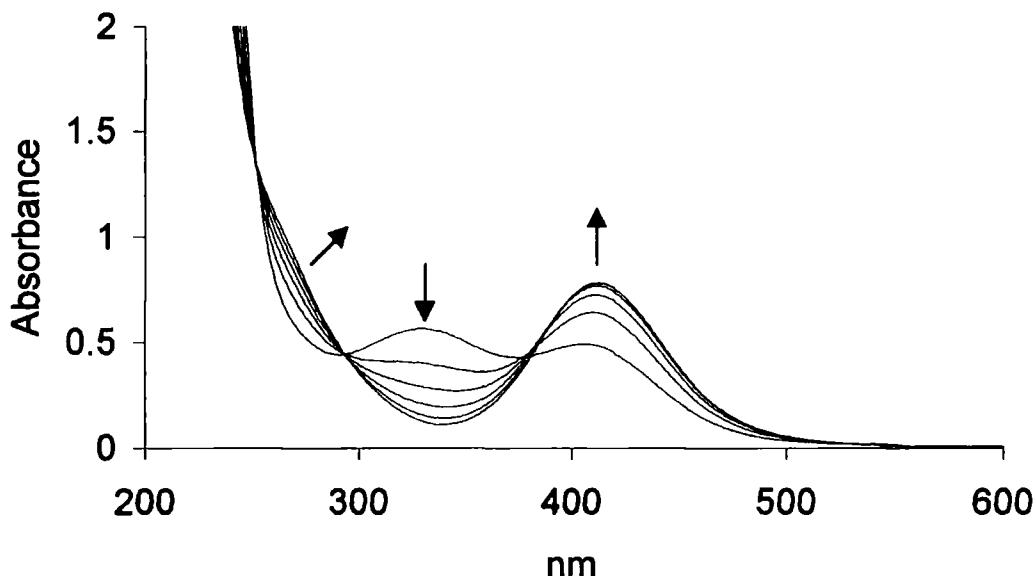
(a) GSNO only, (b) $[\text{NaHS} \cdot x\text{H}_2\text{O}] = 0.10 \text{ mol dm}^{-3}$ and (c) $[\text{Na}_2\text{S} \cdot 9\text{H}_2\text{O}] = 0.10 \text{ mol dm}^{-3}$.

The discrepancies in the two metal sulfide reactions are peculiar, and not dictated by pH. This can be presumed as the peak at 410nm is still produced when the ratio of $[\text{Na}_2\text{S} \cdot 9\text{H}_2\text{O}]$ to $[\text{RSNO}]$ is reduced to 1:1 (figure 4.7), and the pH of the medium (pH 9.80) is the same as that for $0.10 \text{ mol dm}^{-3} \text{ NaHS} \cdot x\text{H}_2\text{O}$ (pH 9.72). The 'colourful' set of spectra bear clear isosbestic points at 254, 293, and 379nm, and also specify that the product absorbs at $\lambda \sim 275\text{nm}$. Hydrosulfide plays an instrumental part in the decay mechanism of the orange-yellow species, as it fades at a slower rate at low $[\text{Na}_2\text{S} \cdot 9\text{H}_2\text{O}]$.

In the wake of these discoveries, the $\text{RSNO}/\text{Na}_2\text{S} \cdot 9\text{H}_2\text{O}$ reaction was probed more deeply to learn if it could be adopted as an analytical or spectrophotometric technique.

Figure 4.7

Repeat scan spectra (time interval = 25 seconds) for the reaction of GSNO ($1 \times 10^{-3} \text{ mol dm}^{-3}$) and $\text{Na}_2\text{S} \cdot 9\text{H}_2\text{O}$ ($1 \times 10^{-3} \text{ mol dm}^{-3}$) in distilled water (pH 9.80), with $[\text{EDTA}] = 1 \times 10^{-4} \text{ mol dm}^{-3}$



4.4.2 Denitrosation of Other S-Nitrosothiols

A 'league table' of nitrosothiol reactivity can be created if the time for $\text{Abs}_{410\text{nm}}$ to reach an upper limit is crudely translated as the rate of reaction between a RSNO ($1 \times 10^{-3} \text{ mol dm}^{-3}$) and $\text{Na}_2\text{S} \cdot 9\text{H}_2\text{O}$ ($1 \times 10^{-2} \text{ mol dm}^{-3}$) (table 4.18). The order is akin to that revealed for the RSNO/ SO_3^{2-} system in section 4.2.3, e.g. a β - NHCOCH_3 or β - CO_2H substituent restricts reactivity.

Plotting the final absorbance at 410nm versus the concentration of nitrosothiol introduced to $0.25 \text{ mol dm}^{-3} \text{ Na}_2\text{S} \cdot 9\text{H}_2\text{O}$ (table 4.19), enables the deduction of the extinction coefficient ($\epsilon_{410\text{nm}}$) of the coloured species at this wavelength. SPEN (figure 4.8) and SNCys yield $\epsilon_{410\text{nm}}$ values of 772 and 774 $\text{mol}^{-1} \text{ dm}^3 \text{ cm}^{-1}$. Hypothetically, the calibration of $\epsilon_{410\text{nm}}$ using authentic RSNO solutions could authorise its use in the quantification of nitrosothiol levels in test assays. For this application, it must be guaranteed that no other constituents interact with $\text{Na}_2\text{S} \cdot 9\text{H}_2\text{O}$ to give a false absorption at 410nm.

Table 4.18

Abs_{410nm} formation times during the reaction of S-nitrosothiols ($1 \times 10^{-3} \text{ mol dm}^{-3}$) and Na₂S.9H₂O ($1 \times 10^{-2} \text{ mol dm}^{-3}$) in distilled water (pH 11.70), with [EDTA] = $1 \times 10^{-4} \text{ mol dm}^{-3}$

S-Nitrosothiol ^a	Time/min
SNCys	< 0.5
SPEN	< 0.5
GSNO	< 1
SNAC	6
SNAP	33
SNOCAP	40
SMSA	90

↓
Decreasing reactivity

a. See table 4.8 for structures.

Table 4.19

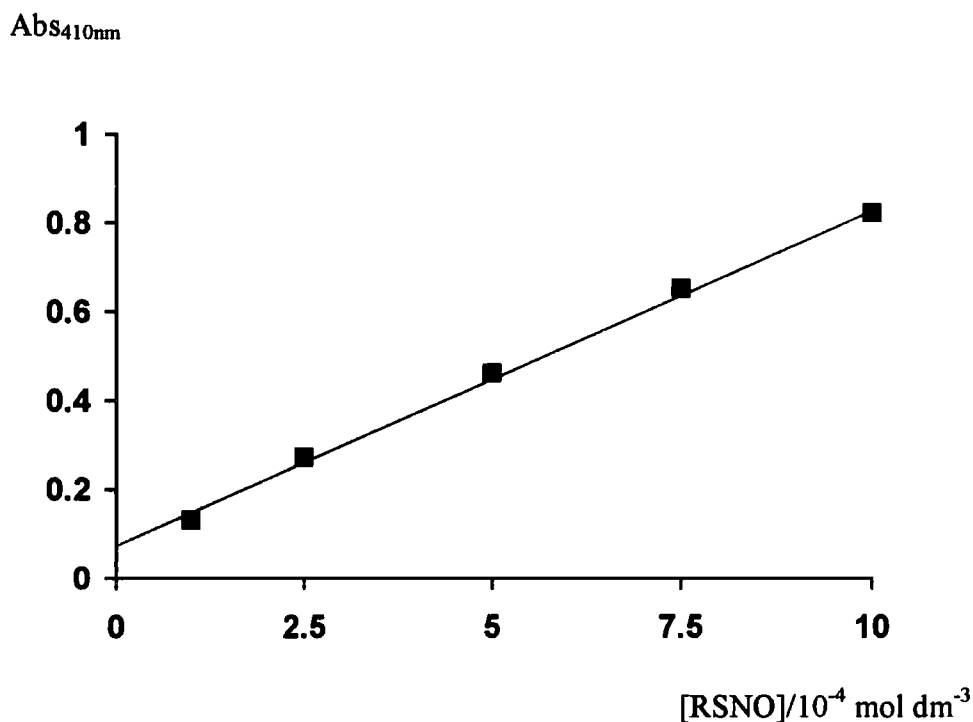
Absorbance (410nm) as a function of added [RSNO] for the reaction of SPEN or SNCys and Na₂S.9H₂O (0.25 mol dm^{-3}) in distilled water (pH 12.94), with [EDTA] = $1 \times 10^{-4} \text{ mol dm}^{-3}$

[RSNO] / $10^{-4} \text{ mol dm}^{-3}$	SPEN Abs _{410nm} ^a	SNCys Abs _{410nm} ^a
1.0	0.131	0.157
2.5	0.272	0.304
5.0	0.462	0.505
7.5	0.652	0.694
10	0.822	0.856
$\epsilon_{410nm}/\text{mol}^{-1} \text{ dm}^3 \text{ cm}^{-1}$	772 ± 17	774 ± 29

a. Measured after 2 minutes.

Figure 4.8

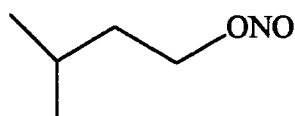
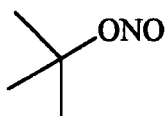
Plot of Abs_{410nm} against $[RSNO]$ for the reaction of SPEN and $Na_2S \cdot 9H_2O$



4.4.3 Denitrosation of O- and N-Nitroso Compounds

Leis et al⁵ have commented upon the emergence of a yellow colour when MNTS is reacted with HS^- at pH 7. To find out whether this visual transformation was widespread through all nitroso compound/ $Na_2S \cdot 9H_2O$ reactions, experiments were repeated with an alkyl nitrite and N-nitrosamine in place of the nitrosothiol. ^tButyl nitrite (4.1) (figure 4.9) and isoamyl nitrite (4.2) operated in an identical way to a RSNO (table 4.20), and the final value of Abs_{410nm} was in agreement with the acknowledged value of ϵ_{410nm} ($\sim 770 \text{ mol}^{-1} \text{ dm}^3 \text{ cm}^{-1}$). The reactivity of isoamyl nitrite was close to that of SNAP, and surpassed ^tBuONO probably on steric grounds. Secondary nitrosamines are renowned for their stability, and showed no signs of reacting within 5 hours.

4.1



4.2

Figure 4.9

Repeat scan spectra (time interval = 20 minutes) for the reaction of ^tbutyl nitrite ($1 \times 10^{-3} \text{ mol dm}^{-3}$) and $\text{Na}_2\text{S}_2\text{O}_8$ ($1 \times 10^{-2} \text{ mol dm}^{-3}$) in distilled water (pH 11.66), with $[\text{EDTA}] = 1 \times 10^{-4} \text{ mol dm}^{-3}$

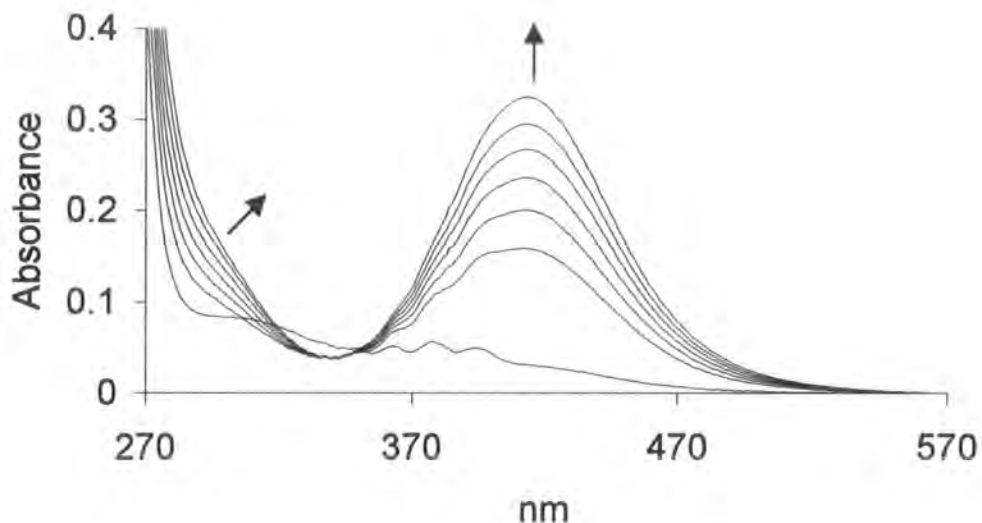


Table 4.20

$\text{Abs}_{410\text{nm}}$ formation times during the reaction of alkyl nitrites or N-nitrosamines ($1 \times 10^{-3} \text{ mol dm}^{-3}$) and $\text{Na}_2\text{S}_2\text{O}_8$ ($1 \times 10^{-2} \text{ mol dm}^{-3}$) in distilled water (pH ~ 11.65), with $[\text{EDTA}] = 1 \times 10^{-4} \text{ mol dm}^{-3}$

RONO^a	Time/min	Final Abs_{410nm}
Isoamyl nitrite	30	0.85
^t Butyl nitrite	360	0.63
RR'NNO^a	Time/min	Final Abs_{410nm}
N-Nitrosopyrrolidine	No reaction	---
N-Nitroso-N-methylaniline	No reaction	---

a. Dissolved in 4% (v/v) 1,4-dioxane.

4.4.4 Nitrosated Product

S-Nitrosated substrates are frequently yellow in appearance, e.g. O_3SSNO^- ²⁶. Assorted nitroso (sulfide) derivatives could theoretically originate from the action of XNO (where X = RS-, RO- etc.) on $Na_2S \cdot 9H_2O$, with thionitrous acid (HSNO), a thionitrite ion (^-SNO), ^-SNO , a SSNO complex, ONSNO, and SNO^+ , all credible candidates. It is our impression however that a **nitrosodisulfide (or perthionitrite) ion ($^-\text{SSNO}$)** is formed. Seel and Wagner³² have observed the instant materialisation of this orange-yellow anion when NO is passed through anaerobic solutions of either Na_2S , NaHS or Na_2S_2 , and the absorption spectra that they describe are exact replicas of those that we have obtained (figures 4.6, 4.7 and 4.9). Spectra display: (i) a main peak with $\lambda_{\text{max}} (H_2O) \sim 409\text{nm}$ (ϵ not given), (ii) a shoulder at $\lambda \sim 290\text{nm}$, and (iii) the diminishment of the two absorbances on standing (over a few days).

4.4.5 Promotion of Reaction by Added Disulfide

If what we detect spectrophotometrically is indeed nitrosodisulfide, its hydrodisulfide or disulfide ion precursor (HSS^- or S_2^{2-}) must somehow be generated from HS^- . One answer to this quandary has been provided by Rao and Gorin³³, and entails a disulfide (e.g. cystine) reacting with $Na_2S \cdot 9H_2O$ in basic media to create RSS^- ($\lambda_{\text{max}} \sim 335\text{nm}$ and $\lambda_{\text{min}} \sim 310\text{nm}$) (equation 4.20). This anion then combines with additional sulfide to give RS^- and HSS^- (equation 4.21), even though the equilibrium constant (K) for the process is perceived as very small (not stated).

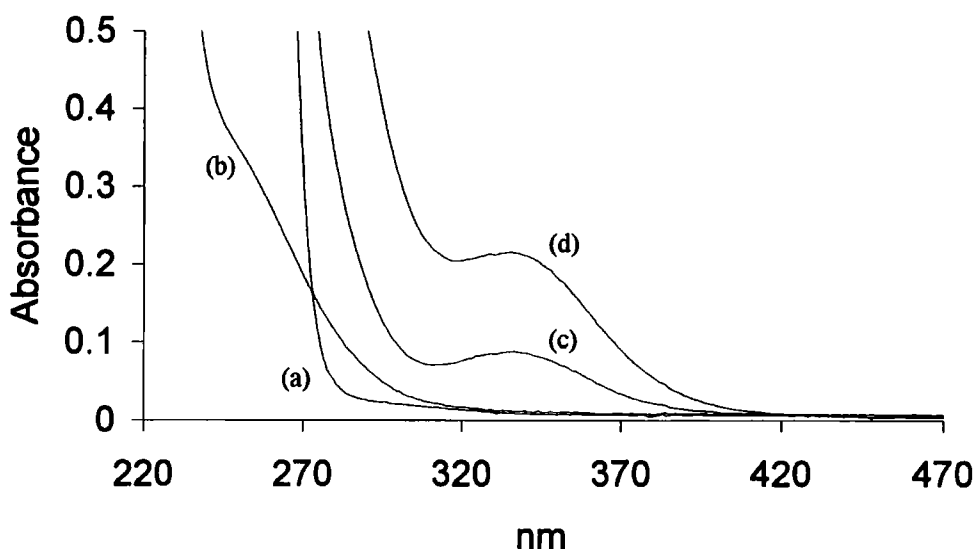


Of course this scenario is only relevant to S-nitrosothiols, as RSSRs are their normal degradation products. Dialkyl peroxides (ROOR), which are the oxygen counterparts to RSSR, do not easily stem from alkyl nitrites³⁴, and so RONO (or MNTS for that matter) must manufacture HSS^- via an alternate route.

To verify the above proposal we checked that RSS^- did emanate from RSSR/HS^- under our reaction conditions (traces (c) and (d) in figure 4.10), by treating oxidised glutathione (GSSG , $1 \times 10^{-3} \text{ mol dm}^{-3}$) with $\text{Na}_2\text{S}\cdot 9\text{H}_2\text{O}$ ($1 \times 10^{-2} \text{ mol dm}^{-3}$).

Figure 4.10

Formation of GSS^- during the reaction of GSSG ($1 \times 10^{-3} \text{ mol dm}^{-3}$) and $\text{Na}_2\text{S}\cdot 9\text{H}_2\text{O}$ ($1 \times 10^{-2} \text{ mol dm}^{-3}$) in distilled water (pH 10.67), with $[\text{EDTA}] = 1 \times 10^{-4} \text{ mol dm}^{-3}$



(a) $\text{Na}_2\text{S}\cdot 9\text{H}_2\text{O}$ ($1 \times 10^{-2} \text{ mol dm}^{-3}$), (b) GSSG ($1 \times 10^{-3} \text{ mol dm}^{-3}$), (c) $\text{Na}_2\text{S}\cdot 9\text{H}_2\text{O}$ ($1 \times 10^{-2} \text{ mol dm}^{-3}$) and GSSG ($1 \times 10^{-3} \text{ mol dm}^{-3}$) – 1 minute after mixing and (d) As (c) – 60 minutes after mixing.

Added GSSG ($1 \times 10^{-3} \text{ mol dm}^{-3}$) was then shown to effect an amazing enhancement in the rate of formation of $\text{Abs}_{410\text{nm}}$, when GSNO ($1 \times 10^{-3} \text{ mol dm}^{-3}$) was mixed with $\text{Na}_2\text{S}\cdot 9\text{H}_2\text{O}$ ($1 \times 10^{-3} \text{ mol dm}^{-3}$) (i.e. figure 4.12 with respect to figure 4.11). The RSS^- entity was confirmed at these GSSG and HS^- concentrations in a separate test (as in figure 4.10), and leaving a GSSG/HS^- solution to settle for 60 minutes before addition to GSNO had a more profound effect (i.e. a greater $[\text{RSS}^-]$ present). These findings substantiate the theory that RSS^- may be the central intermediate that controls the formation of SSNO . Because the ratio of $[\text{GSSG}]$ to $[\text{Na}_2\text{S}\cdot 9\text{H}_2\text{O}]$ was 1:1, pH 12 buffer had to be used to maintain an alkaline pH. The reaction with no GSSG was appreciably slower at pH 12 (figure 4.11) than at pH 9.80 (figure 4.7), and thus perhaps $\text{RSS}^-/\text{HSS}^-$ are partially destroyed by OH^- .

Figure 4.11

Repeat scan spectra (time interval = 50 seconds) for the reaction of GSNO ($1 \times 10^{-3} \text{ mol dm}^{-3}$) and $\text{Na}_2\text{S} \cdot 9\text{H}_2\text{O}$ ($1 \times 10^{-3} \text{ mol dm}^{-3}$) in pH 12.0 buffer, with $[\text{EDTA}] = 1 \times 10^{-4} \text{ mol dm}^{-3}$

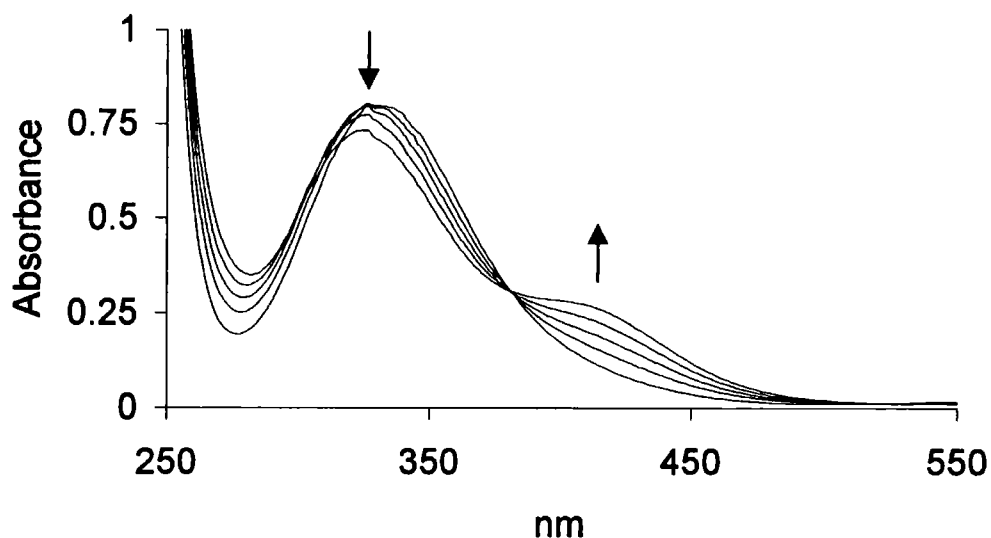
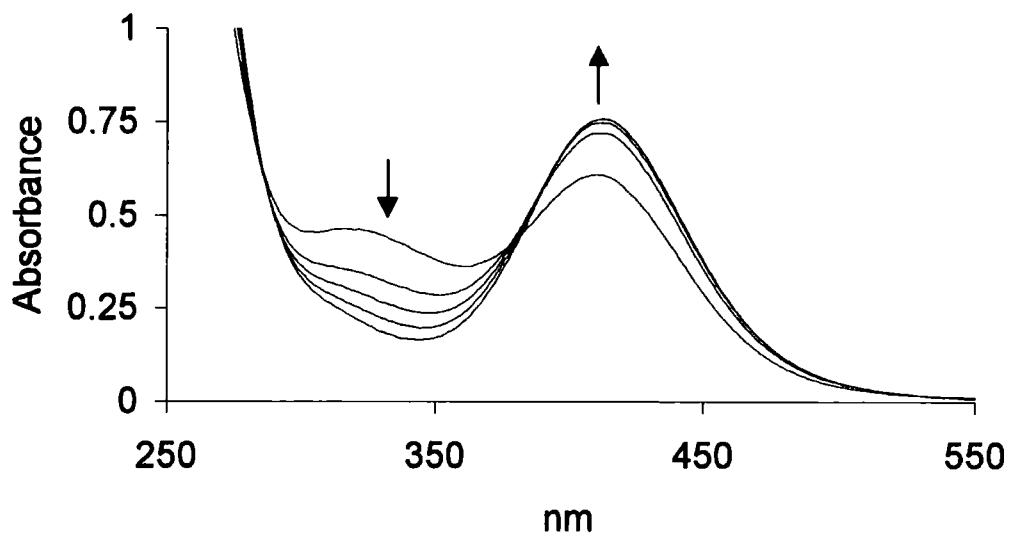


Figure 4.12

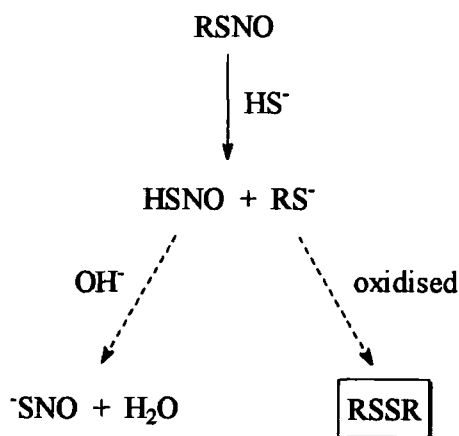
Repeat scan spectra (time interval = 50 seconds) for the reaction of GSNO ($1 \times 10^{-3} \text{ mol dm}^{-3}$) and $\text{Na}_2\text{S} \cdot 9\text{H}_2\text{O}$ ($1 \times 10^{-3} \text{ mol dm}^{-3}$)/GSSG ($1 \times 10^{-3} \text{ mol dm}^{-3}$) in pH 12.0 buffer, with $[\text{EDTA}] = 1 \times 10^{-4} \text{ mol dm}^{-3}$



4.4.6 Mechanism of Anion Formation

A number of observations have been made about the pathway via which the nitrosodisulfide anion forms from a RSNO and $\text{Na}_2\text{S}\cdot 9\text{H}_2\text{O}$. In our opinion the reaction is split into two parts; (i) the source of disulfide, and (ii) the RSSR stimulated creation of HSS^- and its subsequent nitrosation.

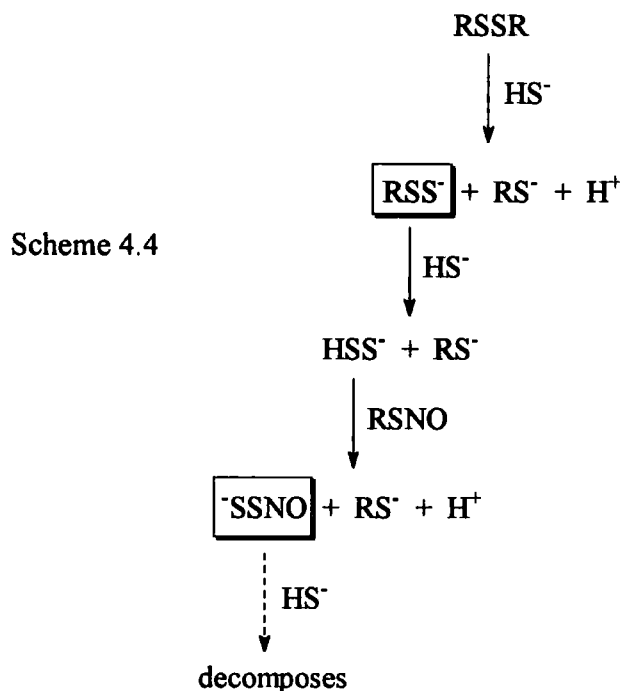
In section 3.2.6.2 penicillamine disulfide was characterised as the product of the base assisted oxidation of penicillamine in aqueous solution. Penicillamine and a N-nitrosamine resulted from the attack of a secondary amine at the nitroso N-atom of SPEN. We have no evidence to support the following notion, but a comparable initial interaction between the powerful nucleophile, HS^- , and a RSNO, may rapidly form thionitrous acid (HSNO) or a thionitrite anion (^-SNO) (scheme 4.3).



Scheme 4.3

More significantly, RS^- would also be formed, and at $\text{pH} > 9.5$ would be continually changed into RSSR. Further studies are needed to ascertain the minimum quantity of RSSR required to initiate the second stage of reaction (see below), but this may only be minuscule.

Reaction would next proceed by the known paths discussed in section 4.4.5 (equations 4.20 – 4.21), and the RSNO finally nitrosate the hydrodisulfide ion to afford the orange-yellow anion, $^-\text{SSNO}$ (scheme 4.4). This is itself susceptible to decomposition via HS^- , and so we see a loss of colour over time that quickens with increasing $[\text{HS}^-]$.



4.5 Conclusion

Sulfur species (e.g. sulfites) are regularly ingested by human beings, as these substances are present in pharmaceuticals, foods, and alcoholic drinks³⁵. Public water supplies and the air that we breathe also contain high levels of sulfur contaminants³⁶ (e.g. SO₂), as effluent streams from the paper/textile sectors and combustion gases from the traditional heavy industries are rich in inorganic materials. In this chapter S-nucleophiles, epitomised by SO₃²⁻, have been portrayed as extremely proficient scavengers of -NO from S-nitrosothiols under physiological conditions (much more so than N-nucleophiles). Episodes of this type are crucial to the biological functions of a RSNO, as nitrogenous products unrelated to nitric oxide are often derived. They may help explain why sulfites are toxic to mammals and sometimes cause respiratory/bronchial disorders³⁷, e.g. asthma.

References

- 1 C.D. Ritchie, *J. Am. Chem. Soc.*, 1975, **97**, 1170.
- 2 R.G. Pearson, H. Sobel and J. Songstad, *ibid.*, 1968, **90**, 319.
- 3 D.J. Barnett, A. Rios and D.L.H. Williams, *J. Chem. Soc., Perkin Trans. 2*, 1995, 1279, D.J. Barnett, J. McAninly and D.L.H. Williams, *ibid.*, 1994, 1131.
- 4 D.R. Arnelle, B.J. Day and J.S. Stamler, *Nitric Oxide; Biology & Chemistry*, 1997, **1**(1), 56.
- 5 J.R. Leis, M.E. Peña and A.M. Rios, *J. Chem. Soc., Perkin Trans. 2*, 1995, 587.
- 6 S.B. Harvey and G.L. Nelsestuen, *Biochim. Biophys. Acta*, 1995, **1267**, 41.
- 7 D. Lyons and G. Nickless in *Inorganic Sulphur Chemistry*, Ed. G. Nickless, Elsevier, Amsterdam, 1968, Ch. 14, p.p. 516.
- 8 R.C. Bransted, *Comprehensive Inorganic Chemistry*, Vol. 8, Van Nostrand, New York, 1961, p.p. 113.
- 9 A.J. Holmes and D.L.H. Williams, to be published.
- 10 A. Simon and K. Waldmann, *Z. Anorg. Allg. Chem.*, 1955, **281**, 113.
- 11 S.B. Oblath, S.S. Markowitz, T. Novakov and S.G. Chang, *J. Phys. Chem.*, 1981, **85**, 1017.
- 12 *Vogel's Textbook of Quantitative Inorganic Analysis*, 4th ed., Longman, 1978, p.p. 755.
- 13 P.W. Riddles, R.L. Blakeley and B. Zerner, *Anal. Biochem.*, 1979, **94**, 75, G.L. Ellman, *Arch. Biochem. Biophys.*, 1959, **82**, 70.
- 14 K. Jones in *Comprehensive Inorganic Chemistry*, Vol. 2, Eds. J.C. Bailar, H.R. Emeleus, R. Nyholm and A.F. Trotman-Dickenson, Pergamon Press, New York, 1973, p.p. 265.
- 15 F. Seel and H. Knorre, *Z. Anorg. Allg. Chem.*, 1963, **322**, 310, F. Raschig, *Z. Angew. Chem.*, 1904, **17**, 1398.
- 16 D.L.H. Williams, *Nitrosation*, Cambridge University Press, 1988, Ch. 7, p.p. 191.
- 17 S.B. Oblath, S.S. Markowitz, T. Novakov and S.G. Chang, *J. Phys. Chem.*, 1982, **86**, 4853, W. Pasiuk-Bronikowska and K.J. Rudzinski, *Chem. Eng. Commun.*, 1982, **18**, 287.
- 18 S.N. Mendiara, E. Ghibaudi, L.J. Perissinotti and A.J. Colussi, *J. Phys. Chem.*, 1992, **96**, 8089.

- 19 G.J. Doyle and N. Davidson, *J. Am. Chem. Soc.*, 1949, **71**, 3491.
- 20 M.N. Ackermann and R.E. Powell, *Inorg. Chem.*, 1967, **6**(9), 1718.
- 21 D. Littlejohn, A.R. Wizansky and S.G. Chang, *Can. J. Chem.*, 1989, **67**, 1596,
S. Naiditch and D.M. Yost, *J. Am. Chem. Soc.*, 1941, **63**, 2123.
- 22 S. Gomiscek, R. Clem, T. Novakov and S.G. Chang, *J. Phys. Chem.*, 1981, **85**,
2567.
- 23 F. Seel and E. Degener, *Z. Anorg. Allg. Chem.*, 1956, **284**, 101.
- 24 V.R. Shenoy and J.B. Joshi, *Wat. Res.*, 1992, **26**(7), 997, D. Littlejohn, K.Y.
Hu and S.G. Chang, *Inorg. Chem.*, 1986, **25**(18), 3131.
- 25 D. Littlejohn and S.G. Chang, *Ind. Eng. Chem. Res.*, 1990, **29**(1), 10.
- 26 M.S. Garley and G. Stedman, *J. Inorg. Nucl. Chem.*, 1981, **43**(11), 2863.
- 27 P. Collings, K. Al-Mallah and G. Stedman, *J. Chem. Soc., Perkin Trans. 2*,
1975, 1734, K. Al-Mallah, P. Collings and G. Stedman, *J. Chem. Soc., Dalton
Trans.*, 1974, 2469.
- 28 G. Stedman and P.A.E. Whincup, *J. Chem. Soc.*, 1963, 5796, C.A. Bunton,
D.R. Llewellyn and G. Stedman, *ibid.*, 1959, 568.
- 29 A.E. Martell and R.M. Smith, *Critical Stability Constants*, Plenum Press, New
York, 1974, Vols. 1, 2 and 5.
- 30 Reference 16, Ch. 6, p.p. 152.
- 31 F.A. Cotton and G. Wilkinson, *Advanced Inorganic Chemistry*, 5th ed., Wiley-
Interscience, New York, 1988, Ch. 13, p.p. 500, H. Kubli, *Helv. Chim. Acta*,
1946, **29**, 1962.
- 32 F. Seel and M. Wagner, *Z. Anorg. Allg. Chem.*, 1988, **558**, 189.
- 33 G.S. Rao and G. Gorin, *J. Org. Chem.*, 1959, **24**, 749.
- 34 A.G. Davies, *Organic Peroxides*, Butterworths, London, 1961, Chs. 1 and 2.
- 35 G.W. Gould and N.J. Russell in *Food Preservatives*, Eds. N.J. Russell and
G.W. Gould, Reinhold, New York, 1991, Ch. 5.
- 36 L.R. Martin in *SO₂, NO and NO₂ Oxidation Mechanisms: Atmospheric
Considerations*, Vol. 3, Ed. J.I. Teasley, Butterworth, Boston, 1984, p.p. 66.
- 37 J.M. Fine, T. Gordon and D. Sheppard, *Am. Rev. Respir. Dis.*, 1987, **136**,
1122.

Chapter 5

Synthesis and Kinetics of Decomposition of Some New S-Nitrosothiols

Chapter 5 : Synthesis and Kinetics of Decomposition of Some New S-Nitrosothiols

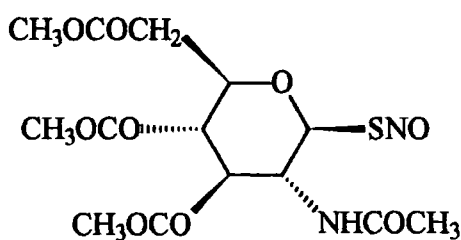
5.1 Introduction

The small list of S-nitrosothiols that have been isolated in the pure form has continued to grow over recent years (reviewed in section 1.2.3). With the notable exception of the “pioneering” solid nitrosothiols, GSNO and SNAP, most S-nitroso species are however unstable at room temperature and rapidly decompose during extraction or work-up in the laboratory. Research efforts have therefore focused upon creating S-nitrosated derivatives that can be stored for prolonged periods and are conveniently transported, yet permit biological compatibility as NO donors. Future administration of these therapeutic drugs to patients may then be possible.

In this section the successful synthesis and characterisation of some novel S-nitrosothiols will be reported, together with the progress made towards other physiologically relevant RSNOs. Kinetic studies concerning their copper catalysed decomposition to NO will also be discussed. Tests revealed some unusual features¹.

5.2 Synthetic Approaches and Biological Activity

5.2.1 2-Acetamido-2-deoxy-S-nitroso-1-thio-β-D-glucopyranose 3,4,6-triacetate (GPSNO)

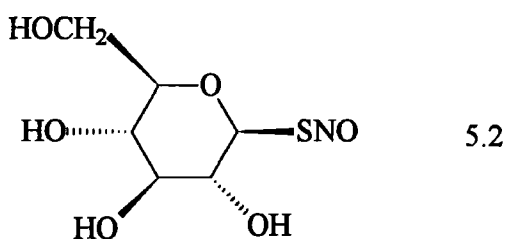


5.1

The S-nitrosothiol, GPSNO (5.1), was prepared as a stable pink solid (section 6.3.2.2) by nitrosation of the thiol precursor using an adaptation of the procedure utilised by Field *et al*² in the manufacture of SNAP. It was characterised via NMR and IR techniques, and offered satisfactory elemental analyses. In aqueous solution GPSNO exhibited the uv-visible absorption maxima representative of S-nitrosothiols, i.e. λ_{\max} (H₂O) at 343 ($\epsilon \sim 450 \text{ mol}^{-1} \text{ dm}^3 \text{ cm}^{-1}$) and 557nm (17). Analysis of a solution of GPSNO ($5 \times 10^{-3} \text{ mol dm}^{-3}$) by the well known Ellman's method³ (sections 3.2.6.2 and 6.2.1.3) indicated that the sample contained a RSH impurity of 1.9%. This remained from the slightly reversible formation of the RSNO⁴ (section 1.2.4.2).

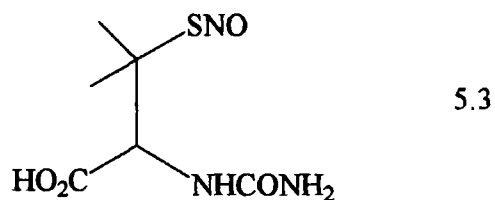
As S-nitroso-1-thiosugars contain hydrophobic and hydrophilic groups, they hold several advantages over most amino acid based nitrosothiols, e.g. enhanced lipid solubility. S-Nitroso-1-thioglucose tetraacetate⁵ (SNAG) is another example within this family of compounds (it has the same structure as GPSNO but the $-\text{NHCOCH}_3$ group is replaced by $-\text{OCOCH}_3$), which although not as stable or pure as GPSNO in solid form, shows substantial vasodilatory properties. SNAG is known to effect cutaneous blood flow in a dose-dependent manner, when transdermally applied to human skin. Similar experiments using GPSNO are awaited with great anticipation.

5.2.2 S-Nitroso-1-thio- β -D-glucose (SNTG)



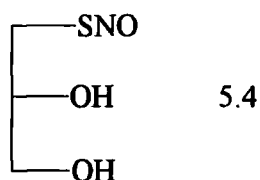
As a consequence of the encouraging results obtained during the fore-mentioned clinical trials, the synthesis of S-nitroso-1-thio- β -D-glucose (5.2) was attempted. Unfortunately SNTG could not be isolated. A sample (containing 1.1% RSH on testing) generated *in situ* from equivalent amounts of thiol and acidified sodium nitrite, did nevertheless afford a uv-visible spectrum with λ_{\max} (H₂O) at 342 ($\epsilon \sim 436 \text{ mol}^{-1} \text{ dm}^3 \text{ cm}^{-1}$) and 557nm (14). Interestingly, ϵ values calculated for SNTG and GPSNO at the 330 - 350nm absorption maxima were comparatively small.

5.2.3 S-Nitroso-N-carbamyl-D,L-penicillamine (SNCP)



SNCP (5.3) was produced as a stable green solid with red reflections, and its analytical data fully assigned (section 6.3.2.3). Its appearance was similar to that of SNAP, a fact not unexpected due to their close structural relationship (the $-\text{CH}_3$ group of the N-acetyl substituent in SNAP is replaced by $-\text{NH}_2$). In the uv-visible spectrum, λ_{max} (H_2O) at 340 ($\epsilon \sim 853 \text{ mol}^{-1} \text{ dm}^3 \text{ cm}^{-1}$) and 590nm (20) were distinguished. Ellman's test determined 1.5% free thiol in an aqueous solution of SNCP.

5.2.4 S-Nitroso-1-thioglycerol (TGSNO)



S-Nitroso-1-thioglycerol (5.4) has a relatively long half-life *in vivo*⁶, i.e. $t_{1/2} \sim 12$ days at pH 7.4 and 37°C (compared to 7 days for GSNO). It also demonstrates some intriguing biological properties⁷. Nitrosation of 1-thioglycerol (3-mercapto-1,2-propanediol) using standard procedures yielded TGSNO as a gelatinous red liquid, which could be stored at $< 4^\circ\text{C}$ in the dark. Samples were too unstable to allow complete purification or characterisation, as they immediately decomposed on exposure to the open atmosphere. The uv-visible spectrum of *in situ* TGSNO did however display λ_{max} (H_2O) at 333 ($\epsilon \sim 881 \text{ mol}^{-1} \text{ dm}^3 \text{ cm}^{-1}$) and 544nm (21). Contaminant levels of 1-thioglycerol present within *in situ* TGSNO were $\sim 0.5\%$.

5.3 S-Nitrosothiol Decomposition

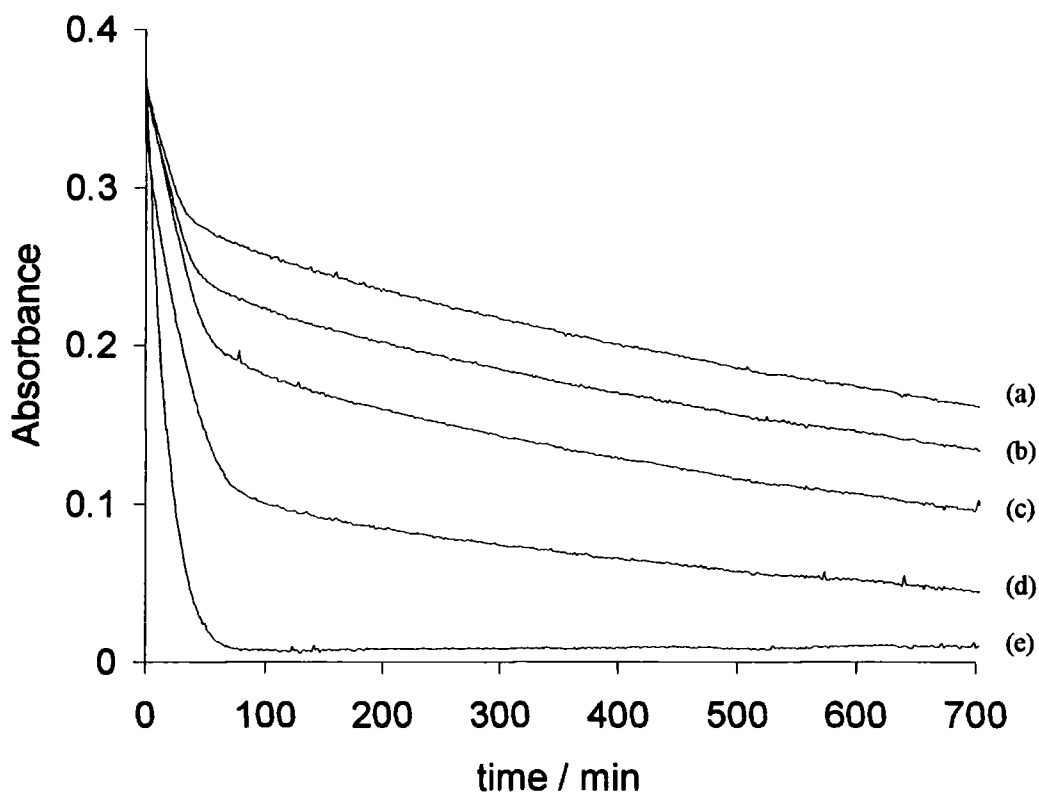
5.3.1 Spectral Characteristics

5.3.1.1 Effect of Varying Added Cu^{2+}

Copper ions catalyse S-nitrosothiol decay in aqueous systems⁸ (section 1.3.3.1). The decomposition of $1 \times 10^{-3} \text{ mol dm}^{-3}$ GPSNO (prepared from dissolution and dilution of a solid sample) as a function of added Cu^{2+} ($0.1 - 5.0 \times 10^{-5} \text{ mol dm}^{-3}$), was therefore studied at physiological pH (7.4) and 25°C . This involved using a spectrophotometer to monitor the change in absorbance at 343nm (λ_{max}) with time. The traces resulting from this series of reactions are represented in figure 5.1.

Figure 5.1

Absorbance-time plots (343nm) for the decomposition of GPSNO ($1 \times 10^{-3} \text{ mol dm}^{-3}$) in pH 7.4 buffer, in the presence of varied Cu^{2+}



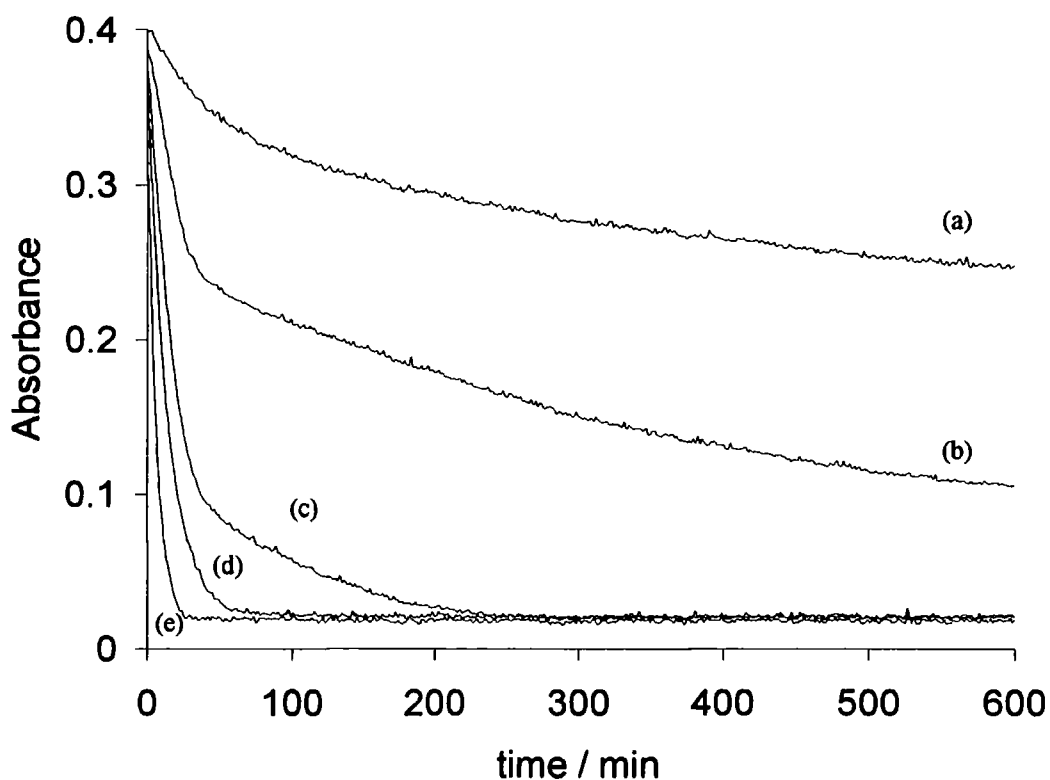
(a) no added Cu^{2+} , (b) $[\text{Cu}^{2+}] = 0.1 \times 10^{-5} \text{ mol dm}^{-3}$, (c) $[\text{Cu}^{2+}] = 0.5 \times 10^{-5} \text{ mol dm}^{-3}$,
(d) $[\text{Cu}^{2+}] = 1.0 \times 10^{-5} \text{ mol dm}^{-3}$ and (e) $[\text{Cu}^{2+}] = 5.0 \times 10^{-5} \text{ mol dm}^{-3}$.

The plots obtained are clearly unusual and are of an intermediate kinetic order that did not permit rate measurements. On a qualitative scale, the initial rate of GPSNO decay is seen to increase as higher concentrations of Cu^{2+} are introduced. Two sequential reaction components seem to be evident at $[\text{Cu}^{2+}] \leq 1.0 \times 10^{-5} \text{ mol dm}^{-3}$. The first process is fast in comparison to the second, but ceases at incomplete conversion of GPSNO. The subsequent pathway then appears to be uniform in each run and unaffected by $[\text{Cu}^{2+}]$. Overall, reaction only proceeds towards completion when $[\text{Cu}^{2+}] \sim 5.0 \times 10^{-5} \text{ mol dm}^{-3}$. This takes less than 70 minutes.

To examine whether this decomposition pattern was general to nitrosothiols containing a 1-thiosugar fragment, the previously described experiment was repeated using SNTG (generated *in situ*) instead of GPSNO (figure 5.2).

Figure 5.2

Absorbance-time plots (342nm) for the decomposition of SNTG ($1 \times 10^{-3} \text{ mol dm}^{-3}$) in pH 7.4 buffer, in the presence of varied Cu^{2+}



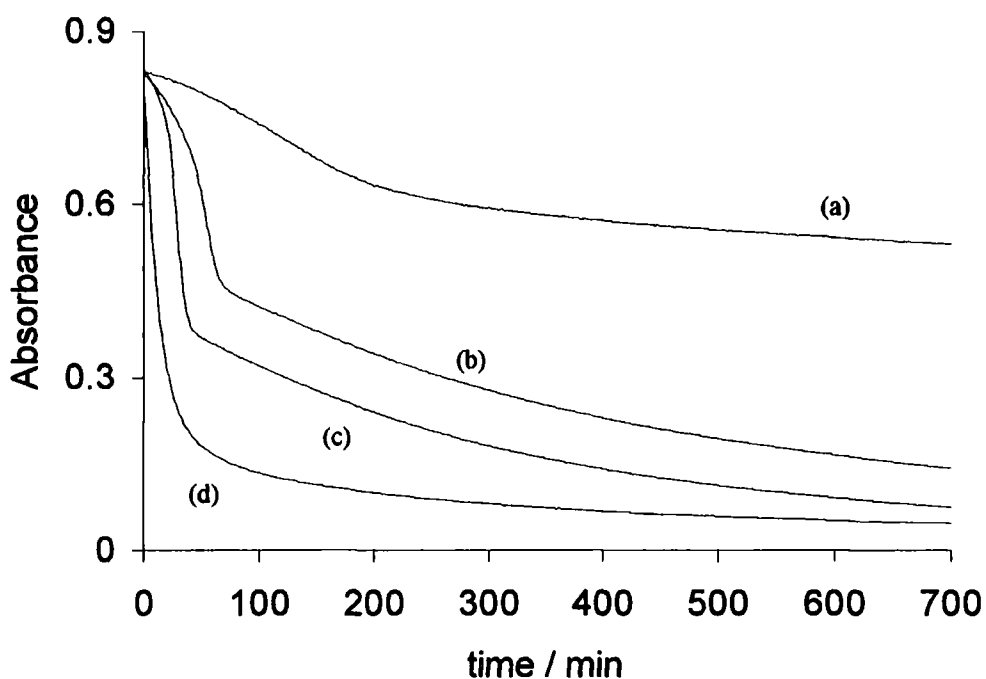
(a) no added Cu^{2+} , (b) $[\text{Cu}^{2+}] = 0.1 \times 10^{-5} \text{ mol dm}^{-3}$, (c) $[\text{Cu}^{2+}] = 0.5 \times 10^{-5} \text{ mol dm}^{-3}$,
 (d) $[\text{Cu}^{2+}] = 1.0 \times 10^{-5} \text{ mol dm}^{-3}$ and (e) $[\text{Cu}^{2+}] = 5.0 \times 10^{-5} \text{ mol dm}^{-3}$.

The set of traces recorded using SNTG complement those of GPSNO. Such behaviour is probably related to the presence of the nitrosothiol sugar unit in some manner. $[\text{Cu}^{2+}] \sim 1.0 \times 10^{-5} \text{ mol dm}^{-3}$ is now sufficient to lead to total SNTG decomposition. The consecutive reaction is just as pronounced as that for GPSNO, and again almost unaltered with changing $[\text{Cu}^{2+}]$.

Spectral features of this nature are not just restricted to S-nitrososugars. Figure 5.3 graphically depicts similar studies using *in situ* TGSNO, in which Cu^{2+} concentrations of $0.5 - 2.5 \times 10^{-5} \text{ mol dm}^{-3}$ were added. Two reactions are apparent, but significant induction periods also evident (traces (a) – (c)). These are shortened as $[\text{Cu}^{2+}]$ increases, and at $[\text{Cu}^{2+}] \sim 2.5 \times 10^{-5} \text{ mol dm}^{-3}$ are removed altogether. Reduction of Cu^{2+} to Cu^+ (the catalytic reagent necessary for RSNO decay) by RS^- , has previously been given as a reason for such time-lags prior to reaction^{8,9}.

Figure 5.3

Absorbance-time plots (333nm) for the decomposition of TGSNO ($1 \times 10^{-3} \text{ mol dm}^{-3}$) in pH 7.4 buffer, in the presence of varied Cu^{2+}



(a) no added Cu^{2+} , (b) $[\text{Cu}^{2+}] = 0.5 \times 10^{-5} \text{ mol dm}^{-3}$, (c) $[\text{Cu}^{2+}] = 1.0 \times 10^{-5} \text{ mol dm}^{-3}$ and (d) $[\text{Cu}^{2+}] = 2.5 \times 10^{-5} \text{ mol dm}^{-3}$.

Limited quantities of SNCP ruled out an in-depth kinetic analysis. Work by Dicks¹⁰ (using an *in situ* sample) has however established that Cu^+ mediated decomposition of SNCP is typical of "normal" S-nitrosothiols, and does not resemble the trends discussed for GPSNO, SNTG and TGSNO. Excellent first-order plots were observed upon Cu^{2+} ($0.3 - 1.0 \times 10^{-5} \text{ mol dm}^{-3}$) addition, and a second-order rate constant of $780 \text{ mol}^{-1} \text{ dm}^3 \text{ s}^{-1}$ estimated (k_2 in rate = $k_2[\text{RSNO}][\text{Cu}^{2+}]$). SNCP was more reactive than SNAP ($k_2^{11} \sim 20 \text{ mol}^{-1} \text{ dm}^3 \text{ s}^{-1}$). This has been attributed to the fact that $-\text{NHCONH}_2$ is more effective at binding Cu^+ than $-\text{NHCOCH}_3$.

5.3.1.2 Addition of Metal Ion Chelating Agents

To distinguish the suspected metal-ion catalysed reaction from any other, parallel experiments were conducted with and without the transition metal ion chelator, EDTA ($1 \times 10^{-3} \text{ mol dm}^{-3}$). The decay of GPSNO ($1 \times 10^{-3} \text{ mol dm}^{-3}$) at $[\text{Cu}^{2+}] = 1 \times 10^{-5} \text{ mol dm}^{-3}$ was followed (figure 5.4).

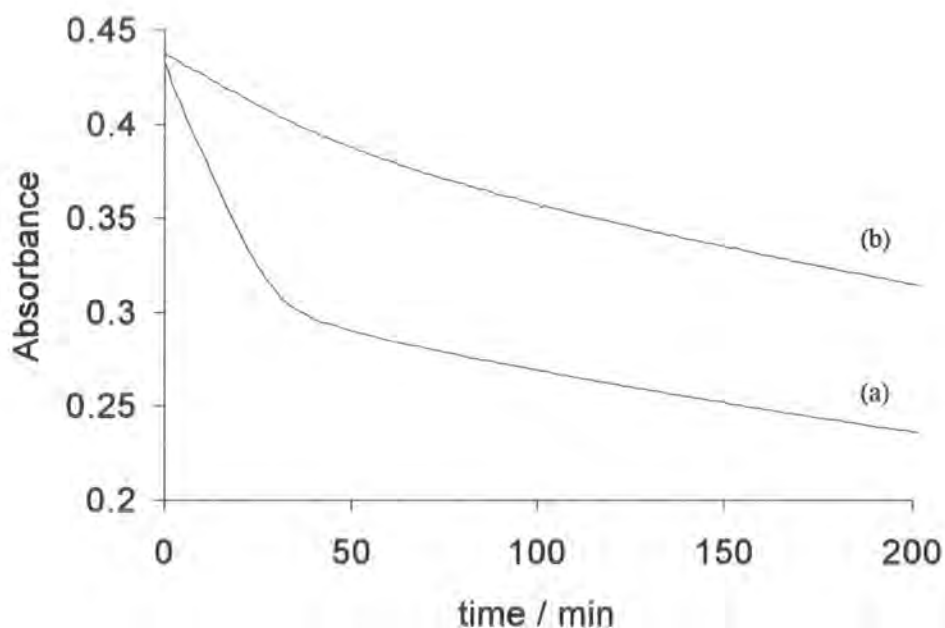
The time-drive spectra obtained prove that the faster component of reaction is metal ion catalysed, as EDTA completely suppresses this pathway in trace (b). The specific Cu^+ chelator, neocuproine, also had the same effect (not shown). As expected, the initial reaction is therefore copper(I) catalysed. On the other hand, the slower second stage of reaction is unchanged by $\text{Cu}^{2+}/\text{Cu}^+$ chelation. It appears to be the thermal reaction that is common to most S-nitrosothiols¹² (section 1.3.2). If this is a first-order process, a rate constant (k') of $1.08 \times 10^{-4} \text{ s}^{-1}$ can be calculated for the thermal decomposition of GPSNO (table 5.1). This half-life of 107 minutes compares reasonably with the value of 33 minutes quoted for SNAG in the literature⁵. Most RSNOs are more stable towards thermal decay than these S-nitrososugars. S-Nitrosocysteine (SNCys) for example has a half-life of 3300 minutes⁸.

The above findings were verified via the addition of EDTA (not shown) at a point equal to 15 minutes in trace (a) of figure 5.4. It halted the Cu^+ path. Addition after 100 minutes had no effect. In both, only the thermal reaction remained.

The behaviour of SNTG (not shown) was identical to GPSNO, and a half-life of 152 minutes measured for the thermal reaction (table 5.1).

Figure 5.4

Absorbance-time plots (343nm) for the decomposition of GPSNO ($1 \times 10^{-3} \text{ mol dm}^{-3}$) in pH 7.4 buffer, in the presence of Cu^{2+} ($1.0 \times 10^{-5} \text{ mol dm}^{-3}$) and no/added EDTA



(a) without EDTA and (b) with EDTA ($1.0 \times 10^{-3} \text{ mol dm}^{-3}$).

Table 5.1

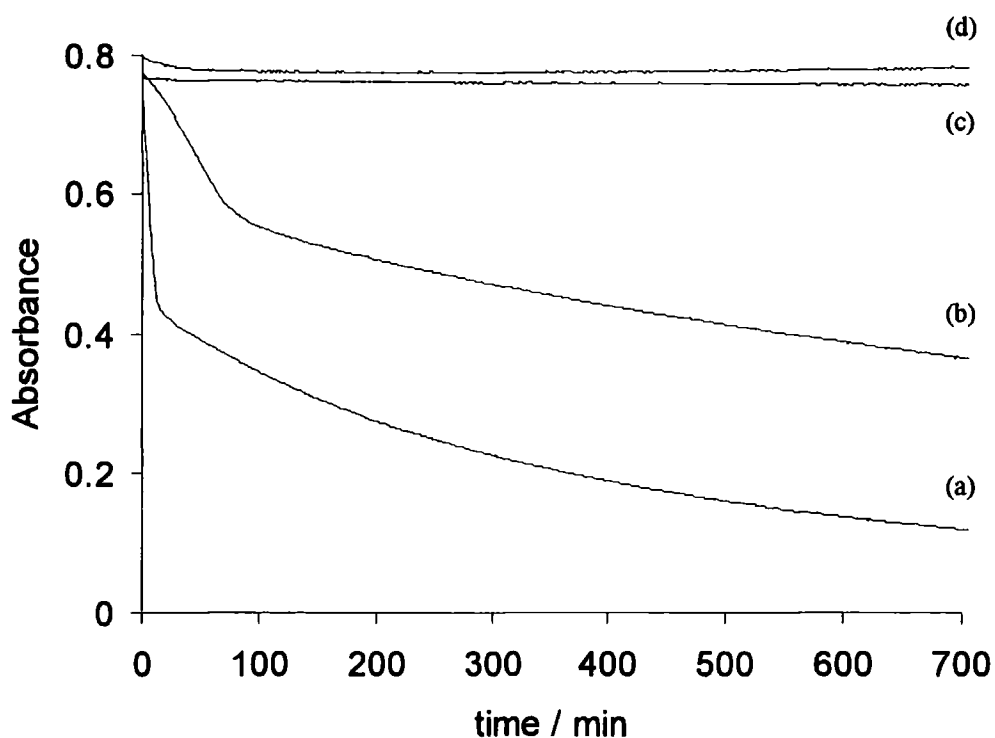
Kinetic data for the thermal induced decomposition of some S-nitrosothiols in pH 7.4 buffer at 25°C

S-Nitrosothiol	$k'/10^{-5} \text{ s}^{-1}$	Half-life (mins)
GPSNO	10.8 ± 0.6	107
SNTG	7.6 ± 0.1	152
SNAG	~ 35.0	33
SNCys	~ 0.35	3300

Adding EDTA (or neocuproine) to test solutions containing TGSNO ($1 \times 10^{-3} \text{ mol dm}^{-3}$) and Cu^{2+} ($1 \times 10^{-5} \text{ mol dm}^{-3}$), before (figure 5.5) or during the course of the reaction (not shown), had a different effect than for GPSNO and SNTG.

Figure 5.5

Absorbance-time plots (333nm) for the decomposition of TGSNO ($1 \times 10^{-3} \text{ mol dm}^{-3}$) in pH 7.4 buffer, in the presence of Cu^{2+} ($1.0 \times 10^{-5} \text{ mol dm}^{-3}$) and varied [EDTA]



(a) no added EDTA, (b) $[\text{EDTA}] = 1.0 \times 10^{-5} \text{ mol dm}^{-3}$, (c) $[\text{EDTA}] = 2.0 \times 10^{-5} \text{ mol dm}^{-3}$ and (d) $[\text{EDTA}] = 5.0 \times 10^{-5} \text{ mol dm}^{-3}$.

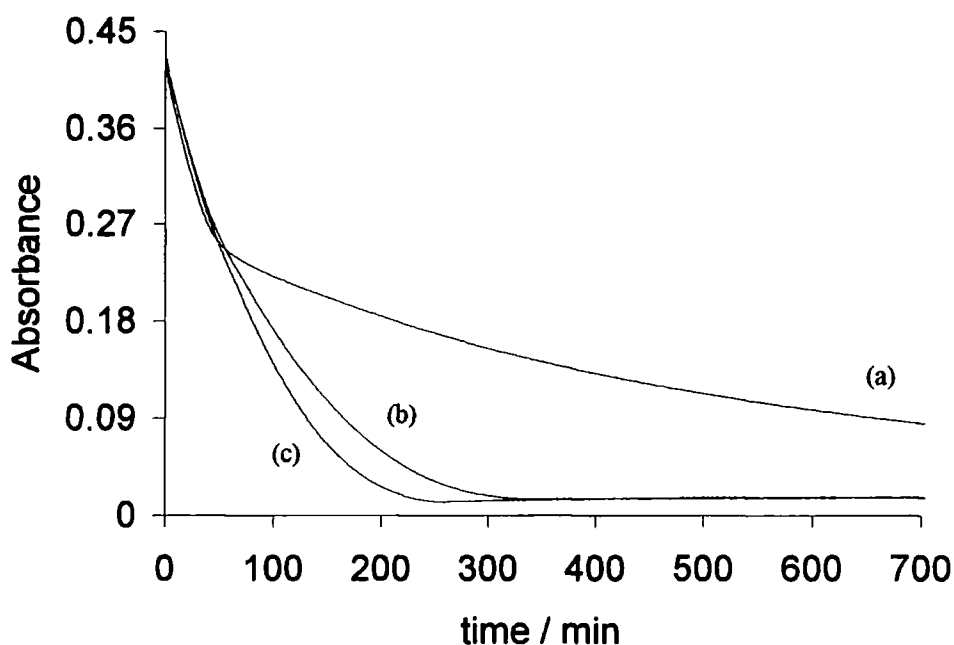
As the concentration of EDTA is increased each reaction component is inhibited, until at $[\text{EDTA}] \geq 2.0 \times 10^{-5} \text{ mol dm}^{-3}$ **both** are completely stopped. No nitrosothiol decay is then evident. The latter stage of decomposition cannot now be a thermal reaction, and must somehow involve Cu^+ .

5.3.1.3 Addition of Ascorbate

At concentrations $\leq 1 \times 10^{-4} \text{ mol dm}^{-3}$ the ascorbate anion (cf. thiolate) can reduce the Cu^{2+} ion to Cu^+ , and so promote S-nitrosothiol decomposition⁸. Figure 5.6 demonstrates the influence of ascorbate ($0.5 - 1.0 \times 10^{-4} \text{ mol dm}^{-3}$) upon the stability of GPSNO ($1 \times 10^{-3} \text{ mol dm}^{-3}$) at pH 7.4, when $[\text{Cu}^{2+}] = 1.0 \times 10^{-5} \text{ mol dm}^{-3}$.

Figure 5.6

Absorbance-time plots (343nm) for the decomposition of GPSNO ($1 \times 10^{-3} \text{ mol dm}^{-3}$) in pH 7.4 buffer, in the presence of Cu^{2+} ($1.0 \times 10^{-5} \text{ mol dm}^{-3}$) and varied [ascorbate]



(a) no added ascorbate, (b) $[\text{ascorbate}] = 0.5 \times 10^{-4} \text{ mol dm}^{-3}$
and (c) $[\text{ascorbate}] = 1.0 \times 10^{-4} \text{ mol dm}^{-3}$.

The addition of this reducing agent leads to a significantly faster reaction. It induces quantitative decay of GPSNO within ~ 350 minutes. Reaction is over in a sufficiently short period, so that it only proceeds via the Cu^+ pathway and the thermal component is eradicated.

Ascorbate served the same purpose in leading to the total decomposition of SNTG and TGSNO (not shown). Any induction periods or secondary reactions were extinguished.

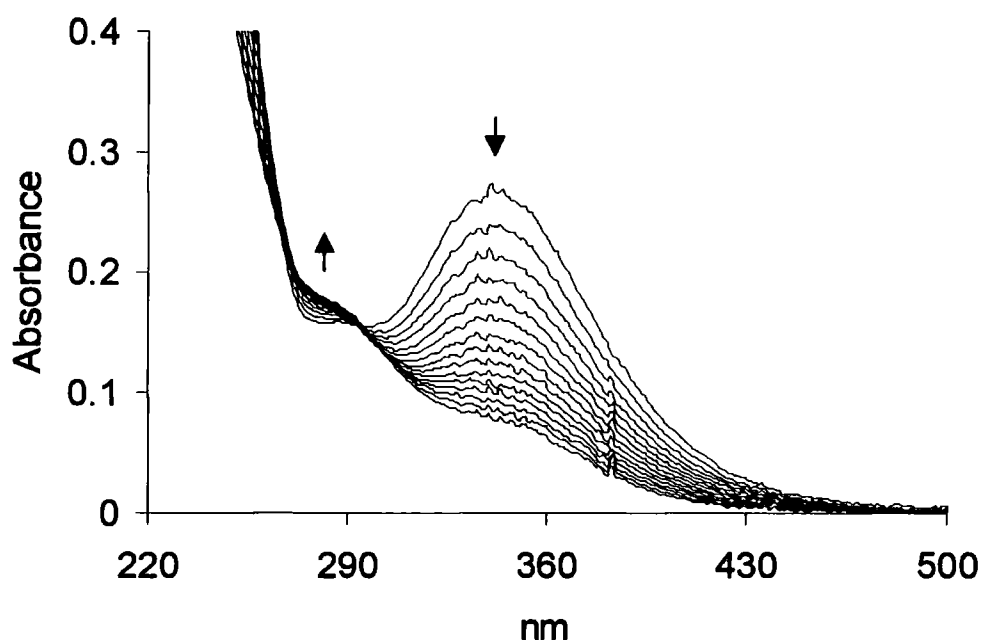
At high concentration ($> 1 \times 10^{-3} \text{ mol dm}^{-3}$) the role of ascorbate changes to that of a nucleophile. It can then undergo electrophilic nitrosation by S-nitrosothiols¹³ (section 1.3.5.4).

5.3.1.4 Formation of a Copper(II)-Disulfide Complex

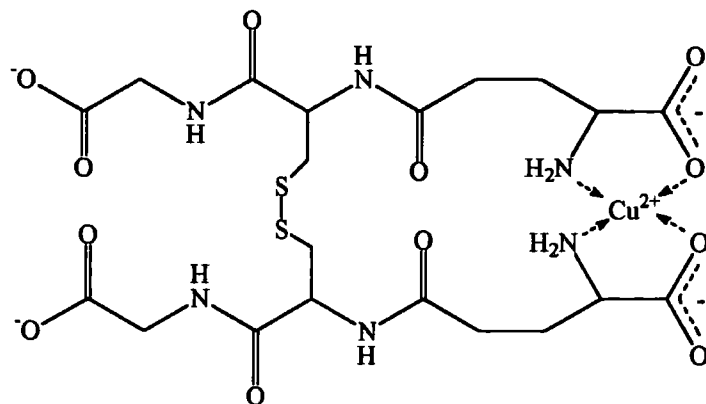
Decomposition of GPSNO ($1 \times 10^{-3} \text{ mol dm}^{-3}$) at $[\text{Cu}^{2+}] = 5.0 \times 10^{-5} \text{ mol dm}^{-3}$, was next recorded using a spectrophotometer set in the repeat scan mode (figure 5.7).

Figure 5.7

Repeat scan spectra (time interval = 4 minutes) for the decomposition of GPSNO ($1 \times 10^{-3} \text{ mol dm}^{-3}$) in pH 7.4 buffer, in the presence of Cu^{2+} ($5.0 \times 10^{-5} \text{ mol dm}^{-3}$)



The resultant spectra enable the decrease in the RSNO absorbance peak at 343nm to be followed, but also indicate the formation of a small shoulder at $\sim 280\text{nm}$. Spectroscopic changes of this kind have previously been found during the copper catalysed decay of GSNO¹⁴, particularly at high $[\text{Cu}^{2+}]$ or upon addition of the disulfide (oxidised glutathione, GSSG). At neutral pH a shoulder is slowly formed at 250 - 260nm. It has been assigned as a possible $\text{N}_\sigma \rightarrow \text{Cu}$ charge transfer transition¹⁵ within a 1:1 complex of GSSG and Cu^{2+} (rather than Cu^+). This GSSG- Cu^{2+} complex (5.5) is thought to involve co-ordination of Cu^{2+} by the $-\text{NH}_2$ and $-\text{CO}_2\text{H}$ groups of the hexapeptide. A square planar geometry is probably adopted around the metal centre¹⁶.



5.5

The peak at 280nm in figure 5.7 could therefore represent a stable RSSR-Cu²⁺ complex formed from the disulfide of GPSNO. No attempts were made to speculate on the structure of this species or the nature of its ligand environment.

Similar spectral transformations to those described for GPSNO, were seen in the corresponding reaction using SNTG ($1 \times 10^{-3} \text{ mol dm}^{-3}$) and Cu²⁺ ($5.0 \times 10^{-5} \text{ mol dm}^{-3}$) (not shown). It may be possible that the carbohydrate portion of a disulfide manufactured from a S-nitroso-1-thiosugar, offers a number of legitimate binding sites for Cu²⁺ co-ordination.

Unlike GPSNO and SNTG, the species formed at $\sim 270\text{nm}$ during the decomposition of TGSNO ($1 \times 10^{-3} \text{ mol dm}^{-3}$) at $[\text{Cu}^{2+}] = 5.0 \times 10^{-5} \text{ mol dm}^{-3}$ was unstable. This absorbance gradually disappeared as the reaction progressed (not shown).

5.3.2 Nitrogenous Product Detection

On the basis of the uv-visible spectra explained in section 5.3.1.4, it was presumed that disulfide constituted the major sulfur-derived end product from the reaction of GPSNO, SNTG and TGSNO with added Cu²⁺. It was now necessary to characterise the principal nitrogenous product(s) of nitrosothiol decomposition.

A NO-specific electrode (section 6.1.8) was used to quantify the levels of NO liberated from $1 \times 10^{-5} \text{ mol dm}^{-3}$ S-nitrosothiol, in pH 7.4 buffer at $[\text{Cu}^{2+}] = 5.0 \times 10^{-5} \text{ mol dm}^{-3}$. For this purpose the reaction was performed under anaerobic conditions, via employment of the glucose/glucose oxidase method¹⁷ (sections 2.5 and 6.2.2). The results are summarised in table 5.2, and are expressed as a percentage of the theoretical maximum amount of NO that could be generated.

Table 5.2

Nitric oxide yields from the decomposition of GPSNO, SNTG and TGSNO ($1 \times 10^{-5} \text{ mol dm}^{-3}$) in pH 7.4 buffer, in the presence of Cu^{2+} ($5.0 \times 10^{-5} \text{ mol dm}^{-3}$)

S-Nitrosothiol	% NO
GPSNO	26
SNTG	30
TGSNO	45

The relatively long time scale required for RSNO decomposition did not allow an accurate assessment of the total NO concentrations released. The main reason for this is the susceptibility of NO to oxidation. The values of 26 - 45% NO determined for GPSNO, SNTG and TGSNO, are therefore far from quantitative but not unexpected, e.g. 15% NO was measured by Barnett¹¹ during the reaction of SNAP ($2 \times 10^{-5} \text{ mol dm}^{-3}$) with added Cu^{2+} ($2.0 \times 10^{-5} \text{ mol dm}^{-3}$) in pH 7.4 buffer.

The Griess test¹⁸ (sections 2.4.2 and 6.2.1.2) enabled an evaluation of the nitrite quantities produced from $1 \times 10^{-3} \text{ mol dm}^{-3}$ S-nitrosothiol in aerated solution, when $[\text{Cu}^{2+}] = 5.0 \times 10^{-5} \text{ mol dm}^{-3}$. These are shown in table 5.3.

The yield of NO_2^- from TGSNO was almost 100%. Quantitative nitrite production is usual in the copper catalysed decay of most aliphatic S-nitrosothiols⁸. A different story exists for GPSNO and SNTG however, as only ~ 50% nitrite was observed. These findings are difficult to explain. Further studies are needed to verify if this discovery is common to more S-nitroso-1-thiosugars.

Table 5.3

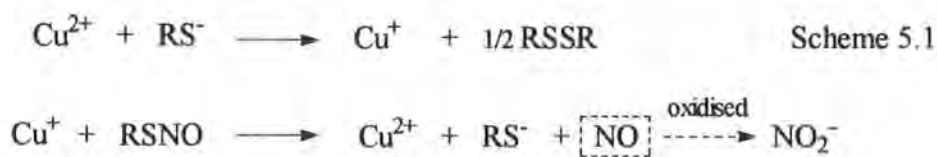
Nitrite yields from the decomposition of GPSNO, SNTG and TGSNO
 ($1 \times 10^{-3} \text{ mol dm}^{-3}$) in pH 7.4 buffer, in the presence of Cu^{2+} ($5.0 \times 10^{-5} \text{ mol dm}^{-3}$)

S-Nitrosothiol	% NO_2^-
GPSNO	51
SNTG	57
TGSNO	97

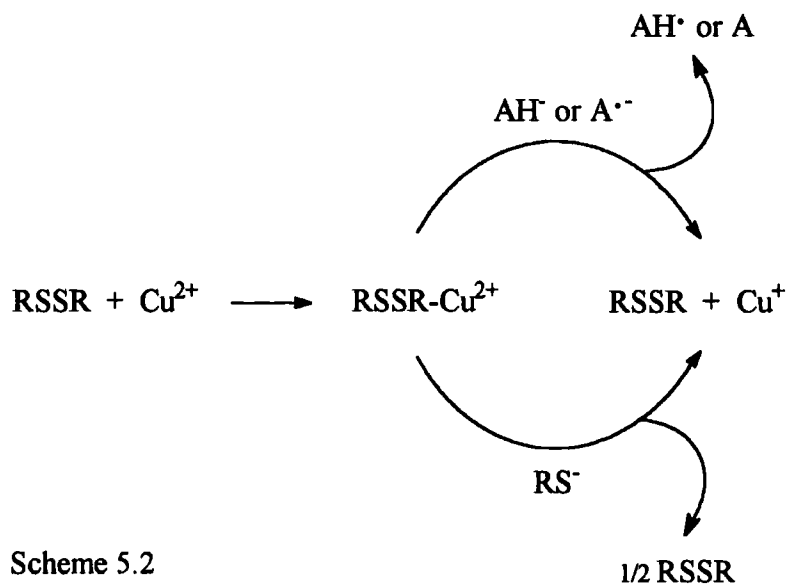
5.3.3 Mechanism of S-Nitrosothiol Decay

The elucidated reaction mechanism which accounts for the decomposition of GPSNO, SNTG and TGSNO in Cu^{2+} enriched aqueous buffer at physiological pH, reflects the range of spectral evidence gathered and product analyses discussed.

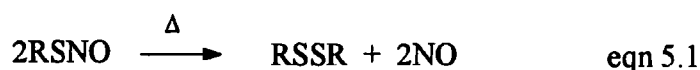
Thiolate levels within *in situ* samples of SNTG and TGSNO, or a solution of dissolved GPSNO, are high enough (< 2%) to effect the reduction of Cu^{2+} to Cu^+ . The initial (faster) component of the two stage reaction seen for each S-nitrosothiol, is therefore consistent with Cu^+ mediated decay to release NO (scheme 5.1).



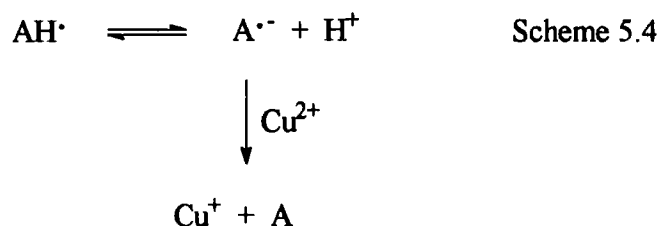
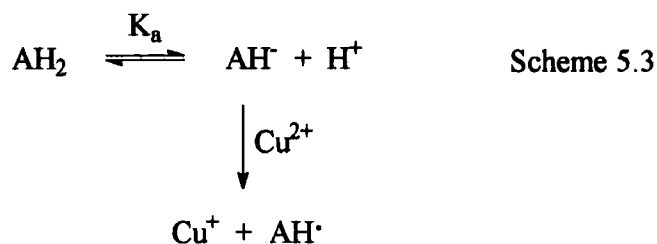
As RSNO decomposition continues, Cu^{2+} ions are increasingly chelated out of solution by the disulfide product (scheme 5.2). A RSSR-Cu^{2+} complex is formed to the detriment of the reaction rate. At lower added $[\text{Cu}^{2+}]$ this complexation leads to incomplete conversion of RSNO, as "free" copper levels are depleted to almost zero. The stability of the complex then dictates the second slower component of reaction.



The situation can be explained using the pathways outlined in scheme 5.2. In the case of TGSNO, the bound form of Cu^{2+} is accessible to reduction by RS^\cdot . Cu^+ and RSSR can be regenerated, and so the absorbance shoulder formed at 270nm (i.e. RSSR-Cu^{2+}) is slowly removed over time. Reaction still then proceeds, but is substantially slower than in the reduction of free Cu^{2+} . Alternatively, the Cu^{2+} complexes of the disulfides derived from GPSNO and SNTG appear to be too stable to be disrupted by the RS^\cdot present. The absorbance shoulders at $\sim 280\text{nm}$ now remain during the course of the reaction, and Cu^+ is not available in solution. Only a rather large thermal reaction is then evident (equation 5.1).



The ascorbate mono-anion (AH^\cdot) is the conjugate base of ascorbic acid (AH_2) ($\text{pK}_a^{19} \sim 4.0$ at 25°C). AH^\cdot and $\text{A}^{\cdot-}$ (created from the radical intermediate AH^\cdot) are effective reagents in the reduction of aqueous copper(II) ions²⁰ (schemes 5.3 – 5.4), and thereby promote the initial Cu^+ catalysed reaction of GPSNO, SNTG and TGSNO. They may also be effective reductants of any complexes formed (scheme 5.2), if reaction does not reach completion via the first component alone. Dehydroascorbic acid (A) is a possible by-product of these redox processes.



5.4 Conclusion

Two original S-nitrosothiols, namely 2-acetamido-2-deoxy-S-nitroso-1-thio- β -D-glucopyranose 3,4,6-triacetate (GPSNO) and S-nitroso-N-carbamyl-D,L-penicillamine (SNCP), have been prepared as pure solids and characterised.

The kinetics of GPSNO decomposition in pH 7.4 buffer have been followed, together with those of S-nitroso-1-thio- β -D-glucose (SNTG) and S-nitroso-1-thioglycerol (TGSNO). Two parallel reactions were noted for each compound. The first component has been interpreted as Cu^+ catalysed, and is attenuated by complexation of Cu^{2+} by RSSR. The second is thought to be a degradation pathway dependent upon the availability of chelated Cu^{2+} to reduction. In the case of GPSNO or SNTG this is merely an overlaid thermal reaction, but for TGSNO it is an impaired variant of the copper(I) reaction.

References

- 1 A.P. Munro and D.L.H. Williams, *Can. J. Chem.*, 1999, **77**, 550.
- 2 L. Field, R.V. Dilts, R. Ravichandran, P.G. Lenhert and G.E. Carnahan, *J. Chem. Soc., Chem. Commun.*, 1978, 249.
- 3 P.W. Riddles, R.L. Blakeley and B. Zerner, *Anal. Biochem.*, 1979, **94**, 75, G.L. Ellman, *Arch. Biochem. Biophys.*, 1959, **82**, 70.
- 4 P.H. Beloso and D.L.H. Williams, *J. Chem. Soc., Chem. Commun.*, 1997, 89.
- 5 A.R. Butler, R.A. Field, I.R. Greig, F.W. Flitney, S.K. Bisland, F. Khan and J.J.F. Belch, *Nitric Oxide; Biology and Chemistry*, 1997, **1**(3), 211.
- 6 W.R. Mathews and S.W. Kerr, *J. Pharm. Exp. Ther.*, 1993, **267**(3), 1529.
- 7 A.R. Butler, personal communication, J.S. Stamler, O. Jaraki, J. Osborne, D.I. Simon, J. Keaney, J. Vita, D. Singel, C.R. Valeri and J. Loscalzo, *Proc. Natl. Acad. Sci., USA*, 1992, **89**, 7674.
- 8 A.P. Dicks, H.R. Swift, D.L.H. Williams, A.R. Butler, H.H. Al-Sa'doni and B.G. Cox, *J. Chem. Soc., Perkin Trans. 2*, 1996, 481, S.C. Askew, D.J. Barnett, J. McAninly and D.L.H. Williams, *ibid.*, 1995, 741.
- 9 A.P. Dicks, P.H. Beloso and D.L.H. Williams, *ibid.*, 1997, 1429.
- 10 A.P. Dicks, Ph.D. Thesis, University of Durham, 1997.
- 11 D.J. Barnett, Ph.D. Thesis, University of Durham, 1994.
- 12 D.L.H. Williams, *J. Chem. Soc., Chem. Commun.*, 1996, 1085.
- 13 A.J. Holmes and D.L.H. Williams, *ibid.*, 1998, 1711.
- 14 H.R. Swift, Ph.D. Thesis, University of Durham, 1996.
- 15 A.R. Amundsen, J. Whelan and B. Bosnich, *J. Am. Chem. Soc.*, 1977, **99**, 6730.
- 16 K. Varnagy, I. Sovago and H. Kozlowski, *Inorg. Chim. Acta*, 1988, **151**, 117.
- 17 A.C.F. Gorren, A. Schrammel, K. Schmidt and B. Mayer, *Arch. Biochem. Biophys.*, 1996, **330**(2), 219.
- 18 *Vogel's Textbook of Quantitative Inorganic Analysis*, 4th ed., Longman, 1978, p.p. 755.
- 19 R.F. Jameson and N.J. Blackburn, *J. Chem. Soc., Dalton Trans.*, 1976, 534.
- 20 J. Xu and R.B. Jordan, *Inorg. Chem.*, 1990, **29**, 2933.

Chapter 6

Experimental Details

Chapter 6 : Experimental Details

6.1 Experimental Techniques

6.1.1 UV-Visible Spectrophotometry

All uv-visible spectra were acquired from freshly prepared solutions in 1cm path length quartz cuvettes on either a Perkin-Elmer Lambda 2/Lambda 12 or Shimadzu UV-2101PC spectrophotometer. These instruments were also used to measure the kinetics of time-dependent reactions. A stopped-flow technique was necessary for more rapid processes ($t_{1/2} \geq 2 \times 10^{-3}$ s) (see section 6.1.2).

Most kinetic measurements were made under pseudo-first order conditions, and the observed rate constants (k_{obs}) determined from the change in absorbance with time at a fixed wavelength. Absorbance-time data were analysed using the computer correlation program "Enzfitter" which is designed for rate calculations. This software enabled k_{obs} to be established on the basis of the derivation below.

For a first order process $A \rightarrow B$, the rate of formation of product B, or loss of reactant A, can be described by;

$$-\frac{d[A]}{dt} = \frac{d[B]}{dt} = k_{\text{obs}}[A] \quad \text{eqn 6.1}$$

Integration yields,

$$\ln[A]_0 - \ln[A]_t = k_{\text{obs}}t \quad \text{eqn 6.2}$$

Where $[A]_0$ and $[A]_t$ are the concentrations of A at times $t = 0$ and $t = t$ respectively.

The Beer-Lambert law ($A = \epsilon cl$, where A is the absorbance, ϵ is the molar extinction coefficient, c is the concentration and l is the path length, 1cm) allows the absorbance at times $t = 0$ and $t = t$ to be represented by equations 6.3 - 6.4.

$$A_0 = \epsilon_A[A]_0 \quad \text{eqn 6.3}$$

$$A_t = \epsilon_A[A]_t + \epsilon_B[B]_t \quad \text{eqn 6.4}$$

Since $[B]_t = [A]_0 - [A]_t$, equation 6.4 can now be written as:

$$A_t = \epsilon_A[A]_t + \epsilon_B[A]_0 - \epsilon_B[A]_t \quad \text{eqn 6.5}$$

At the completion of the reaction, $t = \infty$ and $[B]_\infty = [A]_0$, so;

$$A_\infty = \epsilon_B[A]_0 \quad \text{eqn 6.6}$$

Substituting for $\epsilon_B[A]_0$ into equation 6.5 produces,

$$A_t = \epsilon_A[A]_t + A_\infty - \epsilon_B[A]_t \quad \text{eqn 6.7}$$

Hence,

$$[A]_t = \frac{(A_t - A_\infty)}{(\epsilon_A - \epsilon_B)} \quad \text{eqn 6.8}$$

Likewise at $t = 0$,

$$A_0 = \epsilon_A[A]_0 \quad \text{eqn 6.9}$$

Thus (equation 6.9 minus equation 6.6),

$$(A_0 - A_\infty) = \epsilon_A[A]_0 - \epsilon_B[A]_0 \quad \text{eqn 6.10}$$

and

$$[A]_0 = \frac{(A_0 - A_\infty)}{(\epsilon_A - \epsilon_B)} \quad \text{eqn 6.11}$$

Substituting for $[A]_t$ and $[A]_0$ (equations 6.8 and 6.11) in equation 6.2 gives:

$$k_{\text{obs}} = \frac{1}{t} \ln \frac{(A_0 - A_\infty)}{(A_t - A_\infty)} \quad \text{eqn 6.12}$$

Rearranging therefore leaves,

$$\ln(A_t - A_\infty) = -k_{\text{obs}}t + \ln(A_0 - A_\infty) \quad \text{eqn 6.13}$$

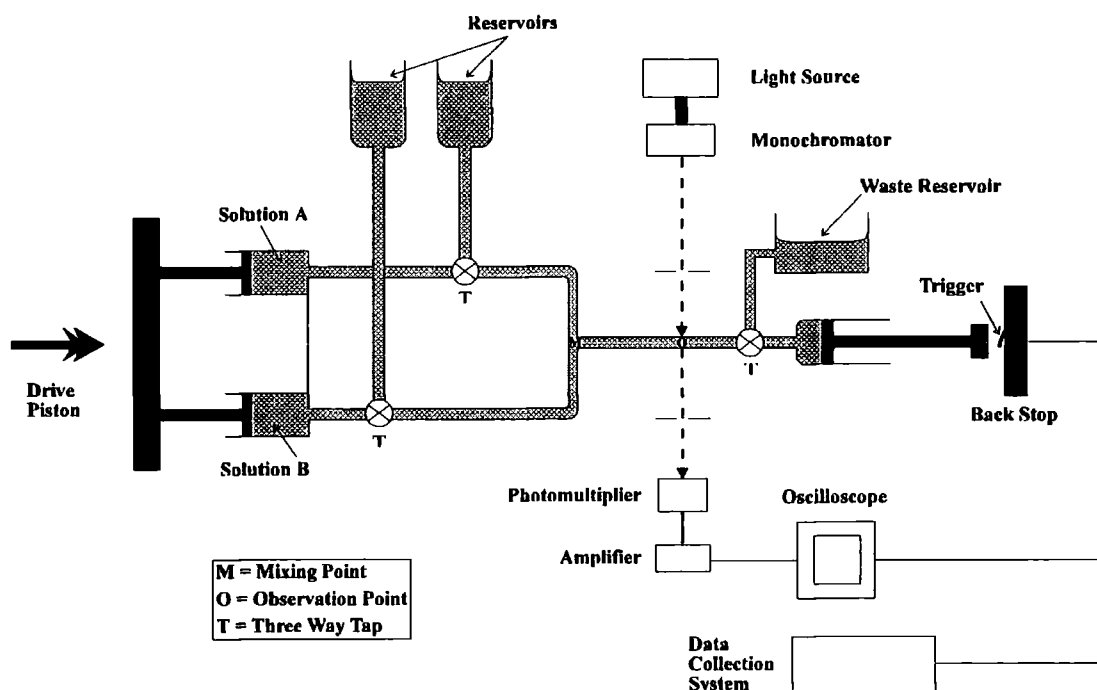
A plot of $\ln(A_t - A_\infty)$ versus t should be a straight line with a gradient equal to $-k_{\text{obs}}$. Absorbance infinity values (A_∞) were noted after a duration of ten half lives and the disappearance of absorbance recorded for a minimum of two half lives.

6.1.2 Stopped-Flow Spectrophotometry

An Applied Photophysics SX-17MV stopped-flow spectrophotometer (figure 6.1) was used to study the kinetics of reactions that were too fast to monitor by conventional means. The reactant solutions (A and B) are held in storage reservoirs and then transferred into two matching syringes to ensure that identical quantities are mixed. The syringes are compressed in unison (using an external air supply), and mixing occurs at *point M* almost instantaneously (ca. 1×10^{-3} s). The mixture next passes into a 1cm path length quartz cell (at *point O*) that is maintained at a constant temperature, and drives the plunger of a separate syringe to trigger a halt in the flow. This action prompts the acquisition of absorbance-time data for the reaction. A beam of monochromatic light (of the desired wavelength) is directed through the cell by fibre optic cable, and the voltage fluctuations that correspond to an absorbance change are suitably interpreted via a photomultiplier. Software incorporated into the stopped-flow hard drive finally transforms the voltage-related data back into an absorbance-time reading that can offer rate information.

Figure 6.1

A stopped-flow spectrophotometer



6.1.3 NMR Spectroscopy

NMR spectra were recorded by Mrs. J. Say using a Varian 400 MHz spectrometer.

6.1.4 IR Spectroscopy

IR spectra were obtained using a Perkin-Elmer 1600 series FTIR spectrometer.

6.1.5 Elemental Analysis

Elemental analysis was performed by Mrs. J. Dostal using a Carlo Erba elemental analyser.

6.1.6 Melting Points

Melting points were attained using an Electrothermal 9100 apparatus.

6.1.7 pH Measurements

All pH readings were taken using a Jenway digital 3020 pH meter (accurate to ± 0.02 pH units). It was calibrated over the range pH 4.0 - 7.0 or pH 7.0 - 10.0 at 25°C according to the nature of the solution to be measured.

6.1.8 Nitric Oxide Specific Electrode

A World Precision ISO-NO nitric oxide sensitive electrode was purchased in order to quantify the NO released from S-nitrosothiols in aqueous solution. Calibration required stock solutions of ascorbic acid (0.1 mol dm^{-3}) and sodium nitrite ($2.5 \times 10^{-3} \text{ mol dm}^{-3}$), which were first left to equilibrate at 25°C for 10 minutes (as the NO detected is influenced by temperature). The ascorbic acid was then placed in a sealed flask and the electrode immersed in the liquid to a depth of 1cm. The digital output reading was zeroed when stable. The contents of the flask were next rigorously purged with N_2 for 5 minutes to prevent the aerial oxidation of NO, and aliquots of NaNO_2 quickly introduced on stirring. A calibration graph of the resultant current (nA) against $[\text{NO}]$ ($\mu\text{mol dm}^{-3}$) could be plotted, assuming the quantitative liberation of NO. Reaction mixtures were easily tested in a similar way.

6.2 Experimental Methods

6.2.1 Product Detection

6.2.1.1 Ammonia Analysis

A 'blank' and a 'test' run had to be performed for each solution analysed. To 1ml of ammonia assay (containing 3.4 mmol dm^{-3} 2-oxoglutarate and $0.23 \text{ mmol dm}^{-3}$ NADPH) was added either 0.1ml distilled water (blank) or 0.1ml reaction solution (test). Cuvettes were left to thermostat at 25°C for 3 minutes, and then the initial absorbance (340nm) of each recorded. To these was added 0.01ml GLDH (bovine liver, 1200 U/ml) and the final absorbance noted 5 minutes later. Equations 6.14 – 6.16 were then used to calculate $[\text{NH}_3]$.

$$\Delta A = (\text{initial absorbance} - \text{final absorbance}) \text{ at } 340\text{nm} \quad \text{eqn 6.14}$$

where;

$$\text{Quantity of ammonia in test sample } (\mu\text{g/ml}) = 30.3 \times (\Delta A_{\text{test}} - \Delta A_{\text{blank}}) \quad \text{eqn 6.15}$$

$$30.3 = 1.11 \times \frac{17}{6.22 \times 0.1} \quad \text{eqn 6.16}$$

17 = RMM of ammonia (g mol^{-1})

6.22 = millimolar absorptivity of NADPH at 340nm

1.11 = volume of liquid in cell (ml)

0.1 = volume of specimen (ml)

6.2.1.2 Nitrite Analysis

The test solution (1ml) was added to 10ml sulfanilimide (3.4g in 100ml 0.4 mol dm⁻³ HCl) and 14ml N-1-naphthylethylenediamine (0.1g in 100ml 0.4 mol dm⁻³ HCl). The total volume was made up to 50ml with distilled water and the volumetric flask thermostatted at 25°C for 10 minutes. The absorbance of 2.5ml reaction solution at 540nm was then recorded.

6.2.1.3 Thiol Analysis

The test solution (2.4ml) was mixed with 0.1ml DTNB (0.05g in 10ml methanol) and the absorbance at 412nm measured after 10 minutes at 25°C.

6.2.2 Enzymatic Deaeration of Solutions

To 100ml of buffer or distilled water was added glucose (0.18g), catalase (1mg) and glucose oxidase (2mg). The solution was left to incubate at 37°C for 60 minutes and then used as normal to prepare reaction mixtures.

6.3 Experimental Materials

6.3.1 Reagents

All reagents were commercial samples of the highest grade and were used without further purification, e.g. the potassium dihydrogenphosphate (KH₂PO₄, 0.15 mol dm⁻³), potassium hydrogen phthalate, potassium chloride, borax (sodium tetraborate decahydrate) and TRIS (tris(hydroxymethyl)aminomethane) used in the preparation of buffer solutions. Solid S-nitrosothiols were synthesised as instructed in the text to follow. High purity distilled water (from the departmental supply) was used at all times. The perchloric acid required for nitrosation was prepared via dilution of 11.76 mol dm⁻³ HClO₄ (standardised using NaOH and a phenol red indicator).

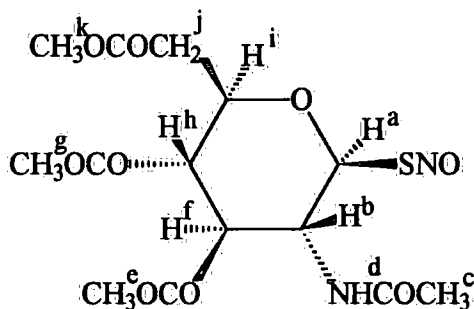
6.3.2 Synthesis of Stable S-Nitrosothiols

6.3.2.1 Symbols and Abbreviations

The following symbols and abbreviations are written for convenience;

δ_H	chemical shift (^1H NMR)
δ_C	chemical shift (^{13}C NMR)
br. s	broad singlet
d	doublet
dd	double doublet
d^6 -DMSO	deuterated dimethyl sulfoxide (99.9 atom % D)
Hz	hertz
J	coupling constant
m	multiplet
m.p.	melting point
MHz	mega hertz
ppm	parts per million
s	singlet
t	triplet
ν_{\max}	IR frequency
w	wide

6.3.2.2 Preparation of 2-Acetamido-2-deoxy-S-nitroso-1-thio- β -D-glucopyranose 3,4,6-triacetate (GPSNO, 6.1)



6.1

All synthetic work was conducted in a reaction vessel covered in foil and immersed in an ice-bath, to minimise photolytic/thermal RSNO decay. An aqueous solution (1.65ml) of sodium nitrite (1.65 mmol, 0.114g) was added dropwise over 2 minutes with vigorous stirring to a mixture of a commercial sample of 2-acetamido-2-deoxy-1-thio- β -D-glucopyranose 3,4,6-triacetate (0.83 mmol, 0.30g) dissolved in 1:1 (v/v) methanol:1 mol dm⁻³ HCl (3.30ml) and concentrated H₂SO₄ (0.17ml). The pale red reaction mixture was stirred for a further 60 minutes and then the precipitate collected by filtration, washed sparingly with ice-cold water, and air dried for 24 hours in the dark to leave a pink solid (0.21g, 65%), m.p. not recorded due to decomposition; ν_{\max} (nujol)/cm⁻¹ 3480 and 3316 (NH), 1922 (SNO), 1743 (COCH₃), 1664 (NHCO), 1572 (NO), 1055 (CN) and 654 (CS); δ_{H} /ppm (400 MHz, *d*⁶-DMSO) 1.69 (3H, s, CH₃^c), 1.95 (3H, s, CH₃^b), 1.96 (3H, s, CH₃^e), 2.01 (3H, s, CH₃^f), 4.06 (1H, d, J = 10.8 Hz, Hⁱ), 4.21 (1H, dd, J = 4.4 and 12.4 Hz, H^j), 4.34 (2H, m, H^b and Hⁱ), 5.02 (1H, t, J = 9.6 and 10 Hz, H^h), 5.41 (1H, t, J = 9.6 and 10 Hz, H^f), 6.64 (1H, d, J = 10.4 Hz, H^a) and 8.21 (1H, d, J = 9.6 Hz, NH^d); δ_{C} /ppm (400 MHz, *d*⁶-DMSO) 20.68, 20.77, 20.82 and 22.78 (CH₃), 50.90 (CH₂), 62.07, 68.54, 73.61, 75.76 and 85.31 (C), 169.59, 169.79, 169.99 and 170.33 (CO); Elemental analysis calculated for C₁₄H₂₀N₂O₉S: C, 42.85; H, 5.15; N, 7.14%, Found: C, 42.99; H, 5.03; N, 6.57%.

6.3.2.3 Preparation of S-Nitroso-N-carbamyl-D,L-penicillamine (SNCP)

An aqueous solution (1.86ml) of sodium nitrite (1.86 mmol, 0.128g) was added in one portion to a stirred mixture of (\pm)-N-carbamylpenicillamine* (0.93 mmol, 0.178g) dissolved in 1:1 (v/v) methanol:11.7 mol dm⁻³ HCl (3.72ml) and concentrated H₂SO₄ (0.19ml). The precipitate produced was separated by filtration, washed with ice-cold water, and then dried *in vacuo* in the dark for 12 hours to give a green powder with red reflections (0.11g, 54%), m.p. not recorded due to decomposition; ν_{\max} (nujol)/cm⁻¹ 3475 and 3363 (NH₂), 1921w (SNO), 1681 (CO), 1557 and 1494 (NO), 1039 (CN), 679 (SN) and 661 (CS); δ_{H} /ppm (400 MHz, *d*⁶-DMSO) 1.92 (6H, s, 2 x CH₃), 4.89 (1H, d, J = 9.8 Hz, CH), 5.72 (2H, br s, NH₂) and 6.65 (1H, d, J = 9.8 Hz, NH); δ_{C} /ppm (400 MHz, *d*⁶-DMSO) 25.34 and 26.35 (CH₃), 59.01 (CH), 59.95 (C), 157.79 and 171.78 (CO); Elemental analysis calculated for C₆H₁₁N₃O₄S: C, 32.58; H, 4.98; N, 19.00%, Found: C, 32.30; H, 4.86; N, 18.36%.

* Provided as a gift from the former Wellcome Company.

APPENDIX

Research Colloquia, Seminars, Lectures and Conferences

The Board of Studies in Chemistry requires that each postgraduate research thesis contains an appendix listing:

- A. All research colloquia, seminars and lectures arranged by the Department of Chemistry and by the Durham University Chemical Society during the period of the author's residence as a postgraduate student;
- B. All research conferences attended and papers presented by the author during the period when research for the thesis was carried out;
- C. Details of the postgraduate induction course.

**A. Colloquia, Lectures and Seminars from Invited Speakers Organised by
the Durham University Chemistry Department, 1996-1999**

(* denotes lectures attended)

- 09.10.96 Prof. G. Bowmaker, University of Auckland, New Zealand
Co-ordination and Materials Chemistry of the Group 11 and
Group 12 Metals: Some Recent Vibrational and Solid State
NMR Studies
- * 14.10.96 Prof. A.R. Katritzky, University of Gainesville, Florida, USA
Recent Advances in Benzotriazole Mediated Synthetic
Methodology
- * 16.10.96 Prof. Ojima, State University of New York, USA
Silylformylation and Silylcarbocyclisations in Organic
Synthesis
- 22.10.96 Prof. B.J. Tighe, University of Aston, UK
Synthetic Polymers for Biomedical Application – Can we meet
Nature's Challenge?
- * 30.10.96 Dr. P. Mountford, University of Nottingham, UK
Recent Developments in Group IV Imido Chemistry
- 06.11.96 Dr. M. Duer, University of Cambridge, UK
Solid State NMR Studies of Organic Solid to Liquid-
Crystalline Phase Transitions
- * 19.11.96 Prof. R.E. Grigg, University of Leeds, UK
Assembly of Complex Molecules by Palladium Catalysed
Queueing Processes
- 27.11.96 Dr. R. Templer, Imperial College London, UK
Molecular Tubes and Sponges
- 04.12.96 Prof. K. Muller-Dethlefs, University of York, UK
Chemical Applications of Very High Resolution ZEKE
Photoelectron Spectroscopy
- * 11.12.96 Dr. C. Richards, University of Wales, Cardiff, UK
Stereochemical Games with Metallocenes
- * 15.01.97 Dr. V.K. Aggarwal, University of Sheffield, UK
Sulfur Mediated Asymmetric Synthesis
- * 16.01.97 Dr. S. Brooker, University of Otago, New Zealand
Macrocycles: Exciting yet Controlled Thiolate Co-ordination
Chemistry

- 22.01.97 Dr. N. Cooley, BP Chemicals, Sunbury, UK
Synthesis and Properties of Alternating Polyketones
- 29.01.97 Dr. J. Clarke, UMIST, UK
What can we learn about Polymers and Biopolymers from
Computer-Generated Nanosecond Movie Clips?
- * 04.02.97 Dr. A.J. Bannister, University of Durham, UK
From Runways to Non-Metallic Metals – A New Chemistry
Based on Sulfur
- * 05.02.97 Dr. A. Haynes, University of Sheffield, UK
Mechanism in Homogeneous Catalytic Carbonylation
- 06.02.97 Prof. P. Bartlett, University of Southampton, UK
Immobilisation of Enzymes in Electrochemically Polymerised
Films
- * 18.02.97 Prof. Sir J. Black, Sir James Black Foundation/King's College
London, UK
My Dialogues with Medicinal Chemists
- 19.02.97 Prof. B. Hayden, University of Southampton, UK
The Dynamics of Dissociation at Surfaces and Fuel Cell
Catalysts
- * 25.02.97 Prof. A.G. Sykes, University of Newcastle, UK
The Synthesis, Structures and Properties of Blue Copper
Proteins
- 26.02.97 Dr. A. Ryan, UMIST, UK
Making Hairpins from Rings and Chains
- * 04.03.97 Prof. C.W. Rees, Imperial College London, UK
Some Very Heterocyclic Chemistry
- 05.03.97 Dr. J. Staunton, University of Cambridge, UK
Tinkering with Biosynthesis: Towards a New Generation of
Antibiotics
- 11.03.97 Dr. A.D. Taylor, ISIS Facility, Rutherford Appleton
Laboratory, UK
Expanding the Frontiers of Neutron Scattering
- * 19.03.97 Dr. K. Reid, University of Nottingham, UK
Probing Dynamical Processes with Photoelectrons
- 17.04.97 Prof. D. Geschke, University of Leipzig, Germany
NMR of Liquid Crystalline Polymers

- 22.04.97 Prof. G.B. Hammond, University of Massachusetts, USA
A Synthron Approach to Selective Fluorination of Organic Molecules using Vinyl and Propargyl Phosphonates
- 20.05.97 Prof. J. Jin, President, Korean Chemical Society, Korea
Poly PPV and Derivatives – Synthesis, Structures and Properties
- * 27.05.97 Dr. M. Meuwly, University of Bristol, UK
Physical Models for Proton-Bound Ionic Complexes
- 13.06.97 Prof. H. Yu, University of Wisconsin, USA
Dynamics of Macromolecular Monolayers
- 26.09.97 Dr. Y.L. Slovokhotov, Nesmeyanov Institute of Organoelement Compounds, Russian Academy of Sciences, Moscow, Russia
Single-Crystal X-Ray Studies of Novel Fullerene Derivatives
- 02.10.97 Dr. T. Umemoto, Daikin Company, Japan
Power-Variable Electrophilic Trifluoromethylating Agents
- * 08.10.97 Prof. E. Atkins, University of Bristol, UK
Advances in the Control of Architecture for Polyamides; From Nylons to Genetically Engineered Silks for Monodisperse Oligoamides
- * 15.10.97 Dr. R.M. Ormerod, Keele University, UK
Studying Catalysts in Action
- 21.10.97 Prof. A.F. Johnson, Interdisciplinary Research Centre, Leeds, UK
Reactive Processing of Polymers: Science and Technology
- * 22.10.97 Prof. R.J. Puddephatt, University of Western Ontario, Canada
RSC Lecture – Organoplatinum Chemistry and Catalysis
- * 23.10.97 Prof. M.R. Bryce, University of Durham, UK
New Tetrathiafulvalene derivatives in Molecular, Supramolecular, and Macromolecular Chemistry: Cooling the Electronic Properties of Organic Solids
- 27.10.97 Prof. W. Roper, University of Auckland, New Zealand
Silyl Complexes of Ruthenium and Osmium
- 11.11.97 Prof. V. Gibson, Imperial College London, UK
Metallocene Polymerisation
- 12.11.97 Dr. J. Frey, University of Southampton, UK
Spectroscopy of Liquid Interfaces: From Bio-organic Chemistry to Atmospheric Chemistry

- 20.11.97 Dr. L. Spiccia, Monash University, Melbourne, Australia
Polynuclear Metal Complexes
- 25.11.97 Dr. R. Withnall, University of Greenwich, UK
Illuminated Molecules and Manuscripts
- * 26.11.97 Prof. R.W. Richards, University of Durham, UK
A Random Walk in Polymer Science
- * 02.12.97 Dr. C. Ludman, University of Durham, UK
Demonstration Lecture - Explosions
- 03.12.97 Prof. A.P. Davis, Trinity College, Dublin, Ireland
Steroid-Based Frameworks for Supramolecular Chemistry
- 04.12.97 Dr. L. Hanton, University of Otago, New Zealand
Transition Metal Complexes of Conformationally Versatile
Ligands Containing Pyridine and Sulfur
- * 10.12.97 Prof. M. Page, University of Huddersfield, UK
The Mechanism and Inhibition of Beta-Lactamases
- 21.01.98 Prof. D. Cardin, University of Reading, UK
Aspects of Metal and Carbon Cluster Chemistry
- 27.01.98 Prof. R. Jordan, University of Iowa, USA
Cationic Transition Metal and Main Group Metal Alkyl
Complexes in Olefin Polymerisation
- 04.02.98 Prof. P. Fowler, University of Exeter, UK
Classical and Non-Classical Fullerenes
- 10.02.98 Dr. J.P. Connelly, University of Montpellier, France
Proteins Under Pressure – How do they take the Stress?
- * 18.02.98 Prof. G. Hancock, Oxford University, UK
Surprises in the Photochemistry of Tropospheric Ozone
- * 24.02.98 Prof. R. Ramage, University of Edinburgh, UK
Synthesis and Folding of Proteins
- 25.02.98 Dr. C. Jones, University of Wales, Swansea, UK
Low Co-ordination Arsenic and Antimony Chemistry
- 11.03.98 Prof. M.J. Cook, University of East Anglia, UK
How to Make Phthalocyanine Films and what to do with them
- * 17.03.98 Prof. Rotello, University of Massachusetts, USA
The Interplay of Recognition and Redox Processes: From
Flavoenzymes to Devices

- * 18.03.98 Dr. J. Evans, Oxford University, UK
Materials which Contract on Heating (From Shrinking Ceramics to Bullet Proof Vests)
- 18.03.98 Dr. R. Denning, Oxford University, UK
Second Order Optical Non-Linearity, Mixed Valence and Hyper-Raleigh Scattering
- * 26.03.98 Prof. G.S. Wilson, University of Kansas, USA
The Application of Microbiosensors to Continuous *in vivo* Monitoring
- 23.04.98 Prof. T. Cass, Imperial College London, UK
Protein design: Engineering Novel Functions in Bioelectronics
- 06.07.98 Dr. S. Althorpe, Steacie Institute for Molecular Sciences, NRCC, Ottawa, Canada
New Theoretical Methods for State-to-State Reactive Scattering
- 29.07.98 Dr. A. Cooper, University of Cambridge, UK
Polymer Synthesis in Supercritical Carbon Dioxide
- * 07.09.98 Prof. K. Shull, Northwestern University, Evanston, Illinois, USA
Axisymmetric Adhesion Tests of Soft Materials
- 07.10.98 Dr. S. Rimmer, Polymer Centre, University of Lancaster, UK
New Polymer Colloids
- * 09.10.98 Prof. M.F. Hawthorne, UCLA, Los Angeles, USA
Carboranes: Exploitation of their Unusual Geometries and Reactivities
- 21.10.98 Dr. P. Unwin, University of Warwick, UK
Dynamic Electrochemistry: Small is Beautiful
- * 23.10.98 Prof. J.C. Scaiano, University of Ottawa, Canada
In Search of Hypervalent Free Radicals
- 26.10.98 Dr. W. Piers, University of Calgary, Canada
Reactions of the Highly Electrophilic Boranes $\text{HB}(\text{C}_6\text{F}_5)_2$ and $\text{B}(\text{C}_6\text{F}_5)_3$ with Zirconium and Tantalum Based Metallocenes
- * 28.10.98 Prof. J.P.S. Badyal, University of Durham, UK
Tailoring Solid Surfaces
- 04.11.98 Dr. N. Kaltsoyannis, University College London, UK
Computational Adventures of d- & f-Element Chemistry
- 11.11.98 Dr. M. Wills, University of Warwick, UK
New Methodology for the Asymmetric Transfer Hydrogenation of Ketones

- 12.11.98 Dr. S. Loeb, University of Windsor, Ontario, Canada
From Macrocycles to Metallo-Supramolecular Chemistry
- 18.11.98 Dr. R. Cameron, University of Cambridge, UK
Biodegradable Polymers
- * 30.11.98 Prof. Hudson, University of Kent, UK
Front-Side S_N2 Reactions
- 01.12.98 Prof. N. Billingham, University of Sussex, UK
Plastics in the Environment – Boon or Bane?
- * 02.12.98 Dr. M. Jaspers, University of Aberdeen, UK
Bioactive Compounds Isolated from Marine Invertebrates and
Cyanobacteria
- 19.01.99 Prof. J. Mann, University of Reading, UK
The Elusive Magic Bullet and Attempts to find it
- * 27.01.99 Prof. K. Wade, University of Durham, UK
Foresight or Hindsight? Some Borane Lessons and Loose Ends
- 03.02.99 Dr. C. Schofield, Oxford University, UK
Studies on the Stereoelectronics of Enzyme Catalysis
- * 17.02.99 Dr. B. Horrocks, University of Newcastle, UK
Microelectrode Techniques for the Study of Enzymes and
Nucleic Acids at Interfaces
- 03.03.99 Prof. B. Gilbert, University of York, UK
Bimolecular Damage by Free Radicals: New Insights through
ESR Spectroscopy
- * 10.03.99 Dr. A. Harrison, University of Edinburgh, UK
Designing Model Magnetic Materials
- 17.03.99 Dr. J. Robertson, Oxford University, UK
Recent Developments in the Synthesis of Heterocyclic Natural
Products
- 13.05.99 Prof. N. Richards, University of Florida, USA
Chemical Perspectives on the Enzymology of Asparagine
Biosynthesis

B. Conferences Attended

1. 6th European Symposium on Organic Reactivity (Louvain-la-Neuve, Belgium, 24 - 29th July 1997).
Poster Presentation "*Measurement of Nitric Oxide Release From Some New S-Nitrosothiols*".
2. Postgraduate Winter School on Organic Reactivity – WISOR VII (Bressanone, Italy, 9 - 17th January 1998).
Poster Presentation "*Mechanistic Studies of Thiolate Ion Induced S-Nitrosothiol Decomposition*".
3. Royal Society of Chemistry Organic Reaction Mechanisms Group Annual seminars attended -
 - (i) Glaxo-Wellcome (Stevenage, 19th September 1997).
Poster Presentation "*Measurement of Nitric Oxide Release From Some New S-Nitrosothiols*".
 - (ii) Zeneca (Huddersfield, 18th September 1998).
Oral Presentation "*Reactivity of Sulfur and Nitrogen Nucleophiles Towards the Nitroso Group of S-Nitrosothiols*".
4. North East Universities Graduate Symposium (Sponsored by ICI and The Royal Society of Chemistry, University of Newcastle, 15th April 1999).
Oral Presentation "*New Aspects of RSNO Chemistry*".

C. First Year Induction Course, October 1996

The course consists of a series of one hour lectures on the services available in the department.

1. Introduction, research resources and practicalities
2. Safety matters
3. Electrical appliances and hands-on spectroscopic services
4. Departmental computing
5. Chromatography and high pressure operations
6. Elemental analysis
7. Mass spectrometry
8. Nuclear magnetic resonance spectroscopy
9. Glassblowing techniques

